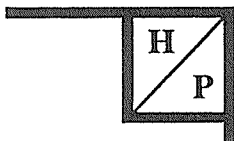
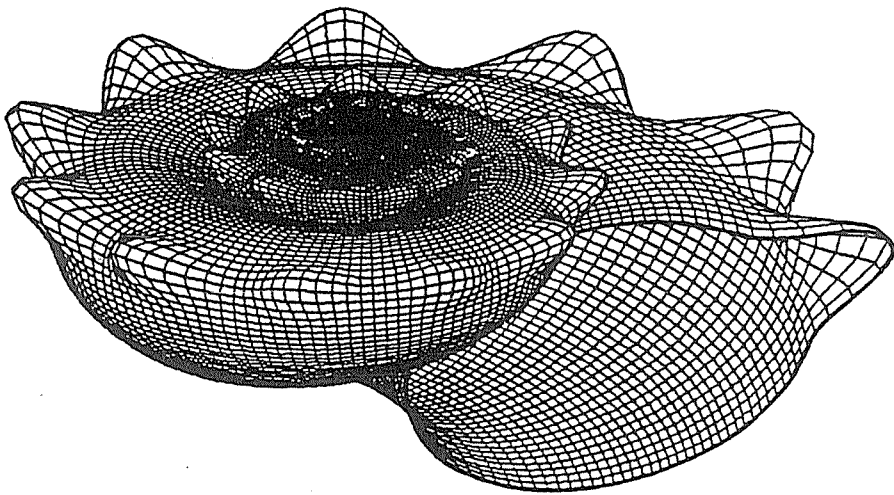


A PIONEERING MONOGRAPH IN CONCHOLOGY

foundations of
**THEORETICAL
CONCHOLOGY**

Second Edition

C. R. Illert and R. M. Santilli



HADRONIC PRESS, INC.

ABOUT THE FIRST AUTHOR

Christopher Roy Illert was born and educated in Australia. Currently, he is Associate Professor of Theoretical Biology at the Institute for Basic Research, Florida, U.S.A. He has served on the mathematics staff at Wollongong University in New South Wales and at the Computer Graphics Department of the Uki campus of the Science-Art Research Center. After graduating in 1973 from the Flinders University of South Australia, he scuba-dived extensively round the Australian coastline and became a member of the Marine Aquarium Research Institute of Australia, the Malacological Societies of South Australia and Australia, and the International Oceanographic Foundation. Over the years his studies of shells have been published in popular glossy magazines such as SEA & SHORE, SHELLS & SEA LIFE, UNDERWATER GEOGRAPHIC and AUSTRALIAN NATURAL HISTORY. His mathematical contributions have appeared in scholarly journals ranging from MATHEMATICAL BIOSCIENCES, IEEE COMPUTER GRAPHICS AND APPLICATIONS, IL NUOVO CIMENTO, HADRONIC JOURNAL and HADRONIC JOURNAL SUPPLEMENT and have been well received. Two of his publications have been selected as amongst the most outstanding contributions to a field of science this century and reprinted in Vol. 15 of the SPIE MILESTONE SERIES, Washington, D.C., USA, 1990. Prof. Illert is the organizer of various scientific meetings, including the First International Conchology Conference held in Australia in 1995.

For the second author see the inside back cover.

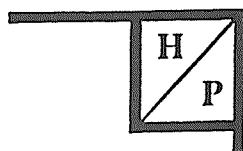
CHRISTOPHER ROY ILLERT

and

RUGGERO MARIA SANTILLI

foundations of
**THEORETICAL
CONCHOLOGY**

Second Edition



HADRONIC PRESS, INC.

Copyright © 1995 by Hadronic Press, Inc.
35246 US 19 North # 115, Palm Harbor, FL 34684 USA

All rights reserved.
No part of this book may be reproduced, stored in a retrieval system
or transmitted in any form or by any means
without the written permission
of the copyright owner.

U. S. Library of Congress
Cataloging in publication data:

C. Illert and R. M. Santilli

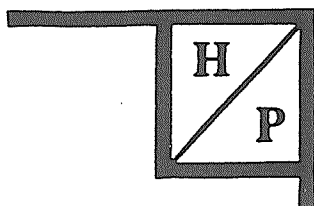
Foundations of Theoretical
Conchology

Second Edition

with Bibliography

Additional data supplied on request

ISBN 0-911767-92-4



HADRONIC PRESS, INC.

35246 US 19 North # 115, Palm Harbor, FL 34684, USA

TABLE OF CONTENTS

PART I: MATHEMATICAL REPRESENTATIONS OF SEA SHELLS FROM SELF-SIMILARITY IN NON-CONSERVATIVE MECHANICS

By C. R. Illert

Introduction, 1

1: Clocksprings mechanics, 5

2: Gnomons, scale invariance and self-similarity, 27

3: Solutions to the Euler equations, 72

4: Conclusions, 101

References, 104

Acknowledgments, 106

About colored plates, 107

PART II: REPRESENTATION OF SEA SHELLS VIA ISOTOPIC AND GENOTOPIC GEOMETRIES

by R. M. SANTILLI

1: Introduction, 112

2: Elements of the isoeuclidean geometry, 129

3: Elements of the genoeuclidean geometry, 158

Appendix A: Isotrigonometry, 162

Appendix B: Isospherical coordinates, 170

Appendix C: The universal isorotational symmetry of sea shells, 175

Acknowledgments, 183

References, 183

COLORED PLATES, 184

PART I :

**MATHEMATICAL REPRESENTATIONS OF SEA
SHELLS FROM SELF-SIMILARITY IN
NON-CONSERVATIVE MECHANICS**

Christopher Roy Illert

2/3 Birch Crescent
East Corrimal, N.S.W. 2518
Australia

and

The Institute for Basic Research
P. O. Box 1577
Palm Harbor, FL 34682
U. S. A.

CONTENTS

INTRODUCTION:	1
SECTION 1: CLOCKSPrING MECHANICS	5
<i>Living Clocksprings 5. First-Order Discrete Mechanics 10. Second-Order Discrete Mechanics 14. The Dissipative Hook-ean Lagrangian 21.</i>	
SECTION 2: GNOMONS, SCALE-INVARIANCE & SELF-SIMILARITY	27
<i>Triangular-Number Gnomons 27. Triangle & Cone Gnomons 28. Rectangular Gnomons 32. Solen 33. Crescentic Gnomons 38. Scallop 40. Self-similarity & Rotation about an Axis 43. Torus 43. Chalice 47. Coni-spiral Gnomons in 3D, 50. Ammonite, Euomphalopterus 61. Turbo 62, 63. Phanerotinus, Angaria 64. The Self-similarity Differential Equation 65.</i>	
SECTION 3: SOLUTIONS TO THE EULER-EQUATION	72
<i>Real-Space Clockspring Trajectories 72. The Conispiral 73. Möbius Conoidal Spires 75. Hyperbolic Clocksprings 81. Wrinkled Ramm Cones 84. Heteromorphs 86. Cylindrical Sine-Spirals 88. Spiral Lissajous Figures 90. Branching Clocksprings and Acausality 92. Janospira 93. Charged Lepton Decay and Neutrino Production 96.</i>	
REFERENCES: 101. ACKNOWLEDGEMENTS: 106. DESCRIPTIVE TEXT FOR COLORED PLATES: 107. COLORED PLATES: 183	

INTRODUCTION

Seashells are remarkable geometrical objects, being approximately self-similar throughout growth, and governed by laws and physical principles which are scale-invariant. Collectively shells pose a non-trivial dynamical problem which can be rigorously formulated (in complex-space) and completely understood. And, once we understand this general problem, it becomes evident that shell-geometries are of interest beyond conchology, malacology and paläontology, with broad implications for theoretical mechanics generally.

Shells are non-trivial geometrical shapes: the end-product of 500 million years of evolution in the oceans of our planet ... perhaps one of the greatest simulations of all time, dwarfing anything done by humans on super-computers. Shells are static real-world "snapshots" of dynamic forces and torques in action, providing solid examples that can be held in the hand: examples of, amongst other things, the onset of "chaos" (including "temporal chaos", see Section 3.2) in "dissipative" scale-invariant systems.

The fossil shell NIPPONITES MIRABILIS is a wonder of nature and a magnificent example: its principal growth-trajectory starts off in a predictable planar coil but becomes increasingly loopy, like the suture-line on a tennis ball, ultimately executing wild serpentine meanders resembling turbulent fluid flow (i.e. a vortex-street wrapped in a spiral). And the growth-trajectory that we see (hereafter called a CLOCKSPRING) is only the real part of a more general (perhaps even geodesic) curve through a multi-dimensional complex-space. Even the underlying physical principles (such as HOOKE'S LAW) only emerge coherently, and seem to make sense, within our full complex-space formalism (as in Section 1). Real-space E^3 just doesn't seem adequate.

So are seashell geometries profound enough to tell us that we live in a world that doesn't quite make sense unless we assume that it has at least five space-like and one time-like dimensions? How seriously should we take them? Certainly, if we do take shell geometries seriously, our insights are all the more powerful because they emerge from totally classical, non-quantum, reasoning.

To some extent, much of this could be shrugged-off were it not for the fact that even in the purely real formalism (as given in Section 3.1) the critical physical constants associated with trajectory "curvature" and "torsion" often have to be complex numbers. Furthermore, a whole class of branching shell-geometries exist, exhibiting a feature called "temporal chaos" that implies hidden dimensions, acausal influences, or both. In this class are shells such as JANOSPIRA NODUS, and others beside, all required by theory and observed in nature despite the fact that their geometries could only be produced by forces that "act-at-a-distance" (both backward and forward) through time itself, thereby violating causality as we "know" it!

Such oddities, suspected by theoreticians such as Kanatani⁷ but ignored for lack of real-world examples, can now be convincingly demonstrated simply by reaching into the nearest shell cabinet. The proof is in the "seeing", so to speak, and as this is the way that Nature itself "does" theoretical mechanics, we might do well to learn from it ... no matter how surprising.

Not only do shells teach the significance of complex curvature and torsion in differential geometry (results not mentioned in any standard text on the subject), and the causal implications of self-similar non-conservative systems, but they also show that sensible, physically-meaningfull Lagrangians exist in nonconservative mechanics. Just because things sometimes happen "dissipatively" in the real-world, does not mean that there isn't an optimal fashion for them to proceed. This has been known for most of our present century, but denied by a small portion of the modern mathematical community concerned with Liapunov Function theory which, of course, advocates the use of conservative Lagrangians to model non-conservative systems ... a total contradiction in terms, rather like hammering a square peg into a round hole!

Santilli's book²⁹ in 1979 gave a history of this misconception as it relates to the inverse problem in variational calculus yet, still, by 1982, research papers (such as the one by Chen & Russell³⁰) were still appearing in the mathematical literature advocating the use of conservative Lagrangians for nonconservative systems. In the cited case³⁰ it was admitted that the approach was unsatisfactory, in their words "primitive and ad hoc", and yet the Quarterly of Applied Mathematics refused to print the correct Lagrangian for the problem (when I supplied it) and, surprisingly enough, even produced a spirited referee response which echoed almost word-perfect the notions of Bauer and Synge from the 1930's. In fact, there's absolutely nothing in several centuries of theoretical mechanics to even suggest that anything "more general than the concept of energy" either exists or makes sense. Liapunov Functions are a nonsense.

Mistakes happen all the time, we've all made them, and that's how knowledge progresses. But when at least a portion of the mathematical community don't seem to want to correct a serious oversight, one which has been perpetuated on and off since the 1920's, then there is an interesting sociological phenomenon in progress. Why would Liapunov Function theorists simply choose to ignore

nonconservative Lagrangians, or arbitrarily discount them as "purely mathematical" objects devoid of physical meaning? Perhaps it is because mathematical equations, and logic alone, simply aren't enough to convince some people. What may be needed is a physically convincing, real-world example of a non-conservative system, one whose Lagrangian can be derived from first principles. If this can be achieved then we may overcome the psychological barriers, and progress most of the way toward convincing all mathematicians that there is a better way to deal with "dissipative" systems. If the seashell problem is able to provide such an example, then it will indeed have served an important role in theoretical (as well as applied) mechanics.

In any case, from a solid empirical base encompassing 100,000 or so (living and extinct) molluscan shell varieties, the horizons of seashell mathematics reach outwards cutting into the fabric of other, better-known branches of modern physics ranging from elasticity theory and fluid dynamics, perhaps to subatomic particles. Indeed, the incremental nature of shell growth, emphasised in Sections 1.2 to 1.4, conjures notions of a succession of "force impulses" discretely deflecting straight-line trajectory increments into continuous-looking spirals. The whole metaphysical atmosphere resembles Feynman Diagram interpretations, and quantum-electrodynamic accounts of charged particle motion in external fields. Just how far this analogy extends, and how relevant it is, still remains largely to be seen but we make a start in Section 3.2 by offering the "example" of charged Lepton decay and Neutrino production in terms of discrete vector sums (1.3) which, in the limit, become circle-integrals.

Although constants associated with various modes of complicated shell-coiling are already being determined to several significant figure accuracy^{16, 15}, THEORETICAL CONCHOLOGY itself is a relatively new science which has emerged in the last two decades. Its literature is sparse and scattered, and no textbook on the subject has yet been made available by large publishers. For this reason we discuss literature from a diversity of sources in more detail than might otherwise be the case, as well as presenting new and previously unknown results. Such coverage should provide the best basis from which to grasp the logical development and significance of the subject, its relevance to other areas of science, and the theoretical problems which still lurk unresolved at the frontiers.

Chris ILLERT (1991).

1.1 LIVING CLOCKSPRINGS?

In 1908 *Harold Sellers Colton*¹ communicated, to the Philadelphia Academy of Sciences, the results of his extensive field and aquarium studies of the feeding-habits of marine snails. He found that some carnivores used their shell-aperture to force open the oysters and cockles on which they fed. It was a complicated process with the snail's soft-body muscles, coiled as they are about the shell's central axis (the columella), being able to create a torque that rotated the shell as a whole thereby enabling the current shell-aperture to be used as a tool to "bulldoze" bivalves open.

The dynamics of this process is rather like twirling the winding spindle of a tensile clockspring whose outermost end is anchored (satisfying a "fixed-end" boundary condition; see Case 3, in Section 3.1). Indeed, this is the kind of image suggested in 1914 by *Theodore Andrea Cook*², in his book "the Curves of Life", though he was apparently unaware of *Colton's* earlier fieldwork and apologised to the reader for making the analogy!

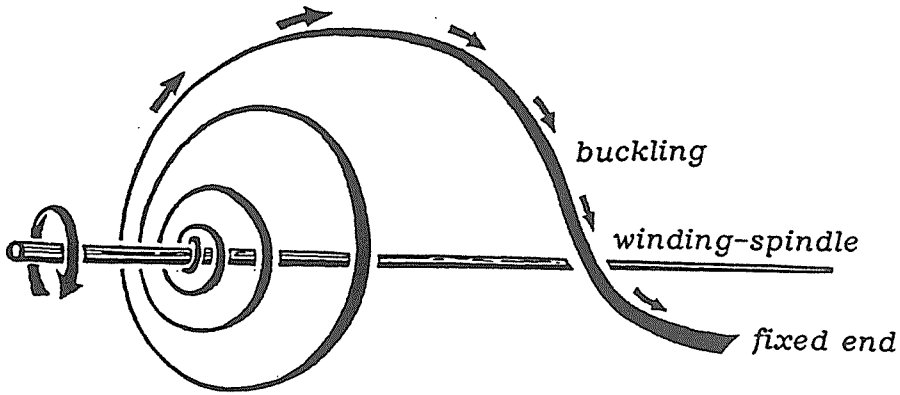
A succession of conchologists and malacologists have since confirmed *Colton's* finding that many marine snails (including volutes, bonnets, helmets, olives, harps and whelks) all to some extent physically twirl their shells, using them like clocksprings during the normal course of feeding. Some of these researchers include *Warren* (1916), *Copeland* (1918), *Clench* (1939), *Megelhaes* (1948),

Carricker (1951), *Nielsen*³ (1975) and *Illert*⁴ (1979/80/81). The history of this strand of thought is summarized in a four-part series of articles by *Illert*⁶ (1985) which also supplies a number of less well known literature references.

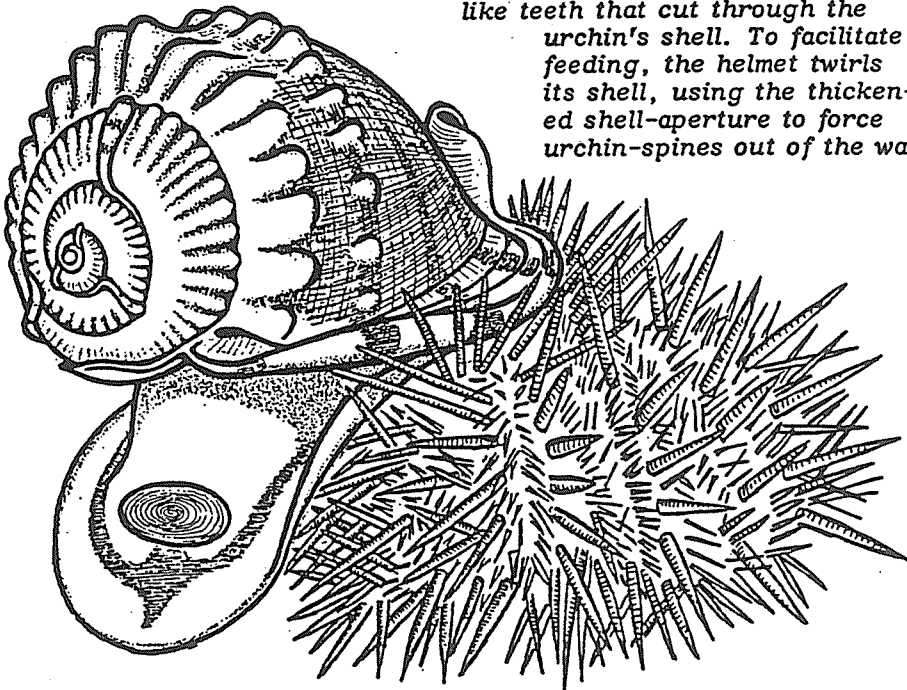
There can be little doubt that the forces acting on the shell are considerable, and the spring analogy appropriate, as some snails use their shells to bore through sand, wood or solid rock. The common abalone has a muscular foot capable of supporting 4000 times its body-weight ... have you tried to pry one off a rock? *Wainwright*⁵ (1969), realizing that the stresses were so great that small cockles or scallops sometimes just shattered, implanted strain-gauges to physically measure the forces involved. *Nielsen*³ (1975) found that even the predatory snails sometimes fractured their own shell-apertures, and *Illert*⁴ (1979/80) realized that this was why some snails such as the South Australian Helmet, *Cassis bicarinata*, have a specially thickened apertural band (called a "varix") to reinforce their shell and prevent it from breaking when it is used to "bulldoze" seaurchin spines away during the course of feeding. >>

Another kind of "clockspring" geometry is represented by the cowrie shell. The juvenile starts coiling in a regular spiral way but, by maturity, the aperture curves inward and growth stops. The cowrie wanders about with its shell exterior covered by a fleshy skin, called the "mantle", emanating through the shell's apertural slit. If a fish or other predator grabbed at the cowrie's exposed mantle-skin, and would not let go, then the cowrie would try to withdraw back through the apertural slit by levering on the rigid shell. In this grim tug-of-war the fulcrum of

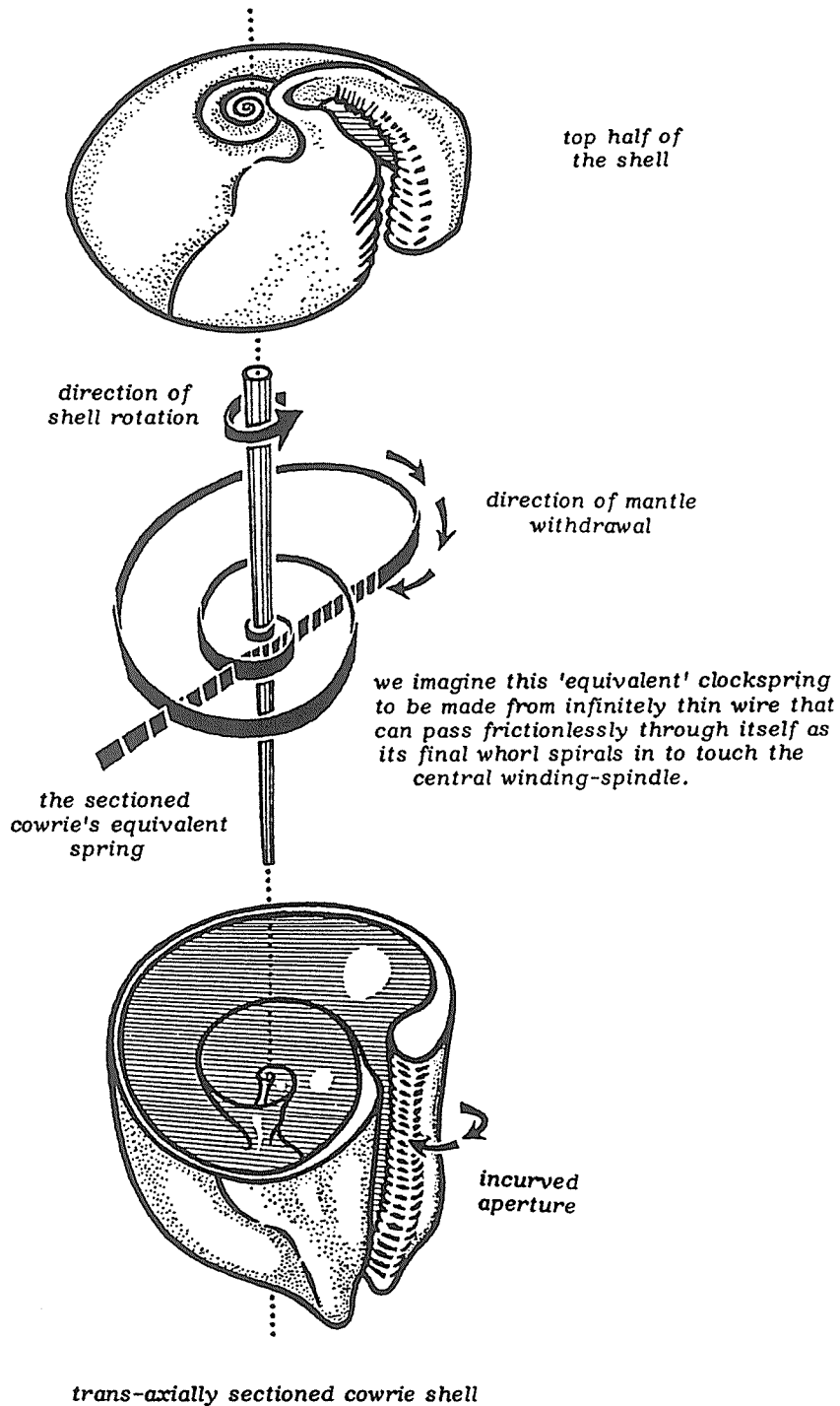
CLOCKSPRING OF THE FIRST KIND



the South Australian helmet, *CASSIS BICARINATA*, is carnivorous; eating sea-urchins with an extendable elephant-like trunk containing saw-like teeth that cut through the urchin's shell. To facilitate feeding, the helmet twirls its shell, using the thickened shell-aperture to force urchin-spines out of the way



CLOCKSPRING OF THE SECOND KIND



forces is the shell aperture; this is probably why most cowries have apertural crenulations ("teeth") enhancing their "grip" during such attacks.

All this biological evidence suggests that, although different species have different reasons for doing so, they produce shells that don't just coincidentally resemble optimal tensile clocksprings, as originally suggested by Cook, but that they actually function as such in order to best dissipate stresses incurred during the normal course of life. We would expect some version of *Hooke's Law*, for elastic springs, to underlie all naturally occurring shell geometries: it seems self-evident from the lifestyles of the creatures themselves.

It is, of course, one thing to claim that this mathematics exists, and quite another thing to find it! The rest of Section 1 is devoted to the task of creating an internally consistent, logical and powerful "clockspring mechanics". By the end of Section 1 we have a mechanics which is too powerful and too general; the Hookean (matrix) constant of proportionality k , and one other (matrix) constant Ω , will remain undetermined. This is why Section 2 is devoted to deriving, and explaining, two symmetry constraints (respectively equations (2.41) and (2.42)) arising in a natural way from self-similarity, from which the structure of the two matrices can be deduced (as in (2.45)) or inferred (as in (2.46) & (2.47)). But, although we know the form of these two matrices, the constant terms within them are still arbitrary. Section 3 therefore shows various classes of clockspring trajectories which satisfy the Euler equation ((1.38) = (3.1)) for different values of the arbitrary constants λ and μ .

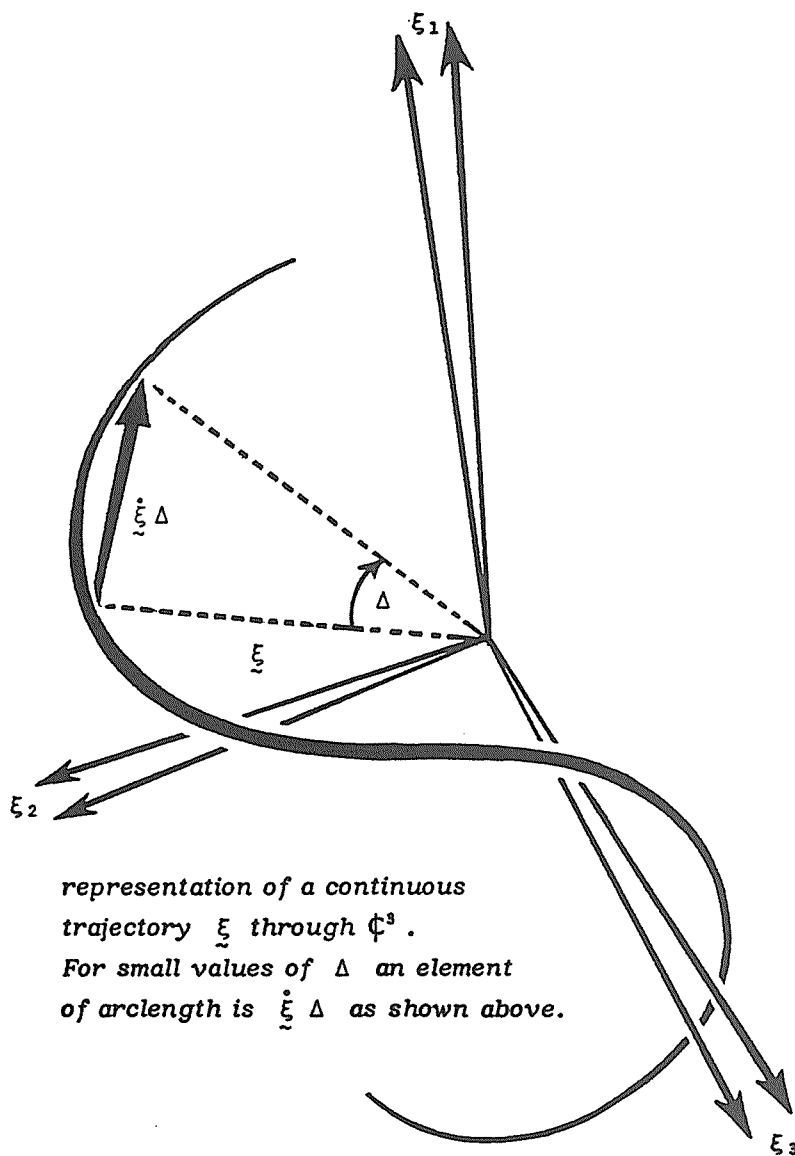
1.2 FIRST ORDER DISCRETE MECHANICS

Consider a vector-valued function $\underline{\xi}(\phi) = (\xi_1(\phi), \xi_2(\phi), \xi_3(\phi))$ describing a continuous, twice-differentiable trajectory through some generalised multi-dimensional space: say $\underline{\xi} : [0, \infty) \rightarrow \mathbb{C}^3$. A physically meaningful formulation of the seashell problem does not seem attainable solely in E^3 . It was attempted by Illert⁶ in 1983 but even the real-space equations themselves suggested a complex-space formalism (the Euler equations becoming diagonalised only in complex coordinates $\underline{\xi}$). Of course, all our complex space equations have their real-space counterparts ("projections") but something of the logical rationale is lost in them. The actual problem to which real-world seashells are the solution can only be fully appreciated in more than three real-space dimensions. We will consider ourselves to have done well if we can, by imposing a geometrically simplifying symmetry, reduce the space in which we formulate the problem down from \mathbb{C}^3 to $\mathbb{C}^2 \times E^1$.

Continuing then, with the above-discussed trajectory $\underline{\xi}$, a suitable quantity of arc-length is defined as follows

$$\frac{d \underline{\xi}}{d \phi} \quad d \phi \quad \equiv \quad \dot{\underline{\xi}} \quad \Delta \quad . \quad \dots (1.1)$$

The diagram opposite is a geometrical "cartoon" whose purpose is to convey a visual image of what our equations mean.



Of course real-world seashells grow incrementally along their respective trajectories so let us consider a sequence of points,

$$\left\{ \xi(s\Delta) \equiv \xi_s \in \mathbb{C}^3 \right\}$$

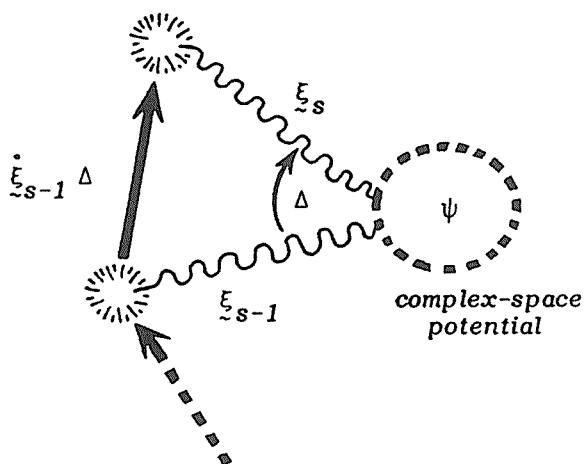
for some small constant Δ , and integers $s = 1, 2, 3, \dots, n$, through which our continuous trajectory $\xi(\phi)$ passes.

We may also, in principle, introduce at this stage the notion of a generalised complex-space potential (either an "attractor" or "repulser"), denoted $\psi(\xi_s)$, which acts impulsively at the points ξ_s generating a discretized approximation to $\xi(\phi)$ according to a simple vector recursion relationship

$$\xi_s = \xi_{s-1} + \dot{\xi}_{s-1} \Delta . \quad \dots (1.2)$$

This is rather like Newton's equation $x = x_0 + vt$ and simple iteration gives

$$\begin{aligned} \xi_n &= \xi_{n-1} + \dot{\xi}_{n-1} \Delta \\ &= (\xi_{n-2} + \dot{\xi}_{n-2} \Delta) + \dot{\xi}_{n-1} \Delta \\ &= (\xi_{n-3} + \dot{\xi}_{n-3} \Delta) + \dot{\xi}_{n-2} \Delta + \dot{\xi}_{n-1} \Delta \\ &= \text{etc.} \\ &= \xi_1 + \sum_{s=1}^{n-1} \dot{\xi}_s \Delta . \quad \dots (1.3) \end{aligned}$$

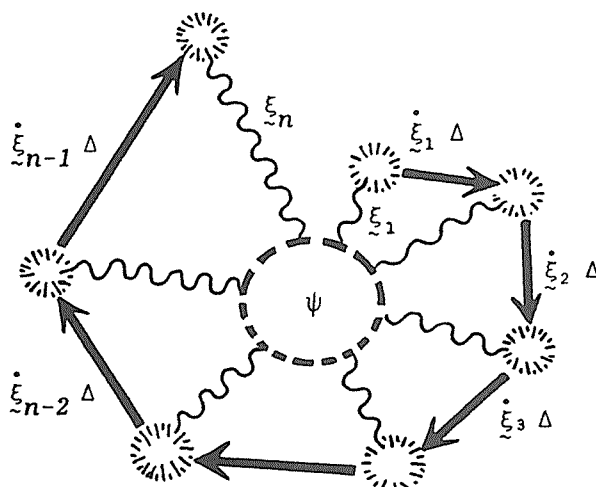


eq. (1.2) describes the alteration of a straight-line trajectory, through the impulsive action of a "potential" ψ . We can represent this process diagrammatically, as shown (LEFT).

the simple vector addition in eq. (1.3) may thus be viewed as a trajectory which is modified by the potential several times.

Consecutive points link to their nearest neighbours by straight-line segments as shown (RIGHT).

Our first order mechanics thus provides a mental picture (cartoon) which assists our visualisation of the mathematical framework.



In the limit as Δ becomes very small, and n very large, it makes sense to replace the discrete quantity $n\Delta$ by a continuous variable ϕ . The summation in eq. (1.3) becomes an integral and we thus obtain the trivial result

$$\xi(\phi) - \xi(0) = \int_0^\phi \dot{\xi}(\tau) d\tau \quad \dots (1.4).$$

1.3 SECOND ORDER DISCRETE MECHANICS

First-order mechanics helps us visualise the potentials ψ that discretely modify our trajectories, but it tells us little about the form of the potential functions, themselves, and nowhere defines "acceleration". We need to generalise eq.(1.2) into a second-order mechanics of the form

$$\xi_{s+1} = f(\Delta, \xi_s, \dot{\xi}_s, \ddot{\xi}_s), \quad \dots (1.5)$$

for some function f . *Reverberi*⁸ chose the first few terms of a Taylor Series, but *Kanatani*⁷ has suggested that the accuracy of this kind of second order mechanics can be improved by choosing f such that

$$\xi_{s+1} \cong \xi_s + \dot{\xi}_s \Delta + \ddot{\xi}_s \Delta^2, \quad \dots (1.6)$$

along with the auxillary definitions of "instantaneous growth velocity" (at location s)

$$\dot{\xi}_s = (\xi_{s+1} - \xi_s) / \Delta, \quad \dots (1.7)$$

and "instantaneous acceleration" at the same location (expressed in terms of the rate of change of these growth-velocities)

$$\ddot{\xi}_s = (\dot{\xi}_s - \dot{\xi}_{s-1}) / \Delta \quad \dots (1.8).$$

From the introductory discussion in Section 1.1 we have reason to believe that the forces behind seashell geometries are both Hookean and nonconservative (after all, shells grow from nothing

into something, in the process taking energy and materials from their external environments, so they must be considered to be "thermodynamically open" systems interacting with sources and sinks). This means that we are dealing with accelerations (hence forces) such that

$$\ddot{\xi}_s = k \bar{\xi}_s - \Omega \dot{\xi}_s, \quad \dots (1.9)$$

for a constant $[3 \times 3]$ diagonal matrix k (the Hookean constant of proportionality) and Ω (the Boycott constant of proportionality for the velocity dependent "dissipative" term). Generally the constants in Ω are related to the magnitudes of static torques and axial compression forces acting within the shell structure, whereas k is a measure of elasticity. Also the quantity $\bar{\xi}_s$, appearing in eq.(1.9), is the average radius-vector at location s defined as follows

$$\bar{\xi}_s = \frac{1}{2} (\xi_{s+1} + \xi_{s-1}) \quad \dots (1.10).$$

Thus substituting eqs.(1.10) and (1.7) into (1.9) gives

$$\begin{aligned} \ddot{\xi}_s &= \frac{1}{2} k (\xi_{s+1} + \xi_{s-1}) - \Omega (\xi_{s+1} - \xi_s) / \Delta \\ &= (\frac{1}{2} k - \Omega / \Delta) \xi_{s+1} + (\Omega / \Delta) \xi_s + \frac{1}{2} k \xi_{s-1}, \end{aligned} \quad \dots (1.11)$$

hence we have

$$\Delta^2 \ddot{\xi}_s = (\frac{1}{2} k \Delta^2 - \Omega \Delta) \xi_{s+1} + \Omega \Delta \xi_s + 0(\Delta^2) \quad \dots (1.12).$$

We can ignore the small term of order $O(\Delta^2)$ and substitute eq.(1.12) back into the general equation of motion (1.6) to obtain the following result

$$\begin{aligned} \xi_{s+1} \approx (1 + \Omega \Delta) \xi_s + \Delta \dot{\xi}_s + (\tfrac{1}{2} k \Delta^2 - \Omega \Delta) \xi_{s+1} \\ \dots (1.13). \end{aligned}$$

The temptation is, of course, to simplify eq.(1.13) even further by cancelling the two terms containing $\Omega \Delta$. But if we look back carefully at eq.(1.12) we see that they had different origins: one in a ξ_s term, and the other in a ξ_{s+1} term, so they are not quite the same. One piece of the $\Omega \Delta$ term properly belongs with the acceleration coefficient $(\tfrac{1}{2} k \Delta^2 - \Omega \Delta)$ whilst the other properly belongs in the displacement coefficient $(1 + \Omega \Delta)$. They are significant terms of order Δ and must both remain in eq.(1.13). To cancel them would be equivalent to assuming a conservative system wherein eq.(1.9) reduces to $\ddot{\xi}_s = k \bar{\xi}_s$.

LEMMA # 1

$$\int_a^b g(\tau) d\tau \approx \tfrac{1}{2}(b-a)(g(b) + g(a)) \quad \dots (1.14).$$

This will not be proved as it is the well known Trapezoid Integration formula which can be found in any standard text on numerical analysis and improves in accuracy if $b - a$ is small.

LEMMA # 2

$$\frac{1}{2} \Omega \Delta (\xi(\Delta) + \xi(0)) \cong \Omega \int_0^{\Delta} \xi(\tau) d\tau \quad \dots (1.15).$$

This result follows from Lemma 1 for small values of Δ .

LEMMA # 3

$$\frac{1}{4} k \Delta^2 (\xi(\Delta) + \xi(0)) \cong k \int_0^{\Delta} \int_0^{\tau} \xi(\mu) d\mu d\tau \quad \dots (1.16).$$

PROOF:

It follows from Lemma 1 that

$$\int_0^{\tau} \xi(\mu) d\mu \cong \frac{1}{2} \tau (\xi(\tau) + \xi(0)).$$

Using Lemma 1 to integrate a second time gives

$$\int_0^{\Delta} \frac{1}{2} \tau (\xi(\tau) + \xi(0)) d\tau \cong \frac{1}{2} \Delta (\frac{1}{2} \Delta (\xi(\Delta) + \xi(0)) + 0),$$

and multiplication throughout, by the matrix k , yields eq.(1.16).

NOTE: these Lemmas are adapted from Reverberi⁸ (1985) with relatively minor modifications.

Eq.(1.13) holds for all real integers s , including the simplest case of all, where $s = 0$, corresponding to the relationship

$$\begin{aligned} \xi(\Delta) \cong (1 + \Omega \Delta) \xi(0) + \Delta \dot{\xi}(0) + (\tfrac{1}{2} k \Delta^2 - \Omega \Delta) \xi(\Delta) \\ \dots (1.17). \end{aligned}$$

In the right-hand-side of this equation we can make the approximation $\xi(\Delta) \cong \tfrac{1}{2}(\xi(\Delta) + \xi(0))$ giving

$$\begin{aligned} \xi(\Delta) \cong (1 + \Omega \Delta) \xi(0) + \Delta \dot{\xi}(0) + (\tfrac{1}{4} k \Delta^2 - \tfrac{1}{2} \Omega \Delta) (\xi(\Delta) + \xi(0)) \\ = (1 + \Omega \Delta) \xi(0) + \Delta \dot{\xi}(0) + k \int_0^{\Delta} \int_0^{\tau} \xi(\mu) d\mu d\tau \\ - \Omega \int_0^{\Delta} \xi(\tau) d\tau \\ \dots (1.18) \end{aligned}$$

by Lemmas 2 and 3,

$$\begin{aligned} = (1 + \Omega \Delta) \xi(0) + \Delta \dot{\xi}(0) - \int_0^{\Delta} (\Omega - (\Delta - \tau) k) \xi(\tau) d\tau \\ \dots (1.19) \end{aligned}$$

by the Reimann-Liouville Integral Theorem*.

*NOTE: the theorem states
$$\int_0^{\Delta} \int_0^{\tau} g(\mu) d\mu d\tau = \int_0^{\Delta} (\Delta - \tau) g(\tau) d\tau$$

Replacing the discrete variable Δ with its continuous counterpart ϕ gives us a general equation of motion

$$\begin{aligned} \xi(\phi) = (1 + \phi \Omega) \xi(0) + \phi \dot{\xi}(0) - \int_0^{\phi} (\Omega - (\phi - \tau) k) \xi(\tau) d\tau \\ \dots (1.20) \end{aligned}$$

which must be valid at least for small angles $\phi \cong \Delta$. Actually we have done better than first appearances might suggest. This equation actually holds for any finite value of the continuous variable ϕ and it describes a huge variety of tensile "clockspring" trajectories through \mathbb{C}^3 . We hereafter refer to eq.(1.20) as the complex-space clockspring equation.

An interesting feature of eq.(1.20) are the terms containing $\xi(0)$ and $\dot{\xi}(0)$. These enable us to readily incorporate into our model the clockspring "fixed-end" boundary conditions (as discussed in Section 1.1). However, if we want to write the integral equation (1.20) as a differential equation it becomes

$$\ddot{\xi}(\phi) + \Omega \dot{\xi}(\phi) - k \xi(\phi) = 0 \quad \dots (1.21)$$

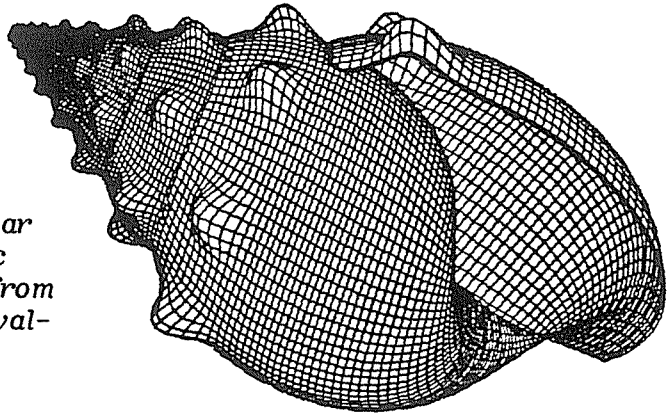
which should be compared with our original discrete relationship eq.(1.9). In Appendix B of his 1987 paper, *Illert*¹⁵ used the Leibnitz rule to differentiate the above eq.(1.20) thereby obtaining (1.21). In Appendix D of the same paper he showed how to Laplace Transform equations of the form (1.20) or (1.21) to obtain various clockspring trajectory solutions. Whilst, in Appendix F, he also discussed the clockspring "fixed end" boundary conditions.

DISCUSSION

We can compare eq.(1.6) with Newton's famous equation of motion $x = x_0 + ut + \frac{1}{2}at^2$. The similarity would have been even greater had we used *Reverberi's*⁶ Taylor Series approximation instead of *Kanatani's*⁷ version. Our eq.(1.7) is the same as eq.(1.2) hence resembling Newton's equation $x = x_0 + vt$. Likewise our eq.(1.8) is a statement of the impulse equation $Ft = mv - mu$. We wanted to form a self-contained, and internally consistent, second order mechanics so it was essential that all these relationships held. It was also important to demonstrate that the equation (1.20) could be derived in a natural way from (1.6), clearly showing the kinds of auxillary conditions and assumptions (such as eq.(1.9)) which had to be made along the way. But there is still one equation from Newtonian mechanics whose counterpart has not yet been discussed: $v^2 - u^2 = 2ax$. Obviously this relates kinetic and potential energies, so it will be dealt with in the next Section when we derive the Lagrangian for our problem.

A turbinate self-similar shell, with ϕ -periodic "knobs", generated from eq. (2.35) using the values:

$$\alpha = 0.061, \quad \tau = 8.6^\circ, \\ \beta_1 = 1.7^\circ, \quad \beta_2 = 0, \quad \beta_3 = 1.1^\circ$$



1.4 THE DISSIPATIVE HOOKEAN LAGRANGIAN

We will define force, \underline{F}_s , in our nonconservative system as follows

$$\ddot{\underline{\xi}}_s = \underline{F}_s - \Omega \dot{\underline{\xi}}_s = k \bar{\underline{\xi}}_s - \Omega \dot{\underline{\xi}}_s \quad \dots (1.22)$$

where $\bar{\underline{\xi}}_s$ was defined along with the constant matrices k and Ω in equation (1.9). Indeed, we can extract eq.(1.9) from (1.22) above. Also we can obtain a more familiar statement of Hooke's law by rearranging (1.22) as follows

$$\underline{F}_s = k \bar{\underline{\xi}}_s = \ddot{\underline{\xi}}_s + \Omega \dot{\underline{\xi}}_s \quad \dots (1.23).$$

We may now repeatedly use (1.8) to expand the velocity term as below

$$\begin{aligned} \underline{F}_s &= k \bar{\underline{\xi}}_s = \ddot{\underline{\xi}}_s + \Omega (\ddot{\underline{\xi}}_s \Delta + \dot{\underline{\xi}}_{s-1}) \\ &= \ddot{\underline{\xi}}_s + \Omega \Delta (\ddot{\underline{\xi}}_s + \ddot{\underline{\xi}}_{s-1} + \dots + \ddot{\underline{\xi}}_1 + \dot{\underline{\xi}}_0 / \Delta) \\ &\cong \ddot{\underline{\xi}}_s + s \Delta \Omega \ddot{\underline{\xi}}_s \quad \left\{ \begin{array}{l} \dots \text{ assuming} \\ \text{the velocity term} \\ \text{is negligible} \end{array} \right. \\ &= (1 + s \Delta \Omega) \ddot{\underline{\xi}}_s \\ &\cong e^{s \Delta \Omega} \ddot{\underline{\xi}}_s \quad \dots (1.24). \end{aligned}$$

Thus Hooke's Law emerges naturally in our nonconservative system provided the forces are appropriately scaled to reflect the influx or outflow of energy.

We can use eq.(1.24) to define a quantity which has dimensions of $[force] \times [time]$ as follows

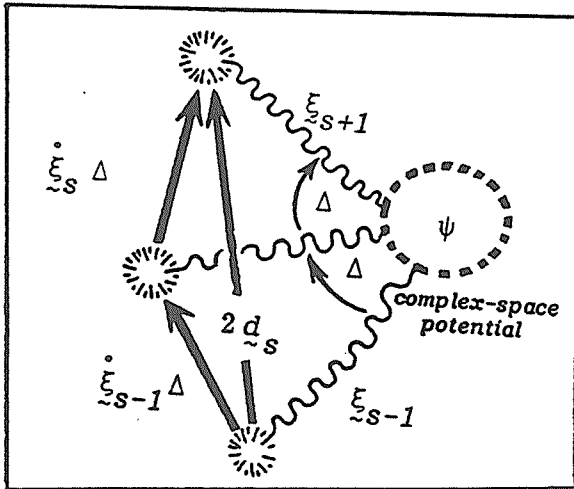
$$\tilde{F}_s \Delta = e^{\Omega s \Delta} \ddot{\tilde{\xi}}_s \Delta$$

which, because of (1.8), can be expressed entirely in terms of velocities as below

$$= e^{\Omega s \Delta} (\dot{\tilde{\xi}}_s - \dot{\tilde{\xi}}_{s-1}) \quad \dots (1.25)$$

and this is just a discrete version of Newton's so-called "impulse" equation; $Ft = mv - mu$, adapted to our nonconservative system.

We now need to define two new quantities, respectively the "mean growth increment" \tilde{d}_s and the "average growth velocity" $\overline{\dot{\tilde{\xi}}}_s$, at the location s , related to each other as shown in the below diagram:



$$\begin{aligned} 2\tilde{d}_s &= \tilde{\xi}_{s+1} - \tilde{\xi}_{s-1} \\ &= (\tilde{\xi}_{s+1} - \tilde{\xi}_s) + (\tilde{\xi}_s - \tilde{\xi}_{s-1}) \\ &= \dot{\tilde{\xi}}_s \Delta + \dot{\tilde{\xi}}_{s-1} \Delta \\ &= \frac{1}{2} (\dot{\tilde{\xi}}_s + \dot{\tilde{\xi}}_{s-1}) 2\Delta \\ &= \overline{\dot{\tilde{\xi}}}_s 2\Delta \quad \dots (1.26). \end{aligned}$$

At present we are mainly interested in the relationship

$$2 \underset{\sim}{d}_s / \Delta = (\dot{\underset{\sim}{\xi}}_s + \dot{\underset{\sim}{\xi}}_{s-1}) \dots (1.27).$$

We can obtain a quantity with dimensions of [energy], hence a measure of the work expent growing from location $s-1$ to location s , simply by multiplying the left-hand-sides of equations (1.25) and (1.27), and equating the result to the product of the right-hand-sides of equations (1.25) and (1.27) as below

$$e^{\Omega s \Delta} \ddot{\underset{\sim}{\xi}}_s \cdot 2 \underset{\sim}{d}_s = e^{\Omega s \Delta} (\dot{\underset{\sim}{\xi}}_s - \dot{\underset{\sim}{\xi}}_{s-1}) \cdot (\dot{\underset{\sim}{\xi}}_s + \dot{\underset{\sim}{\xi}}_{s-1}) \dots (1.28)$$

which is essentially a discrete version of Newton's equation

$2ax = v^2 - u^2$ adapted to our nonconservative system. Now, as $\ddot{\underset{\sim}{\xi}}_s \cong k \ddot{\underset{\sim}{\xi}}_s = k \frac{1}{2}(\underset{\sim}{\xi}_{s+1} + \underset{\sim}{\xi}_{s-1})$ and $2 \underset{\sim}{d}_s = \underset{\sim}{\xi}_{s+1} - \underset{\sim}{\xi}_{s-1}$, equation (1.28) becomes

$$\begin{aligned} & \frac{1}{4} (\sqrt{k} e^{\frac{1}{2} \Omega s \Delta} \underset{\sim}{\xi}_{s+1})^2 - \frac{1}{4} (\sqrt{k} e^{\frac{1}{2} \Omega s \Delta} \underset{\sim}{\xi}_{s-1})^2 \\ &= \frac{1}{2} (e^{\frac{1}{2} \Omega s \Delta} \dot{\underset{\sim}{\xi}}_s)^2 - \frac{1}{2} (e^{\frac{1}{2} \Omega s \Delta} \dot{\underset{\sim}{\xi}}_{s-1})^2 \dots (1.29) \end{aligned}$$

or

$$\frac{1}{2} (\psi_{s+1} - \psi_{s-1}) = T_s - T_{s-1} \dots (1.30)$$

which is just a statement of conservation of energy: any gain in kinetic energy comes from the nonconservative (source) potential ψ (as discussed previously in Sections 1.2 and 1.3). In passing we note that eqs.(1.29) and (1.30) follow from (1.28) because the two $[3 \times 3]$ matrices, k and Ω , are diagonal.

We now define the discrete equivalent of a Lagrangian

$$L_s = T_s - T_{s-1} - \frac{1}{2} (\psi_{s+1} - \psi_{s-1}) \quad \dots (1.31)$$

and sum it over all growth-increments on the trajectory giving

$$\begin{aligned} E &= \sum_{s=1}^n L_s \\ &= T_n - T_{n-1} + T_{n-1} - T_{n-2} + T_{n-2} - T_{n-3} \\ &\quad + \dots + T_2 - T_1 + T_1 - T_0 + \\ &\quad - \frac{1}{2} (\psi_{n+1} - \psi_{n-1} + \psi_n - \psi_{n-2} + \psi_{n-1} - \psi_{n-3} \\ &\quad + \psi_{n-2} - \psi_{n-4} + \psi_{n-3} - \psi_{n-5} + \dots \\ &\quad + \psi_4 - \psi_2 + \psi_3 - \psi_1 + \psi_2 - \psi_0) \\ &= T_n - T_0 - \frac{1}{2} ((\psi_{n+1} + \psi_n) - (\psi_1 + \psi_0)) \\ &\quad \dots (1.32) . \end{aligned}$$

Thus it makes sense to define our dissipative Hookean potential energy term as

$$U_n = \frac{1}{2} (\psi_{n+1} + \psi_n) \cong \psi_n \quad \dots (1.33) .$$

We thus have a conserved quantity

$$T_n - U_n = T_0 - U_0 , \quad \dots (1.34)$$

for any integer n , and

$$U_n \cong \frac{1}{2} (\sqrt{k} e^{\frac{1}{2}\Omega n\Delta} \xi_n)^2 \quad \dots (1.35).$$

Thus the obvious form for a continuous Lagrangian, in the limit as Δ becomes small and n becomes large, is just

$$\begin{aligned} \mathcal{L}(\phi, \xi(\phi), \dot{\xi}(\phi)) \\ = \frac{1}{2} (e^{\frac{1}{2}\Omega\phi} \dot{\xi})^2 + \frac{1}{2} (\sqrt{k} e^{\frac{1}{2}\Omega\phi} \xi)^2 \end{aligned} \quad \dots (1.36)$$

... a sum of kinetic and (Hookean elastic) potential energies, which can be integrated to give an appropriate "energy" functional

$$\mathcal{E} = \int_0^\gamma \mathcal{L} d\phi \quad \dots (1.37)$$

which needs to be extremised if the seashell growth-trajectories given by eqs.(1.20) and (1.21) are to be energy efficient and "optimal" tensile Hookean "clocksprings". The integration in eq.(1.37) is analogous to the summation in eq.(1.32) and both processes give a quantity related to total energy expent in the growth process. We can easily show that the clockspring trajectories extremise our energy functional by checking that

our Lagrangian satisfies the Euler equations

$$\frac{\partial \mathcal{L}}{\partial \xi_j} - \frac{d}{d\phi} \left(\frac{\partial \mathcal{L}}{\partial \dot{\xi}_j} \right) = 0 \quad \dots (1.38)$$

for $j = 1, 2, 3$ and $\xi(\phi) = (\xi_1(\phi), \xi_2(\phi), \xi_3(\phi))$. Substituting eq.(1.36) into (1.38) yields the differential equation (1.21), verifying that our Lagrangian and Euler equations are indeed compatible, and that we do have an optimisation problem to which clockspring trajectories are optimal energy-efficient solutions.

ADVANCED TOPIC:

Of course (1.36) is not the only Lagrangian satisfying (1.38) to give the "clockspring" Euler equations (1.21) hence (2.50). Santilli²⁹ cites another interesting possibility:

$$\mathcal{L}_j = \left(\frac{2 \dot{\xi}_j + \omega_j \xi_j}{2i \sigma_j \xi_j} \right) \operatorname{atn} \left(\frac{2 \dot{\xi}_j + \omega_j \xi_j}{2i \sigma_j \xi_j} \right) - \frac{1}{2} \ln(\dot{\xi}_j^2 + \omega_j \xi_j \dot{\xi}_j + \omega_j^2 \xi_j^2)$$

where $\sigma_1 = \alpha + \frac{1}{2} \omega_1 + i$, $\sigma_2 = \alpha + \frac{1}{2} \omega_2 - i$, $\sigma_3 = \alpha + \frac{1}{2} \omega_3$, such that $\omega_3 = \mu$ and $\omega_1 = \omega_2 = \lambda$, for the scalar constants α , λ and μ as defined in equations (2.46) and (2.47). More concisely, we have the simple relationship between all these constants

$$\sigma_j = \sqrt{k_j + \frac{1}{4} \omega_j^2}, \quad \text{where } j = 1, 2, 3$$

for the eigenvalues k_j as defined in equation (2.48).

Because of the arctan function, it is possible that this new Lagrangian is multiply acausal (in a sense touched upon in Section 3.2) and therefore suited to the description of repeatedly-branching, multiple clockspring complexes such as Yoichiro Kawaguchi's "corals" and "plants" (as shown in color plates F, G and H). If so, then such Lagrangians may assist our understanding of the onset of "chaos" in relatively "self-similar" branching systems. For now, the best we can do is to describe the onset of "chaos" in nonbranching systems as in Cases 5, 6 and 7 of Section 3.1.

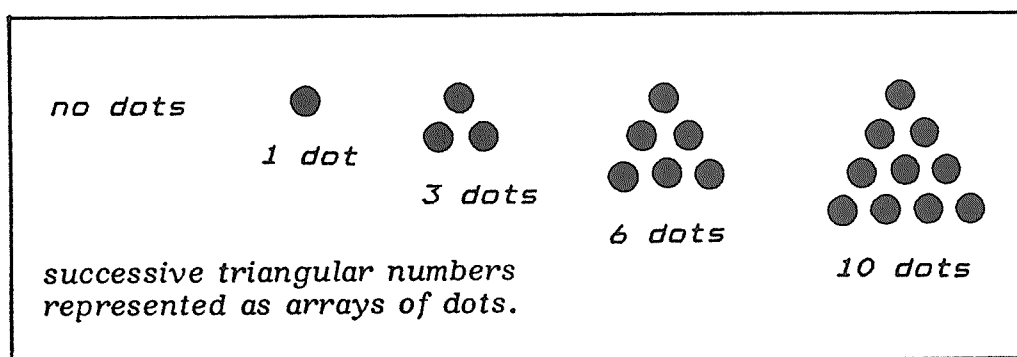
2

GNOMONS, SCALE-INVARIANCE & SELF-SIMILARITY

2.1 TRIANGULAR-NUMBER GNOMONS

Mathematicians in ancient Greece, and probably also Egypt, were familiar with the concept of self-similarity. Aristotle wrote that *"there are certain things which suffer no alteration (except in magnitude) when they grow"* (Categ. 14, 15a, 30).

As an example consider triangular arrays made respectively from 0, 1, 3, 6, 10, 15, ... dots as below.



We see that these "triangular numbers" differ respectively by the "natural numbers" (real integers 1, 2, 3, 4, ...): i.e.

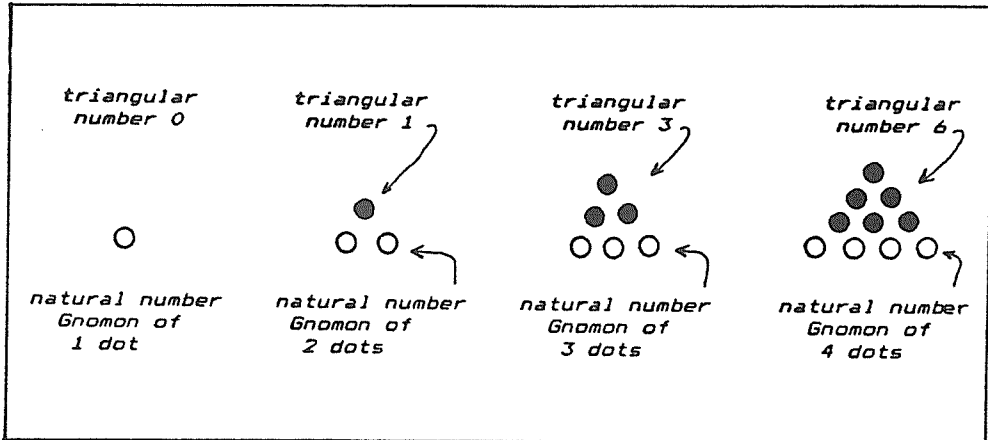
$$1 - 0 = 1, \quad 3 - 1 = 2, \quad 6 - 3 = 3,$$

$$10 - 6 = 4, \quad 15 - 10 = 5, \text{ etc.}$$

... (2.1)

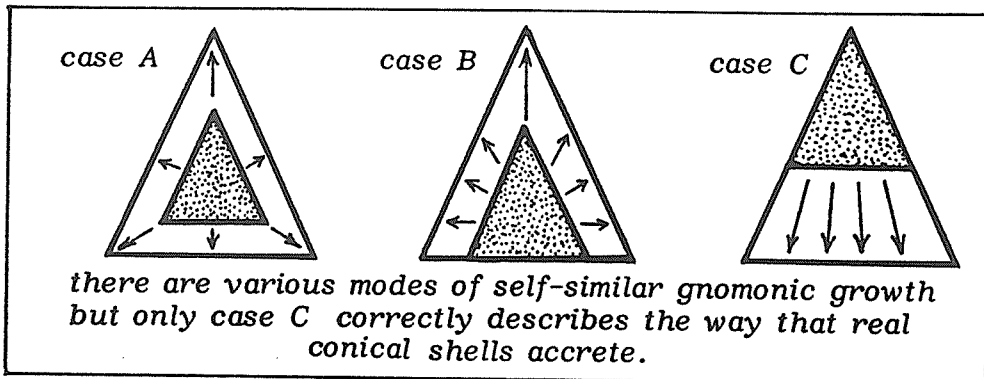
Thus if we adopt Aristotle's definition of a GNOMON as *"any figure which, being added to any figure whatsoever, leaves the resultant figure similar to the original"*, then the natural numbers clearly serve as gnomons to our triangular numbers.

This can be visualised if we denote triangular-number elements by black dots, and natural number elements by white dots, as below.



2.2 TRIANGLE AND CONE GNOMONS

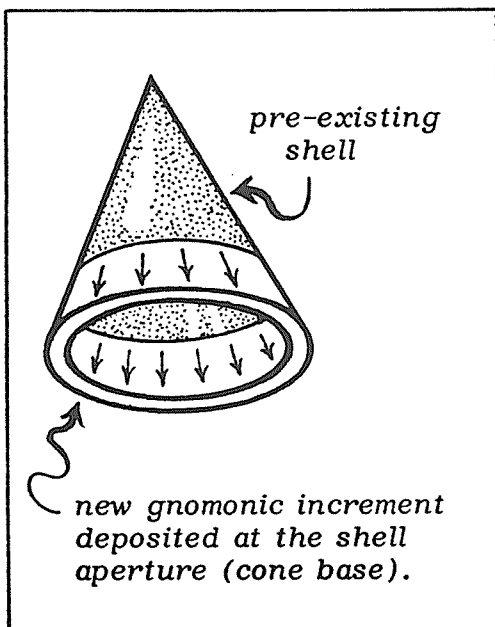
We can extend the concept of gnomons from arrays of dots to rectilinear figures such as the triangle, or even a triangle of revolution (a cone), either of which may enlarge self-similarly through addition of variously shaped gnomons.



The inner stippled triangle (or triangular section) might enlarge equally all round (as in case A), or by increments on

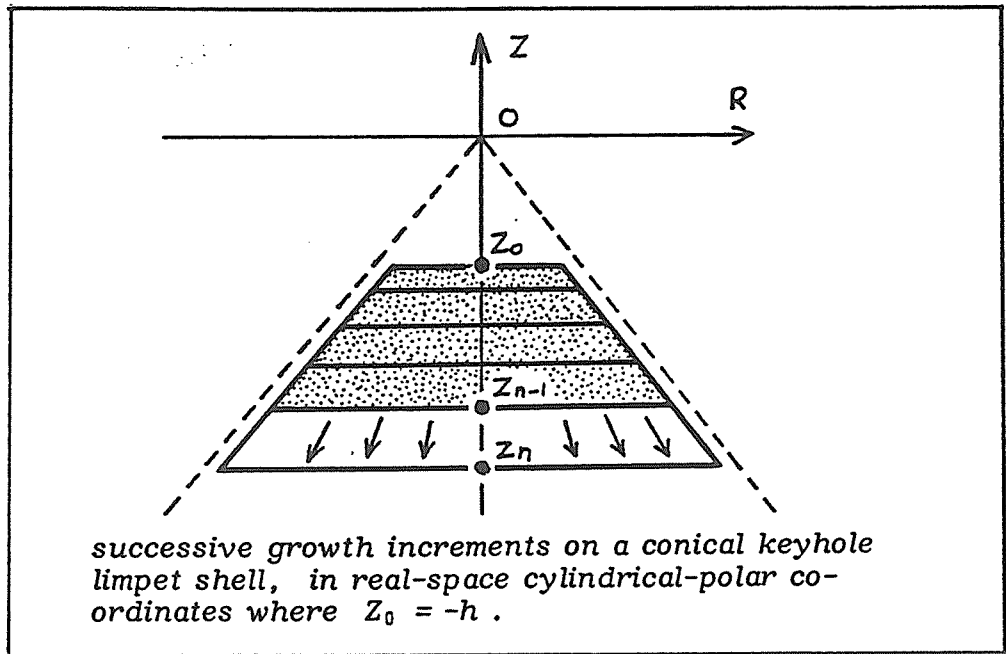
just two sides (as in case B), or by incrementation at the base only (as in case C).

But at least as early as 1709 *Réne Réamur* knew that biological shell material, once formed, remains in being, thereafter incapable of significant change (some sort of bound is placed upon our definition of "significant" change in Section 2.6 when we discuss the Japanese Star Shell). Thus molluscan shells enlarge NOT by growth or magnification in all parts and directions simultaneously (as with the case A triangle, discussed previously) but, instead, at one end only (the base of the conical tube, also



called the shell aperture) through accretion of gnomonic ring-like increments, each similar to its predecessor, so that the whole shell, after every spurt of growth, is still just like what existed before. In this way conical limpet shells grow in size without changing their overall shape: as *Thompson* observed, a juvenile viewed through a magnifying lens is identical to the adult form.

Of course this is not completely true. Some "Keyhole Limpets" have a hole at the cone apex; other limpets coil and develop slits in their adult shells; other molluscs redissolve existing shell material in order to create new shell-growth.



EXAMPLE: axial growth

Consider a conical keyhole limpet shell in real-space cylindrical polar coordinates (R, Z) , as above, such that successive apertural gnomons throughout growth are simple similar rings centred on but perpendicular to the Z -axis;

$$Z_n = C_{n-1} Z_{n-1} = C_{n-1} C_{n-2} \dots C_2 C_1 C_0 Z_0 \dots (2.2)$$

for constants C_j where $j = 0, 1, 2, \dots, n-1$. If all the constants were different, or any were unknown, then eq.(2.2) would not be very usefull. But, fortunately, the Reverend Henry Moseley⁹ in 1838 found that

"to each particular species of [self-similarly growing] shell is annexed a characteristic number, being the ratio of the geometric progression of similar successive linear dimensions".

What this means is that the constants are all approximately the same; i.e.

$$\frac{Z_n}{Z_{n-1}} = C = \text{the same constant for all } n \quad \dots (2.3).$$

Furthermore Moseley's precise "admeasurements" established that gnomons, on self-similarly growing shells, increase in size exponentially. So it makes sense to redefine C in terms of two other constants (α related to the exponential growth-rate, and Δ related to the relative gnomon width) such that

$$C \equiv e^{\ln(C)} = e^{\alpha \Delta} \quad \dots (2.4).$$

Thus eq.(2.2) becomes

$$Z_n = C^n Z_0 = Z_0 e^{\alpha n \Delta} \quad \dots (2.5).$$

On most real-world biological shells there are a large number of growth-increments (n tends to 'infinity'), each of which is very thin (Δ tends to 'zero'), so it is sensible to replace the discrete quantity $n \Delta$ by a continuous variable ϕ (which is a measure of the passage of time, arclength, or angle grown-through), and to introduce a continuous function $Z(\phi)$ such that $Z(0) = -h$ and $Z(n \Delta) = Z_n$. Thus eq.(2.5) becomes

$$Z(\phi) = Z(0) e^{\alpha \phi} = -h e^{\alpha \phi} \quad \dots (2.6).$$

This equation describes the growth ('time-evolution') of the shell's apertural 'generating curve', downward, along the axis of symmetry, as successive gnomons are added.

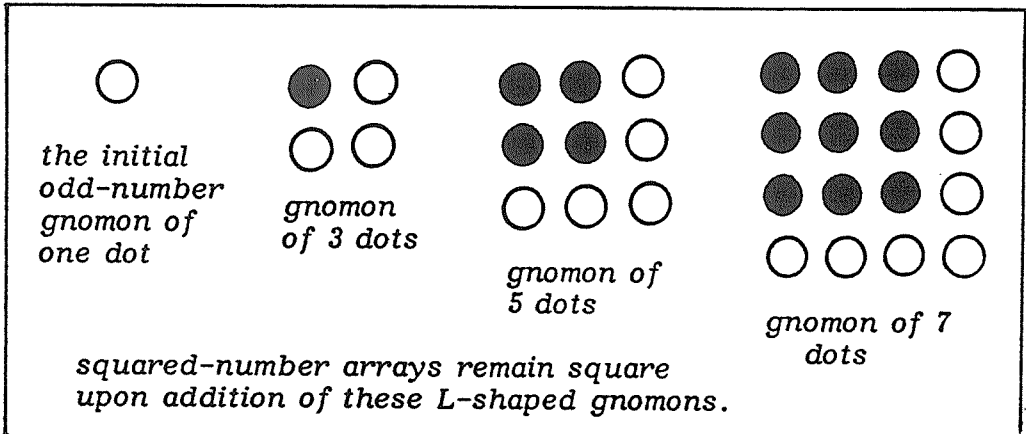
2.3 RECTANGULAR GNOMONS

Just as "triangular-numbers" have natural-numbers for their gnomons, likewise do "squared-numbers" n^2 have successive odd-numbers for their gnomons:

i.e. $0^2 + 1 = 1^2$, $1^2 + 3 = 2^2$, $2^2 + 5 = 3^2$,

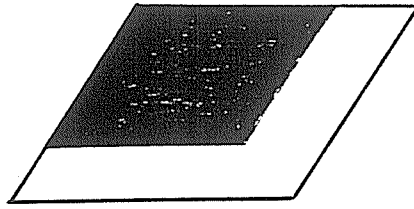
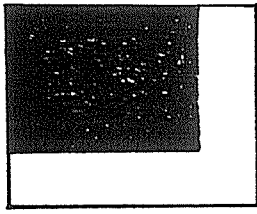
$3^2 + 7 = 4^2$, etc. ... (2.7).

This gnomonic relationship may be represented with L-shaped arrays of dots, whose addition to pre-existing square-arrays yields new larger arrays that are also square. Denoting the squared-number array elements by black dots, and gnomonic odd-number array elements by white dots, eqs.(2.7) become:



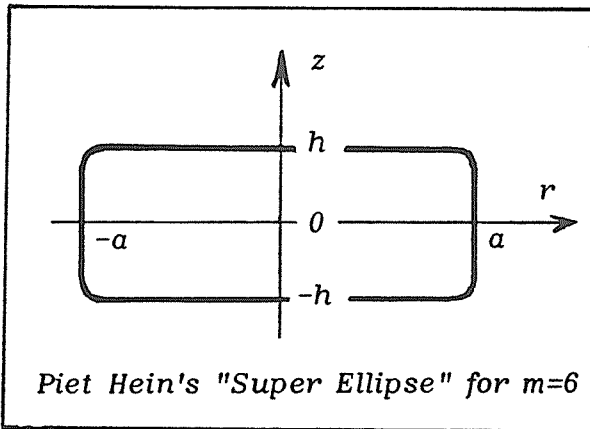
More generally, as Aristotle knew, rectilinear figures such as squares and parallelograms also retain their shapes upon addition of appropriately shaped gnomons (see figure over page).

NOTE: for further discussion see Sir D'Arcy Wentworth Thompson's classic book "On Growth & Form" ¹¹.



quadrilateral figures may increase, through addition of L-shaped gnomons, whilst preserving their original forms.

EXAMPLE: radial growth in the "fingernail" shell (Solen)

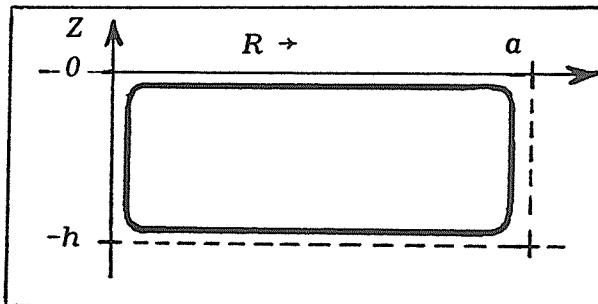


In the September 1965 "Scientific American", Piet Hein gave his famous "Super Ellipse" equation

$$\left(\frac{r}{a}\right)^m + \left(\frac{z}{h}\right)^m = 1 \quad \dots (2.8),$$

which describes various figures that are symmetrical about the origin and can be made as "square" as one likes merely by selecting the constant m to be a sufficiently large positive integer.

A simple coordinate transformation, from (r, z) to (R, Z) , gives

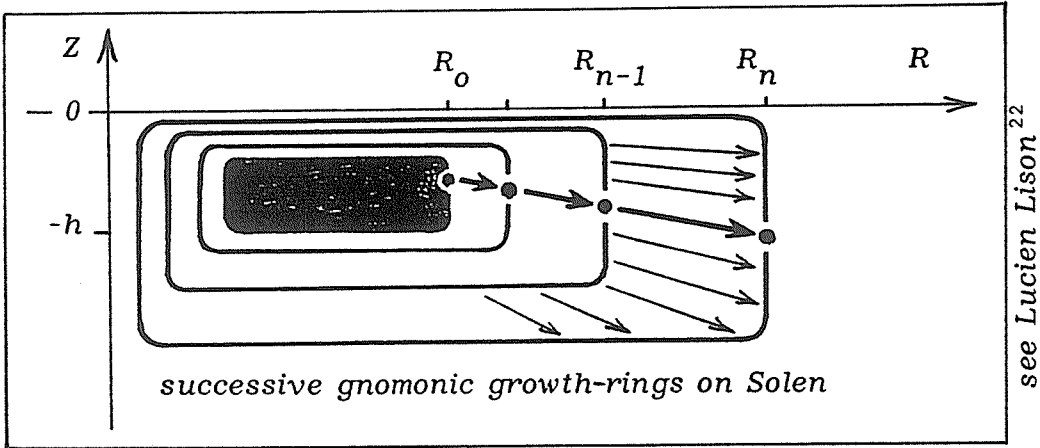


$$\left(\frac{2R - a}{a}\right)^m + \left(\frac{2Z + h}{-h}\right)^m = 1 \quad \dots (2.9).$$

This is the same curve as above, simply relocated to

the fourth quadrant, below the R -axis, such that $0 < R < a$ and $-h < Z < 0$. A simple rearrangement of eq.(2.9) gives a suitable equation that can be used to simulate the growth of the "fingernail" shell (Solen):

$$Z = -\frac{1}{2} h \left(1 - \left(\frac{2R - a}{a} \right)^m \right)^{1/m} - \frac{1}{2} h \quad \dots (2.10).$$



Just like the "squared-numbers" discussed previously, or like Aristotle's squares and parallelograms, the shell Solen also grows by accretion of L-shaped gnomons. If we use the Super Ellipse described by eq.(2.10), with $m = 6$, as the generating figure, then any point on its leading (rightmost) edge undergoes a succession of radial expansions throughout the course of shell-growth, such that

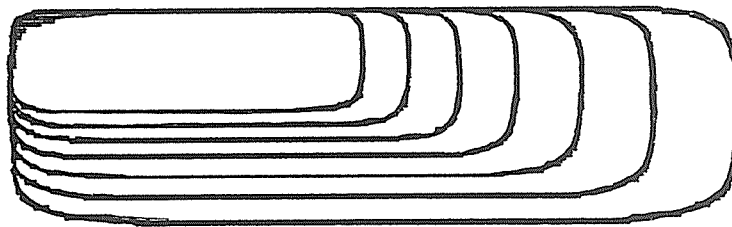
$$R_n = e^{\alpha \Delta} R_{n-1} = R_0 e^{\alpha n \Delta} \quad \dots (2.11).$$

If there are a large number of growth increments ($n \rightarrow \infty$), each very thin ($\Delta \rightarrow 0$), then we may again replace the discrete quantity $n \Delta$ with the continuous (time) variable ϕ to obtain a con-

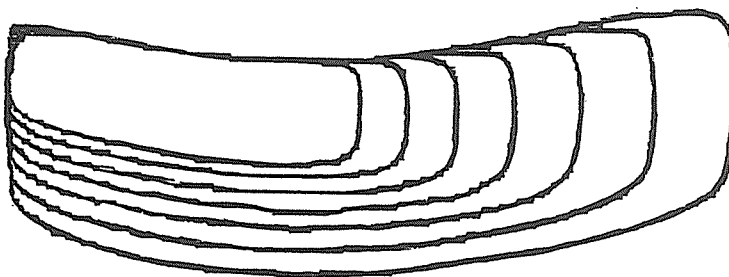
tinuous radial ("time-evolution") function $R(\phi)$, such that $R(n\Delta) = R_n$ and $R(0) = a$:

$$R(\phi) = a e^{\alpha\phi} \quad \dots (2.12).$$

This equation describes the "time-evolution" of an apertural point, in the radial direction. Compare it with equ.(2.6). We can think of the Super-Elliptical "generating-curve" as being made from many such points, each of which obeys eqs.(2.6) and (2.12). A typical computer program for drawing these various growth-stages is given over the page.



Solen marginatus (Pennant, 1777).
(generated with the computer
program given at the top of page 36)



Ensis ensis (Linne, 1758).
(generated with the computer program
on page 36, plus the extra lines of
code).

the "fingernail" shell SOLEN

```
10 Rmin = -0.5
20 Rmax = 16
30 Zmin = -10
40 Zmax = 0.5
50 a = 15
60 h = 4
70 m = 6
80 α = 0.6

100 FOR φ = -2 TO -0.6 STEP 0.2
110   FOR g = -1 TO 1 STEP 2
120     FOR R = 0 TO a STEP a/100
130       Z = -g*0.5*h*(1-((2*R-a)/a)↑m)+(1/m)-0.5*h
140       R1 = EXP(α*φ)*R
150       Z1 = EXP(α*φ)*Z
160       GOSUB 500
170       Z0 = z1
180       R0 = R1
190     NEXT R
200   NEXT g
210 NEXT φ
220 END

500 REM plot subroutine
510 R1 = (R1-Rmin)/(Rmax-Rmin)*600
520 Z1 = (Z1-Zmin)/(Zmax-Zmin)*180
530 Z1 = 180-Z1
540 IF NOT R = 0 THEN
550   LINE (R0,Z0)-(R1,Z1)
560 END IF
570 RETURN
```

Additional program lines for the optional ENSIS modification:

```
155 GOSUB 300
...
300 REM the D'Arcy Thompson grid transformation
310 π = 3.1418
320 q = 0.5*SIN(2*π*R1/a)
330 z1 = z1-q
340 RETURN
```


This simple BASIC program runs on an Amiga 500 computer with a Commodore 1081 color monitor. With minor changes it would also run on a Macintosh except that, last time we looked into the matter, the Apple version of BASIC was inferior: for one thing, it lacked an END IF statement, forcing the programmer to compress large quantities of logic on single lines. We have therefore used the more powerful Amiga version.

The program uses Piet Hein's Super-Ellipse, as given by our equation (2.10) [see line 130 in the program] with major diameter $a = 15$ and minor diameter $h = 4$ and exponent $m = 6$ [see lines 50, 60 & 70]. The horizontal R-axis is scaled to range between $-\frac{1}{2}$ and 16 [lines 10, 20] whilst the vertical Z-axis ranges between -10 and $\frac{1}{2}$ [lines 30, 40]. The R-loop [lines 120 to 190] uses our eq. (2.10) to plot the top half of the Super-Ellipse then, when g changes sign [loop lines 110-200], the R-loop [lines 120-190] is called upon again - this time to plot the bottom half of the Super-Ellipse: note the presence of g in line 130. The GOSUB statement [line 160] simply accesses the PLOT subroutine [lines 500-570]. Line 510 simply scales values of R so they fit upon the T.V. screen which is (on the Amiga 500 computer) 600 pixels wide. Line 520 likewise scales values of Z so they fit on a screen 180 pixels high. Because the T.V. screen has its origin in the top left-hand corner, plotting vertical values downward, hence upside-down, line 530 inverts the Z axis ready for plotting. In order to join two points $(R0, Z0)$ and $(R1, Z1)$ with a straight-line segment [line 550], we must first actually have two-such points: so line 540 checks that this is so. If it is, it draws a line, if not it returns immediately to the R-loop to generate another point. The end result of all the inner loop [lines 110-200] is a single, complete, Super-Ellipse. But a time factor is introduced by the outer ϕ -loop [lines 100 and 210] and our equations (2.6) and (2.12) which appear respectively in lines 140 and 150. Each time, as ϕ increases in increments of 0.2, from -2 to -0.6, the ϕ -loop generates a new growth-ring. After this process has run its course we end up with a succession of Super-Ellipsoidal growth-rings as an approximation to the "continuous" surface of the "Fingernail" shell (Solen). Each new ring adds gnomonically to the pre-existing surface closely mimicing the way that real shells grow.

2.4 CRESCENTIC GNOMONS

It may have become evident, from the example of the "Finger-nail" shell that points about the aperture of a self-similarly accreting shell, expand exponentially and in proportion in both *axial* and *radial* directions simultaneously, such that

$$\frac{Z_n}{R_n} = \frac{Z_{n-1}}{R_{n-1}} = \dots = \frac{Z_o}{R_o} = \frac{\pm h}{a} \quad \dots (2.13)$$

hence the continuous relationships

$$\frac{Z(\phi)}{\pm h} = \frac{R(\phi)}{a} = e^{\alpha \phi} \quad \dots (2.14)$$

which follow also from equs.(2.6) and (2.12). Thus the growth-trajectory of any single point of the apertural generating curve, within the (R, Z) plane, may be written in vector notation as

$$\begin{pmatrix} R_n \\ Z_n \end{pmatrix} = e^{\alpha n \Delta} \begin{pmatrix} R_o \\ Z_o \end{pmatrix} \quad \dots (2.15)$$

which, in continuous notation, becomes

$$\underbrace{\begin{pmatrix} R(\phi) \\ Z(\phi) \end{pmatrix}}_{\text{a trajectory in space as } \phi \text{ varies}} = e^{\alpha \phi} \underbrace{\begin{pmatrix} R(0) \\ Z(0) \end{pmatrix}}_{\substack{\text{its} \\ \text{time} \\ \text{development}}} = e^{\alpha \phi} \underbrace{\begin{pmatrix} a \\ -h \end{pmatrix}}_{\text{a single data point}} \quad \dots (2.16).$$

As ϕ increases the point moves away from the origin, finding itself on successive, different, increasingly larger growth-rings. And a generating curve is made of many such points. Previously we used an equation (2.10) to generate points round the circumference of a Super-Elliptical generating curve. But, more often than not, the generating curve is not given by a simple equation and it is best to select ("digitize") a suitable number of discrete points $P_\theta \in \{(R_\theta, Z_\theta) : \theta = 1, 2, 3, \dots\}$ from about the perimeter of an actual shell aperture, and join them together with straight-line segments. As successive gnomons accrete, during self-similar shell growth, the trajectories of all these points are given by a generalisation of (2.16):

$$\begin{pmatrix} R_\theta(\phi) \\ Z_\theta(\phi) \end{pmatrix} = e^{\alpha\phi} \begin{pmatrix} R_\theta(0) \\ Z_\theta(0) \end{pmatrix} \quad \dots (2.17)$$

or, in the limit when we select so many points about the shell's aperture that θ becomes a "continuous" variable, we can write the continuous surface equation

$$\underbrace{\begin{pmatrix} R(\theta, \phi) \\ Z(\theta, \phi) \end{pmatrix}}_{\text{the resulting surface}} = e^{\alpha\phi} \underbrace{\begin{pmatrix} R(\theta, 0) \\ Z(\theta, 0) \end{pmatrix}}_{\text{initial apertural generating curve}} \quad \dots (2.18)$$

\uparrow
 time
 development

In this equation, θ is some measure of arclength round the shells apertural generating-curve, whilst ϕ is a measure of the passage of time throughout the growth process.

It must be emphasised that eq.(2.16) defines a curve , generated by moving a point through space, in terms of a vector valued function of a single time-related variable ϕ . On the other hand, eq.(2.18) defines a surface , generated by a curve expanding or moving through space, in terms of a vector-valued function of two variables θ and ϕ . A solid volume would likewise be generated by moving a surface through space, and one would need a vector-valued function of three variables θ , ϕ and γ to describe it.

EXAMPLE: *a flat Scallop shell from a digitized generating-curve*

To adequately describe the growing edge of a flat Scallop shell (i.e. its "generating-curve") we need to place it on a sheet of graph paper and digitize about 100 points. If the shell is symmetrical about the R-axis, however, we can halve this number by digitizing only the bottom half (in the present case we used 46 points) then reflecting these same data points through the R-axis to generate the top half of the generating curve. In our program (OPPOSITE) the 46 data points $R_1, Z_1, R_2, Z_2, \dots, R_{45}, Z_{45}, R_{46}, Z_{46}$ are stored in DATA statements [lines 700 to 790]. The horizontal R-axis and vertical Z-axis respectively have their lengths defined in lines 10 to 40. The bottom half of the generating curve is drawn [lines 80 to 150] then RESTORED [line 160] ready for use again, when g changes [lines 70 and 170], to draw the top half of the generating curve. The lines 70 to 170 draw a single, complete, generating curve for any fixed value of ϕ specified by the outer loop [lines 60 to 190]. A second RESTORE statement is needed [line 180] each time the data is to be re-used to draw a totally new growth ring. The vector equation (2.17) is used in lines 100 and 110. The screen scaling and other features in the plot-function are the same as in our previous program. The only really new feature is the READ statement [line 90] and the DATA statements [lines 700 to 790].

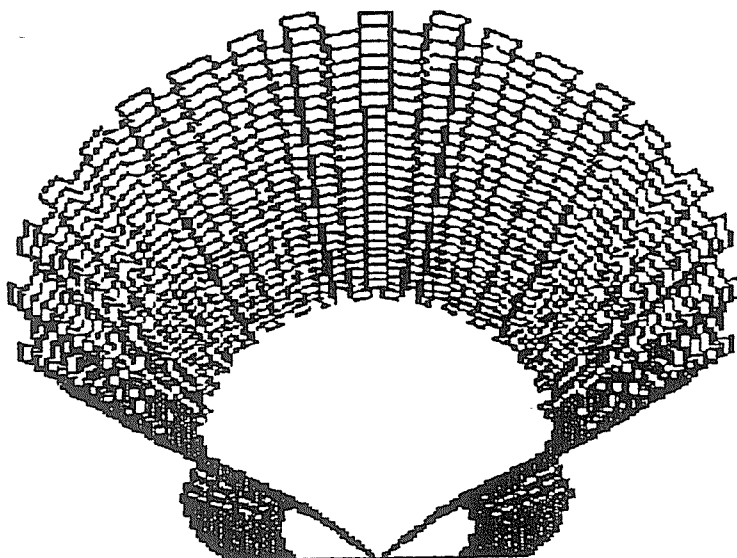
a flat SCALLOP shell

```
10 Rmin = -5
20 Rmax = 15
30 Zmin = -6
40 Zmax = 6
50  $\alpha$  = 0.9

60 FOR  $\phi$  = -0.8 TO 0 STEP 0.03
70   FOR g = -1 TO 1 STEP 2
80     FOR  $\theta$  = 1 TO 48
90       READ R, Z
100      R = EXP( $\alpha*\phi$ )*R
110      Z = EXP( $\alpha*\phi$ )*Z*g
120      GOSUB 500
130      Z0 = Z
140      R0 = R
150    NEXT  $\theta$ 
160  RESTORE
170 NEXT g
180 RESTORE
190 NEXT  $\phi$ 
200 END

500 REM plot subroutine
510 R = (R-Rmin)/(Rmax-Rmin)*600
520 Z = (Z-Zmin)/(Zmax-Zmin)*180
530 Z = 180-Z
540 IF NOT  $\theta$  = 1 THEN
550   LINE (R0,Z0)-(R,Z)
560 END IF
570 RETURN

700 DATA 1.7,-2.3,0.9,-1,0.3,-0.4,0,0,0,-2,0.4,-2.4
710 DATA 1,-2.6,1.7,-2.3,2.6,-4,3.1,-4.4,3.2,-4.7
720 DATA 3.45,-4.7,3.4,-4.5,4,-4.6,4.1,-4.8,4.4
730 DATA -4.8,4.3,-4.6,4.8,-4.4,4.9,-4.7,5.4,-4.6
740 DATA 5.3,-4.4,5.6,-4.2,5.8,-4.4,6.1,-4.2,6,-4
750 DATA 6.4,-3.8,6.5,-3.9,6.9,-3.6,6.8,-3.5,7,-3.2
760 DATA 7.2,-3.4,7.5,-3,7.3,-2.9,7.5,-2.5,7.7,-2.7
770 DATA 8,-2.2,7.8,-2.1,8,-1.8,8.2,-1.9,8.4,-1.5
780 DATA 8.1,-1.4,8.2,-1.1,8.6,-1.2,8.7,-0.8,8.3
790 DATA -0.6,8.4,-0.2,8.7,-0.2,8.7,0
```



a flat Scallop shell generated from a digitized generating-curve, of 92 data-points, using the program on page 41.

If our cylindrical-polar coordinates (R, Z) happen to coincide with the (x, z) plane in a three-dimensional Cartesian system, the surface equation becomes

$$\begin{pmatrix} x(\theta, \phi) \\ y(\theta, \phi) \\ z(\theta, \phi) \end{pmatrix} = \begin{pmatrix} R(\theta, \phi) \\ 0 \\ Z(\theta, \phi) \end{pmatrix} = e^{\alpha\phi} \begin{pmatrix} R(\theta, 0) \\ 0 \\ Z(\theta, 0) \end{pmatrix} = e^{\alpha\phi} \begin{pmatrix} x(\theta, 0) \\ y(\theta, 0) \\ z(\theta, 0) \end{pmatrix} \quad \dots (2.19)$$

which may be written more concisely in Cartesian coordinates as

$$\underbrace{\underline{r}(\theta, \phi)}_{\text{surface}} = e^{\alpha\phi} \underbrace{\underline{r}(\theta, 0)}_{\text{generating curve}} \quad \dots (2.20).$$

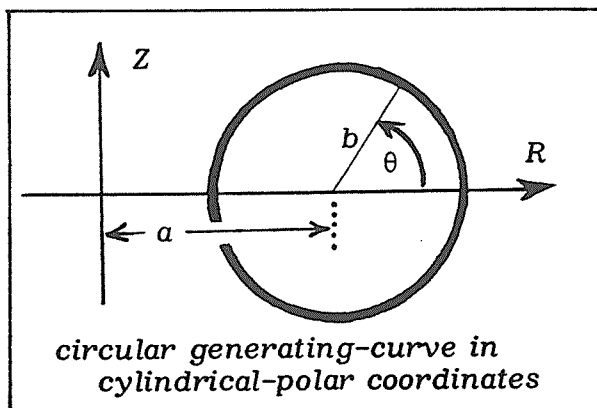
\nearrow
 time development

2.5 SELF-SIMILARITY AND ROTATION ABOUT AN AXIS

So far we have studied two-dimensional, self-similarly-growing surfaces; modelling them with (continuous or digitized) generating curves that expand exponentially in some plane, in accordance with the vector equation (2.20). Both the Scallop and the Fingernail shell were assumed to be completely flat, and even the conical limpets were represented by a flat, vertical, triangular section.

However, few shells in Nature are completely flat; usually at least some rotation occurs about an axis of symmetry which we choose to be the z -axis. Rotation about an axis is another process whereby a simple generating-curve can sweep out a surface in space without changing its shape. We will now consider two examples of *surfaces of revolution*.

EXAMPLE: *a Torus*



Consider a circular generating curve of radius b , and whose centre is displaced a distance a along the R -axis

$$\begin{pmatrix} R(\theta) \\ Z(\theta) \end{pmatrix} = \begin{pmatrix} a \\ 0 \end{pmatrix} + \begin{pmatrix} b \cos \theta \\ b \sin \theta \end{pmatrix}$$

for $\theta \in [0, 2\pi]$... (2.21).

Just as in equations (2.19) and (2.20), we converted cylindrical-polar equations to Cartesian coordinates, we can do the same for eq.(2.21) as follows:

$$\underline{r}(\theta, 0) = \begin{pmatrix} x(\theta, 0) \\ y(\theta, 0) \\ z(\theta, 0) \end{pmatrix} = \begin{pmatrix} R(\theta) \\ 0 \\ Z(\theta) \end{pmatrix} = \begin{pmatrix} a + b \cos \theta \\ 0 \\ b \sin \theta \end{pmatrix} \quad \dots (2.22).$$

If we rotate this generating curve, through an angle ϕ about the z -axis, a surface is swept out in accordance with the general equation

$$\underbrace{\underline{r}(\theta, \phi)}_{\text{toroidal surface}} = \underbrace{\begin{pmatrix} \cos \phi & -\sin \phi & 0 \\ \sin \phi & \cos \phi & 0 \\ 0 & 0 & 1 \end{pmatrix}}_{\text{rotation matrix}} \underbrace{\underline{r}(\theta, 0)}_{\text{generating curve}} \quad \dots (2.23)$$

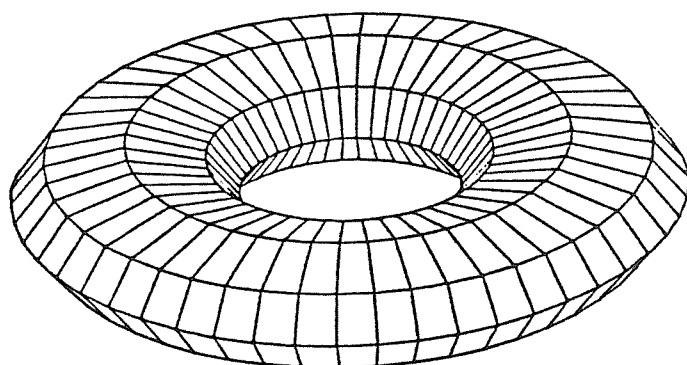
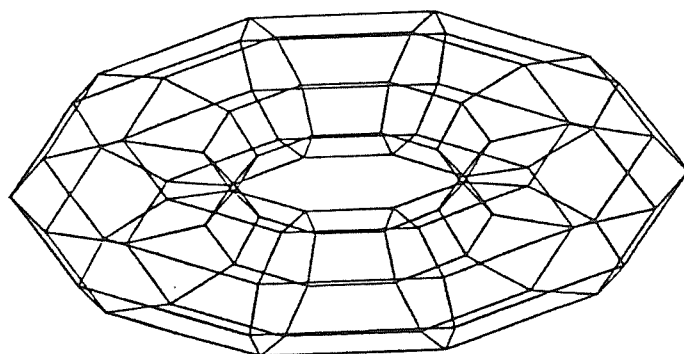
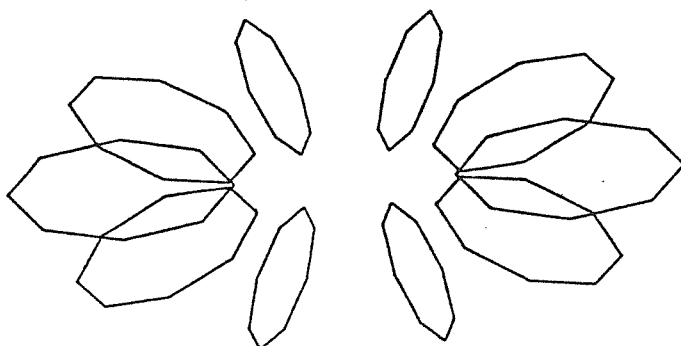
$$\text{i.e.} \quad \begin{pmatrix} x(\theta, \phi) \\ y(\theta, \phi) \\ z(\theta, \phi) \end{pmatrix} = \begin{pmatrix} (a + b \cos \theta) \cos \phi \\ (a + b \cos \theta) \sin \phi \\ b \sin \theta \end{pmatrix} \quad \dots (2.24)$$

for $\theta \in [0, 2\pi]$ and $\phi \in [0, 2\pi]$.

To emphasize the significance of rotation matrices, we will tilt the whole toroidal surface forward (about the x -axis), through an angle β , giving the new surface equation

$$\underline{r}_\beta(\theta, \phi) = \begin{pmatrix} 1 & 0 & 0 \\ 0 & \cos \beta & -\sin \beta \\ 0 & \sin \beta & \cos \beta \end{pmatrix} \begin{pmatrix} \cos \phi & -\sin \phi & 0 \\ \sin \phi & \cos \phi & 0 \\ 0 & 0 & 1 \end{pmatrix} \underline{r}(\theta, 0) \quad \dots (2.25).$$

see the "mazzocchio": Scientific American 247(1): 116-22 (1982)



TORUS generated using the program given on page 46:
see also the color plate A.

```
5  a=1
10 b=0.3
20 Xmin=-1.2*(a+b)
30 Xmax= 1.2*(a+b)
40 Ymin=Xmin
50 Ymax=Xmax
60 Zmin=-3*b
70 Zmax= 3*b
80  $\pi=3.1418$ 
90  $\beta=\pi/6$ 


100 FOR  $\phi=0$  TO  $2*\pi$  STEP  $\pi/20$ 
110   FOR  $\theta=0$  TO  $2.1*\pi$  STEP  $\pi/10$ 
120      $x=(a+b*\cos(\theta))*\cos(\phi)$ 
130      $y=(a+b*\cos(\theta))*\sin(\phi)$ 
140      $z=b*\sin(\theta)$ 
150     GOSUB 300
160     GOSUB 500
170      $x0=x$ 
180      $y0=y$ 
190      $z0=z$ 
200   NEXT  $\theta$ 
210 NEXT  $\phi$ 
220 END

300 REM rotation through angle  $\beta$  about the x-axis
310  $y1=y*\cos(\beta)-z*\sin(\beta)$ 
320  $z1=y*\sin(\beta)+z*\cos(\beta)$ 
330  $y=y1$ 
340  $z=z1$ 
350 RETURN

500 REM plot subroutine
510  $x=(x-Xmin)/(Xmax-Xmin)*600$ 
520  $y=(y-Ymin)/(Ymax-Ymin)*600$ 
530  $z=(z-Zmin)/(Zmax-Zmin)*180$ 
540  $z=180-z$ 
550 IF NOT  $\theta=0$  THEN
560   LINE  $(x0,z0)-(x,z)$ 
570 END IF
580 RETURN
```

◀◀ The computer program (opposite) draws the inclined torus, as given by eq.(2.25). The eqs.(2.24), describing the uninclined toroidal surface, appear as lines 120 to 140 in the program. Line 150 then rotates all points on the toroidal surface through an angle β , about the x -axis, then line 160 plots the points on the screen (joined by straight line-segments) as they are calculated. Again, the way that the θ -loop [lines 110 to 200] is nested inside the ϕ -loop [lines 100 to 210] implies a surface which is generated by rotating a circular generating curve round an axis of symmetry, through an angle ϕ . The step sizes can be made as small as desired, so this computer code defines what we mean by the term "continuous smooth" surface.

EXAMPLE: *Paolo Uccello's Renaissance Chalice*

In generating the toroidal surface, our previous program used a circular generating curve which could be expressed, in eq.(2.22), in terms of simple trigonometrical functions. But, as the previous example of the Scallop shell showed, it is more usefull to generate surfaces from digitized generating curves. *Uccello's Renaissance chalice* drawing can be reproduced by rotating about an axis, a vertical "meridian-line" composed of straight-line segments joining 54 separate data-points (each point (R_θ, Z_θ) corresponding to a different value of θ). These 54 points are stored in DATA statements and respectively called upon by the READ statement within the θ -loop. The points also need to be RESTORED each time the meridian-line is redrawn, in a new position, by the ϕ -loop (see over the page) 

```
1 Rmin=-50
2 Rmax= 50
3 Zmin=-15
4 Zmax= 100
5  $\pi=3.1418$ 
6  $\beta=\pi/6$ 

10 FOR  $\phi=0$  TO  $-\pi$  STEP  $-\pi/30$ 
15   FOR  $\theta=1$  TO 54
20     READ R,Z
25      $x=R*\cos(\phi)$ 
30      $y=R*\sin(\phi)$ 
35     GOSUB 100
40     GOSUB 300
45      $x0=x$ 
50      $y0=y$ 
55      $z0=z$ 
60   NEXT  $\theta$ 
65 RESTORE
70 NEXT  $\phi$ 
75 END

100 REM forward tilting subroutine
105 REM through angle  $\beta$  about the x-axis
110  $y1=y*\cos(\beta)-z*\sin(\beta)$ 
115  $z1=y*\sin(\beta)+z*\cos(\beta)$ 
120  $y=y1$ 
125  $z=z1$ 
130 RETURN

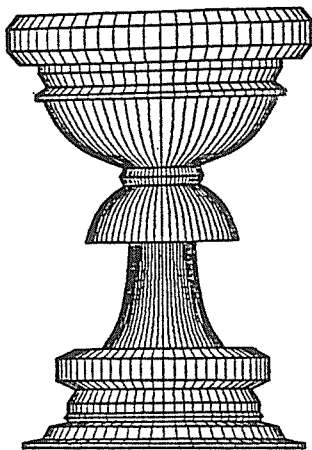
300 REM plot subroutine
305  $x=(x-Rmin)/(Rmax-Rmin)*600$ 
310  $y=(y-Rmin)/(Rmax-Rmin)*600$ 
315  $z=(z-Zmin)/(Zmax-Zmin)*180$ 
320  $z=180-z$ 
325 IF NOT  $\theta=1$  THEN
330   LINE  $(x0,z0)-(x,z)$ 
335 END IF
340 RETURN

500 DATA 37,1,37,2,32,3,30,6,25,7,26,8,25,7,25
505 DATA 11,23,14,28,16,28,21,23,23,18,21,16,23
510 DATA 14.5,25,13,27,12,29,11,31,10.5,33,10,35
```

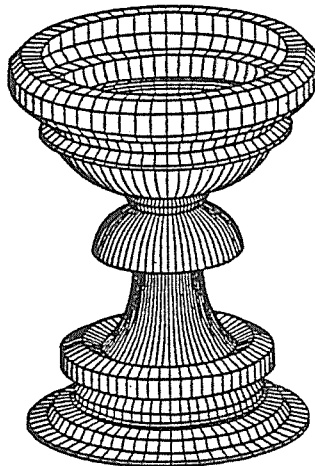
```

515 DATA 9.7,37,9.3,39,9,41,8.8,43,8.8,46,20,46
520 DATA 19.5,48,18.5,50,17.5,52,16,54,14,55.5,12
525 DATA 57,10,58,11,60,10,62,13,63,16,64,19,65
530 DATA 22.5,67,25,69,27,71,28.5,73,30,75,31,77
535 DATA 33,77,33,78,30,80,32,83,32,85,37,85,40,88
540 DATA 40,93,37,96,32,96

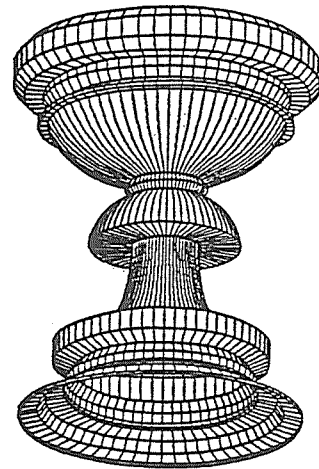
```



$\beta = 0$



$\beta = \pi/6$



$\beta = -\pi/6$

By choosing different values of β in line 6 of the computer program, we can obtain different views of the Renaissance chalice. The tilting subroutine [lines 100 to 130] is responsible for this and it is accessed through line 35. Uccello originally drew his chalice with nothing more than a straight edge and a compass: a monumental feat which we can now mimic with mathematical equations and computers. Other generating curves can be specified in the DATA statements [lines 500 to 540] then this program gives other figures of revolution.

2.6 CONI-SPIRAL GNOMONS IN 3D

We have seen that special surfaces can be generated in 3D from either the *scalar magnification* eq.(2.20), or *rotation* about an axis eq.(2.23), of generating curves which remain self-similar throughout the process. Obviously the next step is to combine both operations together in a more general coordinate transformation equation:

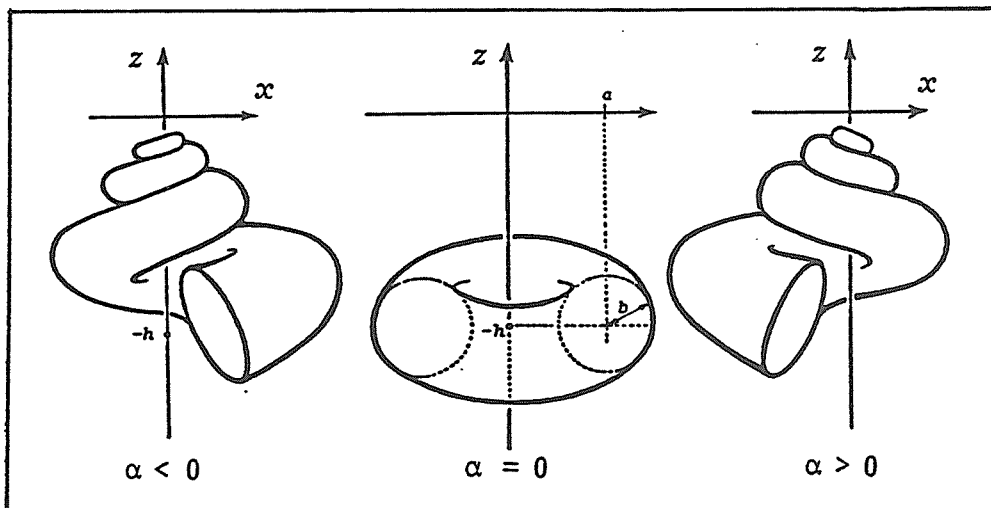
$$\underbrace{\underline{r}(\theta, \phi)}_{\text{surface}} = \underbrace{e^{\alpha\phi}}_{\text{scalar magnification}} \underbrace{\begin{bmatrix} \cos\phi & -\sin\phi & 0 \\ \sin\phi & \cos\phi & 0 \\ 0 & 0 & 1 \end{bmatrix}}_{\text{rotation matrix}} \underbrace{\underline{r}(\theta, 0)}_{\text{generating curve}} \dots (2.26)$$

This vector-transformation should be read from right-to-left: it says that a generating-curve $\underline{r}(\theta, 0)$ is rotated through angle ϕ about the axis of symmetry whilst simultaneously being magnified (equally in all directions) by a scalar factor $e^{\alpha\phi}$. In this way the surface $\underline{r}(\theta, \phi)$ is generated. These are the kinds of surfaces about which Jan Swammerdam, in 1737, wrote

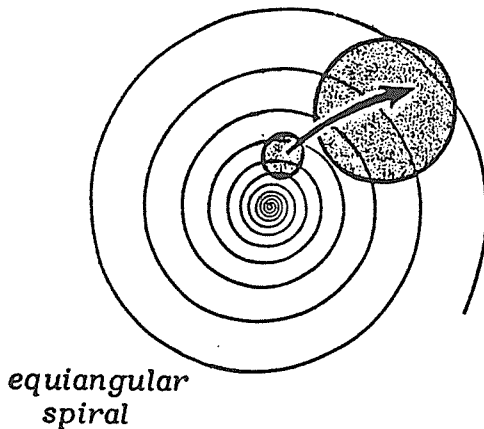
"[a snail shell] must be conceived as a certain oblong, hollow, sharp, and flexible tube, which if rolled and turned round a small iron line or wire, and afterwards this thread or line were drawn away from it, would shew such a perforated pillar [the collumellar umbilicus], which would be the more exact, if those foldings, together with their inclosures, were applied closely to each other, and fastened and united together ... and after this manner are almost all kinds of such little shelly habitations built, in whatever wonderful manner they appear to be turned or constructed."

Thus plani-spiral shells such as the chambered Nautilus have long been viewed as "conical tubes rolled-up into a spiral" in such a fashion that they increase in size without changing their overall form: hence their name "equiangular" spirals. But our transformation eq.(2.26) also applies to conical-spiral, or "turbinate", shellforms as well.

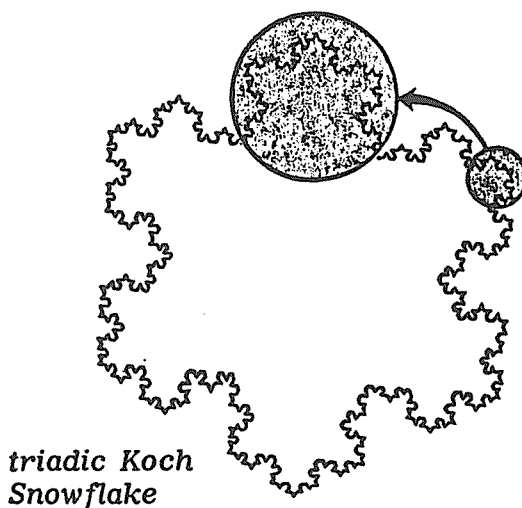
If we delete the rotation matrix from eq.(2.26) it becomes our earlier equation (2.20); alternately if we deleted the exponential scale factor from (2.26) it would become (2.23). Thus the equations (2.20) and (2.23) are, in a sense, limiting cases of each other. Another way to see this is to select different values of α in eq.(2.26): $\alpha = 0$ means that $e^{\alpha\phi} = e^0 = 1$ for all values of the angle ϕ , in which case (2.26) describes figures of revolution as a special case. If $\alpha > 0$ then (2.26) describes dextrally coiled surfaces, and if $\alpha < 0$ they coil sinistrally. Also, if $\alpha \rightarrow \infty$ the exponential scale factor expands so rapidly that it resembles a delta-function, and it accordingly describes conical limpet-like shell forms.



In its own way, eq.(2.26) is the "Lorentz Transformation" in seashell mathematics, summing up a special type of symmetry that determines the form of the Hookean constant matrix in relevant differential equations. The likeness to the Lorentz transformation is strong in other ways too, for (2.26) is a statement that all growth-rings (frames of reference) on the surface are similar and governed by the same equation. It is a statement of self-similarity at all stages of shell growth, and most shells obey this transformation at least to a first approximation.



the equi-angular (logarithmic) spiral $r = e^{\alpha\phi}$ has the remarkable property that we can take any chunk, rotate it through an angle ϕ and magnify it by $e^{\alpha\phi}$, as in equation (2.26), only to find that it exactly maps onto some-other portion of the spiral. As ϕ may be any real value we say this is an example of **CONTINUOUS SELF-SIMILARITY**



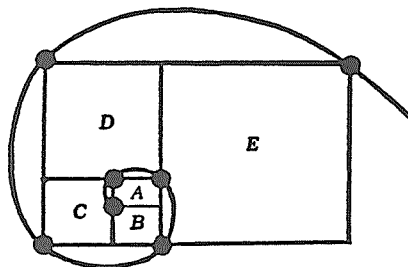
the "triadic snowflake", devised by von Koch in 1904, also obeys a transformation like equation (2.26), but only for discrete angles $\phi = n\Delta$ ($n=1, 2, 3, \dots$), so we need a new transformation (2.27) to capture the essence of this **DISCRETE SELF-SIMILARITY**.

But whereas the Lorentz transformation is a simple "conservative" rotation in space-time, our transformation (2.26) is "dissipative" from the outset because of the exponential scale factor.

Our transformation (2.26) is continuous in the variable ϕ . This means that we can take any "chunk" of an "equiangular" spiral, rotate and magnify it, and it will exactly map onto some other "chunk" elsewhere. But, for some fixed constant Δ , eq.(2.26) can also give the discrete symmetry

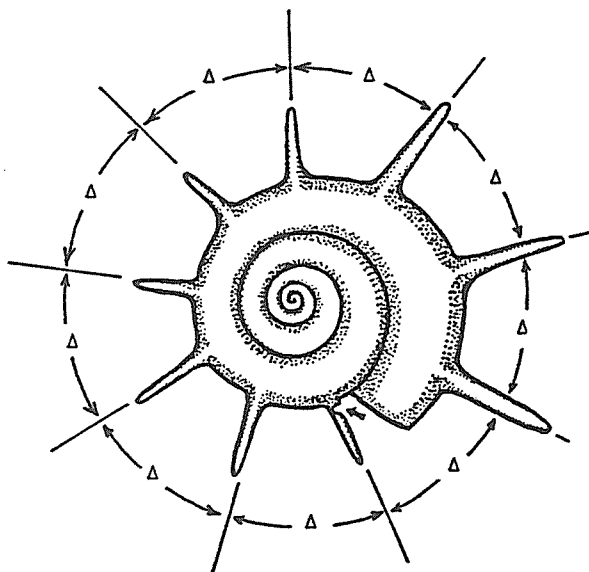
$$\tilde{r}(\theta, \phi + \Delta) = e^{\alpha \Delta} \begin{pmatrix} \cos \Delta, & -\sin \Delta, & 0 \\ \sin \Delta, & \cos \Delta, & 0 \\ 0, & 0, & 1 \end{pmatrix} \tilde{r}(\theta, \phi) \quad \dots (2.27).$$

This discrete symmetry, rather like Bloch's transformation in a crystal lattice, says that some surfaces are made from finite gnomons (each subtending an angle Δ) and that we have to map one gnomon onto another, as a whole. Examples of this occur in Murex shells, Wentletrap shells, frilled cockles and Helmets, to name just a few (see illustrations). Yet this discrete symmetry also applies to certain fractal objects such as the Koch "snowflake", indicating that we are touching a symmetry far deeper than might first have been imagined. Yoichiro Kawaguchi²⁸ has shown that discrete self-similarity can also be a property of repeatedly branching corals, plants such as the cauliflower, and even blood-vessels inside lungs (see color plates F and G). Often, however, self-similarity is disrupted in certain ways and "chaos" subtly modifies branching patterns (see color plate H).



successive chambers in
the pearly NAUTILUS.

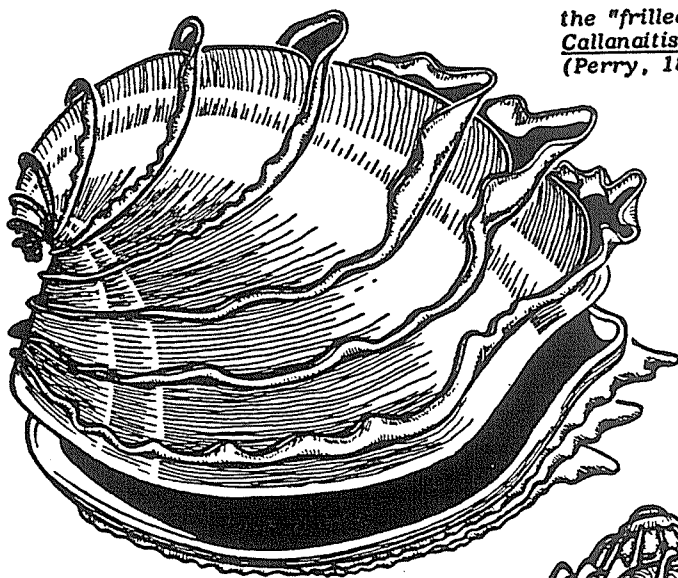
The DISCRETE SELF-SIMILARITY of equiangular spirals, as in eq. (2.27), can easily be demonstrated by starting with a special rectangle, A, whose sides are in the "Golden Proportion" $1:\frac{1}{2}(\sqrt{5}-1)$ or $1:0.618$. Then, choosing as a gnomon the square B, erected upon the original rectangle's larger side, and so on for successive square gnomons C, D, E etc., we can crudely mimic the way that successive internal chambers are added to the equiangular spiral shell of the pearly Nautilus. Interestingly, each gnomon subtends exactly the same angle, Δ , relative to its nearest neighbours on either side. This is more apparent in the Japanese "star shell" (see below) and some other gastropod shell varieties (see opposite page).



$$\Delta = \frac{360^\circ}{9} = 40^\circ$$

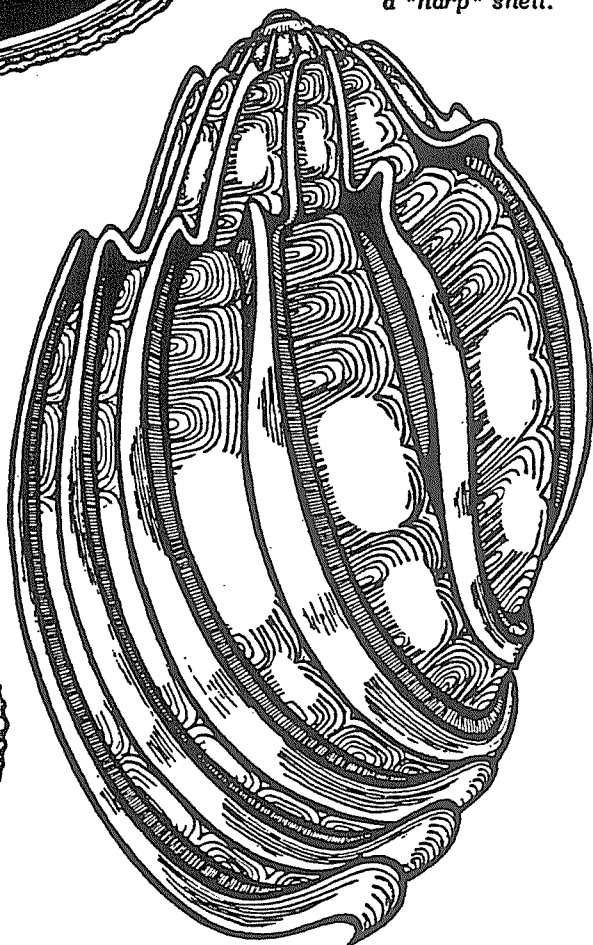
Japanese "star shell"

The Japanese "star shell" Guildfordia yoka (Jousseume) has nine hollow, backward-curving spines round its outer perimeter throughout growth. Each spike subtends the same angle $\Delta = 40^\circ$, relative to its nearest neighbours on either side, showing clearly the significance of the Reinecke angle Δ in eq. (2.27). Note also how the oldest spike, blocking the current shell aperture and obstructing present growth, is being abraided at its base and removed by the mollusc. In this fashion growth may proceed self-similarly again, after the relatively minor modification to existing shell ornamentation.

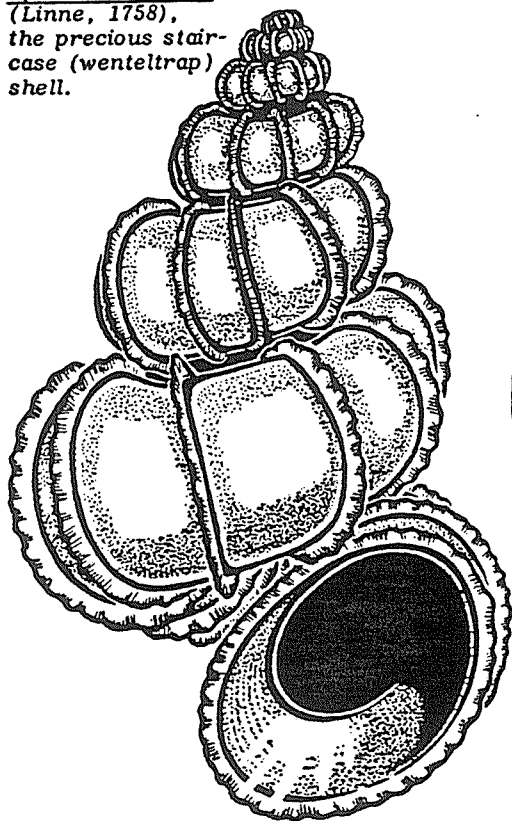


the "frilled cockle"
Callanaitis disjecta
(Perry, 1811).

Harpa articularis
(Lamarck, 1822),
a "harp" shell.



Epitonium scalare
(Linne, 1758),
the precious stair-
case (wenteltrap)
shell.



LEMMA # 4

$$A(\phi) = \begin{pmatrix} \cos \phi, & -\sin \phi, & 0 \\ \sin \phi, & \cos \phi, & 0 \\ 0, & 0, & 1 \end{pmatrix} = e^{\begin{pmatrix} 0, & -1, & 0 \\ 1, & 0, & 0 \\ 0, & 0, & 0 \end{pmatrix} \phi}$$

PROOF:

$$\begin{aligned} A &= \underbrace{\begin{pmatrix} 0, & 0, & 0 \\ 0, & 0, & 0 \\ 0, & 0, & 1 \end{pmatrix}}_B + \underbrace{\begin{pmatrix} 1, & 0, & 0 \\ 0, & 1, & 0 \\ 0, & 0, & 0 \end{pmatrix}}_C \cos \phi + \underbrace{\begin{pmatrix} 0, & -1, & 0 \\ 1, & 0, & 0 \\ 0, & 0, & 0 \end{pmatrix}}_D \sin \phi \\ &= \underbrace{B + C (1 - \phi^2/2! + \phi^4/4! - \dots)}_I + D (\phi - \phi^3/3! + \phi^5/5! - \dots) \\ &= I + D \phi - C \phi^2/2! - D \phi^3/3! + C \phi^4/4! + D \phi^5/5! - \dots \\ &= \sum_{s=0}^{\infty} \begin{pmatrix} 0, & -1, & 0 \\ 1, & 0, & 0 \\ 0, & 0, & 0 \end{pmatrix}^s \phi^s/s! , \quad \text{because } D^2 = -C \end{aligned}$$

which is the power series expansion for the exponential, $e^{D\phi}$, as required.

COROLLARY:

$$e^{\alpha \phi} \begin{pmatrix} \cos \phi, & -\sin \phi, & 0 \\ \sin \phi, & \cos \phi, & 0 \\ 0, & 0, & 1 \end{pmatrix} = e^{\begin{pmatrix} \alpha, & -1, & 0 \\ 1, & \alpha, & 0 \\ 0, & 0, & \alpha \end{pmatrix} \phi} \equiv e^{\zeta \phi}$$

for the constant matrix ζ defined as above.

Using the notation and the substance of the preceding Corollary, eq.(2.26) can now be written in compact exponential notation as

$$\underline{r}(\theta, \phi) = e^{\zeta \phi} \underline{r}(\theta, 0) \quad \dots (2.28)$$

whilst eq.(2.27) likewise becomes

$$\underline{r}(\theta, \phi + \Delta) = e^{\zeta \Delta} \underline{r}(\theta, \phi) \quad \dots (2.29).$$

Equation (2.29) follows trivially from (2.28) because the exponents of multiplied exponentials are additive. Thus it is easier to prove important results using the compact exponential notation as above.

EXAMPLE:

Consider the following three matrices

$$U_z(\beta_1) = \begin{pmatrix} \cos \beta_1, & -\sin \beta_1, & 0 \\ \sin \beta_1, & \cos \beta_1, & 0 \\ 0, & 0, & 1 \end{pmatrix}, \quad U_y(\beta_2) = \begin{pmatrix} \cos \beta_2, & 0, & -\sin \beta_2 \\ 0, & 1, & 0 \\ \sin \beta_2, & 0, & \cos \beta_2 \end{pmatrix},$$

$$\text{and } U_x(\beta_3) = \begin{pmatrix} 1, & 0, & 0 \\ 0, & \cos \beta_3, & -\sin \beta_3 \\ 0, & \sin \beta_3, & \cos \beta_3 \end{pmatrix} \quad \dots (2.30).$$

The first matrix, $U_z(\beta_1)$, represents a rotation through angle β_1 about the z-axis, and such a matrix was first introduced in our eq.(2.23). The matrix $U_y(\beta_2)$ represents a rotation through an angle β_2 about the y-axis. The third matrix $U_x(\beta_3)$ is a rotation through angle β_3 about the x-axis, and such a matrix was previously used in our eq.(2.25).

Consider also the following vectors

$$\tilde{T}_x = \begin{pmatrix} 1 \\ 0 \\ 0 \end{pmatrix}, \quad \tilde{T}_y = \begin{pmatrix} 0 \\ 1 \\ 0 \end{pmatrix} \quad \text{and} \quad \tilde{T}_z = \begin{pmatrix} 0 \\ 0 \\ 1 \end{pmatrix} \quad \dots (2.31).$$

\tilde{T}_x represents a translation through one distance-unit, along the direction of the x-axis. \tilde{T}_y represents a unit-translation along the y-axis. \tilde{T}_z represents a unit-translation along the z-axis.

Now we could, for example, use the generating-curve suggested in eq.(2.22): substituting it into eq.(2.26) would give rise to a plani-spiral (nautilus-like) surface. Alternately we could use a generating curve of the form

$$\begin{aligned} \tilde{r}(\theta, 0) &= a \tilde{T}_x + 0 \tilde{T}_y - h \tilde{T}_z + b \begin{pmatrix} \cos \theta \\ 0 \\ \sin \theta \end{pmatrix} \\ &= \begin{pmatrix} a \\ 0 \\ -h \end{pmatrix} + b \begin{pmatrix} \cos \theta \\ 0 \\ \sin \theta \end{pmatrix} \quad \dots (2.32) \end{aligned}$$

which is a circle of radius b , lying entirely in the x - z plane, whose centre-of-mass has been translated a distance a along the x -axis and a distance $-h$ down the z -axis. Such a generating curve would, when substituted into eq.(2.26), produce a variety of conic-spiral (turbinate) shell forms depending upon the values of the constants a , h and α . Illert (1976) plotted the whole range of these forms in his book "Seashell Mathematics".

Although the generating-curve (2.32) is usefull and simple, few real shells have such curves confined to the vertical plane. Most generating curves are tilted or inclined, relative to the coiling axis, and quite often they are elliptical instead of circular. So a more general generating curve would be elliptical, with major and minor radii respectively b_1 and b_2 , such that the shell tube radius is given by the equation

$$b = b(\theta) = b_1 \cos \theta + b_2 \sin \theta \quad \dots (2.33).$$

Furthermore, in the most general case (see *Illert*¹² 1983 and *Cortie*¹³ 1989), the generating curve might be inclined through angles β_1 , β_2 and β_3 respectively about the z , y and x axes. Thus our generating curve might be of the form

$$\underline{r}(\theta, 0) = \begin{bmatrix} a \\ 0 \\ -h \end{bmatrix} + U_z(\beta_1) U_x(\beta_3) U_y(\beta_2) \begin{bmatrix} b \cos \theta \\ 0 \\ b \sin \theta \end{bmatrix} \quad \dots (2.34).$$

We can substitute in the matrices for the respective rotations, as defined in eq.(2.30), then substitute the resulting generating curve into eq.(2.26) to obtain the final surface-equations:

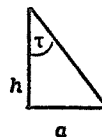
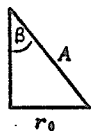
$$\begin{aligned} x(\theta, \phi) &= e^{\alpha \phi} [a \cos \phi + b \cos(\theta + \beta_2) \cos(\phi + \beta_1) \\ &\quad + b \sin(\beta_3) \sin(\theta + \beta_2) \sin(\beta_1 + \phi)] , \\ y(\theta, \phi) &= e^{\alpha \phi} [a \sin \phi + b \cos(\theta + \beta_2) \sin(\phi + \beta_1) \\ &\quad - b \sin(\beta_3) \sin(\theta + \beta_2) \cos(\phi + \beta_1)] , \\ z(\theta, \phi) &= e^{\alpha \phi} [-h + b \sin(\theta + \beta_2) \cos(\beta_3)] \quad \dots (2.35). \end{aligned}$$

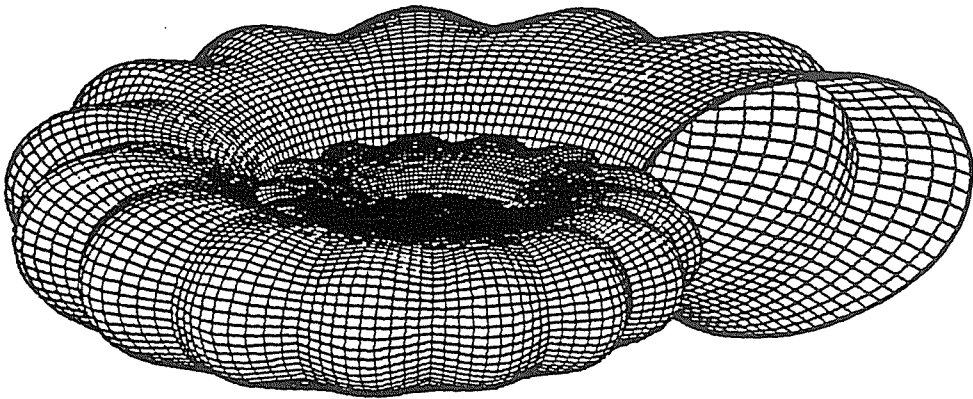
In 1983 Illert¹² suggested variously inclining the shell generating curve (through two main angles β_3 and β_1) as in eq.(2.34):

"... the generating curve ... has been inclined about an axis parallel to the x-axis. It could also have been tilted about an axis parallel to the z-axis, in which case a slightly different rotation matrix would be needed ...".

By 1989 Mike Cortie¹³ had introduced a third mode of inclination, through angle β_2 , and used the most generally oriented generating curve (2.34) to successfully model a variety of real-world shells such as those following on pages 61 to 64 and on page 20. Of course, working in isolation, Cortie developed a nonstandard notation but his equations are equivalent to those already given here (see the below conversion table), relying on the substitution of the generating curve (2.34), into (2.26), to give the general surface equations (2.35). The knobs and corrugations are produced on the following simulations through defining special tube-radius functions, $b = b(\theta, \phi)$ a little more complicated than (2.33), and substituting them into (2.35). The resulting images are visually pleasing and quite realistic.

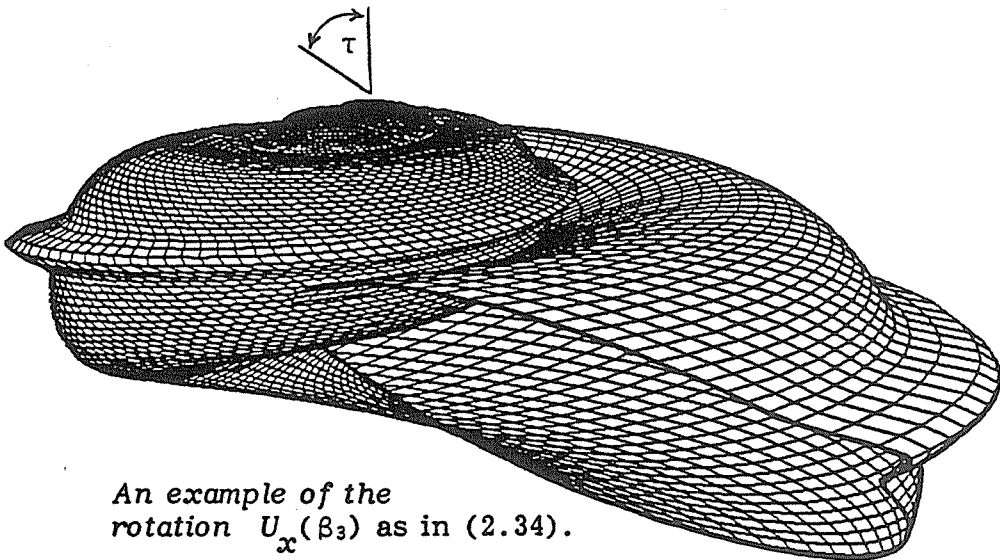
Cortie's notation ¹³ (1989)	Illert's standard notation ¹² (1983)
α $\cot \alpha$ s θ β $\left\{ \begin{array}{l} A \sin \beta = r_0 \\ -A \cos \beta \end{array} \right.$ $R(s)$ Ω, ϕ, μ	ψ α θ ϕ τ $\left\{ \begin{array}{l} a \\ -h \end{array} \right.$ $b(\theta)$ $\beta_1, \beta_2, \beta_3$





A planispiral (apex-angle $2\tau \approx 180^\circ$) ammonite shell with almost "orthoclinal" growth-lines (i.e. the generating curve is perpendicular to the direction of growth at all stages of development):

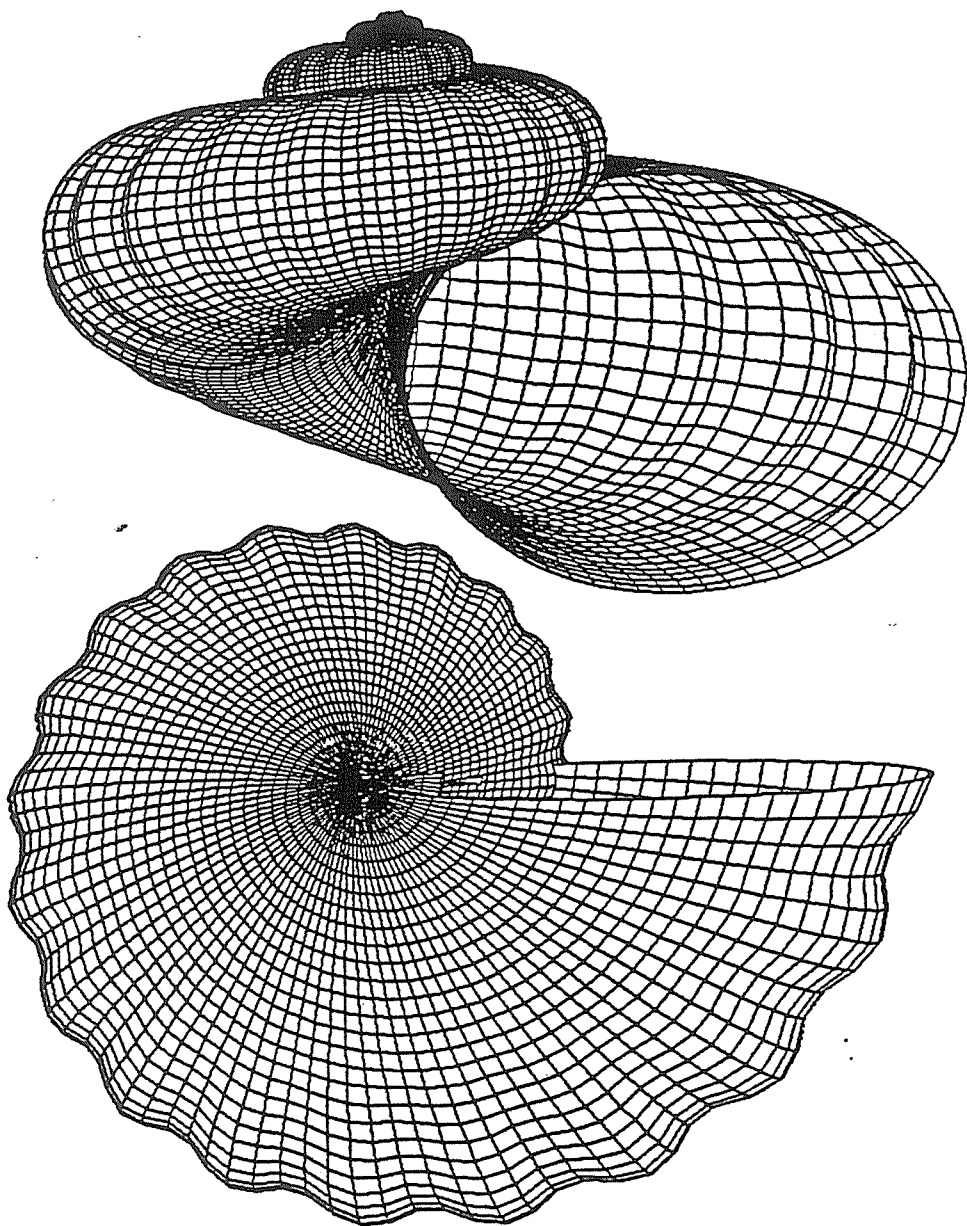
$$\alpha = 0.1214, \quad \tau = 89.95^\circ, \quad \beta_1 = \beta_2 = \beta_3 = 1.1^\circ.$$



An example of the rotation $U_x(\beta_3)$ as in (2.34).

Euomphalopterus ($\times 2$) has "prosoclinal" (forward-leaning, $\beta_3 \gg 0$) growth-lines:

$$\alpha = 0.1725, \quad \tau = 45.3^\circ, \quad \beta_1 = \beta_2 = 0, \quad \beta_3 = 60.2^\circ.$$

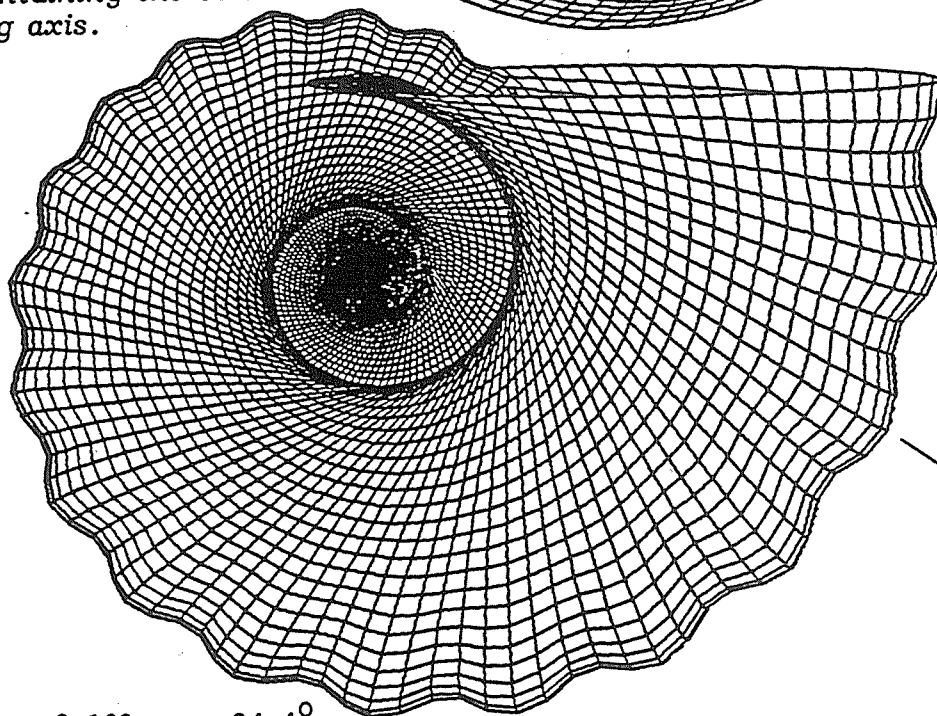


Two views of a corrugated turbo shell whose generating-curve always lies (approximately) in the plane containing the coiling axis (i.e. the z-axis):

$$\alpha = 0.162, \quad \tau = 35^{\circ}, \quad \beta_1 = \beta_2 = 0, \quad \beta_3 = 5.16^{\circ}.$$

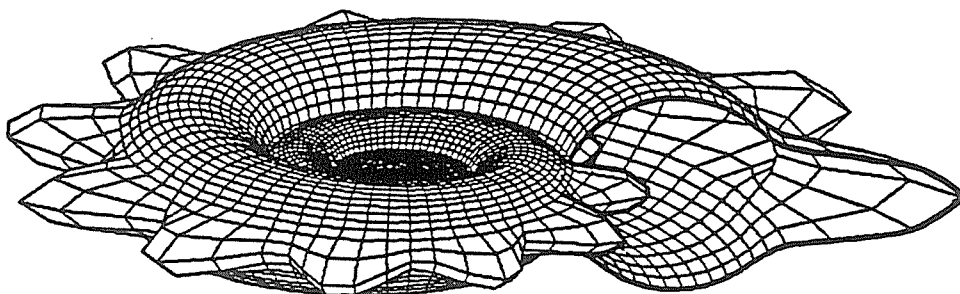
An example of the rotation $U_z(\beta_1)$ in eq. (2.34).

the same shell
as opposite, but
with its generating
curve significantly
inclined ($\beta_1 \gg 0$)
relative to the plane
containing the coil-
ing axis.



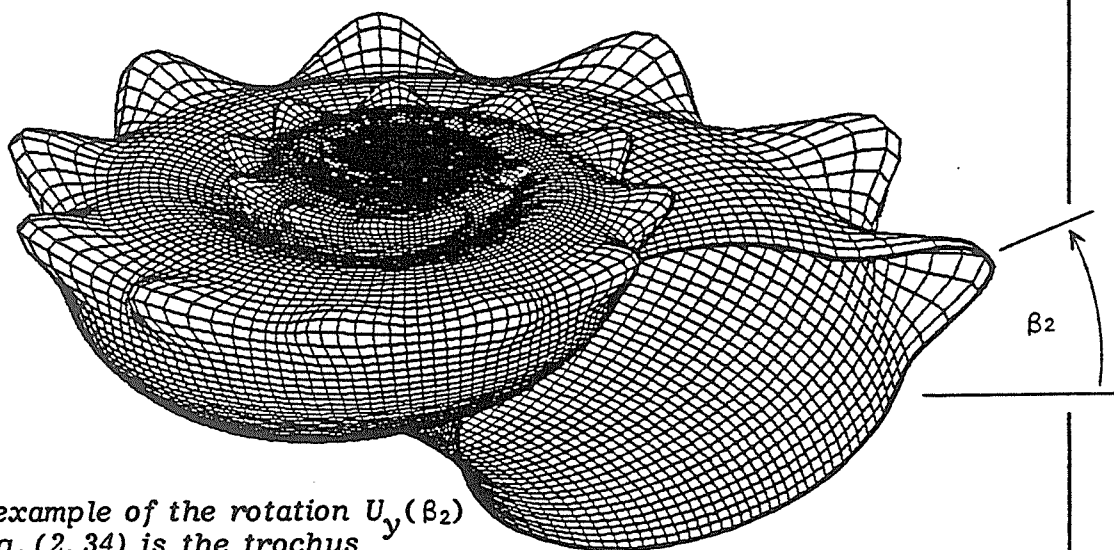
$$\alpha = 0.162, \quad \tau = 34.4^\circ,$$

$$\beta_1 = -40^\circ, \quad \beta_2 = 0, \quad \beta_3 = 5.2^\circ.$$



A planispiral ($2\tau = 180^\circ$) shell ($\times 1$), *Phanerotinus* sp., with unrotated ($\beta_2 \approx 0$) generating-curve hence the horizontally-pointing knobs:

$$\alpha = 0.1214, \quad \tau = 90^\circ, \quad \beta_1 = \beta_2 = \beta_3 = 1.1^\circ \text{ (almost zero).}$$



An example of the rotation $U_y(\beta_2)$ in eq. (2.34) is the trochus *Angaria delphinus* ($\times 1$). It has its generating-curve significantly rotated ($\beta_2 \gg 0$) about its centre of mass, within the original plane, thus giving rise to knobs which point upward at 29.8° relative to the coiling-plane.

$$\alpha = 0.1214^\circ, \quad \tau = 45.26^\circ, \\ \beta_1 = \beta_2 = 5.2^\circ, \quad \beta_3 = 29.8^\circ$$

2.7 THE SELF-SIMILARITY DIFFERENTIAL EQUATION

With the coordinate transformation for self-similar surfaces expressed in the easily differentiable form (2.28) we have

$$\frac{\partial \tilde{r}}{\partial \phi} = \zeta \tilde{r} \quad \dots (2.36)$$

$$\frac{\partial^2 \tilde{r}}{\partial \phi^2} = \zeta^2 \tilde{r} \quad \dots (2.37)$$

$$\frac{\partial^S \tilde{r}}{\partial \phi^S} = \zeta^S \tilde{r} = \alpha^S \begin{pmatrix} C_S & -S_S & 0 \\ S_S & C_S & 0 \\ 0 & 0 & 1 \end{pmatrix} \tilde{r} \quad \dots (2.38)$$

where $C_S = ((\alpha+i)^S + (\alpha-i)^S)/(2\alpha^S)$
and $S_S = i((\alpha-i)^S - (\alpha+i)^S)/(2\alpha^S)$.

These are important "self-similarity" constraints which must be installed into any differential equation that we devise for sea-shell surfaces. Hopefully they will enable us to determine the structure of the unknown Hookean constant matrix. But, first, there is a problem. Once we consider surface equations containing higher-order derivatives, the question immediately arises as to how the generating curve must orient itself in order to correctly turn sharp corners during growth. This question does not arise in first-order mechanics because the trajectories there are all "equiangular" spirals and, once the generating curve is correctly oriented (using, say, equation (2.35)), it remains similarly oriented throughout growth. But second-order mechanics implies growth-trajectories more complicated than just the equiangular spiral.

The so-called *Frenet* conditions that need to be imposed upon the generating curve have been discussed elsewhere by *Willem Bronsvoort*¹⁸ (1985), *Chris Illert*¹⁵ (1989) and to some extent also *Takashi Okamoto*¹⁶ (1988). But we can't tackle such matters until we have worked out the general clockspring trajectory equation.

To simplify matters we will shrink all shell-tubes $\tilde{r}(\theta, \phi)$ onto their "principal growth trajectories" $\tilde{T}(\phi)$: i.e. the imaginary path along the centre of the shell tube, traced out by the centre-of-mass of the generating curve throughout growth. In the previous example we simply shrink $b \rightarrow 0$ for all values of θ in eq.(2.34) thereby reducing the generating curve to a single point at its centre of mass

$$\lim_{b \rightarrow 0} \tilde{r}(\theta, 0) \rightarrow \begin{pmatrix} a \\ 0 \\ -h \end{pmatrix} \equiv \tilde{T}(0) \quad \dots (2.39).$$

As ϕ varies in eq.(2.35) this point traces out the principal growth trajectory

$$\tilde{T}(\phi) = \begin{pmatrix} x(\phi) \\ y(\phi) \\ z(\phi) \end{pmatrix} = e^{\zeta\phi} \tilde{T}(0) = e^{\alpha\phi} \begin{pmatrix} a \cos\phi \\ a \sin\phi \\ -h \end{pmatrix} \quad \dots (2.40)$$

but this is, of course, only for first-order "equiangular" surfaces as in eq.(2.35). Second order theory would have more complicated trajectories $\tilde{T}(\phi)$. The question is, "what are they? and how do we find them?". The first step lies in realizing that the equations (2.36) to (2.38) are also satisfied by the principal growth trajectory, hence it follows immediately that

$$\dot{\tilde{T}} = \zeta \tilde{T} \quad \dots (2.41)$$

and
$$\ddot{\tilde{T}} = \zeta^2 \tilde{T} \quad \dots (2.42).$$

But from equations (1.9) and (1.21) we are seeking a real-space clockspring trajectory equation of the form

$$\ddot{\tilde{T}} = \underbrace{K \tilde{T}}_{\text{Hookean elastic term}} - \underbrace{G \dot{\tilde{T}}}_{\text{velocity dependent externally applied force term}} \quad \dots (2.43)$$

for unknown constant matrices K and G . We can immediately install the first "self-similarity" condition (2.41) into eq.(2.43), eliminating the velocity term as follows

$$\ddot{\tilde{T}} = K \tilde{T} - G \zeta \tilde{T} = (K - G \zeta) \tilde{T} \quad \dots (2.44)$$

but the second "self-similarity" constraint (2.42) must also hold so (2.44) gives the result

$$K - G \zeta = \zeta^2 \quad \text{hence} \quad K = \zeta^2 + G \zeta \quad \dots (2.45).$$

Thus the two "self-similarity" constraints (2.41) and (2.42) have determined the structure of the Hookean elastic constant matrix in our real-space differential equation (2.43) in terms of the known matrix ζ and the other unknown matrix G .

In the book "Seashell Mathematics" (1976), Illert considered the simplest possible case where G is taken to be a simple real scalar constant -2α , and this did give a biologically meaningful shell geometry corresponding to the landsnail *Marisa cornuarietis* (as discussed by Sowerby in 1820, and Adams in 1858) but it was only one special case and, if one thinks about equation (2.43), the assumption that G be the same scalar constant for all three spacial directions essentially means that coiling about the axis of symmetry is coupled to translation along it by a force of the same magnitude in both processes.

In 1928 A.E. Boycott had noticed that coiling about the axis of symmetry proceeded to a large extent independently of axial translation throughout shell growth. So at the very least, we should assume a matrix of the form

$$G = \begin{pmatrix} \lambda, & 0, & 0 \\ 0, & \lambda, & 0 \\ 0, & 0, & \mu \end{pmatrix} \quad \dots (2.46)$$

where λ is a scalar constant related to the magnitude of the winding-force (torque) responsible for coiling *about* the axis of symmetry (in our case z), whilst μ is a scalar constant related to the magnitude of axial compression/extension forces which regulate shell-whorl translation *along* the coiling axis. In other words, we are allowing for *axial-growth* (as discussed in Section 2.2) to proceed at a different rate to *radial growth* (as discussed in Section 2.3). If the forces of axial and radial growth happen to be equal $\lambda = \mu$, then G is equivalent to a scalar constant in that one special case. But, assuming a Boycott matrix of the form (2.46), the Hookean matrix in eq.(2.45) becomes

$$K = \begin{pmatrix} \alpha^2 + \lambda\alpha - 1, & -(2\alpha + \lambda), & 0 \\ (2\alpha + \lambda), & \alpha^2 + \lambda\alpha - 1, & 0 \\ 0, & 0, & \alpha^2 + \alpha\mu \end{pmatrix} \quad \dots (2.47).$$

The three eigenvalues of K are $k_1 = (\alpha + i)(\alpha + i + \lambda)$, $k_2 = (\alpha - i)(\alpha - i + \lambda)$ and $k_3 = \alpha(\mu + \alpha)$, corresponding to the respective eigen-vectors $(i, 1, 0)$, $(1, i, 0)$ and $(0, 0, 1)$. By constructing a matrix S whose vertical rows correspond to these eigenvectors, we can reduce K to a diagonal matrix with these eigenvalues down its diagonal

$$K = S^{-1} k S \quad \dots (2.48)$$

where

$$k = \begin{pmatrix} k_1, & 0, & 0 \\ 0, & k_2, & 0 \\ 0, & 0, & k_3 \end{pmatrix}, \quad S = \begin{pmatrix} 1, & i, & 0 \\ i, & 1, & 0 \\ 0, & 0, & 1 \end{pmatrix}$$

$$\text{and} \quad S^{-1} = \begin{pmatrix} \frac{1}{2}, & -\frac{1}{2}i, & 0 \\ -\frac{1}{2}i, & \frac{1}{2}, & 0 \\ 0, & 0, & 1 \end{pmatrix}.$$

Actually we don't need to know S^{-1} because we can write our real-space clockspring equation (2.43) as follows

$$\mathcal{D} \tilde{T} = K \tilde{T} = S^{-1} k S \tilde{T} \quad \dots (2.49)$$

for the differential operator $\mathcal{D} = \frac{\partial^2}{\partial \phi^2} + G \frac{\partial}{\partial \phi}$.

This whole differential equation can be left-multiplied through by the matrix S giving

$$S \mathcal{D} \tilde{T} = S S^{-1} k S \tilde{T}$$

or

$$\mathcal{D} S \tilde{T} = k S \tilde{T}$$

or

$$\mathcal{D} \tilde{\xi} = k \tilde{\xi}$$

we can interchange the matrix S , and the differential operator as the latter is diagonal

... (2.50)

where we have defined $G = \Omega$ and

$$\tilde{\xi} = S \tilde{T} = \begin{pmatrix} x + i y \\ y + i x \\ z \end{pmatrix} \quad \dots (2.51).$$

Actually eq.(2.50) is exactly our earlier equation (1.21), the only difference being that we have now determined the form of the Hookean constant matrix k from the "self-similarity" constraints (2.41) and (2.42). Also, of course, eq.(2.51) gives the appropriate relationship between real-space and complex-space coordinates. As the equations (2.50) are uncoupled we can multiply them through by arbitrary scalar constants, and it is more usual to use the "normalized" coordinates

$$\tilde{\xi} = \begin{pmatrix} (x + i y) / \sqrt{2} \\ (y + i x) / \sqrt{2} \\ \sqrt{2} z \end{pmatrix} \quad \dots (2.52).$$

This transformation has the physical significance that it preserves the axial component of angular momentum.

This is best demonstrated by defining angular-momentum in \mathbb{C}^3 as follows

$$\begin{aligned}\underline{H} &= \underline{\xi} \times \dot{\underline{\xi}} \\ &= (\xi_2 \dot{\xi}_3 - \xi_3 \dot{\xi}_2, \xi_3 \dot{\xi}_1 - \xi_1 \dot{\xi}_3, \xi_1 \dot{\xi}_2 - \xi_2 \dot{\xi}_1),\end{aligned}$$

then expressing it in real-space coordinates using the transformation (2.52) (for which $\xi_1 = (x+iy)/\sqrt{2}$, $\xi_2 = (y+ix)/\sqrt{2}$ and $\xi_3 = \sqrt{2} z$) giving

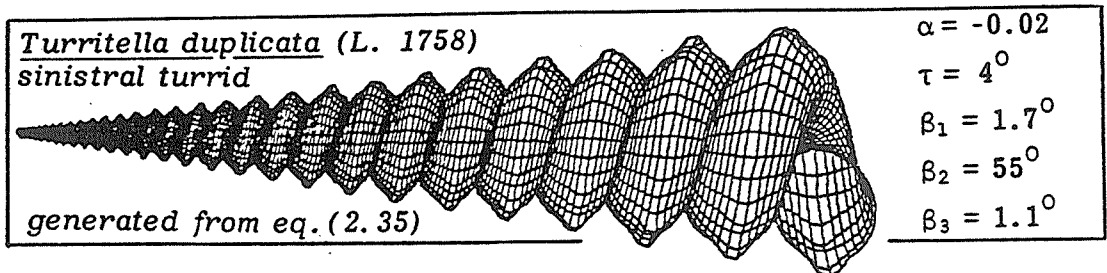
$$\begin{aligned}\underline{H} &= ((y+ix)\dot{z} - z(\dot{y}+i\dot{x}), z(\dot{x}+i\dot{y}) - (x+iy)\dot{z}, \\ &\quad \frac{1}{2}((x+iy)(\dot{y}+i\dot{x}) - (y+ix)(\dot{x}+i\dot{y}))) \\ &= (y\dot{z} - z\dot{y} + i(x\dot{z} - z\dot{x}), z\dot{x} - x\dot{z} + i(z\dot{y} - y\dot{z}), x\dot{y} - y\dot{x}).\end{aligned}$$

Conversely, in E^3 , real-space angular-momentum is usually defined as

$$\underline{h} = \underline{r} \times \dot{\underline{r}} = (y\dot{z} - z\dot{y}, z\dot{x} - x\dot{z}, x\dot{y} - y\dot{x}).$$

As might perhaps be expected $\text{real}[\underline{H}] = \underline{h}$. And, more importantly, we notice that the coordinate transformation (2.52) has left invariant the axial component of angular-momentum:

$$\text{i.e.} \quad \hat{\xi}_3 \cdot \underline{\xi} \times \dot{\underline{\xi}} = \hat{z} \cdot \underline{r} \times \dot{\underline{r}} \quad \dots (2.53).$$



3.1 REAL-SPACE CLOCKSPrING TRAJECTORIES

The *Principal Growth Trajectory*, denoted $\tilde{T}(\phi)$, was previously defined as the spiral curve through the centre of the shell-tube, traced-out by the centre-of-mass of the shell's aperture (generating curve) throughout the course of shell-growth. These coiled curves may be thought of as tensile clocksprings satisfying the following second-order real-space matrix differential equation

$$\left[\frac{\partial^2}{\partial \phi^2} + \Omega \frac{\partial}{\partial \phi} - \zeta^2 - \Omega \zeta \right] \tilde{T}(\phi) = 0 \quad \dots (3.1)$$

where

$$\Omega = \begin{bmatrix} \lambda_1 & 0 & 0 \\ 0 & \lambda_2 & 0 \\ 0 & 0 & \mu \end{bmatrix}, \quad \zeta = \begin{bmatrix} \alpha & -1 & 0 \\ 1 & \alpha & 0 \\ 0 & 0 & \alpha \end{bmatrix} \quad \text{and} \quad \tilde{T}(\phi) = \begin{bmatrix} x(\phi) \\ y(\phi) \\ z(\phi) \end{bmatrix},$$

such that α , λ_1 , λ_2 and μ are constants for any given shell:

- i) α is related to the elasticity of the clockspring wire material,
- ii) λ_1 generally equals λ_2 , so long as they are both real numbers, and $\lambda_1 = \lambda_2 = \lambda$ is related to the magnitude of any winding-force (torque) acting in the xy -plane hence (as *Okamoto*¹⁶ and *Illert*¹⁵ have suggested) it is probably also related to the *curvature* of the spiral trajectory,
- iii) μ is related to the magnitude of any squashing or stretching forces which act along the z -axis hence to the *torsion* of helico-spiral trajectories^{15, 16}.

Equation (3.1) is just (2.49) with the matrices (2.46) and (2.45) installed. Written in full we have

$$\begin{aligned}\ddot{x} + \lambda \dot{x} - (\alpha^2 + \lambda \alpha - 1) x + (2\alpha + \lambda) y &= 0 \\ \ddot{y} + \lambda \dot{y} - (2\alpha + \lambda) x - (\alpha^2 + \lambda \alpha - 1) y &= 0 \\ \ddot{z} + \mu \dot{z} - (\alpha^2 + \mu \alpha) z &= 0 \quad \dots (3.2)\end{aligned}$$

where dots denote $\partial/\partial\phi$. Clearly, as λ and μ are independent parameters which may assume any real or complex value, there are a diversity of clockspring trajectories, solutions to (3.2), and we will now examine as many of them as are known at present.

CASE # 1: *the Coni-spiral*, (real) $\lambda =$ (real) $\mu = -2\alpha \quad \dots (3.3).$

The elasticity of the clockspring wire is any real constant α . So substituting $\lambda = -2\alpha$ into the first two equations in (3.2) gives

$$\begin{aligned}\ddot{x} - 2\alpha \dot{x} + (\alpha^2 + 1) x &= 0 \\ \ddot{y} - 2\alpha \dot{y} + (\alpha^2 + 1) y &= 0 \quad \dots (3.4).\end{aligned}$$

Direct substitution reveals a solution of the form

$$x(\phi) = a e^{\alpha\phi} \cos\phi, \quad y(\phi) = a e^{\alpha\phi} \sin\phi \quad \dots (3.5).$$

Likewise, for a real number $\mu = -2\alpha$, the third equation in (3.2) simplifies down to

$$\ddot{z} - 2\alpha \dot{z} + \alpha^2 z = 0 \quad \dots (3.6)$$

which has a solution of the form

$$z(\phi) = -h e^{\alpha\phi} \quad \dots (3.7)(i).$$

Collectively the equations (3.5) and (3.7)(i) correspond to previously discussed trajectory (2.40): i.e. a "turbinate" spiral lying upon the surface of a cone of base-radius a , and height h . And, depending on the value of α , these conic-spirals can be left-handed, right-handed, or circular (as, for example, in a sea-urchin's test, or a hen's egg).

It was, perhaps, *Pierre Varignon* in 1704 who first demonstrated that a circle is a limiting case of a spiral: just substitute $\alpha = 0$ into equations (3.5) and (3.7), above, to obtain a circle of radius a parallel to the xy -plane, but located a distance $-h$ down the z -axis.

Another solution to (3.6) happens to be

$$z(\phi) = \phi e^{\alpha\phi} \quad \dots (3.7)(ii).$$

This special solution was discussed by *Illert* (1976) in the book "Seashell Mathematics": equations (3.5) and (3.7)(ii) describe the principal growth trajectory of the land-snail *Marisa cornuarietis* (as discussed by *Sowerby* in 1820, and *Adams* in 1858). The most general solution to (3.6) is therefore

$$z(\phi) = (\dot{z}(0) - \alpha z(0)) \phi e^{\alpha\phi} + z(0) e^{\alpha\phi} \quad \dots (3.7)(iii).$$

$$\text{CASE \# 2: } \left. \begin{array}{l} \text{Möbius Conoidal Spires} \\ \text{(real) } \lambda = -2\alpha \\ \text{(real) } \mu \neq -2\alpha \end{array} \right\} \dots (3.8).$$

If μ can assume any real value, except -2α , in the third equation (3.2) then there are two solutions

$$\begin{aligned} z^+(\phi) &= -h e^{-\frac{1}{2}\mu\phi} \cosh((\alpha + \frac{1}{2}\mu)\phi) \\ &= -\frac{1}{2}h (e^{\alpha\phi} + e^{-(\alpha+\mu)\phi}) \end{aligned} \dots (3.9)(i)$$

and

$$\begin{aligned} z^-(\phi) &= -h e^{-\frac{1}{2}\mu\phi} \sinh((\alpha + \frac{1}{2}\mu)\phi) \\ &= -\frac{1}{2}h (e^{\alpha\phi} - e^{-(\alpha+\mu)\phi}) \end{aligned} \dots (3.9)(ii)$$

which we may write collectively as

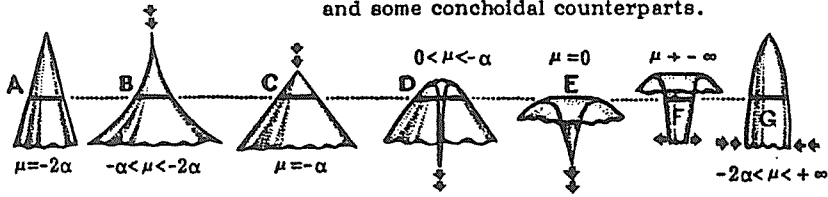
$$z^{\pm}(\phi) = -\frac{1}{2}h (e^{\alpha\phi} \pm e^{-(\alpha+\mu)\phi}) \dots (3.10).$$

But, as $\lambda = -2\alpha$, the solutions for $x(\phi)$ and $y(\phi)$ are still given by the equations (3.5). Hence, assuming axial symmetry, we can define cylindrical-polar coordinates as follows

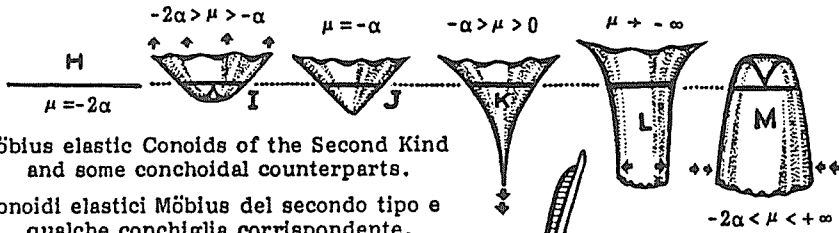
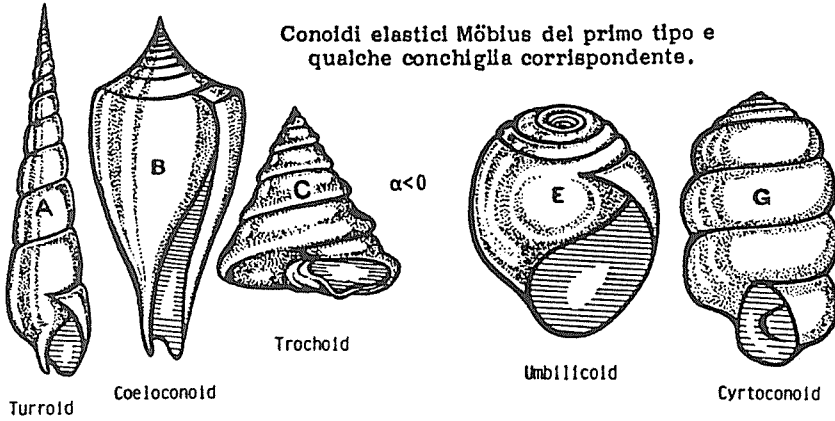
$$\begin{aligned} R(\phi) &= \sqrt{x^2(\phi) + y^2(\phi)} \\ &= ((a e^{\alpha\phi} \cos\phi)^2 + (a e^{\alpha\phi} \sin\phi)^2)^{\frac{1}{2}} \\ &= a e^{\alpha\phi} \end{aligned} \dots (3.11).$$

Substituting (3.11) back into (3.10) enables us to eliminate the variable ϕ , giving the purely cylindrical-polar relationships

Möbius elastic Conoids of the First Kind
and some conchoidal counterparts.

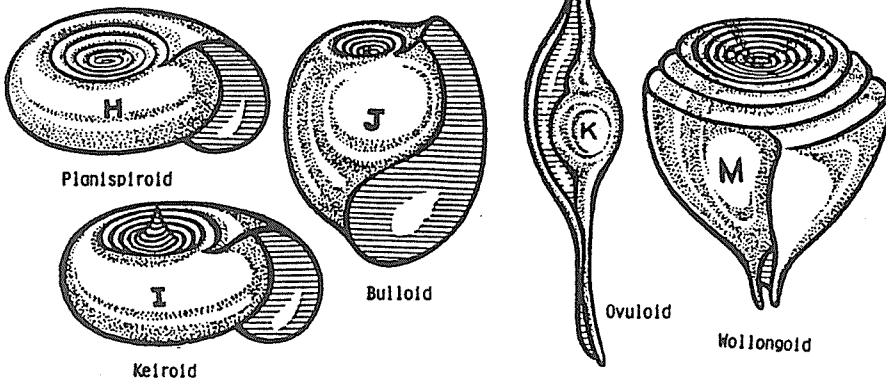


Conoidi elastici Möbius del primo tipo e
qualche conchiglia corrispondente.



Möbius elastic Conoids of the Second Kind
and some conchoidal counterparts.

Conoidi elastici Möbius del secondo tipo e
qualche conchiglia corrispondente.

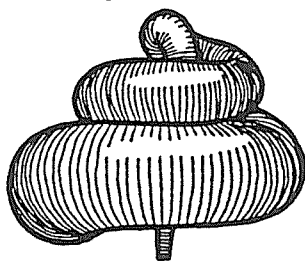


also see color plates A and B

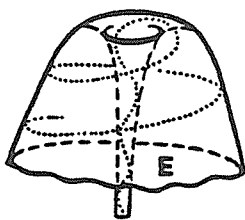
$$\frac{z^{\pm}}{h} = -\frac{1}{2} \left(\frac{R}{a} \pm \left(\frac{R}{a} \right)^{-(1+\mu/\alpha)} \right) \quad \dots (3.12).$$

This equation describes two different families of surfaces, of revolution, upon which our clockspring trajectories lie. Those surfaces of revolution given by (3.12), with the plus sign, are called *Möbius Elastic Conoids of the FIRST KIND*. Their counterparts satisfying (3.12), with the minus sign, are called *Möbius Elastic Conoids of the SECOND KIND*. Various shell-spires, as they occur in Nature, corresponding to these conoids, are shown opposite. Additionally, conoids of various kinds can be superimposed (added together) to describe more complicated spires with recurve and compound curvatures (see Illert¹⁵ (1987) and (Dec. 1990)). It is important to notice that, as μ assumes different values, the conoids (opposite) appear to be axially compressed or stretched.

Some exotic shells start growing along the shell-axis, only to reverse their growth-direction and begin spiralling about their liner protoconch.

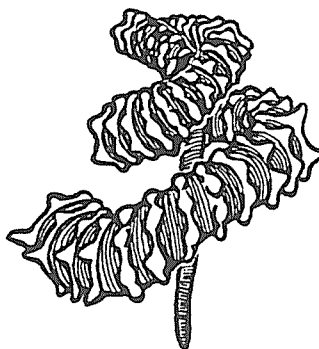


Eubostrychoceras muramotoi
after Okamoto



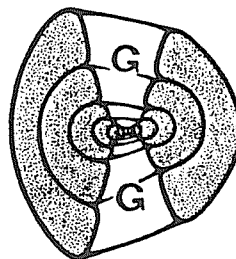
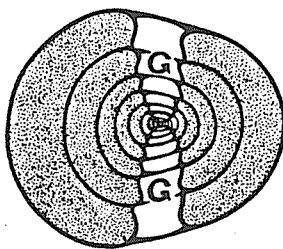
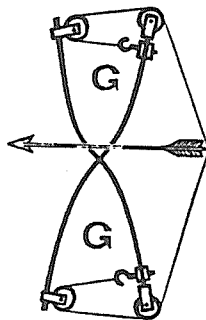
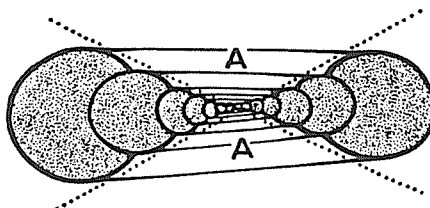
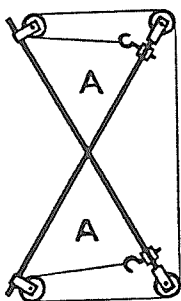
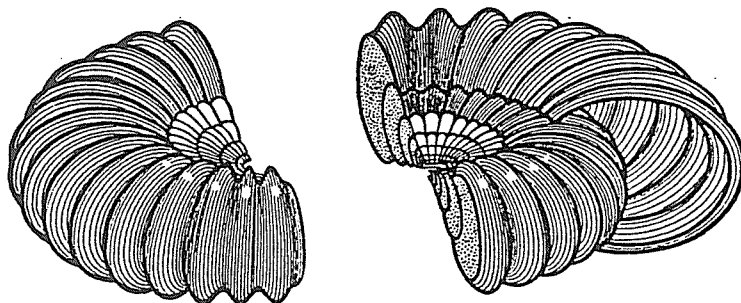
The surface, upon which the protoconch growth-trajectory lies, Okamoto's "hyperbola of revolution", is actually one of our type E möbius conoids

Juvenile stage of
Madagascalites ryu
after Okamoto

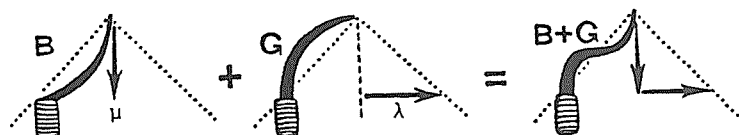
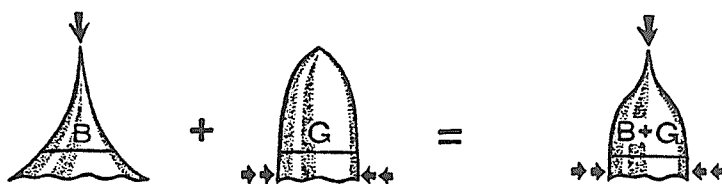


also see color plate F

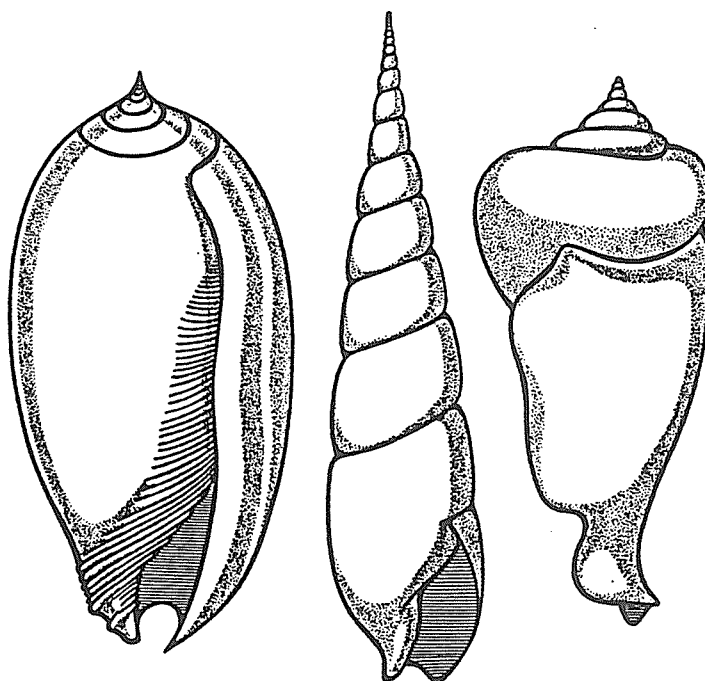
see ref. ¹⁵, Dec. 1990



sectioned ammonite shells provide an explanation for conoid meridian lines in terms of elastic bow armatures.



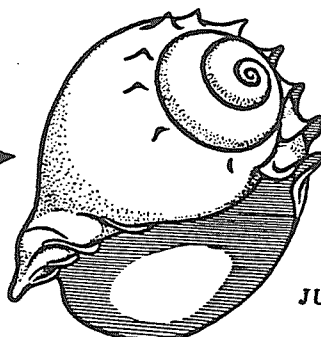
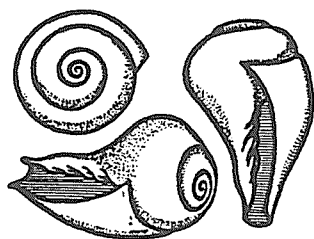
superposition of different conoid meridian-lines produces the optimal, superpowerful, Turkish recurved elastic bow armature



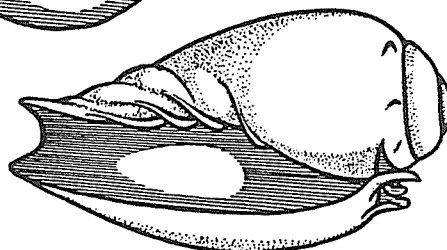
some Olive, Turrid and stromb shells have recurved spires

see Scientific American 264(6): 50-56 (June, 1991)

EARLY PROTOCONCH ($\times 2$)



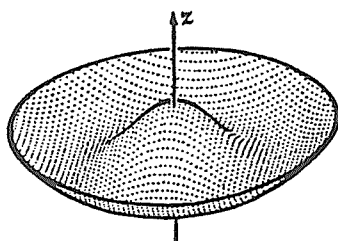
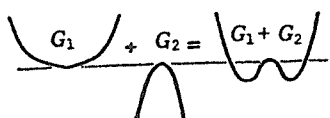
JUVENILE ($\times 2$)



ABOVE: the Baler Shell protoconch a few weeks after hatching ($\times 2$).

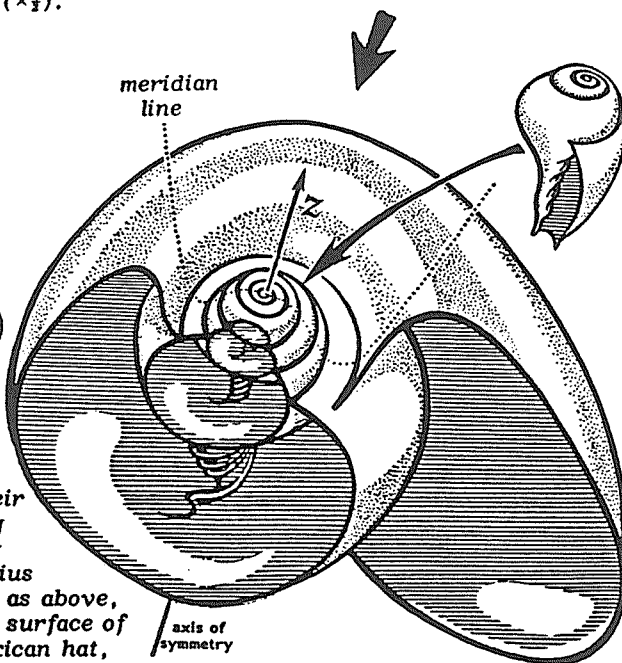
RIGHT: a juvenile with convex almost hemispherical spire, and spikes developing round the shoulder of the outermost whorl ($\times 2$).

BELOW RIGHT: adult Baler Shell shown in section to highlight the upswept outermost whorls ($\times \frac{1}{2}$).



Some shell-spires change their direction of translation along the axis-of-symmetry during growth. By adding two Möbius Elastic Conoids (G_1 and G_2), as above, we can generate an aspheric surface of revolution, resembling a Mexican hat, which resembles the undulations of the spire of the mature Baler Shell (RIGHT).

meridian line



ADULT ($\times \frac{1}{2}$)

CONOID SUPERPOSITION AND COMPOUND SEASHELL-SPIRES
(Sovrapposizione di conoidi per produrre compòsite geometrie guglia)

CASE # 3: *Hyperbolic Clocksprings*
 (real) $\lambda \neq -2\alpha$... (3.13).

The *hyperbolic clocksprings* are best appreciated if we initially choose them to lie entirely in the xy -plane. Another way of saying this is that we choose the trivial solution $z=0$ in eq.(3.2). In any event, with $\lambda \neq -2\alpha$, the first two equations (3.2) have the solutions

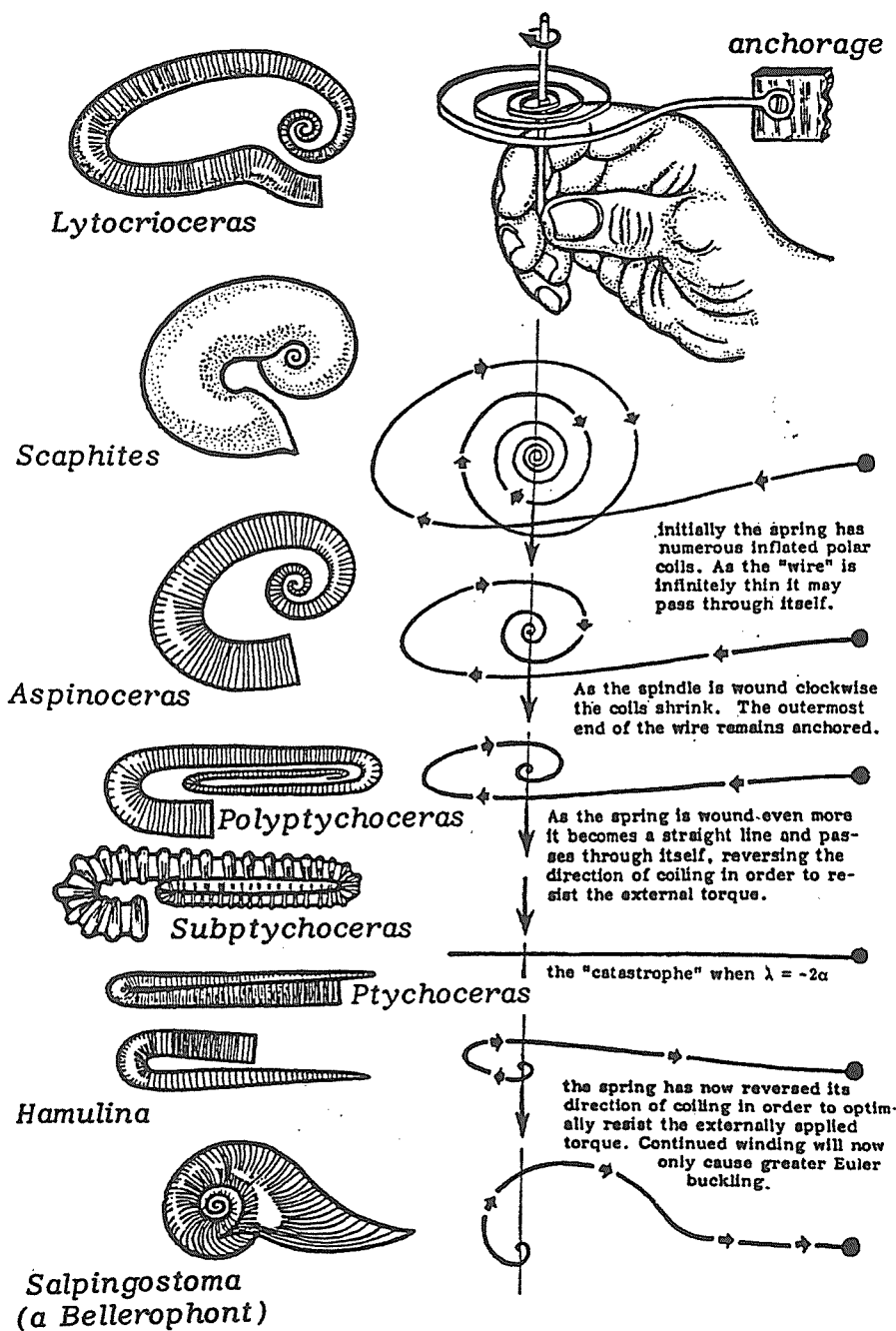
$$\begin{aligned} x(\phi) &= a e^{-\frac{1}{2}\lambda\phi} \cosh((\alpha + \frac{1}{2}\lambda)\phi) \cos\phi \\ y(\phi) &= a e^{-\frac{1}{2}\lambda\phi} \sinh((\alpha + \frac{1}{2}\lambda)\phi) \sin\phi \end{aligned} \quad \dots (3.14)$$

the so called *hyperbolic clocksprings of the FIRST KIND*;
 and also

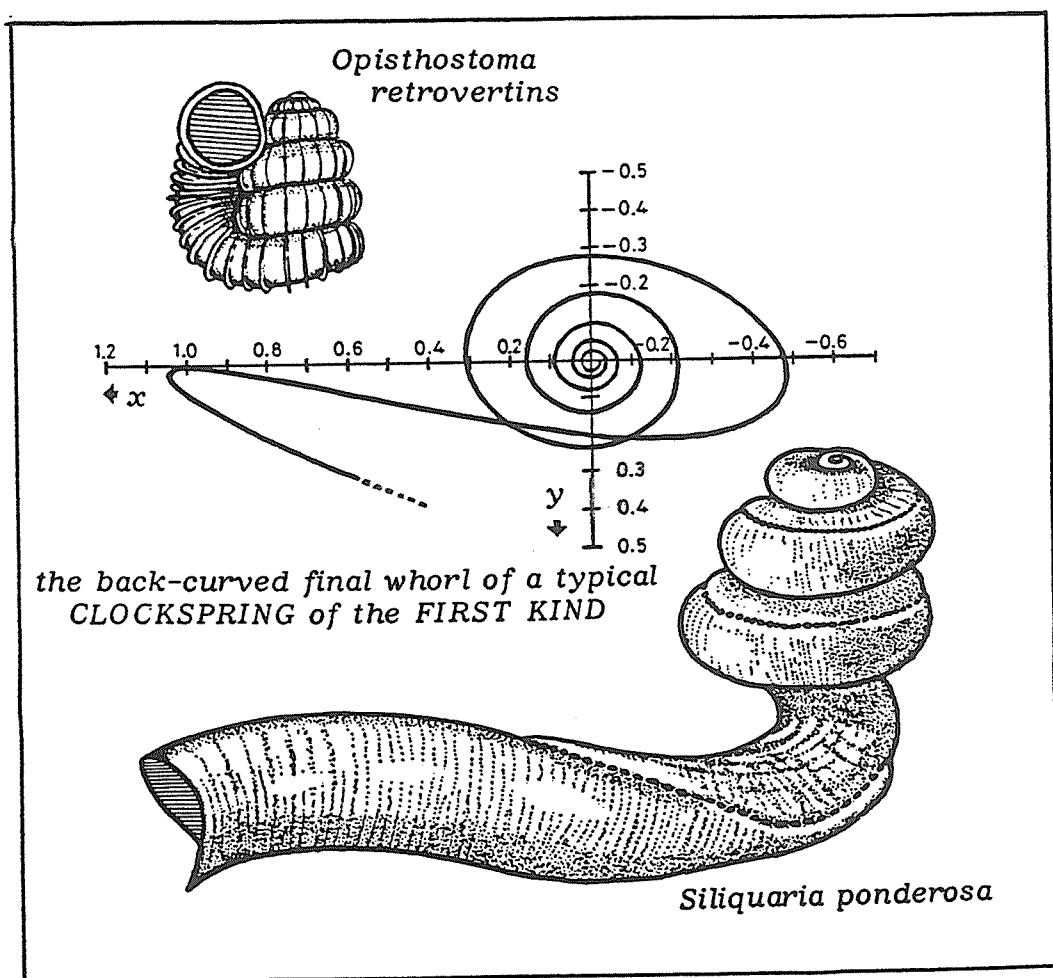
$$\begin{aligned} x(\phi) &= a e^{-\frac{1}{2}\lambda\phi} \sinh((\alpha + \frac{1}{2}\lambda)\phi) \cos\phi \\ y(\phi) &= a e^{-\frac{1}{2}\lambda\phi} \cosh((\alpha + \frac{1}{2}\lambda)\phi) \sin\phi \end{aligned} \quad \dots (3.15)$$

the *hyperbolic clocksprings of the SECOND KIND*. By inspection it should be obvious that clocksprings of the First Kind are anchored at the point $(x(0), y(0)) = (a, 0)$, whereas those of the Second Kind pass through the origin such that $(x(0), y(0)) = (0, 0)$. Check by substituting $\phi=0$ back into (3.14) and (3.15) respectively. We can now understand the significance of the "fixed end" boundary condition obeyed by the urchin-eating Helmet discussed in Section 1.1, and see how to mathematically formulate such a constraint using equations (3.14). Conversely we would use equations (3.15) to model the cowrie-shell whose in-curved aperture was also mentioned in Section 1.1.

CLOCK-SPRINGS OF THE FIRST KIND



Of course these clocksprings need not be confined to a flat plane. Either of (3.14) or (3.15) could be combined with either of the $z(\phi)$ solutions given in eq.(3.10), or maybe with either of the simpler solutions (3.7)(i) or (3.7)(ii), and perhaps with other solutions yet to be discussed or discovered, to give a variety of complicated three-dimensional spirals, any of which may be superimposed (added together) to give composite spirals. The important thing is that, as λ varies, the clocksprings actually tighten or loosen their coils as if acted on by an external torque applied to the winding-spindle (axis of symmetry).



$$\text{CASE \# 4: } \left. \begin{array}{l} \text{wrinkled Ramm Cones} \\ \text{(real) } \lambda \neq -2\alpha \\ \mu = \text{any real number} \end{array} \right\} \dots (3.16).$$

Some interesting trajectories arise if we allow the hyperbolic clocksprings (3.14) and (3.15) to lie upon surfaces of revolution; not unlike the conoids in Case 2. Consider, for example, clock-springs of the First Kind given by (3.14) and a cylindrical polar coordinate $R(\phi)$ given parametrically as follows

$$\begin{aligned} R^+(\phi) &= \sqrt{x^2(\phi) + y^2(\phi)} \\ &= \frac{1}{2} a (e^{2\alpha\phi} + e^{-2(\alpha+\lambda)\phi} + 2e^{-\lambda\phi} (\cos^2\phi - \sin^2\phi))^{\frac{1}{2}} \end{aligned} \dots (3.17)$$

which satisfies the boundary condition

$$R^+(0) = a \dots (3.18)$$

the "fixed-end" constraint that characterizes clocksprings of the First Kind (in this case giving a fixed "neutral" ring of radius a for all values of λ).

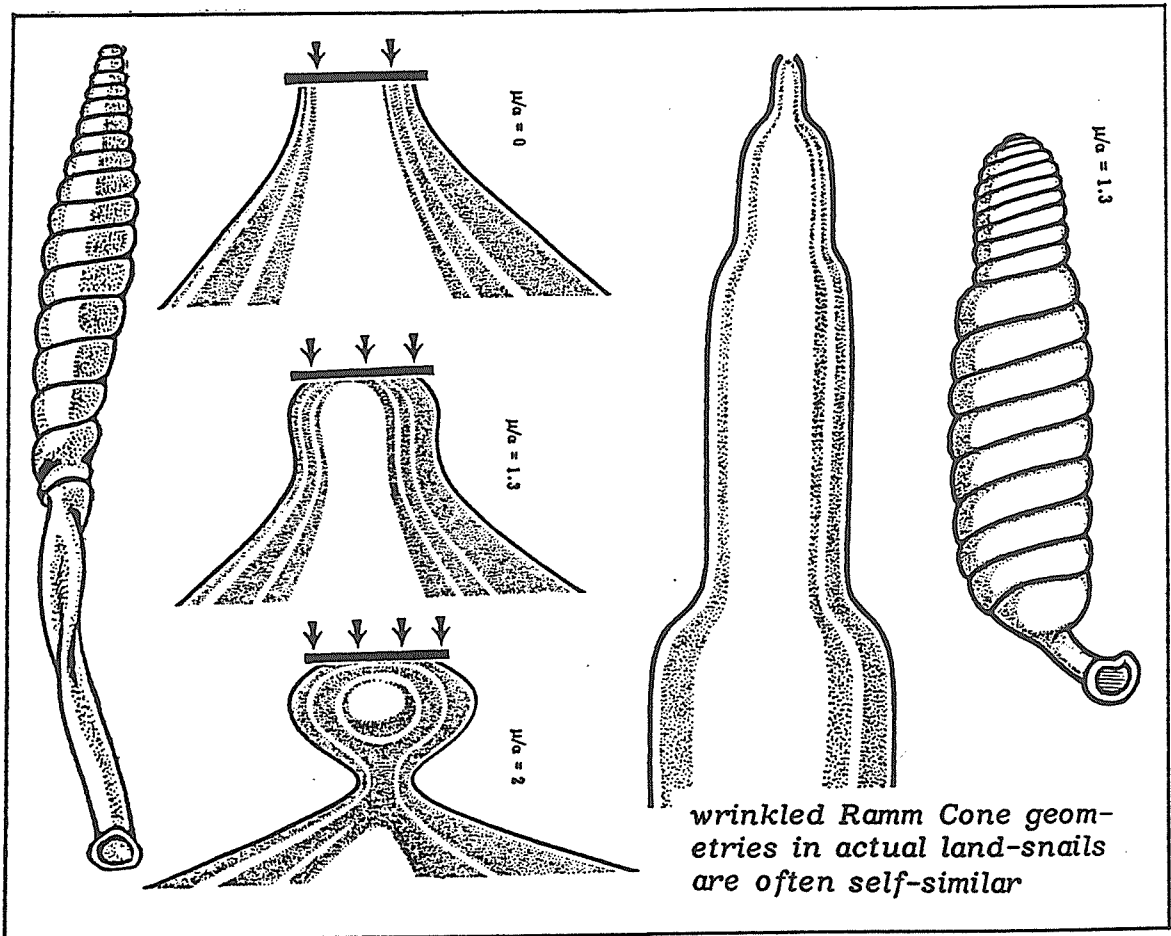
Likewise clocksprings of the Second Kind (3.15) have a corresponding cylindrical-polar radius given parametrically as follows

$$\begin{aligned} R^-(\phi) &= \frac{1}{2} a (e^{2\alpha\phi} + e^{-2(\alpha+\lambda)\phi} - 2e^{-\lambda\phi} (\cos^2\phi - \sin^2\phi))^{\frac{1}{2}} \\ &\dots (3.19) \end{aligned}$$

which satisfies the boundary condition

$$R^-(0) = 0 \dots (3.20).$$

Now, either of the radial functions (3.17) or (3.19) can be combined with any of the functions $z(\phi)$ given by the equations (3.7) or (3.10). Specifically, combining R^+ with z^- can give wrinkled *Ramm Cones*; trajectories on such surfaces of revolution are multiple-tiered and *self-similar*. Combining R^- with z^+ can yield a whole class of *Edwards Conoids* of finite height, some of which are completely closed and similar to pine-cones or sea-urchin shells (tests). These are fundamentally different to the conoids previously discussed in Case 2 which were infinitely tall and open at (at least) one end.



CASE # 5: *Heteromorphs*
 complex values of λ

The constant λ in the *Boycott* matrix (2.46) is real-valued, corresponding in some way to the magnitude of nett winding-force (torque) about the axis of symmetry Z . Obviously, the greater this winding torque, the tighter the coils of the spring spiral hence the smaller the instantaneous "curvature" at each point on the trajectory. Thus our constant λ is some kind of measure of trajectory-curvature, and the tightness of coiling in a general sense, so it is sometimes called the "normalised" curvature (see *Okamoto*¹⁶ and *Illert*¹⁵).

In general, complex values of "normalised curvature" λ correspond to trajectory-transverse oscillations in the coiling-plane (i.e. the xy -plane). This is a result that one won't find in the standard text-books on Differential Geometry. It has only come to light through our study of seashell geometries. To appreciate what is being said here it helps to recall that, so long as λ_1 and λ_2 were both real in equation (3.1), we could put $\lambda_1 = \lambda_2 = \lambda$ as in the original *Boycott* matrix (2.46). But if they are both complex then their imaginary components might not be equal. Indeed, if we select

$$\begin{aligned}\lambda_1 &= -2\alpha - \ln(\epsilon) + i 2\gamma \\ \lambda_2 &= -2\alpha - \ln(\epsilon) + i (2\gamma + \pi) \quad \dots (3.21)\end{aligned}$$

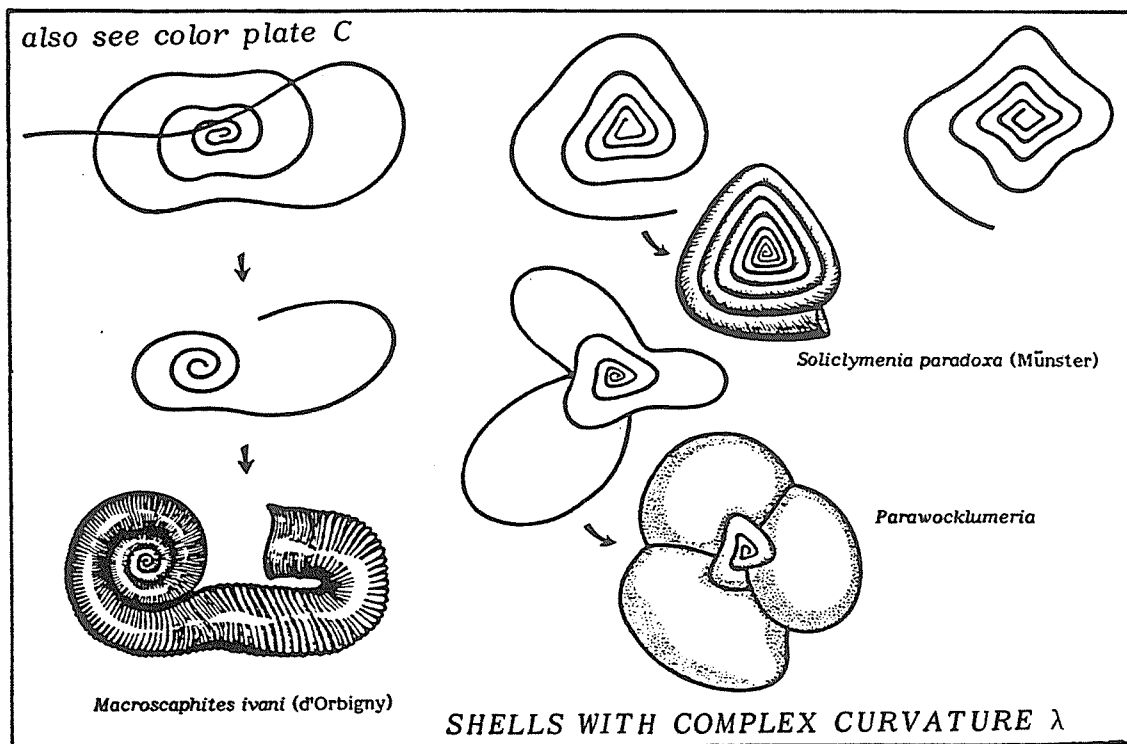
the real components are the same, but there is a phase difference in the imaginary terms. Thus a hyperbolic clockspring trajectory of the First Kind

$$\begin{aligned}
 x(\phi) &= a (e^{\alpha\phi} + e^{-(\alpha + \lambda_1)\phi}) \cos\phi \\
 y(\phi) &= a (e^{\alpha\phi} - e^{-(\alpha + \lambda_2)\phi}) \sin\phi
 \end{aligned}
 \quad \dots (3.22)$$

becomes

$$\begin{aligned}
 \text{real}[x(\phi)] &= a e^{\alpha\phi} (1 + \varepsilon^\phi \cos(2\gamma\phi)) \cos\phi \\
 \text{real}[y(\phi)] &= a e^{\alpha\phi} (1 + \varepsilon^\phi \cos(2\gamma\phi)) \sin\phi
 \end{aligned}
 \quad \dots (3.23).$$

Now, depending upon the value of γ , we can describe spiral trajectories with multiple bumps (called "apses"): if $2\gamma = 2$ we are describing heteromorphic Ammonites with two apses like *Macroscaphites*; if $2\gamma = 3$ we have three-apsed trajectories as in *Solicyclymenia paradoxa* and *Parawocklumeria* (see Illert¹⁵, October 1990).



$$\text{CASE \# 6: } \left. \begin{array}{l} \text{cylindrical Sine-Spirals} \\ \text{(real) } \lambda = -2\alpha \\ \text{(complex) } \mu = \alpha - \beta - i(\gamma - \frac{1}{2}\pi) \end{array} \right\} \dots (3.24).$$

For $\lambda = -2\alpha$ we obtain the equiangular spiral in the coiling plane, as given by equations (3.5). But complex values of μ , the measure of axial squashing and stretching forces, result in trajectory-transverse oscillations *perpendicular* to the coiling plane. This physical consequence of complex values of *torsion* is not to be found in standard texts on Differential Geometry and has only been uncovered through studying real-world shell geometries. Typically we are dealing with trajectories of the form

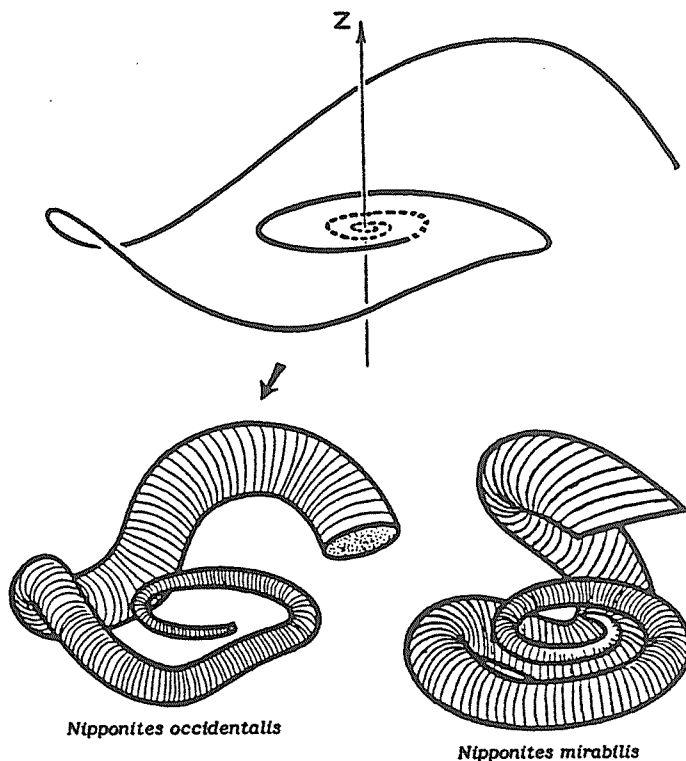
$$z(\phi) = b e^{(\beta + i(\gamma - \frac{1}{2}\pi))\phi} \dots (3.25)(i)$$

alternately written as

$$\text{real}[z(\phi)] = b e^{\beta\phi} \sin(\gamma\phi) \dots (3.25)(ii).$$

We can demonstrate the validity of the solution (3.25)(i) simply by substituting it into the third of the equations (3.2), in the process determining μ (as in 3.24 above). Typically these cylindrical sine-spirals, given by equations (3.5) and (3.25), start coiling in a regular planispiral fashion soon thereafter developing trajectory-transverse oscillations, of increasing magnitude, perpendicular to the plane of coiling as with the fossil ammonite *Nipponites occidentalis* (shown opposite). Some, however, like the juvenile *Nipponites mirabilis* curve back over themselves requiring a more complicated trajectory equation (see the discussion in Case 7).

SHELL GEOMETRIES EXHIBITING THE EFFECTS OF COMPLEX TORSION μ



Nipponites occidentalis starts coiling in a regular planispiral fashion but soon develops trajectory-transverse oscillations perpendicular to the plane of coiling. This kind of trajectory is called a cylindrical Sine-Spiral.

Nipponites mirabilis starts off in a similar fashion, but its looping whorls overhang significantly and a more complicated trajectory equation is needed.

CASE # 7: *spiral Lissajous Figures*
(the miraculous Nipponites)
complex λ and complex μ

Complex values of curvature

$$\lambda_1 = -2\alpha - \ln(\epsilon) + i 2\gamma$$

$$\lambda_2 = -2\alpha - \ln(\epsilon) + i (2\gamma + \pi)$$

and also complex values of torsion

$$\mu = \alpha - \beta - i (\gamma - \tfrac{1}{2} \pi)$$

... (3.26)

produce the most incredibly sinuous spiral Lissajous Figures
... as in the fossil Ammonite *Nipponites mirabilis*. Typical
trajectories satisfying equation (3.1) and the conditions (3.26)
are of the form

$$\text{real}[x(\phi)] = a e^{\alpha\phi} (1 + \epsilon^\phi \cos(2\gamma\phi)) \cos\phi$$

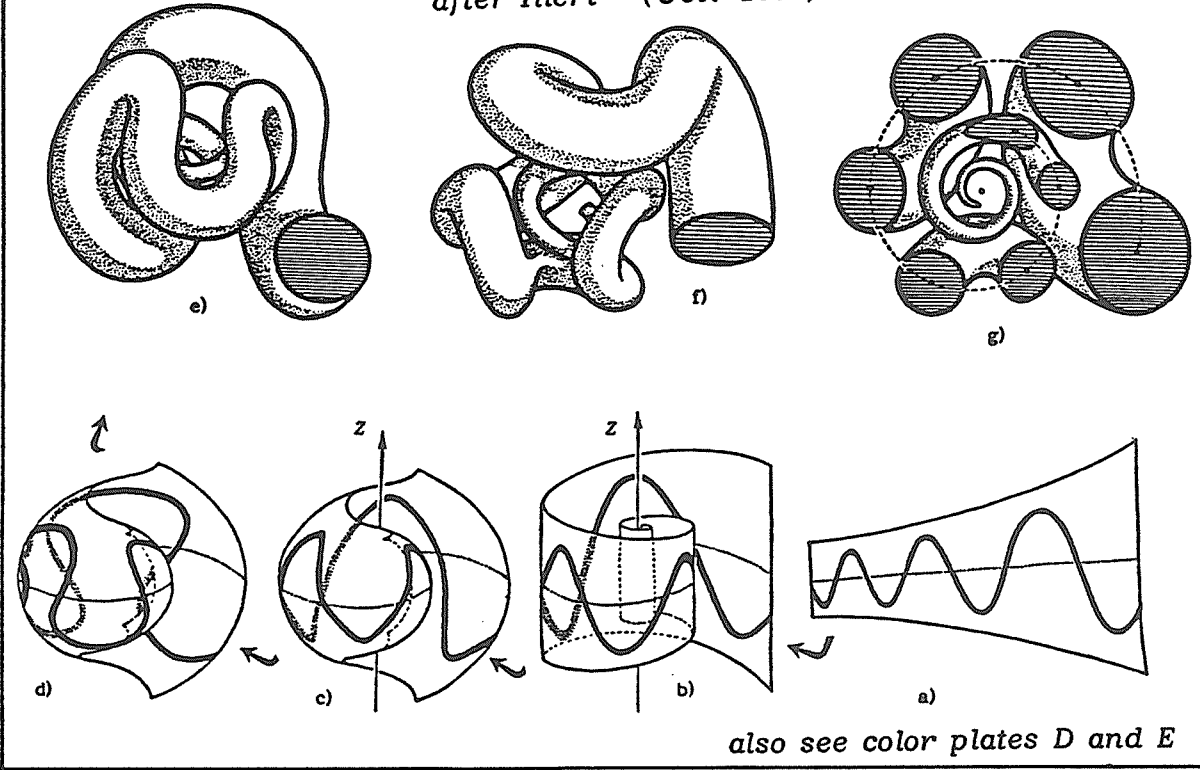
$$\text{real}[y(\phi)] = a e^{\alpha\phi} (1 + \epsilon^\phi \cos(2\gamma\phi)) \sin\phi$$

$$\text{real}[z(\phi)] = b e^{\beta\phi} \sin(\gamma\phi) \quad \dots (3.27).$$

Generally we can generate a huge range of Lissajous spirals
assuming that $\epsilon^\phi \cong \epsilon_0$, a constant, throughout growth.
But if we wish to correctly describe the transition from plani-
spiral juvenile growth to the wild serpentine adult trajectories
then it is important to take into consideration the ϵ^ϕ term in
(3.27).

A refinement to our basic trajectory (3.27) has been suggested
by *Takashi Okamoto*:

Nipponites mirabilis
after Illert¹⁵ (Oct. 1990).



$$\begin{aligned} \text{real}[x(\phi)] &= a e^{\alpha\phi} (1 + \epsilon^\phi \cos(2\gamma\phi)) \cos(\phi - f \sin(2\gamma\phi)) \\ \text{real}[y(\phi)] &= a e^{\alpha\phi} (1 + \epsilon^\phi \cos(2\gamma\phi)) \sin(\phi - f \sin(2\gamma\phi)) \\ &\dots (3.28) \end{aligned}$$

where f is a small constant which helps round the trajectory, making it more sinuous and serpentine, like the suture-line on a tennis ball. Thus, with the generalised solutions for $x(\phi)$ and $y(\phi)$ given by (3.28), and $z(\phi)$ as in (3.27), we can not only describe the meanderings of adult *Nipponites* but also planispiral juvenile growth-stages and the transition between them. This is, perhaps, one of the most awesome and challenging growth-trajectories given by our equation (3.1). It is almost conclusive "proof" that our analysis is correct.

3.2 BRANCHING CLOCKSPrINGS AND ACAUSALITY

We return now to the *Newtonian* notions of time-flow, and linear causality, underlying the analysis in Section 1.2 . Equation (1.2) conjured a mental-image of each new point ξ_s (on some continuous trajectory $\xi(\phi)$) being attained by the vector $\dot{\xi}_{s-1} \Delta$, starting from the preceding point ξ_{s-1} , with entire spiral trajectories being created from a sequence of linear steps (as in eq.(1.3)) just like walking round a spiral-staircase.

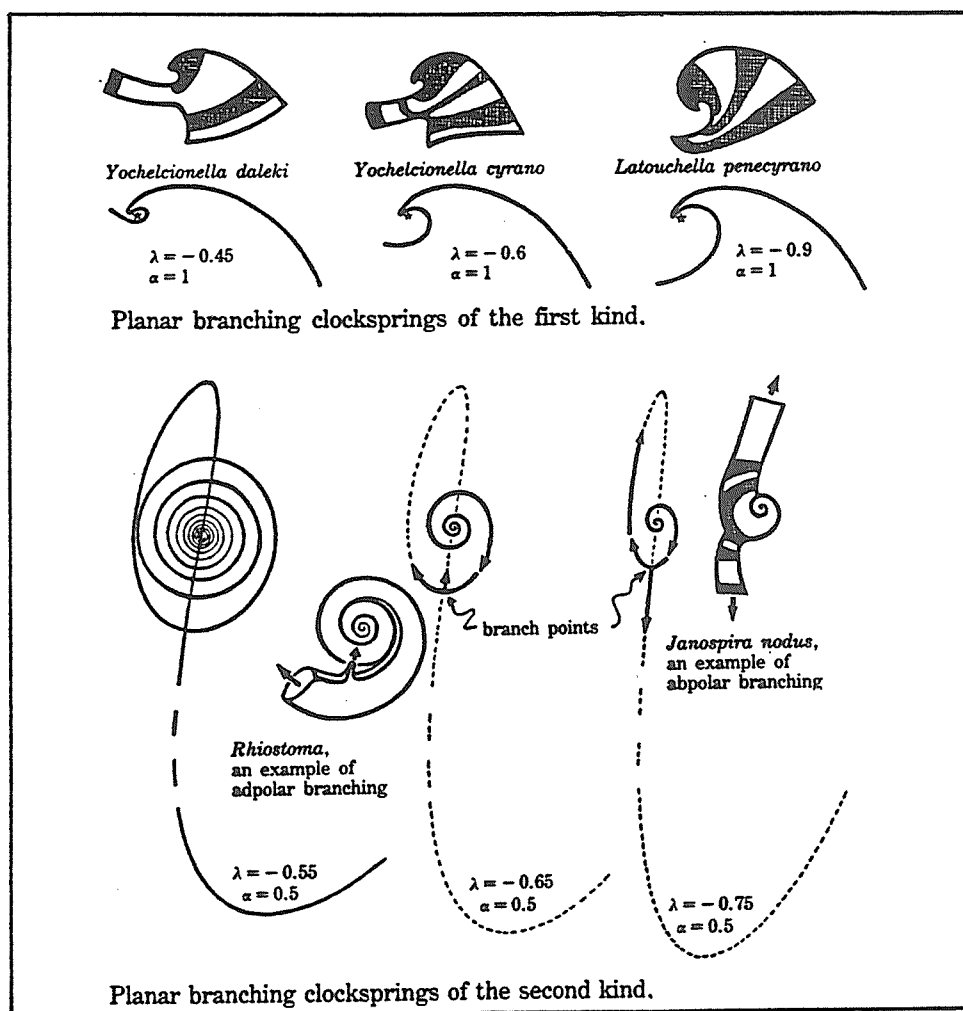
This is all very classical, and "sensible", but we should have realized from the second-order mechanics in Section 1.3 that it isn't quite what's happening. Yes, equation (1.6) looks causal, but the auxillary equations (1.7) and (1.10) require us to "know" ξ_{s+1} (*ahead of time*) in order to respectively define the velocity term $\dot{\xi}_s$ and the (absolutely essential) "average radius" vector $\bar{\xi}_s$. Greenspan and Kanatani⁷ have already remarked upon this acausality within our kind of discrete mechanics. But does it matter? Could it have observable macro-temporal consequences?

Consider the example of clocksprings of the Second Kind


$$\xi(\phi) = a e^{-\frac{1}{2}\lambda\phi} (\sinh((\alpha+\frac{1}{2}\lambda+i)\phi), i \sinh((\alpha+\frac{1}{2}\lambda-i)\phi), 0) \dots (3.29)$$

which, because of eq.(2.52), correspond to the real-space trajectories (3.15) that spiral out from the pole, only to have their outermost whorl loop-back to intersect pre-existing inner whorls. The cowrie shell discussed in Section 1.1 is of this kind but its inturned lip stops short, before any-such intersections could occur.

Yet shells such as *Yochelcionella*, *Rhaphaulus*, *Rhiostoma* and *Spiraculum* all utilize self-intersecting clockspring trajectories; actually **BRANCHING** at points of trajectory-intersection, there after growing simultaneously along two separate branches of the clockspring! Some shells *branch* during the earliest developmental stages (as in *Yochelcionella daleki*, a self-intersecting clockspring of the First Kind, named after a "Dr. Who" science fiction character), whilst others (such as *Janospira nodus*, a self-intersecting clockspring of the Second Kind) wait almost till the end of ontogeny before *branching*.



The palaeontologists who first studied these branching clock-spring geometries described the shells as "curious", "ridiculous" "absurdities" ¹⁷ but we can now see them as the same optimal tensile spirals which other non-branching shells also utilize. And as trajectory-branching seems to occur widely, in unrelated species, the usual "once-off" biological explanations won't suffice ... there is a deeper geometrical principle at work!

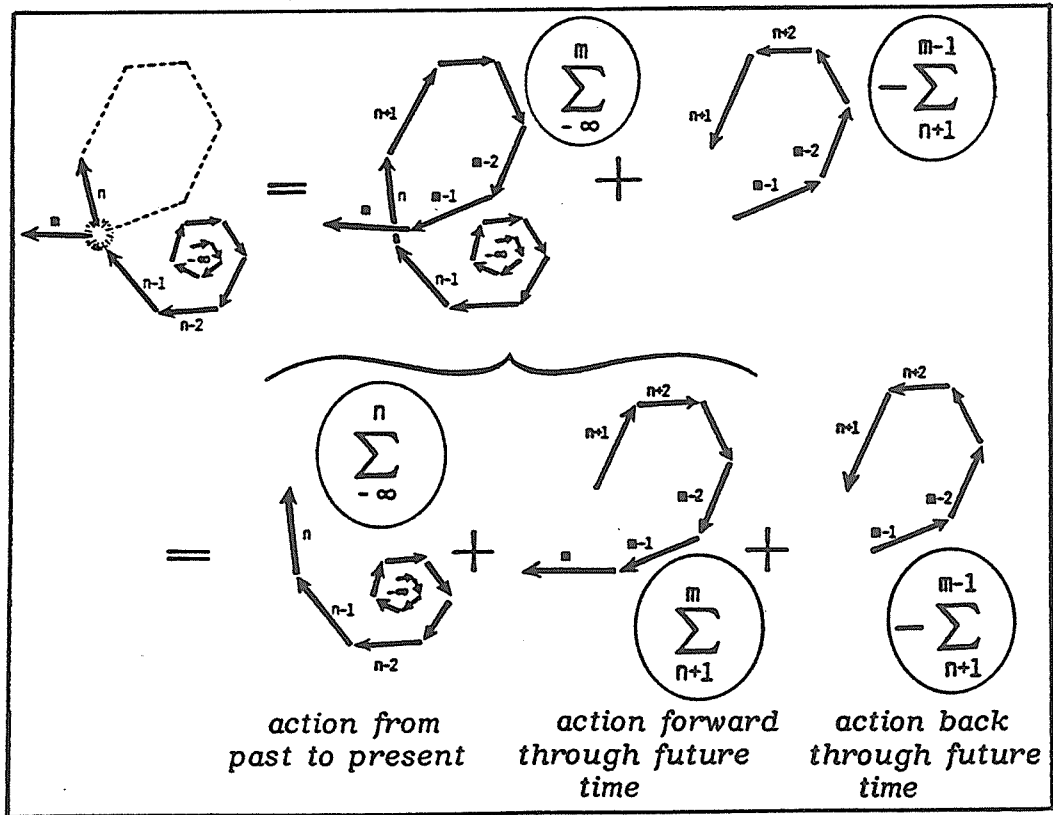
Whilst its clear that the outermost whorl of *Janospira's* trajectory traverses an elongated loop before returning to intersect itself, at the branch-point, we need to carefully think about the causality underlying the actual shell's growth processes. Initially the shell starts spiralling outward from somewhere near the pole ($\phi = -\infty$), eventually reaching the branchpoint ($\phi = n\Delta$) where it duly splits along both trajectory paths! But how can the trajectory at the branchpoint ($\phi = n\Delta$) be causally linked to the *FUTURE* outgoing pathway (located at $\phi = m\Delta$, for $m > n$)? 

It seems as if *Janospira*, at the instant of branching, "knew" (ahead of time) about the existence and location of a future portion of the clockspring trajectory ... even though the outermost whorl had not, at the time of branching, actually looped about to (and indeed, never ultimately would) physically create the future intersection-point. We are talking here, about *action with foreknowledge*, action outside the expected linear *Newtonian* time sequence, rather as if *an impending future event acted BACKWARD THROUGH (future) TIME to influence the present!*

Although highly unusual, this is not logically or physically impossible. *Lila Gatlin* ²⁵ has explained that

"Tolman's paradox forbidding time-reversed information transmission is nonexistent and rests only upon our ingrained thought processes involving, hidden, unnecessary assumptions ... although it will never be possible to design a system that transmits messages from the future upon request from the designer ... this alone does not exclude the possibility that intermittent unrequested messages from the future may sometimes reach a simple computer or, particularly, living organisms, which are masterful information processing systems ... ".

We can more rigorously analyze the causality underlying the branching of *Janospira* by recourse to discrete-growth analysis as in Section 1. We know that the vector-equation (1.6) is the correct approximation to the clockspring trajectory (3.29), particularly if Δ is small and n is large, in which case we can delete the Δ^2 term from (1.6) and think more in terms of (1.3) and a schematic vector-spiral diagram (as below):



The logical rigour of this vectorial analysis makes clearer the causal implications of *Janospira's* geometry. For branching to occur, in the present, there isn't just *Lila Gatlin's* action backwards through time [*minus the sum from $n+1$ to $m-1$*] ... there is also action forward through future time [*the sum from $n+1$ to m*] and we will name this second kind of temporal propagator after *Rupert Sheldrake*²⁶. We see that these acausal temporal fluxes seem to appear in pairs and, in the limit as growth-increment size Δ becomes infinitesimal, we can imagine the finite sums associated with the *Gatlin* and *Sheldrake* propagators becoming circle integrals.

The main thing to realize is that branching clocksprings arise naturally from the same theory that describes all other known shell geometries, and that examples such as *Janospira* occur in Nature. To be predicted by theory and observed in practice is a powerful metaphysical position: how one mentally reconciles the causal implications is a psychological problem.

EXAMPLE: *charged Lepton decay and Neutrino production.*

Instead of being a logical anomaly, the temporal propagators may possibly be a theoretical asset in various contexts. For example, the discrete analysis in Section 1 is not unlike the idea of a particle interacting with a potential according to quantum-field theoretical notions. Although dissipative, because of the exponentials, our Lagrangian (1.36) has a *Kline-Gordonish* look about it. In order to adapt it for the description of spinless uncharged particles we could start by selecting the matrix $\Omega = 0$, and mass $M^2 = -k$ which gives three pos-

sible cases $M = \pm 1 + i\alpha$ or $M = 0 \pm i\alpha$. Ignoring the complex component we might, for example, choose $M = 1$ to represent particles, $M = -1$ to represent antiparticles, and $M = 0$ to represent, say, neutrinos or photons. The complex component α can represent some other aspect of the particle's mass-energy: perhaps *spin* (so if we want to describe *leptons* we just set $\alpha = \frac{1}{2}$).

In any event, if we want to describe *charged* particles then we do not choose $\Omega = 0$ and this has the effect of making our *Kline-Gordon* equation "dissipative": perhaps empowering us to tackle *Bremßstrahlung* emissions of a decelerating charged particle in an external potential. Certainly the preserved z -component of angular momentum $\hat{z} \cdot \underline{r} \times \dot{\underline{r}}$, as in equation (2.53), does suggest a spin-direction due to an external field. If this is the case then we would expect our charged particles to travel in clock-spring trajectories such as (3.29) which sometimes *BRANCH*.

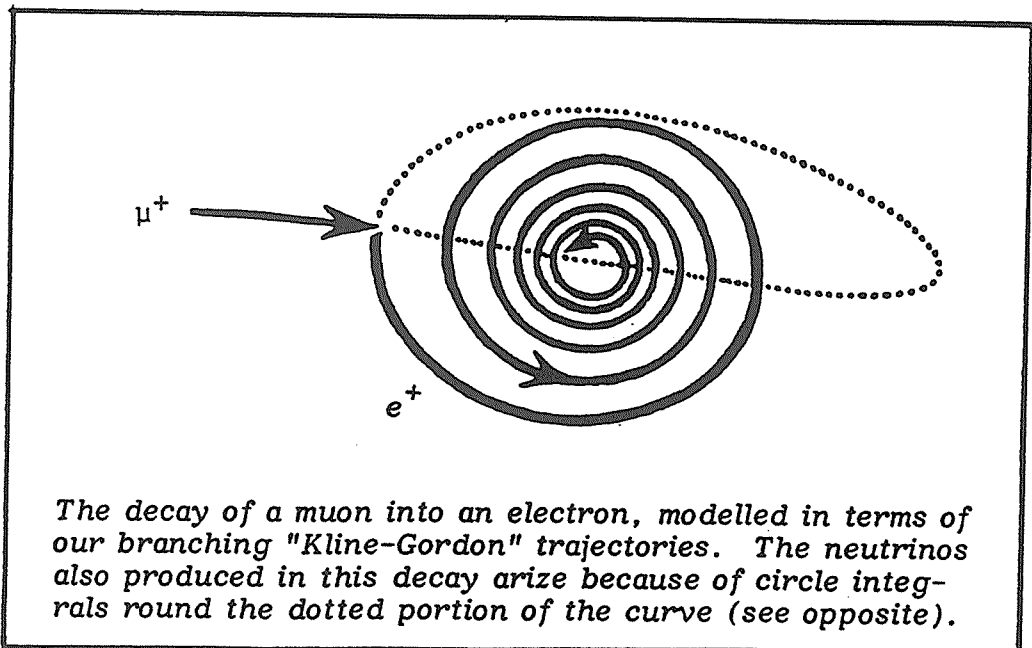
Of course the *Kline-Gordon* equation is normally only used to describe the behaviour of Bosons. But our equations aren't quite the normal version of the *Kline-Gordon* equation. We will persevere with our description of decaying charged Leptons, even if it only applies in the sense of an analogy: like the "clocksprings", "elastic conoids" and "archery-bows" that have been mentioned earlier. At worst the analogy will help us grasp the mathematical meaning, yet perhaps it is more than an analogy. It is for others to decide.

Consider the trajectories (3.14) and (3.15) which depend critically upon the value of λ . This reinforces our guess that trajectory curvature, λ , is related to the elementary particle's charge q .
A. Prosperetti's "zero-order approximation" to the "chronon"

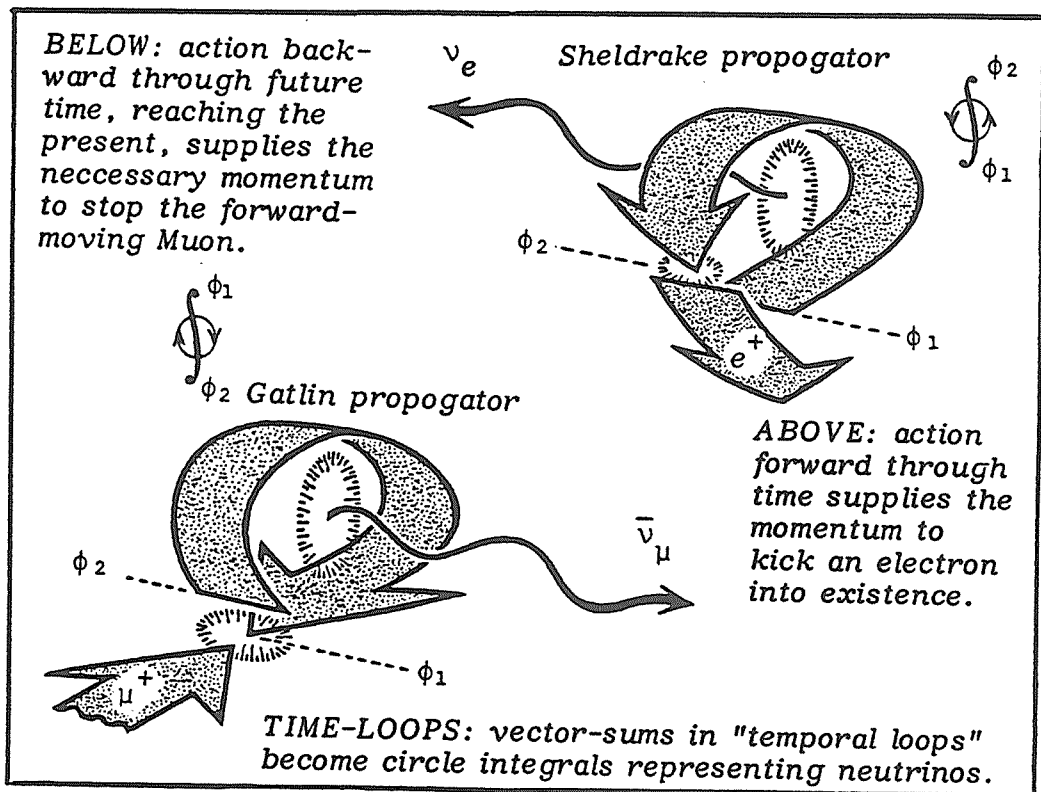
has a q^4 term, so perhaps λ is a simple function of q (see reference²⁷). The main point here, is that there are identifiable quantities in our Lagrangian which might correspond to mass, charge and spin of elementary particles. So let us consider the decay of a charged *MUON* (mass ≈ 105 MeV) into an identically charged *ELECTRON* (mass ≈ 0.5 MeV) in the process giving off a supposedly massless e -*NEUTRINO* and a μ -*ANTINEUTRINO*:

$$\mu^+ \rightarrow e^+ + \bar{\nu}_\mu + \nu_e \quad \dots (3.30).$$

The same branching trajectory that we used for the shell *Jano-spira* can now represent a muon entering from the left (see below) and decaying into an electron which, because of the external field, spirals inward losing kinetic energy. But what about the temporal propagators?



The *Gatlin* temporal propagator can be thought of as a flux, backward through future time, from ϕ_2 to ϕ_1 , supplying the necessary impulse to stop the forward momentum of the muon: it is a μ -*ANTINEUTRINO*. On the other hand, the *Sheldrake* temporal propagator can be thought of as a flux, forward through time, from ϕ_1 to ϕ_2 , supplying the downward momentum necessary to kick the electron into existence: thus it is an e -*NEUTRINO*. So, in our model, the muon-antineutrino is just a time-reversed electron-neutrino and, because they both exist outside the normal time-flow, they must both escape off at the speed of light carrying away recoil momenta. In this model, the time loops have physical meaning.



Perhaps a more modern interpretation of these matters would require us to view the incident muon as NOT being a pointlike *Newtonian* particle with precisely defined position and momentum: instead it might be considered as "smeared over a region of space-time". In which event the branchpoint may be viewed as a temporal version of *Young's* double-slit in the famous optical interference experiment. Thus the incident muon sends temporal propagators out from the branch-point, both backward and forward through time, along both possible paths round the trajectory-loop (*Huygen's Principle*). These two propagators pass frictionlessly through each-other, through space and time, meeting again at the branch-point where they interfere with what's left of the incoming muon that caused them ... thus giving rise to an explosive resonance of destructive interference that results in the observed lepton decay.

One final observation is that the torsion constant in Ω is zero for for zero-mass particles, but may increase to minus infinity for massive particles: thus torsion could supply a measure of *Lorentz-Fitzgerald* contraction of accelerating particles.

The Miraculous Shell:

This graceful spiral seashell,
evolutionary sculpture sublime,
is a clockspring of optimal strength,
and a record of passing time.

Its second-order surface,
round an axis doth twine,
exhibiting ripples and waves,
frozen in calcified lime.

Our extinct fossil Nipponite,
with coils all serpentine,
reconstructed as 'twas in life,
using super-computer time.

3.3 CONCLUSIONS:

In formulating the general problem of seashell geometries we have made the assumptions that 1) seashells grow by the accretion of finite increments thus requiring discrete mathematics for an appropriate description, 2) such growth is necessarily nonconservative thus requiring the use of mathematical methods outside the old-fashioned Lagrangian and Hamiltonian treatments familiar from conservative-stable (hence nongrowing) systems and 3) seashells require the use of novel techniques for their representation based upon the so-called conditions of variational self-adjointness.

These assumptions permitted the first quantitative representation of shell growth verifiable by computer simulation, thus separating personal beliefs and the mediaeval sophistry of the paleontological literature from true fundamental science. We have, after all, a unique second-order coupled differential equation (3.2) describing all of the several major categories of shell geometries found in the real world.

The earliest-published seashell Lagrangians had terms representing kinetic and potential energies but were confined entirely to real Euclidean space E^3 . The model was subsequently improved by lifting the whole problem into what is called ISO-EUCLIDEAN space ϕ^3 (named from the Greek isos-topos meaning preservation of the original configuration). The seashell Lagrangian still has the same form, with terms representing kinetic and potential energies, but they are complex instead of purely real (contrast references ¹² and ¹⁵). The resulting isogeometries seem to obey the axioms of familiar real-space and we made an effort to emphasise the Newtonian-ness of our mechanics in Section 1, yet isospace is in reality curved and forms that are different in normal Euclidean space may be unified in this more general geometry.

Does it matter if space is Euclidean or Iso-Euclidean? Yes, actually! We already know that shell growth trajectories are iso-euclidean but, if we tried to force them into purely Euclidean space, they would wrinkle and the shells would crack or explode. We can roughly convey this from the previously discussed case of *Nipponites mirabilis* (see pages 90 and 91). The first main step toward "Euclideanising" our iso-euclidean Lagrangian (1.36) would be to set

the exponential terms equal to unity (or at least some constant). Now this is a bit too radical for present purposes, but we can go most of the way toward this with minimal effort simply by examining the equations (3.26) and realising that the exponentials in our Lagrangian are of the form $e^{\lambda_1 \phi}$ and $e^{\lambda_2 \phi}$ hence the fastest-varying component in either case will be an ϵ^ϕ term. By setting this equal to a constant ϵ_0 we should start to "see" the effects of forcing iso-euclidean curves to exist in purely euclidean space.

We have already examined the effect of setting $\epsilon^\phi = \epsilon_0$ for the shell *Nipponites mirabilis*. It produces a loopy serpentine lissajous spiral that goes on in a self-similar fashion for ever as in case d) in the figure on page 91. Conversely, in the full iso-euclidean case where ϵ^ϕ is allowed to vary, the shell undergoes a transition from regular plani-spiral juvenile coiling, to increasingly serpentine meanders as in cases f) and g) in the figure on page 91 (see also *Nipponites occidentalis* on page 89).

In other words, the iso-euclidean trajectory of *Nipponites mirabilis* starts coiling in a regular planar spiral before eventually becoming serpentine. But if we force it to exist in a more "Euclideanish" space (by setting $\epsilon^\phi = \epsilon_0$) the whole curve meanders grossly from beginning to end, it is just like stuffing elastic piano-wire into a smaller box thereby forcing it to wrinkle more severely. And these substantial wrinkling effects arise from the rather gentle first approximation to the euclideanisation of an iso-euclidean curve. Full euclideanisation would, no doubt, produce much more dramatic effects ... perhaps with individual geometries exploding like bombs!

There are also other important consequences of isospace. Shells evolving in it appear, on first inspection, to be evolving in normal euclidean space and time in accordance with classical Newtonian dynamics: see equations (1.2), (1.9), (1.8), (1.7), (1.25) and (1.28). But we see from the Lagrangian (1.36) that all associative products must be written in the form $A*B = ATB$ where the iso-unit $T = e^{\frac{1}{2}\Omega\phi}$. But this exponential can equivalently be negative-definite thereby defining an isodual universe wherein time evolves backward, and energy is negative definite. Thus our discovery of action backward and forward through time at branchpoints, constitutes the first manifestation of isodual isogeometries ever seen in nature. The necessity for motion backward through time is precisely the geometric isoduality.

The isoeuclidean geometry was discovered by Prof. Ruggero Maria Santilli in *Hadronic J. Suppl.* 4A, 1 (1988) and was subsequently treated in detail in the monographs:

R. M. Santilli *Isotopic Generalizations of the Galilei and Einstein Relativities*, Hadronic Press, Palm Harbor, FL [1991], Second edition, Ukraine Academy of Sciences, Kiev (1994).

An outline of the isoeuclidean geometry and its application to sea shells is presented by Prof. Santilli in Part II of this volume

REFERENCES

- (1) ... *Francois*, Arch. Exp. G. (2), IX: 240 (1890).
H.S. Colton, Proc. Acad. nat. sci. Philad. 60: 1-30 (1908).
S. Warren, Nautilus (Philad.) 30: 66-68 (1916).
W.J. Clench, New. Engl. Nat. 3: 12-13 (1939).
H. Megelhaes, Ecol. Monogr. 18: 377-409 (1948).
- (2) *T.A. Cook*, "The Curves of Life", Const. & Co., Lond., 1914.
- (3) *C. Nielsen*, Ophelia (Int. J. Mar. Biol.) 13: 87-108 (1975).
- (4) *C. Illert*
 - i) Hawaiian Shell News (new ser. 246) 28(6): 9 (June 1980).
 - ii) Australian Shell News 27: 2 (1979).
 - iii) Of Sea and Shore 12(1): 8-10 (1981).
 - iv) Of Sea and Shore 11(3): 141-2 (1980).
 - v) Scientific Australian 4(7): 8-13 (August 1980).
- (5) *S.A. Wainwright*, Nature 224: 777-779 (1969).
- (6) *C. Illert*
 - i) Shells and Sea Life 16(6): 185 (1985).
 - ii) Shells and Sea Life 16(7): 200 (1985).
 - iii) Shells and Sea Life 16(8): 208 (1985).
 - iv) Shells and Sea Life 16(9): 210 (1985).

(California, USA, ISSN 0747-6078).
- (7) *K.I. Kanatani*, J. Comput. Phys. 53: 181-187 (1984).
R.A. LaBudde & D. Greenspan, J. Comput. Phys. 15: 134
(1974).
- (8) *D. Reverberi*, Z. Angew. Math. Phys. 36(5): 743-56 (1985).
- (9) rev. *H. Moseley*
 - i) Philos. Trans. R. Soc. London: 351-370 (1838).
 - ii) Philos. Mag. (ser. 3) 21(138): 300-305 (1842).
- (10) rev. *J.F. Blake*, Philos. Mag. (ser. 5) 6: 241-263 (1878).

- (11) *Sir D.W. Thompson*, "On Growth & Form", Cambridge University Press, 1917.
- (12) *C. Illert*, *Mathematical Biosciences* 63(1): 21-56 (1983).
- (13) *M.B. Cortie*,
 i) *Suid-Afrikaanse Tydskrif vir Wetenskap (South African Journal of Science)* 85(7): 454-60 (July, 1989).
 ii) *South African Journal of Science* 85(10): 621 (October, 1989).
- (14) *R.M. Linsley*,
 i) *Paleobiology* 3: 196 (1977).
 ii) *American Scientist* 66: 432 (1978).
 iii) *Lethaia* 14: 224 (1981).
 iv) *Malacologia* 20: 153 (1980).
- (15) *C. Illert*,
 i) *il Nuovo Cimento (series D)* 9(7): 791-814 (Luglio, 1987).
 ii) *il Nuovo Cimento (series D)* 11(5): 761-80 (Maggio, 1989).
 iii) *il Nuovo Cimento (series D)* 12(10): 1405-21 (Ottobre, 1990).
 iv) *il Nuovo Cimento (series D)* 12(12): 1611-32 (Dicembre, 1990).
- (16) *T. Okamoto*,
 i) *Journal of the Palaeontological Society of Japan* 36: 37-51 (1984).
 ii) *Palaeontology* 31(1): 35-52 (1988).
 iii) *Palaeontology* 31(2): 281-294 (1988).
 iv) *Palaeobiology* 14(3): 272-286 (1988).
- (17) *B. Runnegar*, *Lethaia* 10: 203 (1977).
E.L. Yochelson, *Lethaia* 10: 204 (1977).
V. Porkorny, *Lethaia* 11: 80 (1978).
- (18) *W.F. Bronsvoort & F. Klok*, *ACM Trans. on Graphics* 4: 291- (1985).
- (19) *C. Pickover*,
 i) *Computers in Physics*, September/October 1990, pages 460-467.
 ii) *Scientific American*, January 1991, pages 90-92 (col. pl. pp 91).
 iii) *IEEE Computer Graphics & Applications* 9(6): 8-11 (Nov. 1989).
- (20) *H. Meinhardt & M. Klinger*, *J. theor. Biol.* 126: 63-89 (1987).
- (21) *A.E. Boycott*, *Proc. Malacol. Soc. London* 18: 8- (1928).
- (22) *L. Lison*,
 i) *Bull. Acad. roy, Belg. Cl. Sci.* 28: 377-390 (1942).
 ii) *Mem. Inst. roy. Sci. nat. Belg. (series 2)* 34: 1-87 (1949).

- (23) C. Pickover,
 i) Leonardo 24(3): 361 (1991).
 ii) "Computers, Pattern, Chaos & Beauty", St. Martin, NY, 1990.
 iii) "Computers & the Imagination", St. Martin's Press, NY, 1991.
- (24) S. Weir, Analysis 48(4): 203-209 (Oct. 1988).
- (25) L. Gatlin, Int. J. theor. Phys. 19(1): 25-29 (1980).
- (26) R. Sheldrake, "New Science of Life", Blond & Briggs, 1981/3.
- (27) A. Prosperetti, il Nuovo Cimento (ser. B) 57(2): 253-68 (1980).
- (28) Y. Kawaguchi
 i) Computer Graphics (Proc. SIGGRAPH) 16(3): 223-232 (July 1982).
 ii) National Geographic, June 1989, pages 719-751.
 iii) Omni, November 1982, pages 110-115.
 iv) in J. Deken, "Computer Images", Thames & Hudson, 1983.
- (29) R.M. Santilli, "Foundations of Theoretical Mechanics, vol. 1",
 Texts & Monographs in Physics, Springer-Verlag, 1979.
- (30) G. Chen & D.L. Russel, Quarterly of Applied Mathematics.
 volume 39(4): pages 433-454 (January 1982).
- (31) C. Illert & C. Pickover,
 i) Underwater Geographic, 33: 27 (Nov/Dec 1991).
 ii) IEEE Computer Graphics & Applications, vol. 12(3), 18-22 (1992).
 iii) Australian Natural History, volume 24(1), pages 60-63 (1992)
- (32) H.B. Moore, National Geographic, 107(3): 427-34 (March, 1955).
- (33) M.J. Wang, il Nuovo Cimento (ser. A) 104(3): 449-52 (Marzo 1991).
- (34) C. Illert, the papers (¹⁵) (i) and (ii) were reprinted in full
in "SPIE Milestone Series" vol. 15: 12-33 (July, 1990).

ACKNOWLEDGEMENTS

The author would like to acknowledge in particular the two things which most influenced his initial work on seashell mathematics: they were Hilary B. Moore's lovely x-ray pictures of shells in the March 1955 "National Geographic" and Sir D'Arcy Wentworth Thompson's monumental book "On Growth and Form". Thanks must also go to Hans Mincham, a well known natural historian who was one of the author's primary-school teachers then, later, curator of invertebrates at the Adelaide Museum; and to the Malacological Societies of South Australia and Australia whose keen amateur membership and lively field-trips fostered a love for seashells. The research reported in this book summarises more than a quarter of

a century of investigation, from those beginnings in Adelaide, and during that time many people and institutions have been of assistance or made contributions. In particular the author would like to thank Bill Cornish, Leon Simon, Peter Tuebner and Ian McCarthy, then all of the Flinders University in South Australia, for guiding the first mathematical investigations culminating in the first publication on this topic in the early 1970's; also Charles Pearce and Ren Potts of Adelaide University for spurring the author on to find several new solutions to the second-order clockspring equation (3.1) in the mid 1970's and for making other valuable suggestions at the time; also Brian Martin, Rita and Gaetano Rando and John Laurent of Wollongong University for generally being supportive throughout the 1980's and assisting with proof-reading and occasional translations, and also Lachlan Chipman for some interesting discussions on philosophy. Special thanks must go to the Science Art Research Centre, and Robert Pope in particular, for encouragement and financial support, assistance with color printing, and also advice on how to draw scientific illustrations effectively with inkpen after the style of the late Frank Hampson whose work the author has always admired and measured his own achievements against. Winston Ponder of the Australian Museum, Sydney, was also supportive and helpful, and Daniela Reverberi proofread and checked the mathematics, and assisted with computer programs. The author is particularly grateful to "Of Sea and Shore" (in particular its editor Tom Rice), "Underwater Geographic" (in particular its editor Neville Coleman), "Il Nuovo Cimento", and the other journals which published his work, making it available to a wide international audience. He is also indebted to Akhlesh Lakhtakia and the international Society of Photo-optical Instrumentation Engineers (SPIE) for deeming the two papers ref.¹⁵ (1987, 1989) to be amongst "the most outstanding milestone achievements in a field of science" published in the international scholarly journals this century, and for reproducing them in full in the "SPIE Milestone Series", volume 15, in 1990.

Specific thanks must go to Mike Cortie of Randburg, South Africa; Yoichiro Kawaguchi of the Nippon Electronics College, Tokyo, Japan; Cliff Pickover of IBM, New York, USA; and Willem Bronsvooort, Koen van Ginkel and Rudi Way of the Delft University of Technology, Delft, the Netherlands; all of whom contributed computer-generated shell images for publication in this present book. In the captions M.C. means Mike Cortie; Y.K. means Yoichiro Kawaguchi; C.P. & C.I. means Cliff Pickover & Chris Illert; W.B. et al means Willem Bronsvooort, Koen van Ginkel and Rudi Way.

THE ILLUSTRATIONS:

M.C. contributed the black and white feltpen images on pages 20, 61, 62, 63, 64, 71.
W.B. et al contributed two images in color plates A and B.
Y.K. contributed six images on color plates F, G, H.
C.P. & C.I. contributed images on color plates A, C, D, E, F.
... all other artwork was hand-drawn by the author C.I.

ABOUT THE COLORED PLATES

Willem Bronsvooort, Koen van Ginkel and Rudi Way have generated the images of shells in plates A and B by sweeping an expanding generating-curve along various turbo-spiral trajectories, thereby creating hollow tubular surfaces. Cliff Pickover, on the other hand, has swept a solid-sphere along Chris Illert's various clockspring trajectories to generate the shells in plates C, D, E and F. If the growth-increments, along the trajectory, are too large we obtain a disjointed "beady" effect ... like a string of pearls (as in the top image on plate A) whereas, if the increments are too small, a very smooth surface results and we lose the ribbed effect that most shells display. Yoichiro Kawaguchi has alternated his generating objects (from cylinder to wedge, to cylinder to wedge, etc) thereby generating an amazing array of branching structures that resemble corals, bryozoans, plants and arteries as in plates F, G and H.

PART II:

**REPRESENTATION OF SEA SHELLS VIA
ISOTOPIC AND GENOTOPIC GEOMETRIES**

Ruggero Maria Santilli

The Institute for Basic Research

Box 1577

Palm Harbor, FL 34682, USA

Fax +1-813-934 9275

E-mail: ibrrms@pinet.aip.org

Abstract

An inspection of the pioneering research in theoretical conchology by Chris Illert [1] indicates that sea shells *appear* to be in our Euclidean space. However, the strict imposition of the axioms of the Euclidean geometry prohibits a quantitative representation of their growth, as verifiable via computer visualization, thus indicating that they belong to a geometry structurally more general than the Euclidean one. In this paper we show that a quantitative, computerizable representation of sea shell growth can be obtained via new geometries recently proposed by this author, called *isoeuclidean and genoeuclidean geometries*, which are based on two new branches of mathematical methods called *isotopic and genotopic*, respectively. Unlike other generalizations, such as Riemannian or Finslerian, the iso- and geno-euclidean geometries are based on the generalization of the trivial unit of the Euclidean geometry $I = \text{diag. } (1, 1, 1)$ into a nonsingular and well behaved 3×3 matrix \hat{I} with an unrestricted functional dependence on all needed local quantities, and then the reconstruction of the entire mathematical methods into a form admitting \hat{I} as the correct left and right unit. The isoeuclidean geometry emerges when \hat{I} is Hermitean and positive-definite, and the broader genogeometry emerges when \hat{I} is not Hermitean, thus requiring the necessary selection of a direction in time. The main result of this paper is that a structural generalization of the *unit* of space and time is requested for a quantitative representation, not only of the growth of seas shells, but also of their bifurcations. The same isotopic and genotopic methods are expected to be applicable to other biological structures. However, yet more complex biological structures are expected to require yet more general mathematical methods, such as the hyperstructures, which can be realized via genotopies with an infinite number of generalized units. In short, the view conveyed in this paper is that genuine advances in theoretical biology require fundamentally novel and advanced mathematical methods.

TABLE OF CONTENTS

1: Introduction, 112

- 1.A: The problem of sea shell growth in space, 112
- 1.B: The problem of sea shell growth in time, 115
- 1.C: Representation of sea shell growth via the isoeuclidean geometry, 116
- 1.D: Representation of sea shell growth via the genoeuclidean geometry, 124
- 1.E: A crucial distinction between physics and biology, 128

2: Elements of the isoeuclidean geometry, 129

- 2.A: Isotopies of the unit, 129
- 2.B: Isotopies of fields, 130
- 2.C: Isospaces, 132
- 2.D: Isotopies of the transformation theory, 140
- 2.E: Isotopies of functional analysis, 140
- 2.F: Isotopies of Lie's theory, 141
- 2.G: Isoeuclidean spaces, 142
- 2.H: Isoeuclidean geometry, 147
- 2.I: Operations in isoeuclidean geometry, 150
- 2.J: Connection with other noneuclidean geometries, 154
- 2.K: Isoeuclidean representation of sea shells, 156

3: Elements of the genoeuclidean geometry, 158

- 3.a: Genounits, 158
- 3.B: Genonumbers, 158
- 3.C: Genoeuclidean geometry, 160

Appendix A: Isotrigonometry, 162

Appendix B: Isospherical coordinates, 170

Appendix C: The universal isorotational symmetry of sea shells, 175

Acknowledgments, 183

References, 183

1: INTRODUCTION

1.1: The problem of sea shall growth in space. Let us consider one of the sea shells studied for the first time by C. Illert [1] via rigorous, quantitative, computerizable, mathematical representations, such as the *Angaria Delphinus* of Fig. 1.

By observing it in our hands, one generally has the impression that the shell belongs to our conventional, three-dimensional Euclidean space $E = E(r, \delta, R)$ with local coordinates $r = \{x, y, z\}$, metric $\delta = \text{diag. } (1, 1, 1)$ and invariant

$$r^2 = x x + y y + z z, \quad (1.1)$$

over the field $R_s = R_s(n, +, \times)$ of real numbers with conventional addition $n+n'$, multiplication $n \times n' = nn'$, and *multiplicative unit of space*

$$I_s = + 1, \quad I_s n = n I_s = n, \quad \forall n \in R, \quad (1.2)$$

where one can assume, e.g., the value $I_s = 1 \text{ mm}$.

The evolution in time would indicate that the *Angaria Delphinus* belongs to a space-time characterized by the Kronecker product $S = E(t, R_t) \times E(r, \delta, R_s)$, where t is our time and $R_t = R_t(t, +, \times)$ is the field of all possible times t , equipped with the conventional addition $t+t'$, multiplication $t \times t' = tt'$, and *multiplicative unit of time*

$$I_t = + 1, \quad I_t t = t I_t = t, \quad \forall t \in R_t, \quad (1.3)$$

where one can assume, e.g., the unit value $I_t = 1 \text{ sec}$. The total representation space would therefore be

$$S(t, r, I_t, I_s) = E(t, R_t) \times E(r, \delta, R_s), \quad (1.4)$$

Note that the sea shell is *at rest* in our hands. As such, the relativistic space-time, such as the Minkowski space M , is excluded (at any rate, if used, it would reduce to the space S under known contraction methods).

To our best knowledge, Illert [1] was the first to show that sea shall growth

cannot be quantitatively represented via conventional space (1.4). He reached this conclusion by noting that the Euler-Lagrangian equations could not be diagonalized in a real-valued space, but they could be diagonalized in a more general complex-valued space.

The problem of sea shell growth in space

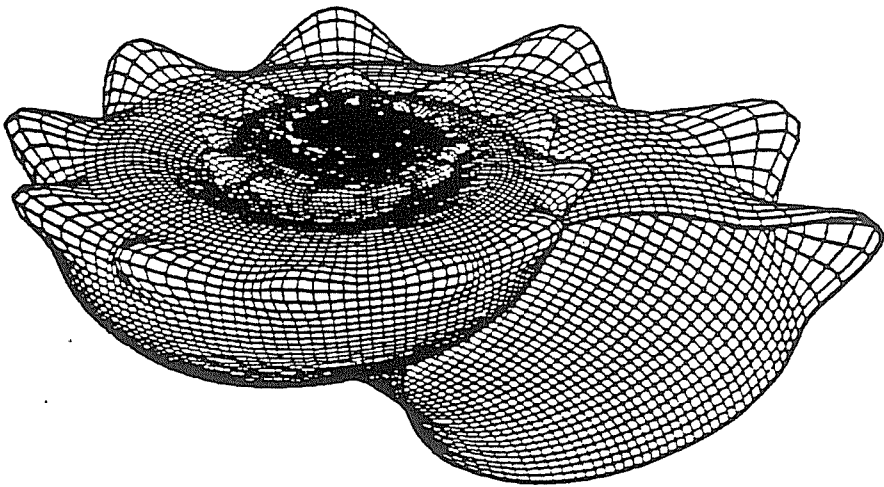


FIGURE 1: Reproduction of the computer visualization of the quantitative representations of growth of the *Angaria Delphinus* reached by Illert [1], p. 64.

The same result can be reached by noting that the strict imposition of the basic axioms of the Euclidean geometry render impossible any quantitative representation of the growth of sea shells such as the *Angaria Delphinus*. We are

here referring to a mathematical representation which is verifiable via computer visualization (since we cannot reproduce shells in laboratory) as well as via other means, such as their predictions.

In different terms, in holding a sea shell in our hands, the limited capabilities of our three Eustachian tubes give us the *impression* that it lives in our three-dimensional Euclidean space, while in reality the sea shell lives in a structurally more general space.

To illustrate the above occurrence, we introduce following Illert [1] a well behaved vector-value function $\xi(\phi) = \xi(\xi_x, \xi_y, \xi_z)$ of a characteristic angle ϕ representing the generic hypersurface of sea shell growth. A finite increment Δ of growth along such hypersurface can be characterized by

$$(d\xi/d\phi) d\phi = (d\xi/d\phi) d\phi \approx (d\phi/d\phi) \Delta \quad (1.5)$$

By recalling that the sea shell grows by finite increments, one must then consider a sufficiently large sequence of finite increments $\xi(\phi) \approx \xi(s\Delta) = \xi_s$ characterized by an integer, $s = 1, 2, \dots, n$, and a sufficiently small Δ , whose derivation is omitted here for brevity (see [loc. cit.], Sect. 1.2).

A quantitative mathematical representation of the sea shell growth then follows via the familiar Euler-Lagrange equations in a given Lagrangian $L(d\xi/d\phi, \xi)$ in the Euclidean space $E(\xi, \delta, R_s)$ whose explicit expression varies from shell to shell [loc. cit.].

The strict imposition of the axioms of the Euclidean geometry demands that the Lagrangian L must be *solely* constructed from *Euclidean scalar products* of the type

$$\xi \times \xi = \xi_x \xi_x + \xi_y \xi_y + \xi_z \xi_z. \quad (1.6)$$

and corresponding forms $(d\xi/dt) \times (d\xi/dt)$, $(d\xi/dt) \times \xi$. This restriction is deeply linked to the notion of *Euclidean distance* between two points 1 and 2

$$D_{\text{Euclidean}} = [(\xi_{1x} - \xi_{2x})^2 + (\xi_{1y} - \xi_{2y})^2 + (\xi_{1z} - \xi_{2z})^2]^{1/2}. \quad (1.7)$$

In fact, any use of products different than (1.6) implies a necessary, consequential,

generalized notion of distance and, therefore, a generalized geometry. The same result can be reached via a number of other ways, e.g., by imposing the fundamental symmetry of the Euclidean geometry, that under the conventional rotational symmetry $O(3)$.

The above restriction then implies that the only possible Lagrangians must have the structure

$$L = K_1 \left[\left(\frac{d\xi}{dt} \right) \times \left(\frac{d\xi}{dt} \right) \right]^n + K_2 \left[\left(\frac{d\xi}{dt} \right) \times \xi \right]^m + K_3 \left[\xi \times \xi \right]^p, \quad (1.8)$$

where n, m, p are positive integers and K_1, K_2 and K_3 are arbitrary constants.

It is then easy to see that *the strict implementation of the Euclidean geometry does not permit a quantitative mathematical representation of sea shell growth in a way conform with evidence*, as established by comparing Lagrangians (1.7) with those needed for actual representations [1].

1.B: The problem of sea shell growth in time. The need for a geometry structurally more general than our Euclidean geometry becomes compelling when time is added in the quantitative representation of sea shell growth.

In fact, the Euclidean geometry and "our" conventional notion of time are manifestly unable to provide *any* representation of the behaviour in the neighborhood of branching points (see Fig. 2). As a matter of fact, the Euclidean notions would imply clear inconsistencies, such as the prediction of an acausal behaviour which is against the physical evidence of the consistent growth of sea shells.

The above occurrence establishes beyond scientific doubt that sea shells evolve in time in a way structurally more general than our own perception of time and, in particular, in a way capable of mastering both directions of time. In fact, the behaviour of sea shells at bifurcation is one specific example of what is commonly referred to as a *space-time machine*, that is, the capability of moving in both space and time in a causal way (see recent studies [2,3] and references quoted therein).

The occurrence has fundamental implications for the selection of an appropriate geometry. In fact, in studying the problem of sea shall growth in *space* *only* one might have the impression that a quantitative representation can be

achieved via the transition from the three-dimensional Euclidean space $E(r, \delta, R_S)$ to the more general three-dimensional Riemannian space $\mathcal{R}(r, g(r), R_S)$; i.e., representing sea shall growth in a *curved space*.

The problem of sea shall growth in time

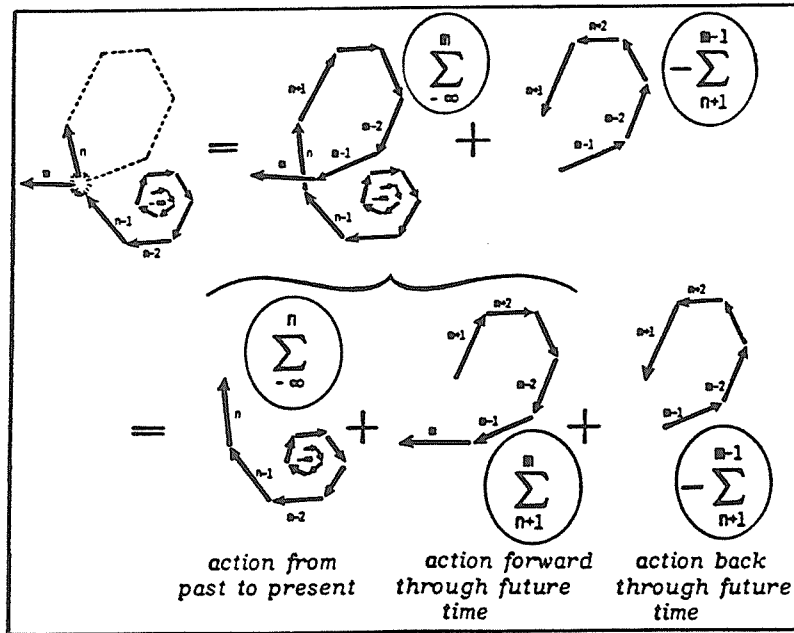


FIGURE 2: A reproduction of the figure of Illert [1], p. 95, on sea shall branching. As one can see, their mathematical representations requires three contributions: 1) one forward from past time; B) one forward to future time; and C) one backward from future time.

This possibility is immediately ruled out by the behaviour at bifurcations, trivially, because the "time arrow" in the transition from the Euclidean to the Riemannian geometry remains the same.

1.C: Representation of sea shell growth via the isoeuclidean geometry. In this

paper we show that a quantitative representation of sea shell growth is permitted by a generalization of the Euclidean geometry proposed by this author in 1988 under the name of *isoeuclidean geometry* (see monographs [4] for the classical treatment and [5] for their operator counterpart). For an in depth mathematical study of the new manifolds underlying the new geometry, here called *Tsagas isomanifolds*, see the recent memoirs by Tsagas and Sourlas [6].

The main idea of the new geometry is *the generalization of the fundamental Euclidean units of space and time*. Let $E(\xi, \delta, R_s)$ be the three-dimensional Euclidean space considered earlier. The covering *isoeuclidean space* is indicated $\hat{E}(\xi, \hat{\delta}, \hat{R}_s)$ and is characterized by the same functions ξ , and the lifting of the trivial space unit $\hat{1}_s = \text{diag. } (1, 1, 1)$ into a sufficiently smooth, bounded, nowhere singular and Hermitean, three-by-three dimensional matrix $\hat{1}$ with unrestricted functional dependence on time t , characteristic angle ϕ , hypersurface ξ and its derivatives of arbitrary order, $d\xi/d\phi$, $d^2\xi/d\phi^2$, as well as any needed additional quantity

$$I_s = \text{diag. } (1, 1, 1) \rightarrow \hat{1}_s(t, \phi, d\xi/d\phi, d^2\xi/d\phi^2, \dots) = \hat{1}^\dagger, \quad (1.9)$$

while, jointly, the Euclidean metric is lifted in the *inverse* amount

$$\delta \rightarrow \hat{\delta} = T_s \delta, \quad \hat{1} = T^{-1}, \quad (1.10)$$

The simplest possible realization is evidently the diagonal one,

$$T_s = \text{diag. } (T_x, T_y, T_z), \quad \hat{1}_s = \text{diag. } (T_x^{-1}, T_y^{-1}, T_z^{-1}). \quad (1.11)$$

The most general possible realization is however the *nondiagonal* form, in which case we shall write

$$T_s = \{ T_{ij}(t, \phi, \xi, d\xi/d\phi, \dots) \}, \quad \hat{1}_s = \{ T_{ij}(t, \phi, \xi, d\xi/d\phi, \dots) \}^{-1}, \quad \det T \neq 0, \quad (1.12)$$

where $i, j = x, y, z$.

A first implication of the isoeuclidean geometry is the generalization of the scalar product (1.6) into the form called *isoscalar product*, which assumed the

following diagonal or general forms

$$\xi \hat{\times} \xi = \xi_x T_x \xi_x + \xi_y T_y \xi_y + \xi_z T_z \xi_z, \quad (1.13a)$$

$$\xi \hat{\times} \xi = \sum_{ij=x,y,z} \xi_i T_{ij} \xi_j. \quad (1.13a)$$

and, consequently, of the distance (1.7) into the form called *isodistance*, which can also be in the diagonal and nondiagonal forms

$$\hat{D}_{\text{Isoeucl.}} = [(\xi_{1x} - \xi_{2x})^2 T_x + (\xi_{1y} - \xi_{2y})^2 T_y + (\xi_{1z} - \xi_{2z})^2 T_z]^{1/2}, \quad (1.14a)$$

$$\hat{D} = [\sum_{ij=x,y,z} (\xi_{1i} - \xi_{2i}) T_{ij}(t, \phi, \xi, \dots) (\xi_{1j} - \xi_{2j})]^{1/2}. \quad (1.14b)$$

The following property is evident from the completely unrestricted functional dependence of the quantities I and \hat{I} , but it is fundamental for the analysis of this paper.

Lemma 1.1: *The isoeuclidean geometry is "directly universal", that is, capable of representing all infinitely possible, integrodifferential deformations of the Euclidean geometry (universality), directly in the considered local variables (direct universality).*

Note that the above direct universality includes the Riemannian geometry as a particular case, although it applies to structurally more general geometries, those in which the basic unit is generalized.

It is then evident that the quantitative representations of sea shell growths achieved by Illert [1] are indeed a particular case of the isoeuclidean geometry. In fact, an inspection of the general Lagrangian of ref. [1], Eq. (1.36), p. 25, i.e.,

$$L = K_1 \frac{d\xi}{d\phi} e^{\Omega\phi} \frac{d\phi}{d\phi} + K_2 \xi e^{\Omega\phi} \xi \quad (1.15)$$

where Ω is another characteristic function of the sea shell considered studied in [1],

sect. 1.3, indicate the particular case in which the 3×3-dimensional isotopic element $T_S = (T_{ij})$ reduced to a one-dimensional scalar function,

$$\xi \hat{\times} \xi = e^{\Omega \phi} \xi \times \xi, \quad A_x = A_y = A_z = e^{-\Omega \phi}. \quad (1.16)$$

The understanding is that more general realizations in three dimension are possible.

The isoeuclidean geometry is the geometry of isospaces $\hat{E}(\xi, \delta, R_S)$. An outline is provided in the subsequent sections. The following main aspects should be indicated in these introductory words.

The new geometry is called an *isotopic image* of the original one because constructed via the so-called *isotopies*, which (according to the Greek meaning of the word) are methods capable of generalizing a given structure in an axiom-preserving way [4,5]. For instance, the trivial unit I and its generalization (1.8), called the *space isounit*, coincide at the abstract level because both nowhere singular, bounded and hermitean, and the same occurs for the scalar products (1.6) and (1.12), as well as for all other aspects. The inverse T of the isounit is called the *space isotopic element* [4,5].

A generalization of the unit implies a consequential, compatible generalization of the *totality* of the mathematical structure of the original geometry, as we shall briefly outline in the next section. For instance, conventional numbers $n, n' \in R_S(n, +, \times)$ are now inapplicable for the new geometry, and must be replaced by generalized numbers called *isonumbers*. Similarly, the conventional notion of angles is no longer applicable because the isoeuclidean space $\hat{E}(\xi, \delta, R_S)$ is a space with the most general known curvature depending not only on ξ (as for the Riemannian spaces), but also on their derivatives of arbitrary order. This implies the loss of the notion of intersecting straight lines which is necessary for the definition of angles. However, for reasons we shall see, generalized angles can indeed be defined, and result to have a rather intriguing connection with the representation of sea shells. Still in turn, this implies the loss of the conventional trigonometry, spherical coordinates, spherical harmonics, and all that. More generally, the lifting of the unit implies a compatible structural generalization of the entirety of functional analysis into a new discipline known as *functional isoanalysis* [4,5]. Any appraisal of the content of this paper via old notions of numbers, angles, trigonometric functions, etc. is generally plagued by a host of inconsistencies which

usually remain undetected.

Another fundamental property which should be known from these introductory words is that *the isoeuclidean geometry coincides with the conventional geometry at the abstract level* [4,5]. This is due to the fact that the metric is indeed generalized $\delta \rightarrow \hat{\delta} = T_S \delta$, but the unit is generalized in an amount *inverse* of the deformation, $1_S \rightarrow \hat{1}_S = T_S^{-1}$, thus implying no geometric change at all.

This property has far reaching implications for conchology because it implies that the shapes we actually see may in the final analysis not be the real ones.

The best way to see this occurrence is by studying one of the novel geometric notions of the isoeuclidean geometry, that of *isosphere*. Consider the deformations of the perfect sphere of radius 1 into a quadric characterized by the deformation of the original axes

$$k\text{-semiaxes} = 1 \rightarrow T_k, \quad (1.17a)$$

$$\xi_x \xi_x + \xi_y \xi_y + \xi_z \xi_z = 1 \rightarrow \xi_x T_x \xi_x + \xi_y T_y \xi_y + \xi_z T_z \xi_z = 1. \quad (1.17b)$$

Suppose now that, jointly, the units of the axis are lifted of an amount inverse of the deformation

$$\text{unit of } k\text{-semiaxis} \rightarrow T_k^{-1}. \quad (1.18)$$

Then the deformation of the original perfect sphere emerges only when projected in the original space $E(\xi, \delta, R_S)$ because, when represented in the appropriate isospace $\hat{E}(\xi, \hat{\delta}, \hat{R}_S)$, all possible surfaces remain indeed perfectly spherical.

Stated in different terms, all possible compact and noncompact quadrics in Euclidean space (including sphere, ellipsoids and paraboloids) are *unified* by the isoeuclidean geometry in the covering notion of isosphere. The capabilities of the new geometry for a quantitative representation of sea shell growth then follows.

The implications are rather deep. In fact, the isoeuclidean geometry indicates that the shape in which a sea shall appears to us, despite its complexity, can indeed be a perfect sphere in its own isospace. In fact, the deformation of the perfect sphere into the most general possible shape in the conventional space

$$E(\xi, \delta, R_s)$$

$$\sum_{k=x,y,z} \xi_k \xi_k = 1 \rightarrow \sum_{ij=x,y,z} \xi_i T_{ij}(t, \phi, \xi, d\xi/d\phi, d^2/d\phi^2, \dots) \xi_j, \quad (1.19)$$

implies the reduction of all infinitely possible shapes of sea shells to only one shape, the perfect sphere in isospace $\hat{E}(\xi, \delta, \hat{R})$. The differentiation between one shape and another is then given by *different isounits* (see Fig. 3).

The isoeuclidean geometry has also a direct implication on the *size* of a sea shell. In fact, if we measure, say, the volume of a sea shell, we can only claim that such a value is the volume of the *projection* of the sea shell in our space. In fact, the volume of the sea shell in its own space can be much bigger or smaller than our measured volume depending on whether the space isounit is much bigger or smaller than $l_s = +1$ mm.

The implication of the corresponding lifting of time are even more intriguing and far reaching. In this case the one-dimensional Euclidean space for time, $E(t, R_t)$, is lifted into the one-dimensional *isoeuclidean space* $\hat{E}(\hat{t}, \hat{R}_t)$ characterized by the lifting of the trivial value $l_t = +1$ into a well behaved, bounded, nowhere singular and real valued (because Hermitean) *scalar* function \hat{l} with an arbitrary functional dependence on all needed quantities

$$l_t \rightarrow \hat{l}_t(t, \xi, d\xi/d\phi, d^2/d\phi^2, \dots). \quad (1.20)$$

In turn, the field of ordinary time $R(t, +, \times)$ is lifted into the field $\hat{R}(t, +, \hat{\times})$ of the so-called *isotime*

$$t \rightarrow \hat{t} = t \hat{l}_t. \quad (1.21)$$

The abandonment of the unit $l_t = +1$ in favor of an arbitrary quantity $\hat{l}_t(t, \xi, \dots)$ then implies the possibility of a quantitative representation of sea shell bifurcations (Fig. 2). In fact, *while ordinary time has only the flow forward, isotime can arbitrarily flow forward or backward depending on the sign of its unit.*

The understanding of isotime require the knowledge that, in the same way

Unification of sea shell shapes into the isosphere

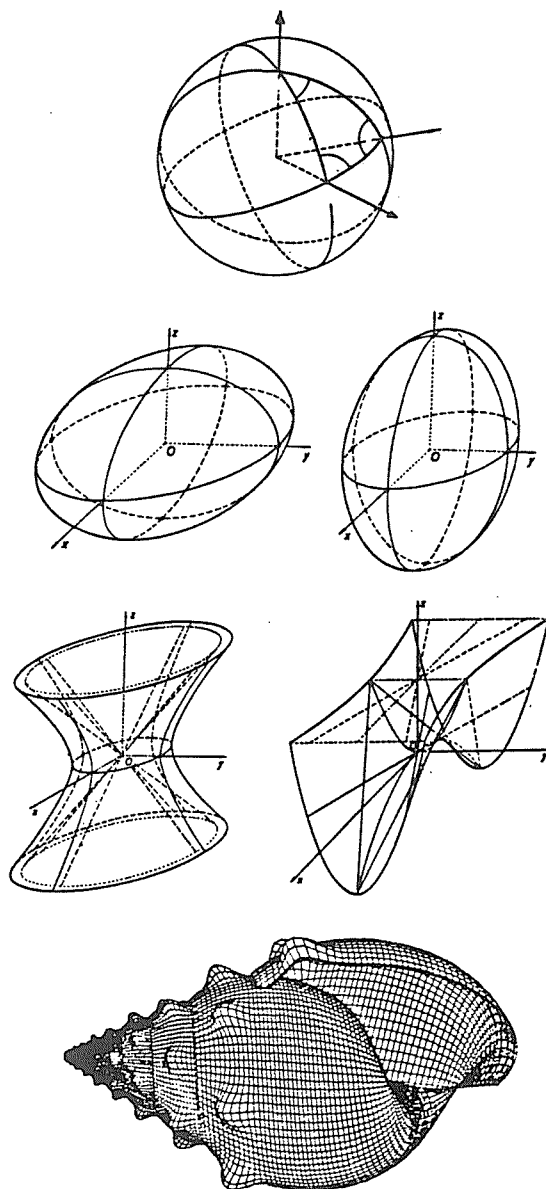


FIGURE 3: We present in this picture a geometric notion which is rather abstract, but which carries deep technical implications for quantitative mathematical studies of sea shells, the fact that *the infinitely possible different shapes of sea shells can be all*

unified into the perfect sphere in isospace, called the *isosphere*. The shapes as we see them with our senses occur only when they are projected in our space $E(\xi, \delta, R_S)$. However, when the shapes are represented in isospace $\hat{E}(\hat{\xi}, \hat{\delta}, \hat{R}_S)$ they are indeed reducible to the perfect sphere under a suitable generalization of the unit. In fact, all infinitely possible shapes in three-dimension can be reduced to the surface $S = \sum_{k=x,y,z} \xi_k T_k(t, \phi, \xi, \dots) \xi_k = 1$ with unrestricted functional dependence of the quantities T_k . It is then evident that, under the assumption of the generalized units T_k^{-1} per each of the three axes, the surface S is a perfect sphere in isospace, evidently because equivalent to the structure $\sum_{k=x,y,z} \xi_k \xi_k = 1$. As an illustration, all the quadrics of this figure and the *turbinate shell* reproduced from Illert [1], p. 20, are all unified in the isosphere (see the appendix for the isospherical coordinates). The reader should be aware that, at this level of generality, there is the emergence of basically novel geometric notions, such as the *sphere with singular unit* (which shall be identified in the next section as of topological class IV, see ref.s [4,5] for comprehensive studies), or the *sphere with a lattice for unit* (to be identified as of class V). These latter notions have no known application in physics, but they appear to have important applications in theoretical biology, evidently due to the much more complex structure of the latter over the former.

as it occurs for spheres and isospheres, *time and isotime coincide at the abstract level*. In particular, our ordinary time t remains completely unchanged, because all changes occur in the *unit* of time.

The way in which time reversal is characterized in the isoeuclidean geometry is also new. In fact, *time reversal* is usually characterized by mapping the value t into the value $-t$ *within the same space*. In isoeuclidean geometry, time inversion is characterized instead by a novel antiautomorphic map introduced by this author in 1985 under the name of *isoduality* [4,5]

$$\mathfrak{I}_t \rightarrow \mathfrak{I}_t^d = -\mathfrak{I}_t. \quad (1.22)$$

In this latter case, time t remains unchanged, and its unit changes sign. In particular, since the unit has changed, isoduality implies the map from the original space to a new space, called *isodual isospace*.

The implications of these novel geometric notions are intriguing indeed. As an example, we have the direct consequence that, when we see with our senses a sea shell in our hands, this does not necessarily means that it evolves with our own

time, because the isounits of time of the sea shell and our own may be different, in which case the two respective evolutions in time may be drastically different even under actual physical contact of our touching the sea shell.

Also, if we see a sea shell growing in time, it does not necessarily mean that it evolved forward to future time, because the *unit* of time can be negative in which case the shell moves backward in time.

Moreover, isogeometries directly affect the *age* of a sea shell. In fact, if we measure the life of a sea shell from its birth, on rigorous scientific grounds we can only claim that this is the age projected in our space-time. The life of the sea shell in its own space-time can be substantially different, that is, it can be much bigger or much smaller than our measured age, depending on whether \hat{t}_t is much bigger or smaller than $t_t = + 1$ sec.

Also, the generalization of the unit of time has the further direct consequence of implying a fully causal, theoretical prediction of the *space-time machine* [2,3], that is, the capability for an elementary particle of performing a closed loop in the forward time-like cone under a certain combination of fields due to matter and antimatter. The reader may be intrigued to know that this author patterned the space-time machine of ref. [3] along the time behaviour of sea shells at bifurcation of sea shells studied by Illert [1]. In fact, for all practical purposes, there is no technical difference between a particle traveling backward and then forward in time and the evolution of a sea shell at bifurcation as in Fig. 2.

1.D: Representation of sea shell growth via the geno-euclidean geometry. A further important characteristic of sea shell growth, fully identified in Illert [loc. cit.] is that they constitute *nonconservative systems*; that is, systems with quantities increasing (or decreasing) in time, as necessary for any growth. Therefore, sea shells constitute a structurally *irreversible* process, that is, an evolution forward in time which is inequivalent to the evolution backward in time.

The isoeuclidean geometry was conceived by this author for a geometrization of *reversible time evolutions*, as expected from the condition of Hermiticity of the basic isounit, $\hat{t}_s = \hat{t}_s^\dagger$. The same geometry can however also represent irreversible processes via the addition of an explicit time dependence such that

$$\hat{1}_s(t, \phi, \xi, \dots) \neq \hat{1}_s(-t, \phi, \xi, \dots) = \hat{1}. \quad (1.23)$$

However a true geometrization of the nonconservative–irreversible character of the sea shells can be better achieved via a further generalization of the isoeuclidean geometry proposed by this author in 1988 under the name of *genoeuclidean geometry* (see also ref.s [4] for classical treatments and ref.s [5] for operator counterpart).

These latter geometry is constructed via more general methods called *genotopies* which (from the Greek meaning of the word) does not preserve the original axioms but induced generalized axioms admitting the original ones as a particular case.

The main difference between the isoeuclidean and the genoeuclidean geometries is that, while the former is characterized by Hermitean units $\hat{1}_\alpha = \hat{1}_\alpha^\dagger$, $\alpha = s, t$, the latter are characterized by units which also also sufficiently smooth, bounded and nowhere singular, but now *nonhermitean*.

This latter generalization is particularly suited for the characterization of all possible directions of time (see Fig. 4 for more details):

1) *Evolution forward to future time*, denoted with the symbol $>$, with *forward time genounit* $\hat{1}_t^>$;

2) *Evolution forward from past time*, denoted with the symbol $<$ with *backward time genounit* $\hat{1}_t^<$ interconnected with the forward one via the conjugation $\hat{1}_t^< = (\hat{1}_t^>)^\dagger$;

3) *Evolution backward from future time*, denoted with the symbol $>^d = ->$, where d stands for the novel conjugation called *isoduality*, with *isodual forward time genounit* $\hat{1}_t^{>d} = -\hat{1}_t^>$;

4) *Evolution backward to past time*, denoted with the symbol $<^d = -<$, with *isodual backward genounit* $\hat{1}_t^{<d} = -\hat{1}_t^<$.

Correspondingly, we have four different space genoeuclidean geometries, two geometries for motion forward to future time and from past times usually denoted with the unified symbol

$$\langle \hat{E} \rangle (\xi, \langle \hat{\delta} \rangle, \langle \hat{R}_s \rangle), \quad \langle \hat{\delta} \rangle = \langle \hat{T}_s \rangle (t, \phi, \xi, \dots) \delta, \quad \langle \hat{1}_s \rangle = (\langle \hat{T}_s \rangle)^{-1}, \quad (1.24)$$

and two isoduals for motion backward in future or past time usually denoted with

the unified symbol

$$\langle E \rangle^d(\xi, \langle \delta \rangle^d, \langle R_s \rangle^d), \quad \langle \delta \rangle^d = \langle T_s \rangle^d(t, \phi, \xi, \dots) \delta, \quad \langle I_s \rangle^d = (\langle T_s \rangle^d)^{-1}, \quad (1.25)$$

where d represents isoduality, with the understanding that only one direction at the time can be used.

When the genogeometry is assumed to be of sufficient generality, the above distinction is lost and all four branches are unified into one single genoeuclidean geometry with smooth interconnections.

An axiomatic representation of the four possible time arrows

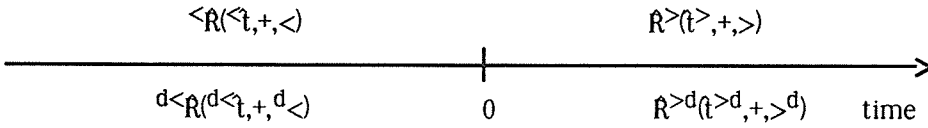


FIGURE 4: A schematic view of the axiomatization of time via genofields introduced by this author [4,5]: the genofield $R^>(\hat{t}^>, +, >)$ with genotime $\hat{t}^> = t I_t^>$, where t is the ordinary time, and genounit $I_t^> = (T_t^>)^{-1} \neq I_t^{>\dagger}$ for *motion forward to future time* $>$; the genofield $\langle R(\hat{t}, +, <)$ with genotime $\hat{t} = \langle I_t t$ and genounit $\langle I_t = (I_t^>)^{\dagger}$ for *motion forward from past time* $<$; the isodual genofield $R^d(\hat{t}^>, +, >^d)$ which is the image of $R^>(\hat{t}^>, +, >)$ under isoduality for *motion backward from future time* $>^d = ->$; and the isodual genofield ${}^d\langle R({}^d\hat{t}, +, {}^d<)$ which is the isodual image of $\langle R(\hat{t}, +, <)$ for *motion backward in past time* ${}^d< = -<$. As one can see, the main element of the characterization is the generalization of the trivial unit $+1$ sec of the current description of time into a (nonsingular and) *nonhermitean* quantity I_t which, being a one-dimensional scalar is a *complex function*. The conjugation under Hermiticity then allows the transition from motion forward to future time to motion forward from past time, while the conjugation under isoduality permits the representation of the remaining two directions. Note the fundamental point here: time t remains the *conventional real time* as ordinarily measured, and only its *unit* is generalized into a nonhermitean quantity. The simplest and most effective realization of the above notion of genotime is that by Jannussis [7] in which the genounit is the *complex quantity* $I_t = n + im$, $n, m \in R(n, +, \times)$. We therefore call *Jannussis complex times* the following four quantities $\hat{t}^> = t I_t^> = t(n + im)$, $\hat{t} = \langle I_t t$

$= t(n - im), \hat{t}^{>d} = t(-n - im), \hat{t}^{<d} = t(-n + im)$, where, again, t is the ordinary real time. Intriguingly, Jannussis' notion of complex time is a quantitative mathematical representation of the notion of absolute time in ancient Greek philosophy. This illustrates again, this time from a different perspective, that there may exist a very large difference between our *perception* of the evolution of sea shells in time, and that actually occurring in the reality.

The capability of the genogeometry to provide a geometrization of irreversible processes is now evident. In fact, the geometry is structurally irreversible because the units for motion forward and backward in time are different.

The genoeuclidean geometry appears to be the most effective for a quantitative study of sea shell growth as well as of other biological entities, because of their intrinsic irreversible structure, as well as their direct universality for all possible systems considered.

A yet more general mathematical formulation can be reached via the so-called *hypergeometries* (see the recent monograph by Vougiouklis [8]). In essence, in all the above models, the generalized unit acquires one specified realization for each given sea shell, i.e., the isotopic or genotopic elements are fixed, as in example (1.14) where $\omega = \exp(\Omega\phi)$. In the hyperstructures these quantities can acquire a finite or infinite *family* of values. The capability of representing even more complex biological structures is then consequential.

In particular, hypergeometries permit the introduction of new notions even more general than those of the iso- and geno-geometries. For instance, the fundamental notion of the latter geometries is that of isonumbers, that is, of "numbers with an arbitrarily generalized but fixed unit" from which the notion of isospace and genospaces are derived. In the transition to hypergeometries the latter notion is generalized into that of *hypernumbers*, that is, of "numbers with a family of generalized units".

In a scientific scene of this type it is recommendable to proceed in stages of increasing complexity. As a first step, we recommend the study of the isogeometries as outlined in Sect.s 2 (see ref.s [4,5] for detailed studies), and the initiation of its application to quantitative mathematical representations of sea shells growth as well as of other biological structures. As a second step we recommend the study of the more general geno-geometries as outlined in Sect. 3 (see

also ref.s [4,5] for more detailed treatments), and the reformulation of the results achieved via isogeometries within this more general setting. As a third step we then recommend the generalization of both isogeometries and genogeometries into hypergeometries via a family of units.

1.E: A crucial geometric distinction between physics and biology. The following additional comment is recommendable since these introductory words.

Physical systems at both the classical [4] and operator [5] levels have clearly show the separation of geometries with positive and negative isounits, in the sense that matter can be entirely represented with isogeometries with positive-definite unit, while antimatter can be entirely represented via their isoduals possessing negative-definite isounits.

Equivalently, we can say that stable elementary particles do not admit bifurcations, in the sense that they can only move forward in time, while antiparticles can only move backward in time (not so for the decay of unstable particles, see Illert [1], p. 98).

This distinction is lost in the transition to biological structures such as a sea shell because, as clearly illustrated by Fig. 2, *each sea shell requires the use of both, geometries with positive-definite and negative-definite isounits.*

From a geometric standpoint, such a distinction is so fundamental that can indeed be used as one way to differentiate between physical and biological structures.

To conclude this introductory words, without any claim of completeness or unicity, in this paper we suggest quantitative treatments of sea shells growth via the hierarchy of generalized geometries of increasing complexity and methodological needs

$$\text{isogeometries} \subset \text{genogeometries} \subset \text{hypergeometries.} \quad (1.26)$$

Such hierarchy should not be surprising to the scholar with young mind. In fact, the complexity of biological structures much more difficult than the sea shell growth, such as the code of a DNA, is such to be simply beyond our comprehension at this time, thus requiring mathematical methods simply beyond our current

imagination, let alone knowledge. The above chain of generalized geometries is expected to be only the *beginning* of further generalizations expected for a true understanding of complex biological structures such as a DNA..

Despite the important achievements reached by mankind until now in biology, we can safely state that our current mathematical and theoretical understanding of biological structures is at its first infancy.

2: ELEMENTS OF ISOEUCLIDEAN GEOMETRY

One of the most insidious aspects for a researcher first approaching isotopic methods is the use of conventional mathematical thinking, because it leads to a number of inconsistencies which remain generally undetected.

In fact, the transition from conventional to the isotopic methods requires a simple yet significant generalization of *all* conventional mathematical tools, which is somewhat reminiscent of, but broader than the mathematical generalization needed in the transition from Newtonian to quantum mechanics. In this section we shall first outline the basic elements of isotopies and then pass to the outline of the isogeometries.

2.A. Isotopies of the unit. The fundamental isotopies from which all others can be uniquely derived are the liftings $I \rightarrow \hat{I}$ of the unit of the current formulation. These liftings were classified by Kadeisvili [9] into:

Class I (generalized units that are smooth, bounded, nondegenerate, Hermitean and positive-definite, characterizing the *isotopies* properly speaking);

Class II (the same as Class I although \hat{I} is negative-definite, characterizing *isodualities*);

Class III (the union of Class I and II);

Class IV (those of Class III plus those with singular isounits); and

Class V (unrestricted generalized units, such as discrete structures, discontinuous functions, etc.).

All isotopic structures identified below also admit the same classification. In this paper we shall generally study isotopies of Class III because they are the

most effective for theoretical conchology, as pointed out in Sect. I. Classes IV and V are vastly unexplored at this writing.

2.B. Isotopies of fields. The fundamental quantities underlying all isotopic theories are given by a novel notion of numbers introduced by this authors in 1980 (for recent physical studies see monographs [4,5], for recent mathematical studies see ref. [10]). Let $F(a,+, \times)$ represent ordinary fields, such as the fields of real R or complex C numbers (the quaternions and octonions [10] will be ignored for simplicity), with generic elements a , addition $a_1 + a_2$, multiplication $a_1 a_2 = a_1 \times a_2$, *additive unit* 0 , $a + 0 = 0 + a \equiv a$, and *multiplicative unit* 1 , $a 1 = 1 a \equiv a \forall a, a_1, a_2 \in F$.

The lifting $I \rightarrow \hat{I}$ requires, for necessary compatibility, a generalization of the conventional associative multiplication ab into the so-called *isomultiplication*

$$a b = a \times b \rightarrow a * b = a T b, \quad T = \text{fixed.} \quad (2.1)$$

where the quantity T is called the *isotopic element*. Whenever $\hat{1} = T^{-1}$, $\hat{1}$ is the correct left and right unit of the new theory, $\hat{1} * a = T^{-1} T a = a * \hat{1} = a T T^{-1} = a, \forall a \in F$, in which case (only) $\hat{1}$ is called the *isounit*. In turn, the liftings $I \rightarrow \hat{I}$ and $\times \rightarrow *$, imply a generalization of the very notion of numbers and of fields into the structure

$$\hat{F} = \{(\hat{a}, *) \mid \hat{a} = a \hat{1}, \quad a = n, c, q \in F, \quad \times \rightarrow * = \times T \times, \hat{1} = T^{-1} = \text{isounit}\}, \quad (2.2)$$

called *isofields*, with elements $\hat{a} \in \hat{F}$ called *isonumbers* [10].

All conventional operations are evidently generalized in the transition from numbers to isonumbers. In fact, we have:

$$\begin{aligned} a + b &\rightarrow \hat{a} + \hat{b} = (a + b) \hat{1}; & a_1 \times a_2 &\rightarrow \hat{a}_1 * \hat{a}_2 = \hat{a}_1 T \hat{a}_2 = (\hat{a}_1 a_2) \hat{1}; \\ a^{-1} &\rightarrow \hat{a}^{-1} = a^{-1} \hat{1}; & a / b = c &\rightarrow \hat{a} \gamma \hat{b} = \hat{c}, \quad \hat{c} = c \hat{1}; & a^{\frac{1}{2}} &\rightarrow \hat{a}^{\frac{1}{2}} = a^{\frac{1}{2}} \hat{1}^{\frac{1}{2}}, \end{aligned} \quad (2.3)$$

etc. Thus, conventional squares $a^2 = aa$ have no meaning under isotopy and must be lifted into the *isosquare* $\hat{a}^{\hat{2}} = \hat{a} * \hat{a}$. The *isonorm* is

$$\uparrow \hat{a} \uparrow = (\bar{a} a) \mathbb{I} = |a| \mathbb{I} \in \mathbb{F}, \quad (2.4)$$

where \bar{a} denote the conventional conjugation, $|a|$ the conventional norm, and \mathbb{I} is positive-definite for isofields of Class I but of undefined character for Class III.

The isotopic character of the lifting $\mathbb{I} \rightarrow \hat{\mathbb{I}}$ is then confirmed by the fact that the isounit $\hat{\mathbb{I}}$ verifies all axioms of \mathbb{I} . In fact,

$$\mathbb{I} * \hat{\mathbb{I}} * \dots * \hat{\mathbb{I}} \equiv \mathbb{I}, \quad \mathbb{I} \hat{\mathbb{I}} \mathbb{I} \equiv \mathbb{I}, \quad \hat{\mathbb{I}}^2 \equiv \mathbb{I}, \quad \text{etc.} \quad (2.5)$$

The *isodual isofields* are characterized by the *isodual map* $\mathbb{I} \rightarrow \mathbb{I}^d = -\mathbb{I}$ and are given by the structures

$$\mathbb{F}^d = \{(\hat{a}^d, +, *^d) \mid \hat{a}^d = a \mathbb{I}^d, \ a = n, c, q \in \mathbb{F}, \ * \rightarrow *^d = \times T^d \times, \ T^d = -T, \ \mathbb{I}^d = -\mathbb{I}\}, \quad (2.6)$$

in which the elements, called *isodual isonumbers*, are given by $\hat{a}^d = -\hat{a}^\dagger$. Thus, for real numbers we have $n^d = -n$ while for complex numbers we have $c^d = -\bar{c}$. Note that the imaginary unit is *isoselfdual*, i.e., invariant under isoduality, $i^d = -\bar{i} \equiv i$, while the conjugation of a complex number is $(n + i \times m)^d = n^d + i^d \times^d m^d = -n + im$. The *isodual isosum* is given by $\hat{a}^d + \hat{b}^d = -(a + b) \mathbb{I}$, while for the *isodual isomultiplication* we have

$$\hat{a}^d *^d \hat{a}^d = \hat{a}^d T^d \hat{a}^d = -\hat{a}^d T \hat{a}^d = -\hat{a} T \hat{a}. \quad (2.7)$$

An important property of the isodual isofields of Class II is that their norm is *negative-definite* because characterized by

$$\uparrow \hat{a}^d \uparrow^d = |a| \mathbb{I}^d = -\uparrow \hat{a} \uparrow. \quad (2.8)$$

The latter property has the nontrivial implications that *physical quantities defined on an isodual isofield, such as time, energy, etc., are negative-definite*.

One can then begin to see the inconsistencies in the use of conventional mathematical thinking under isotopies. For instance, statements such as "two multiplied by two equals four" are correct for conventional methods, but they

generally have no mathematical sense for the covering isotopic methods, evidently because they lack the identification of the basic unit as well as of the multiplication.

Note that the isomultiplication of an isonumber \hat{a} by a quantity Q coincide with the conventional multiplication, $\hat{a} * Q = aT^{-1}TQ \equiv aQ$, and the same occurs for isodual isonumbers $\hat{a}^d *^d Q \equiv aQ$. This may be a reason why isonumbers and their isoduals were *not* discovered in pure mathematics, but rather in physics. In fact, they originate from a novel interpretation of antiparticles, as recalled in Sect. 1 [4,5].

The *theory of isonumbers* is today sufficiently well established new branch of mathematics, and includes:

- (A) **ordinary numbers** with unit 1;
- (B) **isonumbers** with isounits of Class I, $\hat{1} > 0$;
- (C) **isodual numbers** with isodual unit $1^d = -1$;
- (D) **isodual isonumbers** with isounits of Class II, $\hat{1}^d < 0$

(that is, we have *four* different types of real numbers and complex numbers).

The theory of isonumbers needed in theoretical conchology is that of Class III which encompasses and unified all the preceding four types.

In addition, the theory of isonumbers includes generalized numbers of Class IV (this is a basically new notion of number with singular isounits) and Class V (another new type of numbers with distributions or discontinuous functions as isounits) which are not studied in this paper for brevity. The reader should be aware that the distinction between real and complex numbers is lost under isotopies because all possible numbers are unified by the isoreals of class III owing to the freedom in the selection of the isounit $\hat{1}$ [11].

Note also that the lifting $a \rightarrow \hat{a} = a\hat{1}$ is *necessary* for \hat{F} to preserve the axioms of F whenever the isounit $\hat{1}$ is not an element of the original field F , as generally occurring in conchology (for details, see [10]). This implies that the "numbers" suggested for use in theoretical conchology have an *nonlinear-integral* structure.

2.C: Isospaces. Let $F(a, +, \times)$ be a field of real or complex numbers with elements a, b, \dots , conventional sum $a+b$ and multiplication $a \times b = ab$ and related additive and multiplicative units 0, and 1, respectively. A *linear space* $V(\alpha, F)$ [12] is a set of elements $\alpha, \beta, \gamma, \dots$ over a field $F(a, +, \times)$ such to verify the following laws for

all $a, b, c \in F$ and $\alpha, \beta, \gamma \in S$

$$a + b = b + a; \quad a + (b + c) = (a + b) + c; \quad (2.9a)$$

$$\alpha(\beta a) = (\alpha\beta)a; \quad \alpha(a + b) = \alpha a + \alpha b; \quad (a + b)\alpha = \alpha a + \beta a; \quad (2.9b)$$

and, for every $\alpha \in V$, there exists an element $-\alpha$ such that

$$\alpha + (-\alpha) = \alpha - \alpha = 0; \quad (2.10)$$

From the above structural lines one can see the following:

Definition 2.1 [5]: *Given a linear space $V(\alpha, F)$ over a field $F(a, +, \times)$, the Class I "isotopes" $\hat{V}(\alpha, \hat{F})$ of V called "isolinear spaces", are the same set of original elements $\alpha, \beta, \gamma, \dots \in V$ although defined over the isofield of Class I $\hat{F}(\hat{a}, +, *)$ with isomultiplication $\hat{a} * \hat{b} = \hat{a} T \hat{b}$, additive unit 0 , and multiplicative unit $\hat{1} = T^{-1}$, such to preserve all original axioms of V , i.e.,*

$$\hat{a} * (\hat{b} * \alpha) = (\hat{a} * \hat{b}) * \alpha, \quad \hat{a} * (\alpha + \beta) = \hat{a} * \alpha + \hat{a} * \beta, \quad (2.11a)$$

$$(\hat{a} + \hat{b}) * \alpha = \hat{a} * \alpha + \hat{b} * \alpha, \quad \hat{a} * (\alpha + \beta) = \hat{a} * \alpha + \hat{a} * \beta, \quad (2.11b)$$

for all $\alpha, \beta \in \hat{V}$ and $\hat{a}, \hat{b} \in \hat{F}$. The "isodual isolinear spaces" $\hat{V}^d(\alpha, \hat{F}^d)$ are Class II images of $\hat{V}(\alpha, \hat{F})$ under the isoduality

$$\hat{1} \rightarrow \hat{1}^d = -\hat{1}, \quad (2.12)$$

and, as such, are defined over an isodual isofield $\hat{F}^d(n^d, +, *^d)$ of Class II with negative-definite isounit $\hat{1}^d = -\hat{1}$. The "isolinear spaces of class III" are the union of those of Class I and II.

A fundamental property emerging from the above isotopies is the *preservation of linearity in isospace*. As a matter of fact, systems which are nonlinear in conventional spaces, can be turned into an *identical* form which

regains linearity in isospace [5].

This property has important implications for the applications of the isotopic methods, e.g., computer visualization, solution of the equations, etc. In fact, we learn that such methods can turn notoriously difficult nonlinear systems into much more manageable isolinear systems (see later on for more details).

Note also that the field is lifted but the elements of the original vector space remain unchanged. The interested reader can prove as an exercise a number of properties of isolinear spaces and their isoduals via a simple isotopy of the corresponding properties of linear spaces [12]. One which is particularly relevant for these studies follows from the invariance of the elements $\alpha, \beta, \gamma, \dots$ under isotopy as well as under isoduality and can be expressed as follows.

Proposition 2.1 [5]: *The basis of a (finite-dimensional) linear space remains unchanged under isotopy up to possible renormalization factors.*

The above property essentially anticipates the fact that, when studying the isotopies of conventional Lie symmetries, we shall expect no alteration of its basis because a Lie algebra is, first of all, a linear space. In turn, this implies that isotopies preserves the *conventional* generators.

The elements $\alpha, \beta, \gamma \in V$ are called *vectors*. The same quantities when belonging to the isotopes \hat{V} are called *isovectors*. Note the existence of the simpler *isodual vector spaces* $V^d(\alpha, F^d)$ defined over the isodual of a conventional (rather than isotopic) field with *isodual vectors*. Thus, given elements α, β, γ , can be vector, or isovectors, or isodual isovectors depending on the space (i.e., the unit) in which they are defined.

A *metric space* [12] hereon denoted $S(x, g, F)$ is a (universal) set of elements x, y, z, \dots over the fields $F = F(n, +, \times)$ equipped with a nonsingular, and Hermitean map (function) $g: S \times S \Rightarrow F$, such that:

$$g(x, y) \geq 0, \quad (2.13a)$$

$$g(x, y) = g(y, x) \quad \forall x, y \in S; \quad g(x, y) = 0 \text{ iff } a = 0 \text{ or } b = 0 \text{ or both.} \quad (2.13b)$$

$$g(x, y) \leq g(x, z) + g(y, z), \quad \forall x, y, z \in S. \quad (2.13c)$$

A *pseudo-metric space*, hereon also denoted by $S(x,g,F)$, occurs when the above first condition is relaxed. Finally, recall that metric or pseudo-metric spaces over the reals $F = \mathbb{R}$ are used in contemporary physics to characterize our physical space-time. Spaces over the complex numbers, such as the complex Hermitean Euclidean spaces $E(z,\delta,C)$, are used for unitary symmetries, such as $SU(2)$ or $SU(3)$.

Suppose that the space $S(x,g,F)$ is n -dimensional, and introduce the components $x = (x^i)$, $y = (y^j)$, $i = 1, 2, \dots, n$. Then, the familiar way of realizing the map $g(x, y)$ is that via a (Hermitean) *metric* g of the form

$$g(x,y) = x^i g_{ij} y^j, \quad \text{Det. } g \neq 0, \quad g = g^\dagger. \quad (2.14)$$

The axiom $g(x, y) > 0$ for metric spaces then implies the condition that g is positive-definite, $g > 0$.

A celebrated physical example of metric spaces is the Euclidean space in which case the metric is $g = \delta = \text{diag. } (1, 1, 1)$. Pseudo-metric spaces of primary physical relevance are the Minkowski space (with metric $g = \eta = \text{diag. } (1, 1, 1, -1)$), and the $(3+1)$ -dimensional Riemannian spaces with metric $g = g(x)$.

The simplest possible way of constructing an infinite family of isotopes of $S(x,g,F)$ is by introducing n -dimensional isounits of Class I

$$\hat{1} = (\hat{1}_i^j) = (\hat{1}_i^j), \quad i, j, r, s = 1, 2, \dots, n. \quad (2.15)$$

with isotopic elements

$$T = \hat{1}^{-1} = (T_i^j) = (T_i^j), \quad (2.16)$$

Then, we can introduce the notion of the *isomap* $\hat{g}: \hat{S} \times \hat{S} \Rightarrow \hat{F}$ with realization

$$\hat{g}(x, y) = (x^i \hat{g}_{ij} y^j) \hat{1} \in \hat{F} \quad (2.17)$$

where the quantity

$$\hat{g} = T g = (T_i^k g_{kj}), \quad (2.18)$$

is the *isometric* [4,5].

The *basis* $e = (e_i)$, $i = 1, 2, \dots, n$ of an n -dimensional space $S(x, g, F)$ can be defined via the rule

$$g(e_i, e_j) = g_{ij}. \quad (2.19)$$

Then, the *isobasis* is characterized by

$$\hat{g}(\hat{e}_i, \hat{e}_j) = \hat{g}_{ij}. \quad (2.20)$$

The above isotopic generalizations can be expressed as follows.

Definition 2.2 [5]: The “isotopic liftings” of Class I of a given, n -dimensional, metric or pseudometric space $S(x, g, F)$ over the field $F = F(a, +, \times)$ are given by the infinitely possible “isospaces” $\hat{S}(x, \hat{g}, \hat{F})$ characterized by: a) the same dimension n and the same local coordinates x of the original space; b) the lifting of the original metric g into one of the infinitely possible nonsingular, Hermitean “isometric” $\hat{g} = Tg$ with isotopic element T of Class I depending on the local variables x , their derivatives \dot{x} , \ddot{x} , ... with respect to an independent variable t , and any needed additional quantity

$$g \rightarrow \hat{g} = Tg, \quad (2.21a)$$

$$T = T(s, x, \dot{x}, \ddot{x}, \dots), \quad \det T \neq 0, \quad T^\dagger = T > 0, \quad (2.21b)$$

$$\det. g \neq 0, \quad g = g^\dagger, \quad (2.21c)$$

and c) the lifting of the field $F(a, +, \times)$ into an isotope of Class I $\hat{F}(\hat{a}, +, *)$ whose isounit $\hat{1}$ is the inverse of the isotopic element T , i.e.,

$$\hat{1} = T^{-1}, \quad (2.22)$$

with "isocomposition"

$$(x, \hat{y}) = (x, T y) \hat{1} = (T x, y) \hat{1} = \hat{1} (x, T y) = (x^i \hat{g}_{ij} y^j) \hat{1} \in \hat{F}. \quad (2.23)$$

The "isodual isospaces" of Class II $\hat{S}^d(x, \hat{g}^d, \hat{F}^d)$ are given by the image of $\hat{S}(x, \hat{g}, \hat{F})$ under isoduality and are defined by the map

$$\hat{g} \rightarrow \hat{g}^d = T^d g, \quad T^d = -T, \quad (2.24a)$$

$$\hat{1} \rightarrow \hat{1}^d = (T^d)^{-1} = -\hat{1}, \quad (2.24b)$$

with "isodual isocomposition" in \hat{F}^d

$$(x, \hat{y})^d = (x, T^d y) \hat{1}^d = (T^d x, y) \hat{1}^d = \hat{1}^d (x, T^d y) = (x^i \hat{g}_{ij}^d y^j) \hat{1}^d \in \hat{F}^d. \quad (2.25)$$

The "isospaces of Class III" are the unions of those of Class I and II.

A few comments are now in order. The first and geometrically most dominant aspect is that, because of the unrestricted functional dependence of the isotopic element T , the isometrics $\hat{g} = Tg$ are generally of *nonlinear-integral* type.

Thus, the isotopic liftings $\hat{S}(x, g, F) \rightarrow \hat{S}(x, \hat{g}, \hat{F})$ imply a *nonlinear and integral generalization of the original linear-local space*. In particular, isospaces require a suitable integral topology for their rigorous treatment which has been studied by Tsagas and Sourlas [6].

A simple approach to this new topology is the following. All nonlinear and integral terms are embedded, by construction, in the isounits $\hat{1}$. On the other hand, topologies are known to be insensitive to the functional dependence of their own units. This implies the particular integro-differential topology of the isoeuclidean geometries whereby conventional topologies hold everywhere *except at the unit*.

Isospaces can also be distinguished via Kadeisvili's classification depending on the characteristics of the unit (Sect. 1.5) into:

Isospaces properly speaking (Class I),

isodual isospaces (Class II)

Indefinite isospaces (Class III),
Singular isospaces (Class IV], and
General isospaces (Class V).

Theoretical conchology requires the use of isospaces of (at least) Class III.

As indicated earlier, isospaces are bona-fide nonlinear and nonlocal generalizations of the original spaces. Despite the above differences, we have the following

Theorem 2.1 [5]: *Isospaces of Class I $\mathbb{S}(x, \hat{g}, \hat{F})$ (isodual spaces of Class II $\mathbb{S}^d(x, \hat{g}^d, \hat{F}^d)$) are locally isomorphic to the original spaces $\mathbb{S}(x, g, F)$ (isodual space $\mathbb{S}^d(x, g, F^d)$). Isodual spaces of Class III are isomorphic to the union of spaces and isodual spaces.*

The above simple mathematical property has fundamental implications anticipated in the introductory section. In particular, the property implies that the isotopies of Class I of space-time symmetries such as the rotation, Lorentz, Poincaré and unitary symmetries are locally isomorphic to the original symmetries. Nevertheless, the explicit form of the transformations will be generally nonlinear, nonlocal and nonlagrangian when formulated in the original space, thus achieving the desired structural generalization of conventional symmetry transformations.

Note the necessity for these isomorphisms of the *joint* liftings

$$g \rightarrow \hat{g} = Tg \quad \text{and} \quad F \rightarrow \hat{F}, \quad \hat{1} = T^{-1}. \quad (2.26)$$

In fact, a lifting of the type $\mathbb{S}(x, g, F) \rightarrow \mathbb{S}(x, \hat{g}, \hat{F})$, $\hat{g} = Tg$, alone without the joint lifting of the base field *is not* an isotopy and the spaces $\mathbb{S}(x, g, R)$ and $\mathbb{S}(x, \hat{g}, R)$ are generally *non-isomorphic*.

From the above properties we have the following

Proposition 2.2 [5]: *The compositions (x, \hat{y}) on isospaces $\mathbb{S}(x, \hat{g}, \hat{F})$ are isoselfdual, i.e., invariant under isoduality*

$$(x, \hat{y}) = (x^i \hat{g}_{ij} y^j) \hat{1} \equiv (x, \hat{y})^d = (x^i \hat{g}^d_{ij} y^j) \hat{1}^d. \quad (2.27)$$

The above property implies the preservation of causality under isoduality. In fact, the known objections based on causality for motion backward in time refer strictly to the conventional unit +1. The same objections becomes inapplicable for motion backward in time represented via isoduality precisely because of the abstract identity of the two directions of motion identified by the above property.

Scalar functions $f(x)$ on isospaces $\hat{S}(x, \hat{g}, \hat{F})$ are ordinary functions. An *isoscalar function* $\hat{f}(x)$ on $\hat{S}(x, g, F)$ is a function with values on the isofield, i.e.,

$$\hat{f}(x) = f(x) \hat{1} \in \hat{F}. \quad (2.28)$$

It should be indicated that in Definition 2.1 *the local coordinates* $x \in \hat{S}(x, \hat{g}, \hat{F})$ *are assumed to be ordinary scalars and not isoscalars*. One can then build an isospace $\hat{S}(\hat{x}, \hat{g}, \hat{F})$ with *isocoordinates*

$$\hat{x} = x \hat{1}. \quad (2.29)$$

in which case the isocomposition is factorizable into the conventional one

$$\hat{x}^2 = \hat{x}^t * \hat{x} = (x^t x) \hat{1}. \quad (2.30)$$

The interchange between the isotopic element and the isounit

$$T \rightarrow \hat{1} \quad (2.31)$$

is called *isoreciprocity map* [5].

In summary, we have four different formulations of isospaces per each individual Class, given in self-explanatory notations by

$$\hat{S}(x, \hat{g}, \hat{R}(n, +, *)), \hat{S}(x, \hat{g}, \hat{R}(\hat{n}, +, *)), \hat{S}(\hat{x}, \hat{g}, \hat{R}(n, +, *)), \hat{S}(\hat{x}, \hat{g}, \hat{R}(\hat{n}, +, *)). \quad (2.32)$$

The isospaces of primary relevance for theoretical conchology are given by the structures $\hat{S}(x, \hat{g}, \hat{F})$ of Class III of Definition 2.1 specialized to the cases of isoreal and isocomplex fields $\hat{F} = \hat{R}, \hat{C}$.

2.D. Isotopies of the transformation theory. Let $S(r, F)$ be a conventional vector space with local coordinates r over a field F , and let $r' = A(w)r$ be a linear, local and canonical transformation on $S(r, F)$, $w \in F$. The lifting $S(r, F) \rightarrow \hat{S}(r, F)$ requires a corresponding *necessary* isotopy of the transformation theory

$$r' = \hat{U}(\hat{w}) * r = \hat{A}(\hat{w}) T_S r, \quad T \text{ fixed, } r \in \hat{S}(r, F), \quad 1 = T^{-1}, \quad (2.33)$$

called *isotransformations*, with isodual form

$$r' = \hat{A}^d(\hat{w}^d) *^d r = -\hat{A}(\hat{w}) * r. \quad (2.34)$$

Expectedly, isotransformations verify the condition of *isolinearity*

$$A * (\hat{a} * r + \hat{b} * r') = \hat{a} * (A * r) + \hat{b} * (A * r'), \quad \forall r, r' \in \hat{S}(r, F), \quad \hat{a}, \hat{b} \in \hat{F}, \quad (2.35)$$

although their projection in the original space $S(r, F)$ is nonlinear, because $r' = AT(r, \dot{x}, \dots)r$. Isotransformations are also *isolocal* because the theory formally deals with the local variables r while all nonlocal terms are embedded in the isounit. Nevertheless, they too are nonlocal when projected in the original space.

Similarly, isotransformations are *isocanonical* because they are formally derivable from a variational principle on the *isosymplectic geometry* [4,5], although they are noncanonical when projected in $S(x, F)$. Note that nonlinear, nonlocal and noncanonical transforms can always be identically rewritten in isotopic form.

2.E. Isotopies of functional analysis. As indicated earlier, the isotopies imply simple yet nontrivial generalizations of *the totality* of contemporary mathematical structures, beginning from elementary notions such as numbers, and then passing to angles and leading inevitably to a generalization of functional analysis called by Kadeisvili [9] *functional isoanalysis*.

The generalized discipline begins with the isotopy of continuity (whose knowledge is assumed when dealing with technical aspects), and includes the isotopies o : conventional square-integrable, Banach and Hilbert spaces; all operations on them; special functions, distributions and transforms; etc.

Evidently we cannot possibly review this new discipline here to avoid a prohibitive length (see ref. [5] for details). In the appendices we shall outline the isotopies of trigonometry and spherical coordinates because of their fundamental character for conchology.

2.F: Isotopies of Lie's theory. The preceding liftings demand a corresponding compatible lifting of all branches of Lie's theory, including the lifting of enveloping associative algebras, Lie algebras, Lie groups, representation theory symmetries, etc.

The emerging generalized theory was submitted by this author in 1978 under the name of *Lie-isotopic theory*, and it is generally called nowadays *Lie-Santilli theory* [6]. This generalized theory is essentially based on the lifting of the trivial unit $I = \text{diag.} (1, 1, \dots)$ of the conventional formulation of Lie's theory into the most general possible isounit $\hat{1} = T^{-1}$.

The lifting $I \rightarrow \hat{1}$ then implies the generalization of the simplest possible Lie product of contemporary use, $AB - BA$, into a generalized form called *Lie-Santilli isoproduct* [6] $\hat{A}\hat{B} - \hat{B}\hat{A}$, which still verifies the Lie axioms although at a generalized level.

Jointly, (connected) Lie transformation groups represented with the conventional exponentiation

$$A = e^{iXw} = I + (iXw)/1! + (iXw)(iXw)/2! + \dots \quad (2.36)$$

are lifted into the *Lie-Santilli isogroups* with realization in terms of the so-called *isoexponentiation*

$$\hat{A} = \hat{e}^{iXw} = \hat{1} + (iXw)/1! + (iXw)T(iXw)/2! + \dots = \{e^{iXTw}\}\hat{1}. \quad (2.37)$$

where one should note the appearance of a nonlinear-nonlocal quantity T in the exponent. A corresponding nontrivial generalization of all aspects of Lie's theory then follows (see refs [4,5,6] for comprehensive presentations).

The Lie-Santilli theory is also subdivided into five classes. The structure of primary use for theoretical conchology are the following four:

- 1) **conventional Lie theory** with trivial unit $I = \text{diag.} (1, 1, \dots) > 0$;

2) **isodual Lie theory** with isodual unit $1^d = -1 < 0$;

3) **Lie-Santilli isothory** with isounit $\hat{1}_s > 0$; and

4) **isodual Lie-Santilli isothory** with isodual isounits $\hat{1}_s^d = -\hat{1}_s < 0$.

The theory needed for the study of the symmetries of sea shells is the Lie-Santilli theory of Class III which encompasses all the above types.

A result important for theoretical conchology is the following studied in App. C. Recall from Fig 3 the unification of all possible shapes of sea shells into the isosphere. But the Lie-Santilli theory identifies the universal symmetry of the isosphere in the isotopic $\hat{O}(3)$ symmetry, which results to be locally isomorphic to the conventional rotational symmetry $O(3)$. The isorotational symmetry $\hat{O}(3)$ is therefore results to be the symmetry of all possible sea shells.

2.G: Isoeuclidean spaces. The fundamental spaces of this analysis can be introduced via the following:

Definition 2.3 [5]: *The liftings of the conventional n -dimensional Euclidean spaces $E(r, \delta, R)$ over the reals $R(n, +, \times)$ into the "isoeuclidean spaces" of Class I are given by*

$$E(r, \delta, R) \rightarrow \hat{E}(r, \hat{\delta}, \hat{R}), \quad (2.38a)$$

$$\delta = I_{n \times n} \rightarrow \hat{\delta} = T(t, r, \hat{r}, \mu, \tau, n, \dots) \delta, \quad (2.38b)$$

$$\det \delta = 1 \neq 0, \delta = \delta^\dagger \rightarrow \det. \hat{\delta} \neq 0, \hat{\delta} = \hat{\delta}^\dagger, \quad (2.38c)$$

$$R \rightarrow \hat{R}, \quad \hat{1} = T^{-1} = \delta^{-1} \quad (2.38d)$$

$$\begin{aligned} r^2 := (r, r) &= r^i \delta_{ij} r^j \rightarrow \hat{r}^2 = (r, \hat{r}) = (r, \hat{\delta} r) \hat{1} = \\ &= (\hat{\delta} r, r) \hat{1} = \hat{1} (r, \hat{\delta} r) = [r^i \hat{\delta}_{ij} (r, \hat{r}, \dots) r^j] \hat{1} \in \hat{R}, \end{aligned} \quad (2.38e)$$

where the isofield $\hat{R}(\hat{n}, +, *)$ is of Class I. The "isodual isoeuclidean spaces" of Class II are given by the isodual image of the preceding ones

$$\hat{E}(r, \hat{\delta}, \hat{R}) \rightarrow \hat{E}^d(r, \delta^d, \hat{R}^d), \quad (2.39a)$$

$$\hat{\delta} = T \delta \rightarrow \delta^d = T^d \delta = -\hat{\delta}, \quad T^d = -T, \quad (2.39b)$$

$$\hat{R} \rightarrow \hat{R}^d \approx R \hat{1}^d, \quad \hat{1}^d = -\hat{1} \quad (2.39c)$$

$$r^{\hat{2}} = (r, \hat{r}) = (r^i \hat{\delta}_{ij} r^j) \hat{1} \rightarrow r^{\hat{2}d} = (r, \hat{r})^d = (r^i \hat{\delta}_{ij}^d \hat{r}^j) \hat{1}^d \equiv r^{\hat{2}}. \quad (2.39d)$$

The "isoeuclidean spaces of Class III" are the union of those of Class I and II.

Note that the correct formulation of the *isosphere* of fig. 3 is the expression

$$r^{\hat{2}} = (r^i \hat{\delta}_{ij} r^j) \hat{1} = \hat{1}, \quad (2.40)$$

where the multiplication by $\hat{1}$ is *necessary* because the quantity must be an element of the isofield.

For numerous physical applications of the isoeuclidean spaces we refer the interested reader to monographs [4,5]. The following outline may be useful as a comparative basis with applications in theoretical conchology.

A) Geometric applications. Recall that the conventional Euclidean metric $\delta = \text{diag.} (1, 1, 1)$ is a geometrization of the perfect rigid sphere with unit radius. Isotopic elements of the diagonal type

$$T = \text{diag.} (b_1^2, b_2^2, b_3^2), \quad b_k = b_k(t, r, \dot{r}, \ddot{r}, \dots) > 0, \quad k = 1, 2, 3, \quad (2.41)$$

and related isounits

$$\hat{1} = \text{diag.} (b_1^{-2}, b_2^{-2}, b_3^{-2}), \quad (2.42)$$

then permit a *direct representation of the actual nonspherical shape of a given body as well as of all its infinitely possible deformations.*

B) Analytic applications. As well known, Lagrange's equations of motion in

the Lagrangian $L = L(t, r, \dot{r}) = K - V$, where K is the kinetic energy and V the potential energy on a conventional Euclidean space generally represent conservative systems.

A main objective of the isotopies is the representation of arbitrary, generally nonconservative dynamical problems with conventional potential forces, plus contact, nonlinear–nonlocal–nonlagrangian¹ forces due to the medium. In this latter case, the system is represented by *two independent quantities*, the Lagrangian $L = K - V$ and the isounit $\hat{1}$.

In this latter case, *the isounit permits a direct representation of contact, nonlinear–nonlocal–nonlagrangian forces for interior physical conditions*. The Lagrangian L must now be properly written in isoeuclidean space $\hat{E}(r, \hat{\delta}, \hat{R})$, as we shall see shortly.

One can see that *isospaces provide a direct geometrization of the inhomogeneity and anisotropy of physical media in which motion occurs*. In fact, the inhomogeneity can be represented in isospaces, e.g., via a dependence of the isometric $\hat{\delta}$ on the locally varying density μ . The anisotropy, e.g., due to the presence of an intrinsic angular momentum along the direction \vec{n} , is then representable via a factorization of such a preferred direction also in the isometric, much along the Finslerian geometry, for via the differentiations $b_1 \neq b_2 \neq b_3$.

Note that the representation is "direct" because occurring directly in the isometric itself, without any need of operator formulations or any use of artificial or indirect approaches.

Note that the 3-dimensional Euclidean "space" is one. On the contrary, there exist infinitely many 3-dimensional isoeuclidean "spaces". This is evidently due to the infinitely possible isometrics $\hat{\delta}$ representing the infinitely possible physical conditions of interior problems.

C) Algebraic applications: Recall that the unit $I = \text{diag. } (1, 1, 1)$ of the Euclidean space is the fundamental unit of Lie's theory, e.g., the unit of the group of invariance of the sphere, the orthogonal group $O(3)$.

¹ By "nonlagrangian" we mean hereon non-first-order Lagrangians, namely, equations of motion which violate the integrability conditions for their representation via first-order Lagrangians $L = L(t, r, \dot{r})$. Evidently, higher order Lagrangian may exist, e.g., $L = L(t, r, \dot{r}, \ddot{r})$. The point is that, under these latter conditions, there is no (conventional) Hamiltonian. The term "noncanonical" is then used as a synonym of "non-first-order-Lagrangian".

Then, the isounit characterizes a structural generalization of Lie's theory as outlined above.

The following property is a consequence of Theorem 2.1.

Corollary 2.1A: *Isoeuclidean spaces $\hat{E}(r, \delta, \hat{R})$ of Class I (isodual isoeuclidean spaces of Class II $\hat{E}^d(r, \delta^d, \hat{R}^d)$) are locally isomorphic to the conventional Euclidean spaces of the same dimension $E(r, \delta, R)$ (isodual Euclidean spaces of the same dimension $E^d(r, \delta^d, R^d)$). The isoeuclidean spaces of Class III are isomorphic to the union of the original space $E(r, \delta, R)$ and its isodual $E^d(r, \delta, R^d)$.*

We shall say that, from a geometrical viewpoint, Euclidean spaces and their isotopes are equivalent, as ensured by the preservation of the original axioms, as well as the identity of the two spaces at the abstract level.

The isospaces needed for theoretical conchology, including representatives of the evolution in time, can be introduced via the following:

Definition 2.4 [5]: *The "isoeuclidean space-time" of Class I is given by the Cartesian product of two isoeuclidean spaces, one representing space and the other representing time with corresponding isounits $\hat{1}_t$ and $\hat{1}_s$, isocomposition*

$$\hat{E}(t, \hat{R}_t) \times \hat{E}(r, \delta, \hat{R}) : \quad t^2 = (t T_t t) \hat{1}_t \in \hat{R}_t, \quad \hat{1}_t = T_t^{-1}, \quad (2.43a)$$

$$r^2 = (r^t T_s \delta r) \hat{1}_s \in \hat{R}, \quad \hat{1}_s = T_s^{-1}, \quad (2.43b)$$

and diagonal realization

$$T_t = T_t(t, r, \dot{r}, \ddot{r}, \dots) > 0, \quad (2.44a)$$

$$T_s = \text{diag.} (T_x, T_y, T_z), \quad T_k = T_k(t, r, \dot{r}, \ddot{r}, \dots) > 0, \quad k = x, y, z. \quad (2.44b)$$

The "isodual isoeuclidean space-time" of Class II is then given by

$$\hat{E}^d(t, \hat{R}_t^d) \times \hat{E}^d(r, \delta^d, \hat{R}^d): \quad t^{\hat{2}d} = (t T_t^d t) \hat{1}_t^d \in \hat{R}_t^d, \quad (2.45a)$$

$$r^{\hat{2}d} = (r^t T_S^d \delta r) \hat{1}_S^d \in \hat{R}, \quad (2.45b)$$

$$\hat{1}_t^d = (T_t^d)^{-1} = -\hat{1}_t, \quad \hat{1}_S^d = (T_S^d)^{-1} = -\hat{1}_S, \quad (2.45c)$$

$$T_t^d = T_t^d(t, r, \hat{r}, \mu, \tau, n, \dots) < 0, \quad (2.45d)$$

$$T_S^d = -\text{diag.} (T_X, T_Y, T_Z) < 0. \quad (2.45e)$$

The "isodual isoeuclidean space-time of class III" are the union of those of Class I and II.

As it is the case for all other quantities, the above definition implies the existence of four distinguishable nonrelativistic times:

Time, as the usual element t of the field of real numbers $R(t, +, \times)$;

Isotime, the element $\hat{t} = t \hat{1}_t \in \hat{R}(\hat{t}, +, *)$;

Isodual time, the element $t^d = t \hat{1}^d = -t \in R^d(t^d, +, \times^d)$;

Isodual isotime, the element $\hat{t}^d = \hat{t} \hat{1}_t^d = -\hat{t} \in \hat{R}^d(\hat{t}^d, +, *^d)$;

which are all unified in Class III.

Note that time moves backward for isodual time and isodual isotime. In fact, under isoduality, we have the antiautomorphic map

$$t > 0 \quad \rightarrow \quad t^d = t \hat{1}^d = -t < 0, \quad (2.46)$$

and the same result persists under isotopy.

The reader should however keep in mind that such backward motion in time is referred to a *negative-definite unit* and, as such, it is fully equivalent to the forward motion in time referred to a *positive-definite unit*. The equivalence of these two directions of time referred to units opposite in sign is at the foundation of the preservation of causality for the space-time machine of ref. [3], as well as of the isotopic representation of the bifurcations of Figure 4.

2.H: Isoeuclidean geometry. The *isoeuclidean geometry* [4,5] is the geometry of the isoeuclidean spaces on isoreal fields. For clarity, we shall study first the isogeometries of Classes I and II and then pass to the more general Class III.

Recall that in the transition from the Euclidean space $E(r,\delta,R)$ to the Riemannian space in the same dimension $\mathcal{R}(r,g,R)$ there is the loss of angles and trigonometric functions evidently because of the loss of straight lines due to the curvature of the space, as expressed by the Riemannian metric $g = g(r)$.

In the transition from the Euclidean space $E(r,\delta,R)$ to the isoeuclidean spaces $\hat{E}(r,\hat{\delta},\hat{R})$ we acquire the most general possible curvature dependent also in the velocities, accelerations and other quantities, as expressed by the isometric $\hat{\delta} = \hat{\delta}(t, r, \dot{r}, \ddot{r}, \dots)$. Nevertheless, the lifting $E(r,\delta,R) \rightarrow \hat{E}(r,\hat{\delta},\hat{R})$ is an *isotopy*, that is, a generalization which preserves the original axioms.

Since the original space is flat, *the isoeuclidean geometry is isoflat*, that is, the curvature emerges only when $\hat{E}(r,\hat{\delta},\hat{R})$ is projected in $E(r,\delta,R)$ because, within the isospace itself, there is no curvature.

The novel geometric property of isoflatness then permits the reconstruction in $\hat{E}(r,\hat{\delta},\hat{R})$ of angles and trigonometric functions which is precluded in Riemannian spaces.

Let us consider first the isoeuclidean geometry in two dimension with isotopic element and isounit

$$T = \text{diag.} (T_x, T_y), \quad \hat{1} = \text{diag.} (T_x^{-1}, T_y^{-1}). \quad (2.47)$$

Let θ be the angle among two intersecting straight lines in $E(r,\delta,R)$. Then the corresponding angle $\hat{\theta}$ in $\hat{E}(r,\hat{\delta},\hat{R})$, called *isoangle*, is given by

$$\hat{\theta} = \theta (T_x T_y)^{\frac{1}{2}}. \quad (2.48)$$

This result is established by the basic invariance of the space, the isotopic $\hat{O}(2)$ symmetry, and in particular from an inspection of the arguments of the isorotations, or from the isorepresentation theory.

A study of rule (2.48) has indicated that the isoangle $\hat{\theta}$ can also be

interpreted as *the original angle prior to the deformation*. The angle θ in rule (2.48) is then *the angle of deformation measured in our space*. This implies that, *when deforming a circle into an ellipsoid, the directional angle of a point is evidently altered in the Euclidean plane into the angle θ , but the isoeuclidean plane reconstructs the original directional angle $\hat{\theta}$* .

The above results are sufficient to indicate the existence of a consistent and intriguing isotopy of conventional trigonometry, which is studied in more detail in Appendix A.

We are now in a position to study the unification of all possible three-dimensional hypersurfaces in the isosphere (Fig. 3). In essence, the isoeuclidean geometry of Class I preserves the signature of the original metric, $\text{sig. } \hat{\delta} \equiv \text{sig } \delta = (+, +, +)$. The only possible isometrics are given by structures of the type

$$\hat{\delta} = T\delta = \text{diag. } (+ b_x^2, + b_y^2, + b_z^2), \quad b_k \neq 0; \quad (2.49)$$

the isoeuclidean geometry of Class II is characterized instead by the isodual of the preceding metric

$$\delta^d = T^d\delta = \text{diag. } (- b_x^2, - b_y^2, - b_z^2), \quad b_k \neq 0; \quad (2.50)$$

the isogeometry of Class III has an undefined signature of the isometric, and we can write

$$\hat{\delta} = T\delta = \text{diag. } (\pm b_x^2, \pm b_y^2, \pm b_z^2), \quad b_k \neq 0; \quad (2.51)$$

while the isogeometry of Class IV includes all the above, plus the possibility that the individual b 's can be singular.

The surfaces unified by the isosphere of Class I and related symmetry are therefore the following:

1) The sphere

$$O(3): \quad x x + y y + z z = \text{inv.}, \quad (2.52)$$

2) All ellipsoids (prolate or oblate spheroidal ellipsoids)

$$\hat{O}(3): x b_x^2 x + y b_y^2 y + z b_z^2 z = \text{inv.}, \quad (2.53)$$

The surfaces unified by the isosphere of Class II are:

3) The isodual sphere

$$O^d(3): -x x - y y - z z = \text{inv.}, \quad (2.54)$$

4) All isodual ellipsoids

$$\hat{O}^d(3): -x b_x^2 x - y b_y^2 y - z b_z^2 z = \text{inv.}, \quad (2.55)$$

The surfaces unified by the isosphere of Class III are all the above, plus:

5) The hyperbolic paraboloid (paraboloid with two sheets here reinterpreted as the isodual of the elliptic paraboloid)

$$O^d(2.1): -x x + y y - z z = \text{inv.}, \quad (2.56)$$

6) All signature preserving deformations of the hyperbolic paraboloid

$$\hat{O}^d(2.1): -x b_x^2 x + y b_y^2 y - z b_z^2 z = \text{inv.}, \quad (2.57)$$

7) The hyperbolic paraboloid (paraboloid with two sheets here reinterpreted as the isodual of the elliptic paraboloid)

$$O^d(2.1): -x x + y y - z z = \text{inv.}, \quad (2.58)$$

8) All signature preserving deformations of the hyperbolic paraboloid

$$\hat{O}^d(2.1): -x b_x^2 x + y b_y^2 y - z b_z^2 z = \text{inv.}, \quad (2.59)$$

9) All possible surfaces in three-dimensional space of arbitrary order

$$\hat{O}(3) ; x T_x(t, r, \dots) x + y T_y(t, r, \dots) y + z T_z(t, r, \dots) z = \text{inv.} \quad (2.60)$$

as well as all cones of all preceding surfaces (holding when the invariant is null).

The isosphere of Class V implies all the above plus isospheres with arbitrary isounits, e.g., a distribution or a lattice.

As indicated in Sect. 1.C, the unification of all the above surfaces in the perfect sphere in isospace is due to the fact that, jointly with the deformation of the semiaxes of the sphere in Euclidean space, $l_k \rightarrow T_k$, the unit in each direct is deformed of the inverse amount $l_k \rightarrow \hat{l}_k = T_k^{-1}$, $k = x, y, z$, thus preserving the perfectly spherical character.

Note the *direct universality* of the above unification. In fact, given an arbitrary surface in $E(r, \delta, R)$, there always exist three elements T_k , $k = x, y, z$, under which that surface is *identically* represented by Eq. (2.60).

2.I: Operations in isoeuclidean geometry . We consider now the representation of vectors and their operations in the isoeuclidean geometry. Recall that the basis of a vector space is not changed under isotopy (up to possible renormalization factors). Let e_k , $k = 1, 2, 3$, be the unit vectors on $E(r, \delta, R)$ directed along the x, y, z axes, and let \hat{e}_k be the corresponding isobasis in $\hat{E}(r, \delta, \hat{R})$. Then, a vector V can be expressed in isospace as in the conventional case

$$V = x \hat{e}_1 + y \hat{e}_2 + z \hat{e}_3 . \quad (2.61)$$

This is another way of expressing the fact that the vector V is straight in $\hat{E}(r, \delta, \hat{R})$, although its projection in $E(r, \delta, R)$ is curved. As usual under isotopies, *the vectors are not changed, but operations on vectors are changed*. In fact, the scalar product $V_1 \cdot V_2$ of two vectors $V_1 = \{x_1, y_1, z_1\}$ and $V_2 = \{x_2, y_2, z_2\}$ is now lifted into the expression called *isoscalar product*

$$V_1 \odot V_2 = (x_1 T_x x_2 + y_1 T_y y_2 + z_1 T_z z_2) \hat{1} \in \hat{R}(\hat{n}, +, *) . \quad (2.62)$$

Note that, as expected, the isoscalar product preserves the original axioms as necessary under isotopies, i.e.,

$$V_1 \odot V_2 = V_2 \odot V_1, \quad V_1 \odot (V_2 + V_3) = V_1 \odot V_2 + V_1 \odot V_3. \quad (2.63)$$

Moreover, the *isonorm* on $\hat{E}(r, \delta, \hat{R})$ is expressible in terms of the isoscalar product via the rule

$$\uparrow V \uparrow = (V \odot V)^{\frac{1}{2}} \uparrow \in \hat{R}(\hat{n}, +, *). \quad (2.64)$$

Consider now two points $P_1 = \{x_1, y_1, z_1\}$ and $P_2 = \{x_2, y_2, z_2\}$. Then the *isodistance* among them is the quantity

$$\hat{D} = [(x_1 - x_2)g_{11}(x_1 - x_2) + (y_1 - y_2)g_{22}(y_1 - y_2) + (z_1 - z_2)g_{33}(z_1 - z_2)]^{\frac{1}{2}} I. \quad (2.65)$$

it is evidently unique (for each given isounit) and permits a study of the isotopy of the original Euclid axioms.

Note that conventional distances and isodistances do not coincide even when the isotopic element is a constant, $T = N \in R(n, +, \times)$ because in this case

$$\hat{D} = D N^{\frac{1}{2}} N^{-1} = D N^{-\frac{1}{2}} \neq D, \quad (2.66)$$

Similarly, the vectorial product $V_1 \wedge V_2$ is lifted in the expression called *isovectorial product*

$$V_3 = V_1 \hat{\wedge} V_2, \quad V_{3k} = \epsilon_{kij} (g_{ij})^{\frac{1}{2}} x_{1i} (g_{jj})^{\frac{1}{2}} x_{2j}, \quad i, j, k = 1, 2, 3. \quad (2.67)$$

which satisfies the basic axioms of a vector product

$$V_1 \hat{\wedge} V_2 = V_2 \hat{\wedge} V_1, \quad V_1 \hat{\wedge} (V_2 + V_3) = V_1 \hat{\wedge} V_2 + V_1 \hat{\wedge} V_3. \quad (2.68)$$

It is instructive for the interested reader to verify the preservation of *Lagrange's identity* of the Euclidean geometry under isotopies among four vectors A, B, C, D in $\hat{E}(r, \delta, \hat{R})$

$$(A \hat{\wedge} B) \odot (C \hat{\wedge} D) = (A \odot C) * (B \odot D) - (B \odot C) * (A \odot D). \quad (2.69)$$

Isotopies of Euclid's fifth axiom

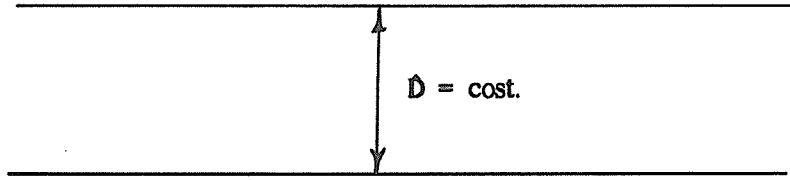


FIGURE 7. A schematic view of Euclid's celebrated Fifth axiom on parallel lines, which can be reformulated in isoeuclidean spaces, thus leading to the notion of *isoparallel lines*.

Other properties can be easily derived by the interested reader via similar procedures.

We now study the notion of *isolagrangian*. Recall that the systems under consideration are non-first-order Lagrangian, i.e., they do not verify the integrability conditions for their representation via Lagrange equations with a Lagrangian $L = L(t, r, \dot{r})$. However, when the same systems are properly represented in isospace, a first-order Lagrangian $\hat{L}(t, r, \dot{r})$ exists, called *isolagrangian*.

The methods for properly writing an isolagrangian are simple and essentially based on the rule that all products, powers, square roots, quotients, etc. have to be isotopic. Let $L(t, r, \dot{r}) = K(\dot{r}) - V(t, r, \dot{r})$ be a conventional Lagrangian where $K(\dot{r}) = \frac{1}{2}m\dot{r} \odot \dot{r}$ is the conventional kinetic energy and $V(t, r, \dot{r})$ is the potential energy (e.g., of the Lorentz force).

The isolagrangian $\hat{L}(t, r, \dot{r}) = \hat{K}(\dot{r}) - \hat{V}(t, r, \dot{r})$ is then characterized by the *isokinetic energy*

$$\hat{K}(\dot{r}) = \frac{1}{2} m \dot{r} \odot \dot{r}, \quad (2.70)$$

while the *isopotential* $\hat{V}(t, r, \dot{r})$ is the original expression for variables r calculated via the rule of the isodistance.

The above isoanalytic representation has been introduced for the representation of nonconservative systems [4,5]. A simple example may be of assistance for application in conchology. Consider an extended free particle in

empty space, which is evidently represented via the kinetic energy alone $L = \frac{1}{2}m\dot{\mathbf{r}} \times \dot{\mathbf{r}} \in E(\mathbf{r}, \delta, R)$, where \mathbf{r} represents the trajectory of the center of mass.

Suppose now that the particle at a given value of time penetrates within a physical medium, thus experiencing nonpotential forces. The drag forces experiences in the latter instance are represented by the isotopic element T , that is, *the transition from motion in vacuum to motion within a physical medium can be represented by the transition from the Euclidean geometry to its isoeuclidean covering*. In turn, the transition is represented by writing the original Lagrangian in isospace, thus reaching the expression $\hat{L} = \frac{1}{2}m\dot{\mathbf{r}} \circ \dot{\mathbf{r}} \in \hat{E}(\mathbf{r}, \hat{\delta}, \hat{R})$. The geometric aspect important for this section is that the two Lagrangians L and \hat{L} coincide at the abstract level for all Class I isospaces.

Numerous classical examples are now available (see ref.s [4,5]). the simplest one is the particle with linear velocity-damping

$$\ddot{\mathbf{x}} + \gamma \dot{\mathbf{x}} = 0, \quad m = 1, \quad \gamma > 0, \quad (2.71)$$

which is merely represented via the particular realization of the isotopic element and isounit

$$T = e^{\gamma t}, \quad \mathbf{1} = e^{-\gamma t}, \quad \gamma > 0. \quad (2.72)$$

as the reader is encouraged to verify (see ref. [6], p. 101). The isorepresentation can be enlarged into the form

$$T = \text{diag.} (b_x^2, b_y^2, b_z^2) e^{\gamma t}, \quad (2.73)$$

exhibiting a feature completely absent in Euclidean geometry, a *direct representation of the actual nonspherical shape of the particle considered* here assumed to be an ellipsoid with semiaxes b_k^2 . The understanding is that the isoeuclidean geometry can also be realized via *nondiagonal isotopic elements*, as requested by the case at hand.

Note that the representation of shape is completely absent in Newton's equation of motion and it is a sole feature of the isoeuclidean geometry. In fact,

after computing the equation of motion, the "shape factor" cancels out.

But perfectly rigid objects do not exist in the physical reality. The isoeuclidean geometry then permits a *direct representation of all infinitely possible deformations of the original nonspherical shape*, which can be easily achieved via a dependence of the characteristics b-quantities in the local pressure, velocity, etc.

In summary, the isoeuclidean geometry has the following primary applications in physics: A) geometrization of the physical medium considered; B) representation of the resistive effects on the motion of extended particles; and C) representation of the actual nonspherical shapes and all their possible deformations.

2.J: Connection with other noneuclidean geometries. A few comments are now in order on the connection between the isoeuclidean geometry and others *non-Euclidean geometries* (see, e.g., ref. [13] and quoted literature). As well known, Euclid's Fifth Axiom lead to a historical controversy that lasted for a millennium, until solved by Lobacevskii in a rather unpredictable way, via the introduction of a new, non-Euclidean geometry today appropriately called *Lobacevskii geometry* (see [loc. cit.]).

As well known, Lobacevskii geometry is also based on certain liftings of Euclidean expressions, although defined on the conventional unit. Thus, the Lobacevskii and isoeuclidean geometries are structurally different.

Nevertheless, it is also important to understand that *the Lobacevskii geometry is a particular case of the projection of the isoeuclidean geometry in the Euclidean plane*. To see this point consider the celebrated Lobacevskii transformations

$$x' = \frac{x + a}{1 + ax}, \quad y' = \frac{y(1 - a^2)^{\frac{1}{2}}}{1 + ax}, \quad |a| < 1, \quad (2.74)$$

which have the peculiar property of carrying straight lines into straight lines and circles into circles (see ref. [13] for details) *while keeping the unit the same*. Now, the isoeuclidean space $E(r, \delta, R)$ in two dimensions can be equivalently reinterpreted as an ordinary Euclidean plane $\bar{E}(r, \delta, R)$ in the new coordinates

$$\bar{x} = T_x^{\frac{1}{2}} x, \quad \bar{y} = T_y^{\frac{1}{2}} y, \quad (2.75)$$

under which we have the identity

$$\bar{x} \bar{x} + \bar{y} \bar{y} = x T_x x + y T_y y. \quad (2.76)$$

It is then evident that Lobacevskii transformations (2.74) are contained as a particular case of the much larger class of isotransformations (2.75).

The connection between Lobacevskii and isoeuclidean geometries can therefore be expressed by saying that:

A) *the Lobacevskii geometry identifies "one" particular lifting of the Euclidean geometry preserving straight lines and circles under the conventional value of the unit; while*

B) *the isoeuclidean geometry identifies "an infinite class" of liftings of the Euclidean geometry which preserve straight lines and circles under a joint lifting of the unit.*

Note finally that the Lobacevskii geometry itself can be subjected to an isotopic lifting which has not been studied here for brevity.²

Numerous other noneuclidean geometries exist in the literature [13]. One particularly intriguing geometry is the so-called *nondesarguesian geometry* studied by Shieber [14], which has a significant connection with these studies because it can also represent nonlagrangian systems.

This latter geometry too is different from the isoeuclidean one, again, because it is based on the conventional unit. However, the underlying mapping between the Euclidean and nondesarguesian geometry is also contained as a particular case of the infinite transformations (2.75) of the isoeuclidean geometry.

These comments are significant to focus the attention on an additional reason for our selection of the isoeuclidean geometry over other possible choices, its "direct universality" of incorporating "all" infinitely possible maps of the Euclidean geometry (including singular maps for Class IV and discrete maps for Class V).

In summary, the isoeuclidean geometry is directly universal for all

² Note that the *isolobacevskii geometry* is no longer contained as a particular case of the isoeuclidean geometry because the original axioms of the two geometries are different.

infinitely possible generalizations of the Euclidean geometry which are: nonlinear in coordinates and their derivatives of arbitrary order, nonlocal-integral in all needed variables, and non-first-order-Lagrangians.

2.K: Isoeuclidean representations of sea shells. A few examples are now in order. Consider the *hyperbolic clocksprings of the first kind in a plane*, ref. [1], Eq. (3.14), p. 81, i.e.,

$$x = e^{-\frac{1}{2}\lambda\phi} \cosh[(\alpha + \frac{1}{2}\lambda)\phi] \cos\phi, \quad (2.77a)$$

$$y = a e^{-\frac{1}{2}\lambda\phi} \sinh[(\alpha + \frac{1}{2}\lambda)\phi] \sin\phi. \quad (2.77b)$$

It is easy to see that in the isoeuclidean plane $E(r, \delta, R)$, $\delta = T\delta$, $T = \text{diag. } (T_x, T_y)$, the above surface reduces to the perfect circle. In fact, under the values of the isotopic element

$$T_x = \{a e^{-\frac{1}{2}\lambda\phi} \cosh[(\alpha + \frac{1}{2}\lambda)\phi]\}^{-2}, \quad (2.78a)$$

$$T_y = \{a e^{-\frac{1}{2}\lambda\phi} \sinh[(\alpha + \frac{1}{2}\lambda)\phi]\}^{-2}, \quad (2.78b)$$

the surface equations reduce to the isopolar coordinates (App. B)

$$x = T_x^{-\frac{1}{2}} \cos(T_x^{-\frac{1}{2}} T_y^{-\frac{1}{2}} \phi), \quad (2.79a)$$

$$y = T_y^{-\frac{1}{2}} \sin(T_x^{-\frac{1}{2}} T_y^{-\frac{1}{2}} \phi), \quad (2.79b)$$

and they do indeed describe a perfect circle in isospace, the isocircle

$$x T_x x + y T_y y = \cos^2(T_x^{-\frac{1}{2}} T_y^{-\frac{1}{2}} \phi) + \sin^2(T_x^{-\frac{1}{2}} T_y^{-\frac{1}{2}} \phi) = 1. \quad (2.80)$$

A similar result evidently occurs for the *hyperbolic clockspring of the second kind*, ref. [1], Eq. (3.15), p. 81, where we have the interchange of T_x and T_y .

Along similar lines, it is easy to see that the *Lissajous spiral*, ref. [1], Eq. (3.27), p. 90, occurring for the *nipponites*, is indeed a perfect sphere in a three-

dimensional isoeuclidean space. In fact, one has to solve the following equations in r and the B 's

$$\begin{aligned} x &= a e^{\alpha \phi} [1 + e^{\phi} \cos(2 \gamma \phi)] \cos \phi = \\ &= r [B_{22}^{-1} \sin(B_{21} B_{22} \theta)] [B_{11}^{-1} \cos(B_{11} B_{12} \phi)], \end{aligned} \quad (2.81a)$$

$$\begin{aligned} y &= a e^{\alpha \phi} [1 + e^{\phi} \cos(2 \gamma \phi)] \sin \phi = \\ &= r [B_{22}^{-1} \sin(B_{21} B_{22} \theta)] [B_{12}^{-1} \sin(B_{11} B_{12} \phi)], \end{aligned} \quad (2.81b)$$

$$z = b e^{\beta \phi} \sin(\gamma \phi) = r B_{21}^{-1} \cos(B_{21} B_{22} \theta), \quad (2.81c)$$

in which case the shells is represented via the isospherical coordinates (App. B) as the perfect sphere in isospace

$$\begin{aligned} x T_x x + y T_y y + z T_z z &= \\ &= r^2 (B_{22}^2 B_{11}^2 \text{isoin}^2 \theta \cos^2 \phi + B_{22}^2 B_{12}^2 \text{isoin}^2 \theta \text{isoin}^2 \phi + \\ &\quad + B_{21}^2 \text{isocos}^2 \theta) = r^2. \end{aligned} \quad (2.82)$$

Similar representations hold for all other possible shapes of sea shells owing to the direct universality of the isoeuclidean geometry. The above examples confirm the geometric unification of all possible sea shells into the isosphere.

Such a geometric unification permits the identification of the *universal symmetry for all possible sea shells as being the isorotational symmetry* $\hat{O}(3)$ of App. C. In turn, the application of the isorotations is particularly intriguing because it permits the study of interconnections between sea shells which simply cannot be studied via the conventional rotational symmetry. This aspect will be studied in a separate work.

The extension of the results with the inclusion of time and the representation of sea shells evolution at bifurcations will be studied in a future

work.

3: ELEMENTS OF THE GENOEUCLIDEAN GEOMETRY

3.A: Genounits. We shall now briefly outline the broader genoeuclidean geometry. As indicated in Sect. 1, the fundamental quantities are the four sufficiently smooth, nonsingular, bounded and *nonhermitean* generalized units, called *genounits*, for the characterization of the four possible time arrows for nonconservative irreversible processes (Fig. 4).

We then have the *space genounits* and related *space genotopic elements* characterized by 3×3 -matrices interconnected by two conjugations, Hermiticity and isoduality

$$\mathbf{l}_s^> = \mathbf{T}_s^>, \quad \mathbf{<l}_s = (\mathbf{l}_s^>)^{\dagger}, \quad (3.1a)$$

$$\mathbf{l}_s^{>d} = -\mathbf{l}_s^>, \quad {}^d\mathbf{<l}_s = -\mathbf{<l}_s, \quad (3.1b)$$

and the *time genounits* and related *time genotopic elements* characterized by a one-dimensional complex function also interconnected by two conjugations, Hermiticity and isoduality.

$$\mathbf{l}_t^> = \mathbf{T}_t^>, \quad \mathbf{<l}_t = (\mathbf{l}_t^>)^{\dagger}, \quad (3.2a)$$

$$\mathbf{l}_t^{>d} = -\mathbf{l}_t^>, \quad {}^d\mathbf{<l}_t = -\mathbf{<l}_t, \quad (3.2b)$$

The above units are distinct in the genoeuclidean geometries of Class I and II, but they are all unified for the case of Class III or higher. The representation of the bifurcation of sea shells then requires the use of genogeometries of at least Class III, while Class I is sufficient for particles in irreversible conditions and Class II is sufficient for antiparticles also in irreversible conditions [4,5].

3.B: Genonumbers. The technical understanding of the genoeuclidean geometry requires the knowledge that they are based on a theory of numbers which is more general than that of isonumbers.

Let $F(\alpha, +, \times)$ be a conventional field (Sect. 2.B) with multiplication $\alpha\beta = \alpha \times \beta$. Its isotopic generalization is characterized by the isoproduct $\alpha * \beta = \alpha T \beta$, $T = T^\dagger =$ fixed. Both products $\alpha\beta$ and $\alpha * \beta$ are based on the assumption that they apply irrespective of whether α multiplies β from the left, or β multiplies α from the right. We can therefore introduce the following:

Definition 3.1 [5,10]: *The multiplication of two numbers α and β is ordered to the right, and denoted $\alpha > \beta = \alpha T^> \beta$, when α multiplies β to the right, while it is ordered to the left, and denoted $\alpha < \beta = \alpha T^< \beta$ when β multiplies α from the left, where $T^>$ and $T^<$ are genotopic elements of Class III.*

Note that the above ordering is compatible with other properties and axioms of number theory. As an example, if the original field F is commutative, it remains commutative in *each* of the above ordering, that is, if $\alpha\beta = \beta\alpha$, then $\alpha > \beta = \beta > \alpha$ and $\alpha < \beta = \beta < \alpha$. The same occurrence holds for other properties, such as associativity while the verification of the left and right distributive laws is evident. Thus, the entire theory of numbers can be reformulated under ordering by characterizing fully acceptable fields.

The point at the foundations of the genoeuclidean geometry is that *the multiplications of the same numbers in different orderings are generally different*, $\alpha > \beta \neq \beta < \alpha$, as requested by the different isounits (3.1), (3.2) whether for space or time genoproducts

$$1^>: 1^> > \alpha = \alpha > 1^> \equiv \alpha, \quad 1^> = (T^>)^{-1} \quad (3.3a)$$

$$1^<: 1^< < \alpha = \alpha < 1^< \equiv \alpha, \quad 1^< = (T^<)^{-1}. \quad (3.3b)$$

The above features permit a dual generalization of isonumbers, one for ordering to the right, yielding the *right genofield*

$$\hat{F}^>(\hat{\alpha}^>, +, *^>), \quad \hat{\alpha}^> = \alpha 1^>, \quad (3.4)$$

whose elements $\hat{\alpha}^>$ are called *right genonumbers*, and one to the left, yielding the *left genofield*

$$\langle \hat{f}(\langle \hat{a}, +, \langle * \rangle, \quad \langle \hat{a} = \langle 1 \rangle \alpha, \quad (3.5)$$

whose elements $\langle \hat{a}$ are called *left genonumbers*. The above two different genofields are often denoted with the unified symbol $\langle \hat{f}(\langle \hat{a}, +, \langle * \rangle)$, with the understanding that the orderings can solely be used individually and not jointly.

Note the need for a prior isotopy $\alpha\beta \rightarrow \alpha T\beta$ in order to construct the above genotopies. In fact, no ordering is evidently meaningful for the conventional multiplication $\alpha\beta = \alpha 1\beta$.

Under the above assumptions, *the product ordered to the right can characterize motion forward in time, while that ordered to the left can characterize motion backward in time*. In different term, the above orderings represent *Eddington's arrows of time*.

Note that the theory of isonumbers is a subcase of that of genonumbers under the simple condition $T^> = \langle T = T = T^\dagger$. This illustrates that the origin of the reversibility can be seen in the appropriate theory of numbers, more specifically, from the fact that their multiplications to the right and to the left are identical, $\alpha > \beta \equiv \alpha < \beta$.

The *isodual genofields* can now be constructed with the familiar isoduality and are denoted with $\langle \hat{f}(\langle \hat{a}^d, +, \langle * \rangle^d)$. Again, the distinction between genofields and their isoduals is lost for Class III. The rest of the isotopic theory can then be generalized accordingly, including isotransformation theory, Lie-Santilli theory, functional isoanalysis, etc. (see ref.s [5] for brevity).

3.C: Genoeuclidean geometry. The theory of isospaces admits a consistent and significant genotopic covering. Let $E(r, \delta, R)$ be a conventional, three-dimensional Euclidean space over the reals R and let $\hat{E}(r, \hat{\delta}, \hat{R})$ be its isotopes over the isoreals \hat{R} . Then, the *genoeuclidean spaces* are given by

$$\hat{E}(r, \hat{\delta}, \hat{R}) : \hat{\delta}^> = T^> \delta, \quad r^{2>} = r^t \delta^> r, \quad 1^> = (T^>)^{-1}, \quad (3.6a)$$

$$\langle \hat{E}(r, \langle \hat{\delta}, \langle \hat{R}) : \langle \hat{\delta} = \delta \langle T, \quad r^{<2} = r \langle \hat{\delta} r^t, \quad \langle 1 = (\langle T)^{-1}, \quad (3.6b)$$

$$1^> = (\langle 1)^\dagger, \quad (3.6c)$$

A most visible difference between genospaces and isospaces is that the invariant in the former is unique for both multiplications to the right and to the left, while in the latter we have the invariants for the multiplication to the right and one to the left are different. We therefore have *two different genospaces one for motion forward in time, and one for motion backward in time.*

The use of conventional transformation theory for genospaces also violates linearity, transitivity and other basic laws. For this reason it must be lifted into the *right and left genotrasformations*

$$r' = \hat{U}^> r = \hat{U}^> T^> r, \quad (3.7a)$$

$$r' = r < \hat{U} = r < T < \hat{U}. \quad (3.7b)$$

The above transformations are, individually one-sided isolinear, isolocal and isocanonical as it occurs for the isotransformations, although they are again different for different orderings of the product.

The *genoeuclidean geometry* is the geometry of genospaces $\langle \hat{E} \rangle(r, \langle \hat{\delta} \rangle, \langle \hat{R} \rangle)$. An important difference between the iso- and genogeometries is that the metric of the former is unique for both directions of time, while the metric of the latter is differentiated depending on the assumed direction of time, $\hat{\delta}^> \neq \hat{\delta}^<$.

This implies the existence of two different deformations of the sphere, one per each direction of time, each of which is mapped into the perfect sphere in genospace. called *genosphere*. Note however that, for purely imaginary genotopic elements, e.g., $T^> = iT$, $T = T^\dagger$, $\hat{\delta} = T\hat{\delta}T$, $\hat{1} = T^{-1}$, the forward genosphere is the negative of the isosphere

$$r^{\hat{2}} = (r^\dagger \hat{\delta}^> r) \hat{1}^> = (r^\dagger i \hat{\delta} r) i \hat{1} = -r^2 = -(r^\dagger \hat{\delta} r) \hat{1}. \quad (3.3.8)$$

Note also that the negative of the isosphere *is not* the isodual isosphere (because the latter coincides with the isosphere). Genotopies can therefore used to alter the sign of the isosphere. More general realizations evidently occur for broader structures of the genometric (for numerous physical applications, see [4,5]).

The extension of the remaining properties of isogeometries into the genotopic form is an instructive exercise for the interested reader, and it is omitted for brevity (see ref.sd [5]). Genoeuclidean representations of sea shells will be done in a future work.

APPENDIX A: ISOTRIGONOMETRY

In Sect. I we pointed out the inapplicability of the conventional trigonometry and related Gauss plane for the characterization of the isocomplex numbers. In this appendix we study the isotopic generalization of trigonometry submitted by this author in 1988 under the name of *isotrigonometry* (see [4,5]).

Consider a conventional two-dimensional Euclidean space $E(r, \delta, R)$, $\delta = \text{diag. (1, 1)}$ over the reals $R(n, +, \times)$. Its fundamental notion is the familiar distance among two points

$$D^2 = (x_1 - x_2)(x_1 - x_2) + (y_1 - y_2)(y_1 - y_2) \in R(n, +, \times), \quad (\text{A.1})$$

which represents the celebrated *Pythagorean theorem* expressing the hypotenuse D of a right triangle with sides A and B ,

$$D^2 = A^2 + B^2. \quad (\text{A.2})$$

A property of the space $E(r, \delta, R)$ is the angle α between two vectors from the origin to points $P_1(x_1, y_1)$ and $P_2(x_2, y_2)$. The trigonometric notion " $\cos \alpha$ " is given by

$$\cos \alpha = \frac{x_1 x_2 + y_1 y_2}{(x_1 x_1 + y_1 y_1)^{\frac{1}{2}} (x_2 x_2 + y_2 y_2)^{\frac{1}{2}}}. \quad (\text{A.3})$$

From the above definition one can derive the entire conventional trigonometry. For instance, by assuming that the points are on a circle of unit radius $D^2 = 1$, we have for $P_1(x_1, y_1)$ and $P_2(1, 0)$ $\cos \alpha = x_1$, for $P_2(0, 1)$ we have $\sin \alpha = y_1$, with consequential familiar property of the Gauss plane

$$\sin^2 \alpha + \cos^2 \alpha = 1, \quad \text{etc.} \quad (\text{A.4})$$

All the above properties lose mathematical and physical significance under

isotopy for numerous independent reasons, such as the loss of the central notion, that of distance, Eq. (A.1), the generally curved character of the lines, etc. The use of conventional geometries, those defined over ordinary fields, is also inapplicable because they are based on the conventional unit l , while under isotopies we must necessarily redefine the unit.

Reconstruction of angles in the isoeuclidean geometry

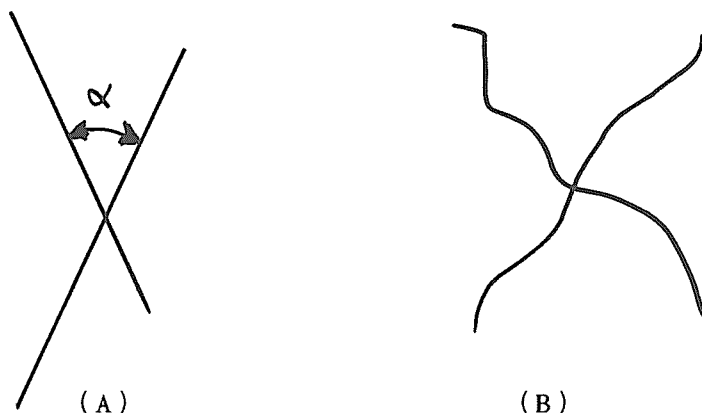


FIGURE . Diagram (A) depicts the origin of the notion of angle in the conventional Euclidean plane from two straight intersecting lines, which can be analytically expressed via the familiar expression (A.2). In the transition to the Isoeuclidean plane, the lines are no longer straight when projected in the original space, thus preventing the conventional definition of angles. However, the isoeuclidean geometry is isostraight, that is, the lines are straight in isospace. This does indeed permit the reconstruction of angles, although in the generalized form of Eq. (A.8). In turn, the possibility of a consistent generalized notion of angle permits the construction of a consistent generalization of trigonometry. Note that this is impossible in the Riemannian and other curves geometries, and it is permitted by the Isoeuclidean geometry because of its fundamental structure, the property that the Euclidean metric is arbitrarily deformed, $\delta \rightarrow \hat{\delta} = T\delta$, thus acquiring the most general possible curvature, but the original unit is deformed of the inverse amount, $l \rightarrow \hat{l} = T^{-1}l$, thus eliminating the curvature in isospace.

These and other reasons have rendered mandatory the generalization of conventional trigonometry under isotopy. Consider the isotopic lifting $E(r, \delta, R)$ into the now familiar *two-dimensional isoeuclidean space* over the isoreals $\hat{R}(n, +, *)$

(Sect. 3.3) here assumed for simplicity in the diagonalized form

$$\hat{E}(r, \hat{\delta}, \hat{R}) : r = (x, y), \hat{\delta} = T\delta = \text{diag.} (T_x, T_y), \hat{R} = \hat{R}(n, +, *), \quad (\text{A.5a})$$

$$\hat{1} = T^{-1} = \text{diag.} (T_x^{-1}, T_y^{-1}), \quad T_k = T_k(t, r, \hat{r}, \dots), k = 1, 2. \quad (\text{A.5b})$$

Consider now two points $P_1(x_1, y_1), P_2(x_2, y_2) \in \hat{E}(r, \hat{\delta}, \hat{R})$. Then the conventional distance (6.A.1) is necessarily (and uniquely) generalized into the *isodistance*

$$\hat{D}^2 = (x_1 - x_2) T_x (x_1 - x_2) + (y_1 - y_2) T_y (y_1 - y_2) \in \hat{R}. \quad (\text{A.6})$$

(where we ignore the factor $\hat{1}$ for simplicity). The above generalized notion of distance evidently characterizes an infinite family of isotopies of the Pythagorean theorem, called *isopythagorean theorem*, according to which the image of expression (A.2) under isotopies is given by

$$\hat{D}^2 = A T_x(t, r, \hat{r}, \dots) A + B T_y(t, r, \hat{r}, \dots) B, \quad (\text{A.7})$$

Suppose now that the two points P_1 and P_2 also represent *isovectors* originating from the origin of $\hat{E}(r, \hat{\delta}, \hat{R})$. The *isoangle* between these two isovectors is given by [4,5]

$$\hat{\alpha} = \alpha (T_x T_y)^{1/2}, \quad (\text{A.8})$$

where α is the original angle.

We can then introduce the notion of *isocosinus* of the isoangle $\hat{\alpha}$ via the definition³

$$\text{isocos } \hat{\alpha} = \frac{x_1 T_x x_2 + y_1 T_y y_2}{\left((x_1 T_x x_1 + y_1 T_y y_1)^{\frac{1}{2}} (x_2 T_x x_2 + y_2 T_y y_2)^{\frac{1}{2}} \right)} \quad (\text{A.9})$$

³ The attentive reader may have noted the conventional square in the denominator. However, the isofactor in the denominator cancels out with that of the numerator, resulting in expression (A.9)

Isopythagorean theorem

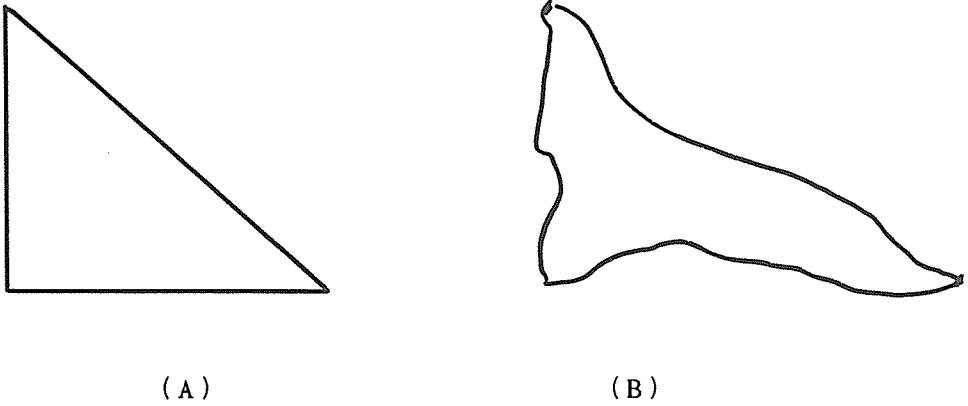


FIGURE 9: A schematic view of the isotopic image of the Pythagorean Theorem which permits the reconstruction of the theorem for figure (B) with arbitrarily curved sides. Its understanding requires the knowledge that *the right triangle (A) remains a right triangle in isoeuclidean space, called "right isotriangle"*. Diagram (B) is only *the projection of the right isotriangle in the conventional Euclidean space*. In fact, the conventional sides are lifted into curves. Then, the original angle α between two generic sides is lifted into the isoangle $\hat{\alpha} = T_X^{\frac{1}{2}} T_Y^{\frac{1}{2}} \alpha$. Despite these generalizations, a relationship between the *isohypotenuse* and the *isosides* still exists, and it is given by Eq. (A.7). As a matter of fact, this is precisely the central geometric meaning of isoeuclidean distance. It may be intriguing and instructive for the interested reader to note that all conventional trigonometry on a plane admits a consistent and nontrivial isotopy. As an example, the original angles of a triangle α, β, γ , which are such that $\alpha + \beta + \gamma = 180^\circ$, are deformed under isotopies into the new values α', β', γ' such that $\alpha' + \beta' + \gamma' \neq 180^\circ$ in the Euclidean plane. However, the peculiarity of the isoeuclidean geometry is such that the deformations $\hat{\alpha} \rightarrow \alpha$, etc. are compensated in such a way that $T_X^{\frac{1}{2}} T_Y^{\frac{1}{2}} \alpha' = \hat{\alpha}$, etc. The sum of the angle of (any) isotriangle is then

$$T_X^{\frac{1}{2}} T_Y^{\frac{1}{2}} (\alpha' + \beta' + \gamma') = \hat{\alpha} + \hat{\beta} + \hat{\gamma} = 180^\circ.$$

All other properties can then be derived accordingly. To understand the novelty one should note that the above generalization of the Pythagorean theorem does not exist in conventional geometries, those constructed with respect to conventional units,

such as the Riemannian or other noneuclidean geometries.

We now assume the two points to be on the surface

$$D^2 = x T_x x + y T_y y = 1, \quad (\text{A.10})$$

and for the values $P_1 (x_1, y_1)$, $P_2 (b_1^{-1}, 0)$, the *isocosinus* $\hat{\alpha}$ becomes

$$x_1 = T_x^{-1/2} \cos \hat{\alpha} = \text{isocos } \hat{\alpha}. \quad (\text{A.11})$$

We can then define the *isosin* $\hat{\alpha}$ by assuming $P_2 (0, T_y^{-1})$ for which

$$y_2 = T_y^{-1/2} \sin \hat{\alpha} = \text{isosin } \hat{\alpha}. \quad (\text{A.12})$$

The following isotopy of property (A.4) then holds

$$T_x \text{isocos}^2 \hat{\alpha} + T_y \text{isosin}^2 \hat{\alpha} = 1 \quad (\text{A.13})$$

The above results characterize the *isopolar coordinates* in the isogauss plane

$$x = \text{isocos } \hat{\alpha} = T_x^{-\frac{1}{2}} \cos (T_x^{\frac{1}{2}} T_y^{\frac{1}{2}} \alpha), \quad (\text{A.14a})$$

$$y = \text{isosin } \hat{\alpha} = T_y^{-\frac{1}{2}} \sin (T_x^{\frac{1}{2}} T_y^{\frac{1}{2}} \alpha). \quad (\text{A.14b})$$

which verify again the isotopic generalization of property (A.4) for $\hat{D} = 1$

$$x T_x x + y T_y y = T_x \text{isosin}^2 \hat{\alpha} + T_y \text{isocos}^2 \hat{\alpha} = 1. \quad (\text{A.15})$$

When the isohypothénuse \hat{D} is not one, we have the value of the sides

$$A = \hat{D} T_x^{-\frac{1}{2}} \cos \hat{\alpha} = \hat{D} \text{isocos } \hat{\alpha}, \quad (\text{2.16a})$$

$$B = D T_Y^{-\frac{1}{2}} \sin \hat{\alpha} = \hat{D} \text{ isosin } \hat{\alpha}, \quad (\text{A.16b})$$

which are again consistent with basic isopythagorean theorem.

In summary, the *isotopy of the trigonometric functions* is given by

$$\cos \alpha \rightarrow \text{isocos } \hat{\alpha} = T_X^{-\frac{1}{2}} \cos (T_X^{\frac{1}{2}} T_Y^{\frac{1}{2}} \alpha), \quad (\text{A.17a})$$

$$\sin \alpha \rightarrow \text{isosin } \hat{\alpha} = T_Y^{-\frac{1}{2}} \sin (T_X^{\frac{1}{2}} T_Y^{\frac{1}{2}} \alpha). \quad (\text{A.17b})$$

The construction of the isotrigonometry in all the necessary details can be conducted accordingly.

Note that the trigonometric functions are deformed both in *intensity* and in their *angle*. These properties render them particularly intriguing in physics, e.g., for the study of deformation of potential wells in nuclear physics, or in theoretical biology, e.g., the study of the shape of sea shells.

The reader should be aware that, despite they apparent simplicity, the isotrigonometric functions are rather general indeed because of the dependence of their angles, $\sin \hat{\alpha} = \sin[\hat{\alpha}(t, r, \dot{r}, \dots)]$, $\cos \hat{\alpha} = \cos[\hat{\alpha}(t, r, \dot{r}, \dots)]$. For isoeuclidean planes of Class I, the factor of the isoangle $(T_X T_Y)^{1/2}$ is *positive-definite* in which case $\sin \hat{\alpha}$ and $\cos \hat{\alpha}$ remain conventional trigonometric functions. For the isoeuclidean plane of Class II the factor $(T_X T_Y)^{1/2}$ still remains positive-definite. Thus *the argument of the isotrigonometric functions is isoselfdual*. However, true generalization emerge for the isoeuclidean plane of Class I because, in this case, the factor $(T_X T_Y)^{1/2}$ can be purely imaginary and the trigonometric functions $\sin \hat{\alpha}$ and $\cos \hat{\alpha}$ become *hyperbolic* functions (see below).

Note that in the formalism of Sect. 2.J, the isocosinus of the angle for two intersecting vectors can be written as the isotopy of the conventional case

$$\text{isocos } \hat{\theta} = \frac{V_1 \odot V_2}{\uparrow V_1 \uparrow * \uparrow V_2 \uparrow}. \quad (2.18)$$

Also, one can introduce the *directional isocosinuses* of a vector

$$\text{isocos } \hat{\alpha} = V_1 / \uparrow V \uparrow, \text{ isocos } \hat{\beta} = V_2 / \uparrow V \uparrow, \text{ isocos } \hat{\gamma} = V_3 / \uparrow V \uparrow. \quad (2.19)$$

Then, we have again the correct lifting of the corresponding conventional identity

$$T_x \text{isocos}^2 \hat{\alpha} + T_y \text{isocos}^2 \hat{\beta} + T_z \text{isocos}^2 \hat{\gamma} = 1. \quad (2.20)$$

here we have ordinary squares rather than isosquares.

The reader can then readily compute the remaining properties of the isotrigonometry. We here limit ourself to mention only a few properties. For instance, *the isotrigonometric functions are also periodic of period 2π* ,

$$\text{isocos} (\hat{\alpha} + 2\pi) \equiv \text{isocos } \hat{\alpha}, \quad \text{isoin} (\hat{\alpha} + 2\pi) \equiv \text{isoin } \hat{\alpha}. \quad (\text{A.21})$$

The following symmetry properties then follow as in the conventional case

$$\text{isocos} (-\hat{\alpha}) \equiv \text{isocos } \hat{\alpha}, \quad \text{isoin} (-\hat{\alpha}) = -\text{isoin } \hat{\alpha}. \quad (\text{A.22})$$

Similarly, the theorems of isoaddition become

$$\text{isoin} (\hat{\alpha} \pm \hat{\beta}) = T_x^{-\frac{1}{2}} (\text{isoin } \hat{\alpha} \text{isocos } \hat{\beta} \pm \text{isocos } \hat{\alpha} \text{isoin } \hat{\beta}), \quad (\text{A.23a})$$

$$\text{isocos} (\hat{\alpha} + \hat{\beta}) = T_x (T_y^{-1} \text{isocos } \hat{\alpha} \text{isocos } \hat{\beta} \pm T_x^{-1} \text{isoin } \hat{\alpha} \text{isoin } \hat{\beta}) \quad (\text{A.23b})$$

$$\text{isoin } \hat{\alpha} + \text{isoin } \hat{\beta} = 2 T_x^{-\frac{1}{2}} \text{isoin } \frac{1}{2} (\hat{\alpha} + \hat{\beta}) \text{isocos } \frac{1}{2} (\hat{\alpha} - \hat{\beta}), \quad (\text{A.23c})$$

$$\text{isocos } \hat{\alpha} + \text{isocos } \hat{\beta} = 2 T_x^{-\frac{1}{2}} \text{isocos } \frac{1}{2} (\hat{\alpha} + \hat{\beta}) \text{isocos } \frac{1}{2} (\hat{\alpha} - \hat{\beta}), \quad (\text{A.23d})$$

etc.

The connection between isotrigonometric functions and isoexponentiation requires the use of the isounit

$$\mathbf{1} = T_x^{-\frac{1}{2}} T_y^{-\frac{1}{2}} = (\det \mathbf{1})^{\frac{1}{2}}, \quad \mathbf{t} = T_x^{\frac{1}{2}} T_y^{\frac{1}{2}} = (\det \mathbf{T})^{\frac{1}{2}} \quad (\text{A.24})$$

under which we have the alternative definition of isotrigonometric functions

$$\hat{e}^{i\hat{\alpha}} = \hat{1} e^{i\hat{\imath}\alpha} = T_y^{-\frac{1}{2}} \text{isocos } \hat{\alpha} + i T_x^{-\frac{1}{2}} \text{isosin } \hat{\alpha}, \quad (\text{A.25})$$

where the isoenvelope is now defined for product $a*b = a\hat{1}b$ and isounit $\hat{1}$. We can then also introduce the *isohyperbolic functions* for $\hat{\imath} > 0$

$$\text{isocosh } \hat{\alpha} = T_x^{-\frac{1}{2}} \cosh(\hat{\imath}\alpha), \quad \text{isosinh } \hat{\alpha} = T_y^{-\frac{1}{2}} \sinh(\hat{\imath}\alpha), \quad (6.A.26)$$

with basic property

$$T_x \text{isocosh}^2 \hat{\alpha} - T_y \text{isosinh}^2 \hat{\alpha} = 1, \quad (\text{A.27})$$

and their derivation via the isoexponentiation

$$\hat{e}^{\hat{\alpha}} = \hat{1} e^{\hat{\imath}\alpha} = T_y^{-\frac{1}{2}} \text{isocosh } \hat{\alpha} + T_x^{-\frac{1}{2}} \text{isosinh } \hat{\alpha}. \quad (\text{A.28})$$

It may be intriguing and instructive for the interested reader to work out additional properties of isotrigonometric and isohyperbolic functions.

However, a peculiar property is that *all distinctions between trigonometric and transcendental functions are lost in the isoeuclidean plane of Class III*, trivially, because in this case the factor $\hat{\imath}$ can be real or imaginary, as indicated earlier.

We close this appendix with the following intriguing property of the isogauss theory

Lemma A.1: *All possible algebraic or transcendental functions $f(x, y) = 0$ in the Gauss plane can be unified into the isocircle in the isogauss plane of Class III*

In fact, for any $f(x, y) = 0$ there always exist elements δ_{ij} such that $f(x, y) \equiv r^i \delta_{ij} r^j - 1$

= 0. The above property can be illustrated via a certain geometric complementarity between the circle $xx + yy = 1$ and the tractrix

$$y e^{1 - (1 - y^2)^{\frac{1}{2}}} + (1 - y^2)^{\frac{1}{2}} = 1 \quad (\text{A.29})$$

It is evident that tractrix (6.B.1) is unified into the isocircle by the diagonal isometric with elements $\delta_{11} = yx^{-2} \exp(1 - (1 - y^2)^{\frac{1}{2}})$, $\delta_{22} = y^{-1}(1 - y^2)^{\frac{1}{2}}$.

APPENDIX B: ISOSPHERICAL COORDINATES

In ref. [5] we have proved that the conventional spherical coordinates in Euclidean space $E(r, \delta, R)$

$$x = r \sin \theta \cos \phi, \quad y = r \sin \theta \sin \phi, \quad z = r \cos \theta, \quad (\text{B.1})$$

with familiar measure

$$ds^2 = dx^2 + dy^2 + dz^2 = dr^2 + r^2 (d\theta^2 + \sin^2 \theta d\phi^2), \quad (\text{B.2})$$

imply a number of inconsistencies when used in isospaces $\hat{E}(r, \hat{\delta}, \hat{R})$, such as the impossibility of separating the radial and angular part in the equations of motion, and other problems, which persist in the use of other *conventional* coordinate systems, e.g., elliptical.

These occurrences have rendered mandatory the construction of the isotopies of the spherical coordinates, called isospherical coordinates, which are the correct coordinates for isospaces $\hat{E}(r, \hat{\delta}, \hat{R})$.

We shall present first the simplest possible derivation of the isospherical coordinates, and then its more general form as needed for the isorepresentation theory of the isotopic $\hat{SO}(3)$ symmetry and other applications. Consider the three-dimensional isoeuclidean space $\hat{E}(r, \hat{\delta}, \hat{R})$ with isometric

$$\hat{\delta} = T \delta, \quad \delta = \text{diag.} (1, 1, 1), \quad T = \text{diag.} (T_x, T_y, T_z). \quad (\text{B.3})$$

Introduce the redefinitions of the Cartesian coordinates

$$\bar{x}_I = x T_x^{\frac{1}{2}}, \quad \bar{y} = y T_y^{\frac{1}{2}}, \quad \bar{z} = z T_z^{\frac{1}{2}}, \quad (\text{B.4})$$

which are such to reduce the isoinvariant in $\hat{E}(r, \hat{\delta}, \hat{R})$ into an identical form in a conventional Euclidean space $E(\bar{r}, \delta, R) \neq E(r, \delta, R)$,

$$r^2 = x T_x x + y T_y y + z T_z z \equiv \bar{x} \bar{x} + \bar{y} \bar{y} + \bar{z} \bar{z} = \bar{r}^2. \quad (\text{B.5})$$

Next, we introduce the *isospherical angles*

$$\hat{\theta} = T_z^{\frac{1}{2}} \theta, \quad \hat{\phi} = T_x^{\frac{1}{2}} T_y^{\frac{1}{2}} \phi, \quad (\text{B.6})$$

defined to coincide with the original angles prior to the deformation. They are derivable from the representation theory of the isorotational group $\hat{O}(3)$ which is here omitted for brevity [5].

Under these assumptions, the *isospherical coordinates* can be first written in the form [5] (see Fig. 10)

$$x = r T_x^{-\frac{1}{2}} \sin (T_z^{\frac{1}{2}} \theta) \cos (T_x^{\frac{1}{2}} T_y^{\frac{1}{2}} \phi) \quad (\text{B.7a})$$

$$y = r T_y^{-\frac{1}{2}} \sin (T_z^{\frac{1}{2}} \theta) \sin (T_x T_y \phi), \quad (\text{B.7b})$$

$$z = r T_z^{-\frac{1}{2}} \cos (T_z^{\frac{1}{2}} \theta), \quad (\text{B.7c})$$

We can then introduce the simplest possible form of the *isomeasure* on $\hat{E}(r, \hat{\delta}, \hat{R})$, that in terms of conventional differentials with the isotopic element independent from the local variables

$$\begin{aligned} ds^2 &= d\bar{x} d\bar{x} + d\bar{y} d\bar{y} + d\bar{z} d\bar{z} = \\ &= dx T_x dx + dy T_y dy + dz T_z dz = \end{aligned}$$

$$\begin{aligned}
&= dr^2 + r^2 [T_z d\theta^2 + T_x T_y \sin^2 \theta d\phi^2] = \\
&\equiv dr^2 + r^2 [d\hat{\theta}^2 + (\sin^2 \hat{\theta}) d\hat{\phi}^2].
\end{aligned} \tag{B.8}$$

The expression of the isomeasure for the general case in which the isotopic element depends on the local variables requires the full use of the differential calculus and, as such, it is omitted for brevity (see ref. [5]).

The isospherical coordinates in form (B.7) are useful for practical calculations, although they are not in their most general possible form because conventional trigonometric functions admit isotopic images. Their formulation in terms of the isotrigonometric functions then permits deeper insights.

Recall from Appendix A that the *isopolar coordinates* expressed in terms of the *isotrigonometric functions* in the *isogauss* (x, y)-plane with isotopic element $T = \text{diag.} (T_x, T_y)$ are given by

$$x = r \text{ isocos } \hat{\phi} = r T_x^{-\frac{1}{2}} \cos [(T_x^{\frac{1}{2}} T_y^{\frac{1}{2}}) \phi], \tag{B.9a}$$

$$y = r \text{ isosin } \hat{\phi} = r T_y^{-\frac{1}{2}} \sin [(T_x^{\frac{1}{2}} T_y^{\frac{1}{2}}) \phi], \tag{B.9b}$$

and verify the *isopythagorean theorem*

$$x T_x x + y T_y y = r^2 (T_x \text{isocos}^2 \hat{\phi} + T_y \text{isosin}^2 \hat{\phi}) = r^2. \tag{B.10}$$

In particular, the isotopic element of the above isotrigonometric functions is *not* that of the isogauss plane, but rather the element T in the isoexponentiation

$$\begin{aligned}
\hat{e}_\phi^{i\phi} &= \mathfrak{l}_\phi e^{i T \phi} = \mathfrak{l}_\phi e^{i \mathfrak{t} \phi} = \mathfrak{l}_\phi (\cos \hat{\phi} + i \sin \hat{\phi}) = \\
&= T_y^{-\frac{1}{2}} \text{isocos } \hat{\phi} + i T_x^{-\frac{1}{2}} \text{isosin } \hat{\phi},
\end{aligned} \tag{B.11a}$$

$$\mathfrak{t} = T_x^{\frac{1}{2}} T_y^{\frac{1}{2}}, \quad \mathfrak{l}_\phi = \mathfrak{t}^{-1}. \tag{B.11b}$$

The next issue is the appropriate isotrigonometric formulation of the

remaining terms in $\hat{\theta}$. At this point there is the emergence of a further degree of freedom which is "hidden" in the *isotopic* theory itself and completely absent in quantum mechanics.

By inspecting structure (B.7) one could conclude that the isogauss plane for the polar angle has the isotopic element $T = \text{diag. } (T_z, 1)$. However, one can also introduce the following redefinition of the isotopic element in three-dimensional space

$$T_x^{\frac{1}{2}} = B_{22} B_{11}, \quad T_y^{\frac{1}{2}} = B_{22} B_{12}, \quad T_z^{\frac{1}{2}} = B_{21}, \quad (\text{B.12a})$$

$$B_{21} B_{22} = B_{11} B_{12}. \quad (\text{B.12b})$$

with solution

$$B_{11}^3 = T_x T_z^{\frac{1}{2}} / T_y^{\frac{1}{2}}, \quad (\text{B.13a})$$

$$B_{12}^3 = T_y T_z^{\frac{1}{2}} / T_x^{\frac{1}{2}}, \quad (\text{B.13b})$$

$$B_{22}^3 = b_1 b_2 / b_3, \quad B_{21} = b_3, \quad (\text{B.13c})$$

$$B_{11}^3 B_{12}^3 = B_{22}^3 B_{21}^3 = T_x^{\frac{1}{2}} T_y^{\frac{1}{2}} T_z, \quad (\text{B.13d})$$

under which we can introduce the *general isospherical coordinates*

$$x = r \text{ isosin } \hat{\theta} \text{ isocos } \hat{\phi} =$$

$$= r [B_{22}^{-1} \sin (B_{21} B_{22} \theta)] [B_{11}^{-1} \cos (B_{11} B_{12} \phi)], \quad (\text{B.14a})$$

$$y = r \text{ isosin } \hat{\theta} \text{ isosin } \hat{\phi} =$$

$$= r [B_{22}^{-1} \sin (B_{21} B_{22} \theta)] [B_{12}^{-1} \sin (B_{11} B_{12} \phi)], \quad (\text{B.14b})$$

$$z = r \text{ isocos } \hat{\theta} = r B_{21}^{-1} \cos (B_{21} B_{22} \theta), \quad (\text{B.14c})$$

with isoidentity

$$x T_x x + y T_y y + z T_z z = \quad (B.15)$$

$$= r^2 (B_{22}^2 B_{11}^2 \text{isoin}^2 \hat{\theta} \text{c} \hat{\phi}^2 + B_{22}^2 B_{12}^2 \text{isoin}^2 \hat{\theta} \text{isoin}^2 \hat{\phi} + \\ + B_{21}^2 \text{isoc} \cos^2 \hat{\theta}) = r^2,$$

Isospherical coordinates

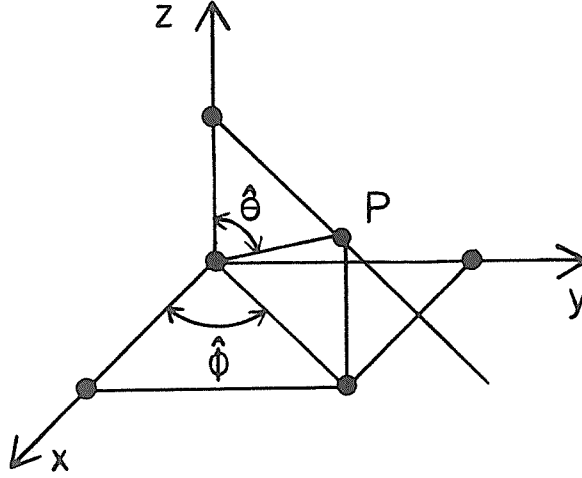


FIGURE 10: A schematic view of the coordinates of a point on the isosphere in isoeuclidean space in three-dimension, Eq.s (B.14). As one can see, the representation coincides at the abstract level with the conventional one in Euclidean space with coordinates (B.1). However, the projection of the former in the space of the latter exhibits the ellipsoidal character of the isosphere.

Redefinitions (B.14) are important for the isorepresentation theory studied in ref.s [5] because they permit the identification of the values of the *isospherical isotopic elements* and *isounits* separately for the θ and ϕ angles

$$T_{\theta} = B_{21} B_{22} \equiv T_{\phi} = B_{11} B_{12}, \quad (B.16a)$$

$$\gamma_{\theta} = B_{21}^{-1} B_{22}^{-1} \equiv \gamma_{\phi} = B_{11}^{-1} B_{12}^{-1}, \quad (B.16b)$$

with evident computational advances.

The "hidden" isotopic degree of freedom in the transition from the decomposition

$$T = \text{diag} (T_x, T_y, T_z) = \text{diag} (T_x, T_y) \times \text{diag} (T_z, 1), \quad (\text{B.17})$$

to the more general form underlying structure (5.5.14)

$$T = \text{diag} (T_x, T_y, T_z) = \text{diag.} (B_{11}^2, B_{12}^2) \times \text{diag} (B_{21}^2, B_{22}^2), \quad (\text{B.18a})$$

$$T_x = B_{22}^2 B_{11}^2, \quad T_y = B_{22}^2 B_{12}^2, \quad T_z = B_{21}^2, \quad (\text{B.18b})$$

is also important for numerous applications of the isotopies.

APPENDIX C : THE UNIVERSAL ISOROTATIONAL SYMMETRY OF SEA SHELLS

As it is well known, the symmetry of the sphere in three-dimensional Euclidean space $E(r, \delta, R)$ is the *rotational symmetry* $O(3)$. As it is equally well known, sea shells are believed not to admit a symmetry owing to their nonspherical shape as well as the increase of the shape itself in time.

In this appendix we introduce, apparently for the first time, the universal isosymmetry for all possible sea shells as being the *isorotational symmetry* $\hat{O}(3)$ identified by this author in 1985 for physical applications (see the detailed studies in ref.s [5]). Such a symmetry is possible following the representation of sea shells in isoeuclidean spaces $\hat{E}(r, \hat{\delta}, \hat{R})$ and the identification of all possible shapes with the *isosphere* (Fig. 3). The proof of the universal isosymmetry $\hat{O}(3)$ of sea shells is therefore reduced to the proof that $\hat{O}(3)$ is the universal symmetry of the isosphere.

Consider the isoeuclidean spaces $\hat{E}(r, \hat{\delta}, \hat{R})$ of Class III with isometric, isotopic element and isounit in the diagonal form

$$\hat{\delta} = T\delta, \quad T = \text{diag.} (T_x, T_y, T_z), \quad T_k = T_k(t, r, \dot{r}, \dots) > 0, \quad \hat{1} = T^{-1}. \quad (\text{C.1})$$

The isotopies we are studying characterize the deformations of the sphere

$$r^2 = r^1 r^1 + r^2 r^2 + r^3 r^3 > 0, \quad (\text{C.2})$$

into all infinitely possible three-dimensional surfaces

$$r^{\hat{2}} = r^k T r^k = + r^1 T_x r^1 + r^2 T_y r^2 + r^3 T_z r^3 = \text{inv.} \quad (\text{C.3})$$

Some of the main properties of isorotations can then be expressed as follows:

Theorem C.1 [5]: *The isosymmetries $\hat{O}(3)$ of all infinitely possible deformations of the sphere on the isoeuclidean spaces $\hat{E}(r, \delta, \hat{R})$, verify the following properties:*

1) *The groups $\hat{O}(3)$ consist of infinitely many different simple groups corresponding to the infinitely many possible deformations of the sphere (explicit forms of the isometric);*

2) *All isosymmetries $\hat{O}(3)$ are locally isomorphic to $O(3)$ for positive-definite isounits or are isomorphic to the isodual $O^d(3)$ for negative-definite isounits; and*

3) *The groups $\hat{O}(3)$ constitute "isotopic coverings" of the conventional group $O(3)$ in the sense that:*

3.a) *The groups $\hat{O}(3)$ are constructed via methods (the Lie-Santilli theory [6]) structurally more general than those of $O(3)$ (the conventional Lie's theory);*

3.b) *The groups $\hat{O}(3)$ represent physical conditions (deformations of the sphere; inhomogeneous and anisotropic interior physical media; etc.) which are broader than those of the conventional symmetry (perfectly rigid sphere; homogeneous and isotropic space; etc.); and*

3.c) *All groups $\hat{O}(3)$ recover $O(3)$ identically whenever $\hat{1} = 1$ and they*

can approximate the latter as close as desired for $\hat{1} \approx I$.

It is generally believed in both the mathematical and physical literature that the rotational symmetry is broken by ellipsoidal deformations of the sphere. This belief is disproved by the Lie–Santilli theory because of the following:

Corollary C.1A [loc. cit.]: *The rotational symmetry is not broken by ellipsoidal deformations of the sphere, but it is instead exact because of the isomorphism $\hat{O}(3) \simeq O(3)$, provided that it is realized at the covering isotopic level with respect to the isounit $\hat{1} = T^{-1}$.*

Note that the *conventional rotations* are indeed no longer a symmetry of the deformed sphere. Corollary C.1A therefore focuses the attention on the difference between the violation of a *symmetry* in conventional spaces and its exact validity for the corresponding isospace. Equivalently, we are here referring to a mechanism of reconstruction of an exact symmetry in isospace when conventionally broken.

The isorotations can be explicitly written in $E(r, \delta, R)$

$$r' = \hat{\mathfrak{R}}(\theta) * r = \hat{\mathfrak{R}}(\theta) T(t, r, \hat{r}, \ddot{r}, \dots) r = \tilde{S}(t, r, \hat{r}, \ddot{r}, \dots) r, \quad \hat{\mathfrak{R}} = \tilde{S} \hat{1}, \quad (C.4)$$

and therefore result to be intrinsically nonlinear. This is due to the fact that the functional dependence of the isotopic elements is completely unrestricted by the isotopies. We therefore have the following

Corollary C.1B [loc. cit.]: *While conventional rotations are linear, local and canonical transformations in $E(r, \delta, R)$, isorotations are isolinear, isolocal and isocanonical in $\hat{E}(r, \hat{\delta}, \hat{R})$, but nonlinear, nonlocal and noncanonical when projected into $E(r, \delta, R)$*

A further important result is the isotopic generalization of the conventional *Euler's theorem* on the general displacement of a rigid body with one point fixed which we can express via the following:



Theorem A.2 [loc. cit.]: *The general displacement of an elastic body with one fixed point is an isorotation $\hat{O}(3)$ of Class I around an axis through the fixed point.*

The above theorem illustrates the use of the classical isorotational symmetry for the characterization of deformable bodies.

A brief outline of the classical isorotational symmetry is the following. First, let us consider the three-dimensional isoeuclidean space $\hat{E}(r, \hat{\delta}, \hat{R})$. Its local coordinates are usually assumed to be *contravariant* and we shall write $r = \{r^k\}$, $k = 1, 2, 3$. Assume that the isometric in its natural form has *covariant* indices

$$\hat{\delta} = (\hat{\delta}_{ij}) = \text{diag.} (T_x, T_y, T_z). \quad (C.5)$$

Its *contravariant* form is then given by

$$(\hat{\delta}^{ij}) = (\hat{\delta}_{ij})^{-1} = \text{diag.} (T_x^{-1}, T_y^{-1}, T_z^{-1}), \quad \hat{\delta}_{ik} \hat{\delta}^{kj} = \delta_j^i. \quad (C.6)$$

We consider now the *isophase space* $T^*\hat{E}(r, \hat{\delta}, \hat{R})$ with local coordinates $a = \{a^\mu\} = \{r, p\} = \{k, p_k\}$, $\mu = 1, 2, \dots, 6$, where the linear momentum p_k is *contravariant*, as usual. The raising and lowering of the indices therefore follows the rules

$$r_k = \hat{\delta}_{ki} r^i = T_k r^k, \quad p^k = \hat{\delta}^{ki} p_i = T_k^{-1} p_k \text{ (no sums)}. \quad (C.7)$$

The classical Lie-Santilli brackets then assume the form⁴

$$\begin{aligned} [A, \hat{B}] &= \frac{\partial A}{\partial r^p} \hat{1}^p_s \frac{\partial B}{\partial p_q} - \frac{\partial B}{\partial r^p} \hat{1}^p_q \frac{\partial A}{\partial p_k} = \\ &= \frac{\partial A}{\partial r^k} T_k^{-1} \frac{\partial B}{\partial p_k} - \frac{\partial B}{\partial r^k} T_k^{-1} \frac{\partial A}{\partial p_k}, \end{aligned} \quad (C.8)$$

To identify the Lie-Santilli algebra $\hat{\mathfrak{so}}(3)$, let us compute first the *classical fundamental isocommutation rules* which are readily given by⁵

⁴ The proof that the above brackets do indeed verify the Lie axioms although in a generalized way is based on the isotopies of the symplectic geometry and, as such, it cannot be reviewed here for brevity (see ref.s [[5] for brevity).

$$([a^\mu, \hat{a}^\nu]) = \begin{pmatrix} [r^i, \hat{r}^j] & [r^i, \hat{p}_j] \\ [p_i, \hat{r}^j] & [p_i, \hat{p}_j] \end{pmatrix} = (\hat{\omega}^{\mu\nu}) = \begin{pmatrix} 0 & 1 \\ -1 & 0 \end{pmatrix}, \quad (C.9)$$

showing the isotopy $I \rightarrow \hat{I}$. However, when considering the isocommutation rules between r_i and p_j we have

$$\begin{pmatrix} [r_i, \hat{r}^j] & [r_i, \hat{p}_j] \\ [p_i, \hat{r}^j] & [p_i, \hat{p}_j] \end{pmatrix} = \begin{pmatrix} 0 & I \\ -I & 0 \end{pmatrix}, \quad (C.10)$$

Lemma C.1: *The classical isocommutation rules between r_i and p_j coincide with the conventional, canonical ones.*

Next, we introduce the generators of the Lie-isotopic algebra $\hat{\mathfrak{so}}(3)$ which, by central assumption, are given by the *conventional, contravariant generators* of $O(3)$,⁶

$$J^k = \epsilon^{kij} r_i p_j = \epsilon^{kij} T_i{}^l p_j. \quad (C.11)$$

The above quantities are called the components of the *isotopic angular momentum* to emphasize the fact that they characterize a generalized notion defined on $T^*\hat{E}(r, \hat{\delta}, \hat{R})$ rather than on $T^*E_2(r, \delta, R)$.

In particular, the magnitude of the conventional angular momentum is given by the familiar expression $J^2 = J^k J_k = \delta^{ij} J_k J_k$, while the magnitude of the isotopic angular momentum is given by⁷

$$J^2 = J * J = J^k * J_k = \hat{\delta}^{ij} J_i * J_j = \hat{\delta}^{ij} J_i T J_j. \quad (C.12)$$

Next, the following isocommutation rules are readily computed

⁵ These rules require the knowledge of the isoderivatives for which $\partial r_i / \partial r^j = \delta_{ij}$ [5].

⁶ Unlike the operator case to be considered soon, note that the quantities r^i and p_j here are ordinary functions and, thus, they do not require the isotopic product $r^i * p_j$. Note also the subtle but important differences of the indices of $\hat{\delta} = (\hat{\delta}_{ij})$, $I = (I^i{}_j)$ and $T = (T_i{}^j)$. Thus, only the tensor $\hat{\delta}_{ij}$ or its inverse $\hat{\delta}^{ij}$ used for lowering or raising indices.

⁷ J^2 is in this case an *isoscalar*, that is, a scalar quantity in isospace. For this reason it must be contracted in the form $J^2 = J^k * J_k$.

$$[J^k, \hat{r}_i] = \epsilon^{kij} r_j, \quad (C.13a)$$

$$[J^k, \hat{p}_i] = \epsilon^{kij} p_j, \quad (C.13b)$$

and evidently coincide with the conventional ones.

The desired *classical isorotational algebras* $\hat{\mathfrak{so}}(3)$ are then given by [3]⁸

$$\hat{\mathfrak{so}}(3): \quad [J^i, \hat{J}^j] = \epsilon^{ijk} J^k, \quad (C.14)$$

namely, the isocommutation rules of $\hat{\mathfrak{so}}(3)$ have the same structure constants as those for the conventional $\mathfrak{so}(3)$. This establishes the local isomorphism $\hat{\mathfrak{so}}(3) \approx \mathfrak{so}(3)$ *ab initio*. For different classical realizations one may consult ref.s [4,5].

The *isocenter* of the enveloping algebra $\hat{\xi}$ is given by the isomagnitude of the isotopic angular momentum, $C^{(2)} = J^2$, as expected. In fact,

$$[J^2, \hat{J}^i] = 2 \epsilon^{kij} J^k J^j \equiv 0. \quad (C.15)$$

The desired *classical isorotational group* $\hat{SO}(3)$ can then be expressed via the isoexponentiations in terms of the conventional generators and parameters (the Euler's angles)

$$\hat{\mathfrak{R}}(\theta) = \left[\prod_{k=1,2,3} e_{|\hat{\xi}}^{\theta_k \omega^{\mu\alpha} \hat{J}_{2\alpha}^{V(\partial J_k / \partial a^V)(\partial / \partial a^\mu)}} \right] \hat{1} = \hat{\mathfrak{S}}(\theta) \hat{1}, \quad (C.16)$$

where the exponentials are expanded in the conventional associative envelope ξ for simplicity.

Note the true realization of the notion of isotopic lifting of a Lie symmetry, consisting of the preservation of the original generators and parameters of the

⁸ Isocommutation rules (6.1.14) disprove another popular belief in Lie's theory, that the compactness or noncompactness of an algebra can be ascertained from the structure constants. In fact, the structure constants ϵ^{ijk} are those of the *compact* $\mathfrak{so}(3)$ algebra, yet isoalgebra (6.1.14) can represent the *noncompact* $\mathfrak{so}(2,1)$ algebra for $T = \text{diag. } (1, 1, -1)$. The latter possibility has been *excluded* from the physical studies of this and of the following sections by restricted the isotopic element to be of Class I.

symmetry, and the isotopic generalization of the structure of the Lie group itself.

The computation of examples is straightforward. For instance, a (classical) *isrotation around the third axis* is given by [5]

$$\begin{aligned} \mathbf{r}' &= \hat{\mathbf{R}}(\hat{\theta}) * \mathbf{r} = \hat{\mathbf{S}}(\hat{\theta}) \mathbf{r} = \\ &= \begin{pmatrix} x' \\ y' \\ z' \end{pmatrix} = \begin{pmatrix} x \cos \hat{\theta} - y T_x^{-\frac{1}{2}} T_y^{\frac{1}{2}} \sin \hat{\theta} \\ x T_x^{\frac{1}{2}} T_y^{-\frac{1}{2}} \sin \hat{\theta} + y \cos \hat{\theta} \\ z \end{pmatrix}. \\ \hat{\theta} &= T_x^{\frac{1}{2}} T_y^{\frac{1}{2}} \theta. \end{aligned} \quad (\text{C.17})$$

It is an instructive exercise for the interested reader to prove the invariance of all possible deformed spheres under the above isotransforms.

We now compute a general isrotation which brings a point P on the isosphere to an arbitrary point Q. Its projection in Euclidean space is the transformation of a point P on an *ellipsoid* into another arbitrary point Q of the same ellipsoid. Such a rotation can be computed via three successive isrotations [5]:

1) An isrotation $\hat{\mathbf{R}}(\hat{\theta}_1)$ of an angle $\hat{\theta}_1 = T_x^{\frac{1}{2}} T_y^{\frac{1}{2}} \theta_1$ in the (x, y)-plane such that $0 \leq \hat{\theta}_1 \leq 2\pi$,

$$\begin{pmatrix} x' \\ y' \\ z' \end{pmatrix} = \begin{pmatrix} \cos \hat{\theta}_1 & -T_x^{-\frac{1}{2}} T_y^{\frac{1}{2}} \sin \hat{\theta}_1 & 0 \\ T_x^{\frac{1}{2}} T_y^{-\frac{1}{2}} \sin \hat{\theta}_1 & \cos \hat{\theta}_1 & 0 \\ 0 & 0 & 1 \end{pmatrix} \begin{pmatrix} x \\ y \\ z \end{pmatrix}, \quad (\text{C.19})$$

2) An isrotation $\hat{\mathbf{R}}(\hat{\theta}_2)$ around the polar axis z of an angle $\hat{\theta}_2 = T_z^{\frac{1}{2}} \theta_2$ such that $0 \leq \hat{\theta}_2 \leq \pi$,

$$\begin{pmatrix} x' \\ y' \\ z' \end{pmatrix} = \begin{pmatrix} 1 & 0 & 0 \\ 0 & \cos \hat{\theta}_2 & -T_y^{\frac{1}{2}} T_z^{-\frac{1}{2}} b_3^{-1} \sin \hat{\theta}_2 \\ 0 & T_y^{-\frac{1}{2}} T_z^{\frac{1}{2}} \sin \hat{\theta}_2 & \cos \hat{\theta}_2 \end{pmatrix} \begin{pmatrix} x \\ y \\ z \end{pmatrix}, \quad (\text{C.20})$$

3) An isrotation $\hat{\mathbf{R}}(\hat{\theta}_3)$ in the (x, y)-plane with angle $\hat{\theta}_3 = T_x^{\frac{1}{2}} T_y^{\frac{1}{2}} \theta_3$ such that $0 \leq \hat{\theta}_3 \leq 2\pi$,

$$\begin{pmatrix} x' \\ y' \\ z' \end{pmatrix} = \begin{pmatrix} \cos \hat{\theta}_3 & -T_x^{-\frac{1}{2}} T_y^{\frac{1}{2}} \sin \hat{\theta}_3 & 0 \\ T_x^{\frac{1}{2}} T_y^{-\frac{1}{2}} \sin \hat{\theta}_3 & \cos \hat{\theta}_3 & 0 \\ 0 & 0 & 1 \end{pmatrix} \begin{pmatrix} x \\ y \\ z \end{pmatrix}. \quad (\text{C.21})$$

We therefore have the *general isorotation* on the isosphere

$$\begin{aligned}
 \mathbf{r}' &= \mathfrak{R}(\hat{\theta}_1, \hat{\theta}_2, \hat{\theta}_3) * \mathbf{r} = \mathfrak{R}(\hat{\theta}_1) * \mathfrak{R}(\hat{\theta}_2) * \mathfrak{R}(\hat{\theta}_3) * \mathbf{r} = \mathfrak{S}(\hat{\theta}_1, \hat{\theta}_2, \hat{\theta}_3) \mathbf{r}, \quad (C.21) \\
 \begin{pmatrix} x' \\ y' \\ z' \end{pmatrix} &= \begin{pmatrix} [\cos \hat{\theta}_1 \cos \hat{\theta}_3 - \sin \hat{\theta}_1 \cos \hat{\theta}_2 \sin \hat{\theta}_3] \\ [T_x^{-\frac{1}{2}} T_y^{-\frac{1}{2}} (\sin \hat{\theta}_1 \cos \hat{\theta}_3 + \cos \hat{\theta}_1 \cos \hat{\theta}_2 \sin \hat{\theta}_3)] \\ [\sin \hat{\theta}_2 \sin \hat{\theta}_3] \\ [-T_x^{-\frac{1}{2}} T_y^{-\frac{1}{2}} (\cos \hat{\theta}_1 \sin \hat{\theta}_3 - \sin \hat{\theta}_1 \cos \hat{\theta}_2 \cos \hat{\theta}_3)] & [T_x^{-\frac{1}{2}} T_y^{-\frac{1}{2}} \sin \hat{\theta}_1 \sin \hat{\theta}_2] \\ [-T_x^{-\frac{1}{2}} T_z^{-\frac{1}{2}} (\sin \hat{\theta}_1 \sin \hat{\theta}_3 + \cos \hat{\theta}_1 \cos \hat{\theta}_2 \cos \hat{\theta}_3)] & [-T_y^{-\frac{1}{2}} T_z^{-\frac{1}{2}} \cos \hat{\theta}_1 \sin \hat{\theta}_2] \\ [T_x^{-\frac{1}{2}} T_y^{-\frac{1}{2}} \sin \hat{\theta}_2 \cos \hat{\theta}_3] & [\cos \hat{\theta}_2] \end{pmatrix} \begin{pmatrix} x \\ y \\ z \end{pmatrix} \\
 \hat{\theta}_1 &= T_x^{-\frac{1}{2}} T_y^{-\frac{1}{2}} \theta_1, \quad \hat{\theta}_2 = T_z^{-\frac{1}{2}} \theta_2, \quad \hat{\theta}_3 = T_x^{-\frac{1}{2}} T_y^{-\frac{1}{2}} \theta_3. \quad (C.22)
 \end{aligned}$$

The *inverse general isorotation* is then given by

$$\mathbf{r} = \mathfrak{R}(\pi - \hat{\theta}_3, \hat{\theta}_2, \pi - \hat{\theta}_1) * \mathbf{r}'. \quad (C.23)$$

The representation of a decaying angular momentum is notoriously not possible with conventional rotations, but it is readily achieved by the isorotations with a functional dependence of the type $T_k^{-\frac{1}{2}} = \exp(-\gamma t)$, under which we have

$$J^k = e^{-\gamma t} \epsilon^{kij} r^i p_j. \quad (C.24)$$

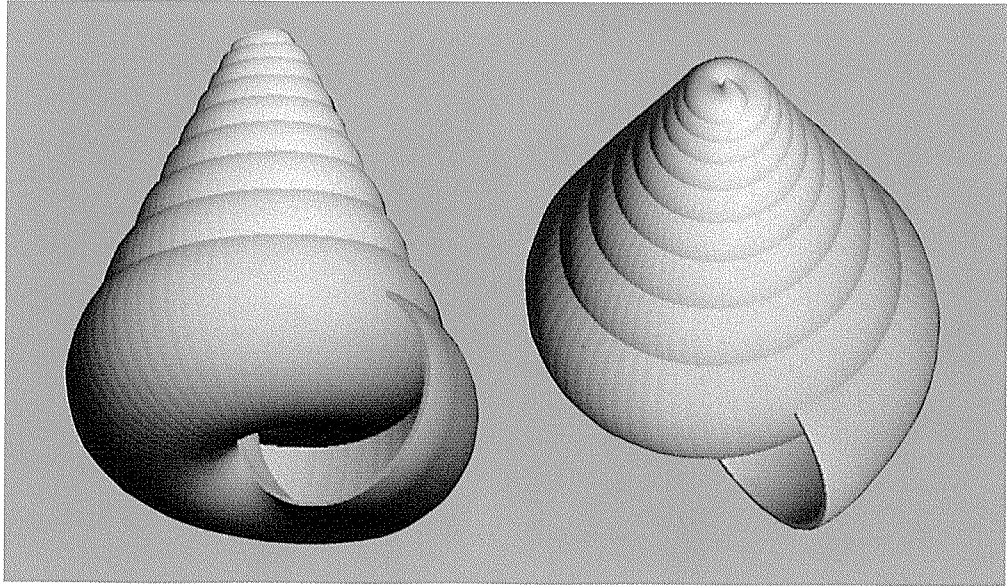
This illustrates the applicability of isorotations, not only for the invariance of the shape of the sea shells, but also their growth in time.

ACKNOWLEDGMENTS

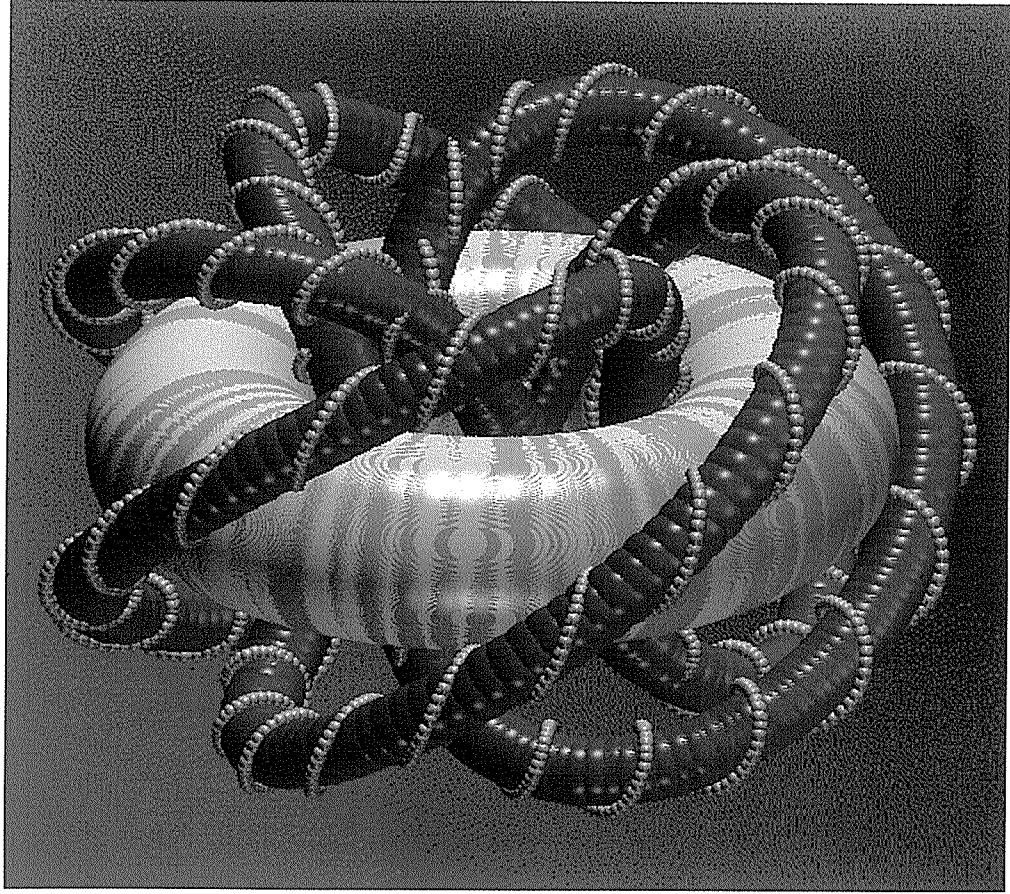
The author would like to express his sincere appreciation and gratitude to C. Illert for invaluable consultations, and to R. Pope for the honor of nominating in his name a Hall of their *Science-Art Research Center* in Australia. Additional thanks are due to G. T. Tsagas, T. Vougiouklis, A. Jannussis and D. Sourlas.

REFERENCES

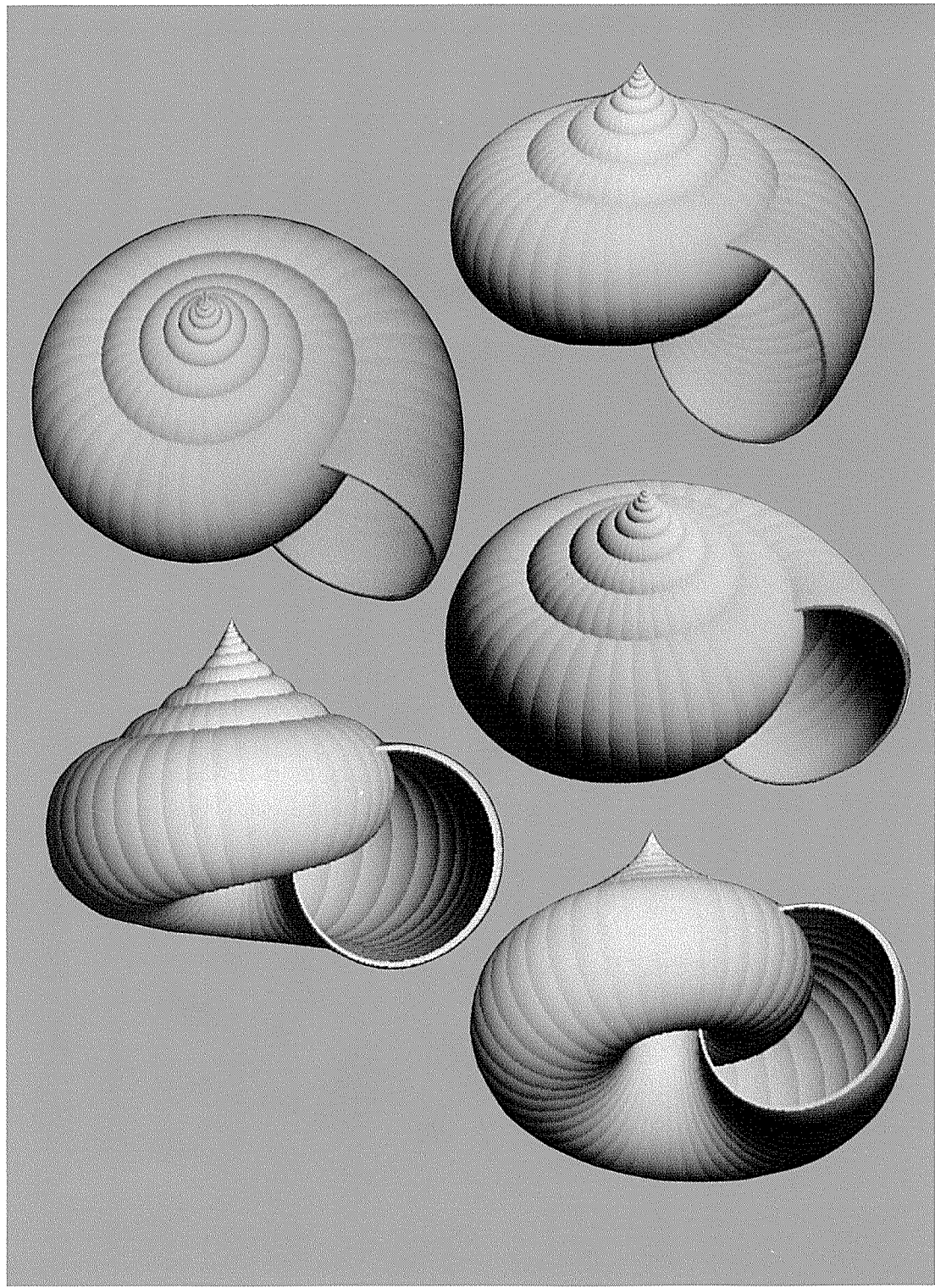
1. C. Illert, *Foundations of Theoretical Conchology*, First Edition, Hadronic Press, Palm Harbor, FL (1992)
2. P. Deutch, Phys. Rev. D **44**, 3197 (1991); L.-X. Li, Phys. Rev. D **48**, 4735 (1993)
3. R. M. Santilli, Hadronic J. **17**, 257 and 285 (1994)
4. R. M. Santilli, *Isotopic Generalization of Galilei's and Einstein's Relativities*, Vol. I: *Mathematical Foundations*, Vol. II: *Classical Isotopies*, Second edition, Academy of Sciences of Ukraine (1994)
5. R. M. Santilli, *Elements of Hadronic Mechanics*, Vol. I: *Mathematical Foundation* (1993), Vol. II: *Theoretical Foundations* (1994), Vol. III: *Experimental Verifications* (in preparation), Academy of Sciences of the Ukraine
6. G. T. Tsagas and D. S. Surlas, Theory of Isomanifolds, Algebras, Groups and Geometries, Vol. **12** (1995), in press; D. S. Surlas and G. T. Tsagas, *Mathematical Foundations of the Lie-Santilli Theory*, Academy of Sciences of Ukraine, Kiev (1993)
7. A. Jannussis, Hadronic J. **13**, 399 (1990)
8. T. Vougiouklis, *Hyperstructures and their Representations*, Hadronic Press, Palm Harbor, FL (1993)
9. J. V. Kadeisvili, *Santilli's Lie-isotopic Generalizations of Contemporary Algebras, Geometries and Relativities*, 2-nd edition, Academy of Sciences of Ukraine (1994); and Algebras, Groups and Geometries **9**, 283 (1992)
10. R. M. Santilli, Algebras, Groups and Geometries **10**, 273 (1992)
11. J. V. Kadeisvili, M. Kamiya and R. M. Santilli, Hadronic J. **16**, 168 (1993)
12. D. K. Fedeev, in *Mathematics, its Content, Method and Meaning*, M.I.T. Press, Cambridge, MA (1963)
13. A. D. Aleksandrov, in *Mathematics, its Content, Method and Meaning*, M.I.T. Press, Cambridge, MA (1963)
14. A. Schoeber, Non-Euclidean and Non-Desarguesian geometries for nonsel-fadjoint systems, Hadronic J. **5**, 1140-1183 (1982)



W.B. et al



C.P. & C.I.

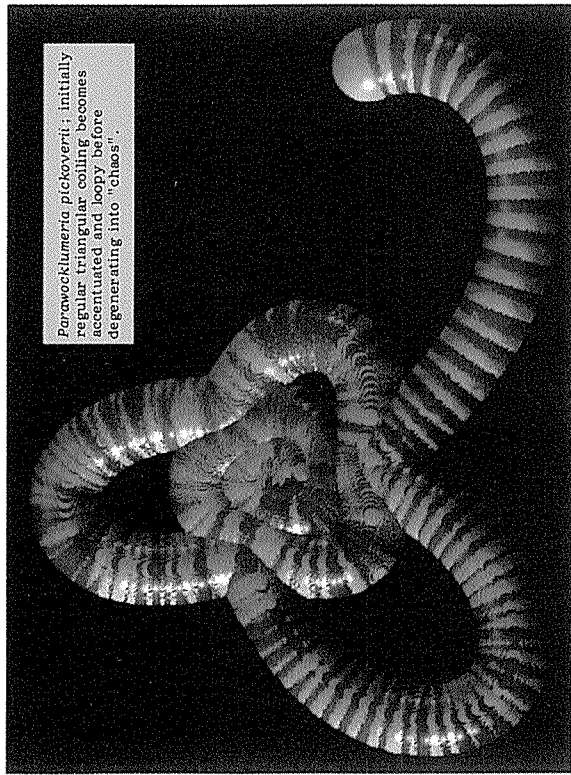


W.B. et al



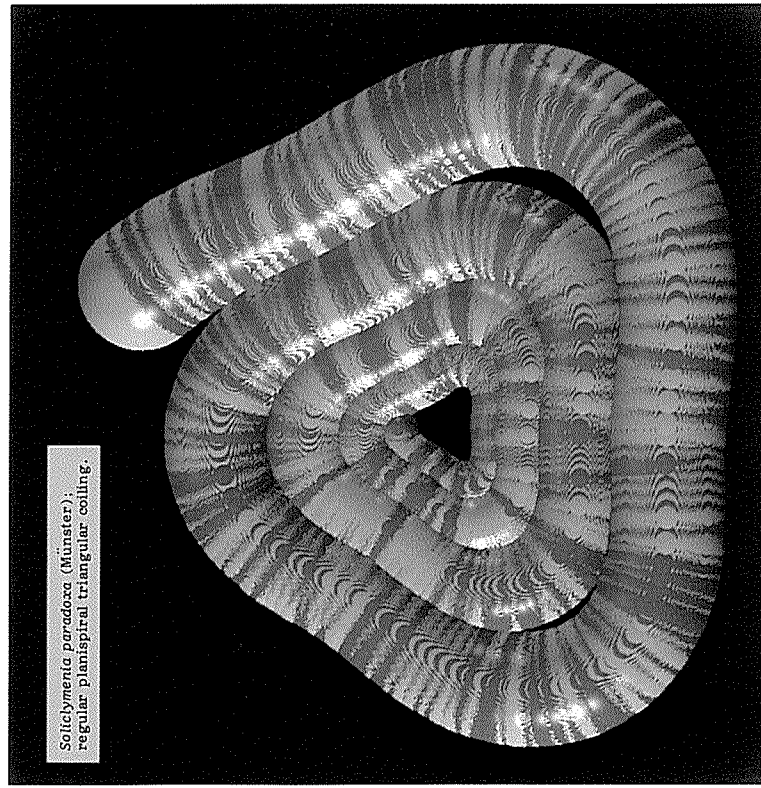
Macroscaphites ivani (d'Orbigny);
found in early Cretaceous strata from
Africa and the European Alps.
Initially regular spiral coiling becomes
elongated.

C.P. & C.I.



Perawocklumeria pickoveri; initially
regular triangular coiling becomes
accentuated and lumpy before
degenerating into "chaos".

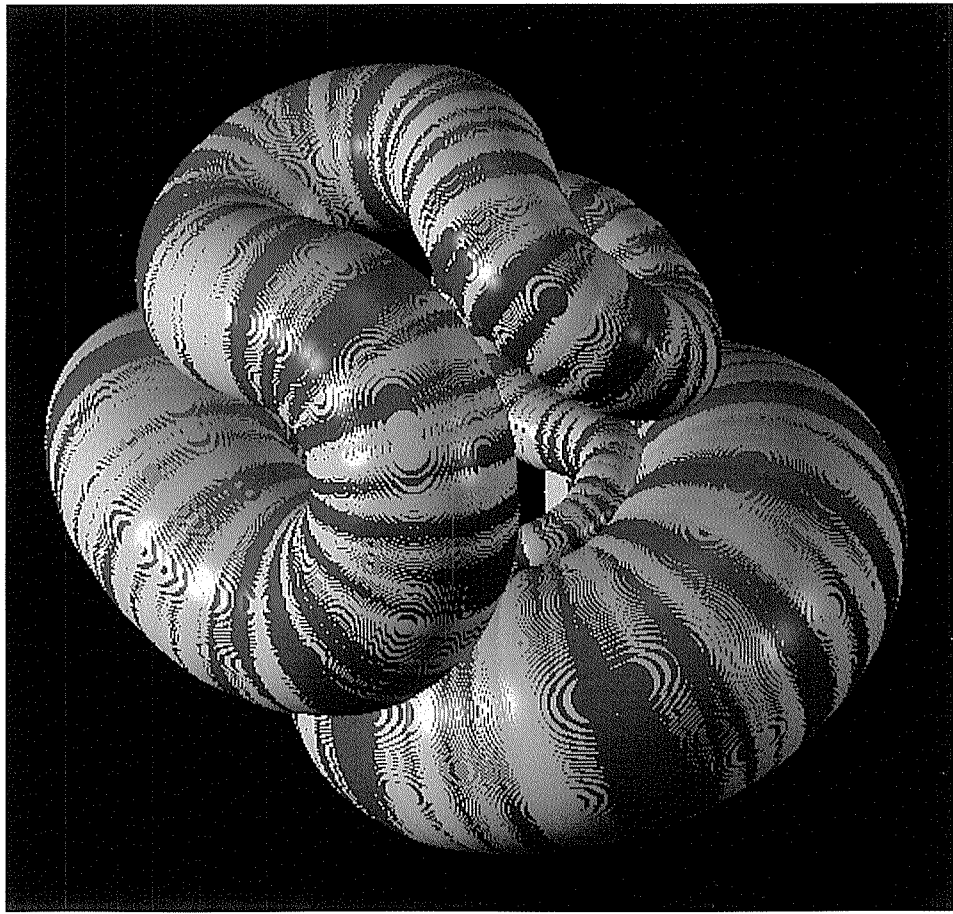
C.P. & C.I.



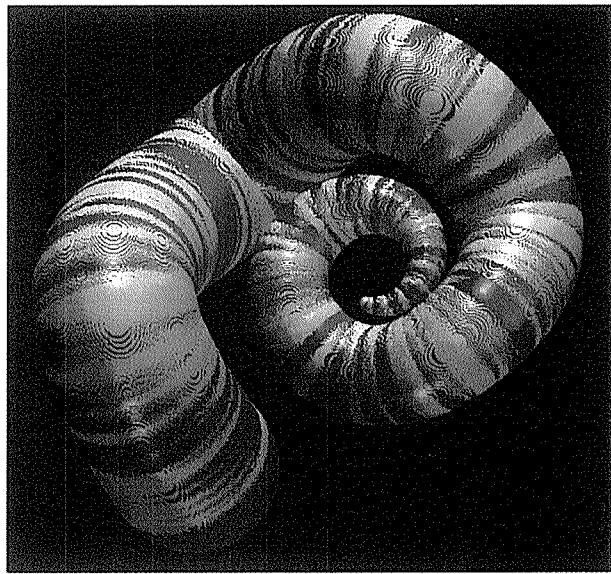
Solilymenia paradoxa (Münster);
regular planispiral triangular coiling.

C.P. & C.I.

These shells demonstrate one kind of breakdown of regular coiling into "chaos". Trajectory-transverse oscillations such as these, within the coiling-plane, are produced in Illert's equations by choosing complex values for the "normalized curvature" constant λ which is basically related to the magnitude of the torque that produces such "buckling": think of a tensile wire coil with its outer-end anchored and the winding spindle being twirled to cause buckling. As these shells grow round sharp corners (bumps in the trajectory called "apses") we have to think about how the generating-curve should orient itself throughout growth. The problem was solved here by sweeping a sphere along the principal growth-trajectory: as it inches along, creating successive growth-increments, the sphere automatically generates a surface in a convincing fashion.



C.P. & C.I.

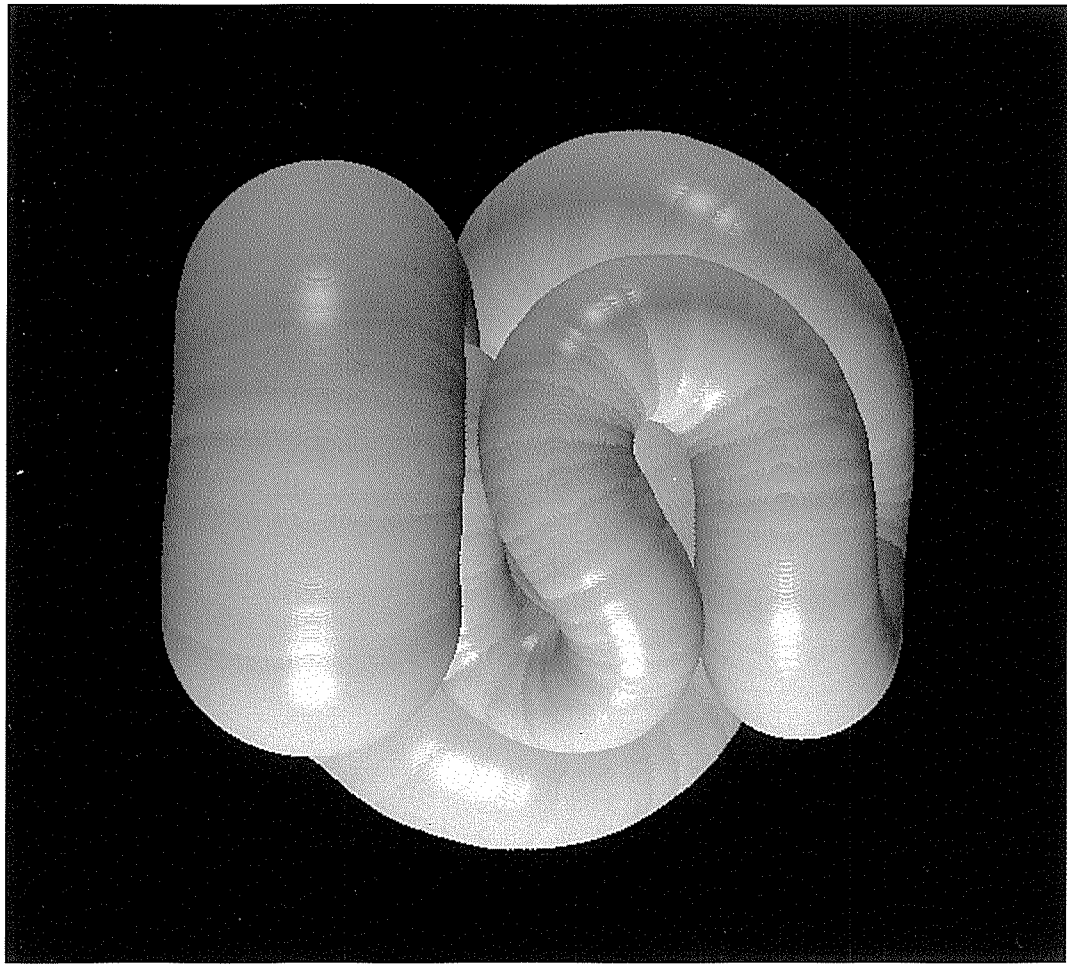


C.P. & C.I.

Nipponites mirabilis (Yabe, 1904): an extinct ammonite whose shape was, for a long time, thought to be arbitrary but has now been shown to obey precise mathematical equations to several significant-figure accuracy.

ABOVE: the juvenile stage begins coiling in a predictable planispiral fashion but, after a time, transverse oscillations set in perpendicular to the coiling plane.

LEFT: by adulthood "chaos" seems to have set in, with outermost whorls meandering in a serpentine fashion ... rather like the suture-line on a tennis ball.



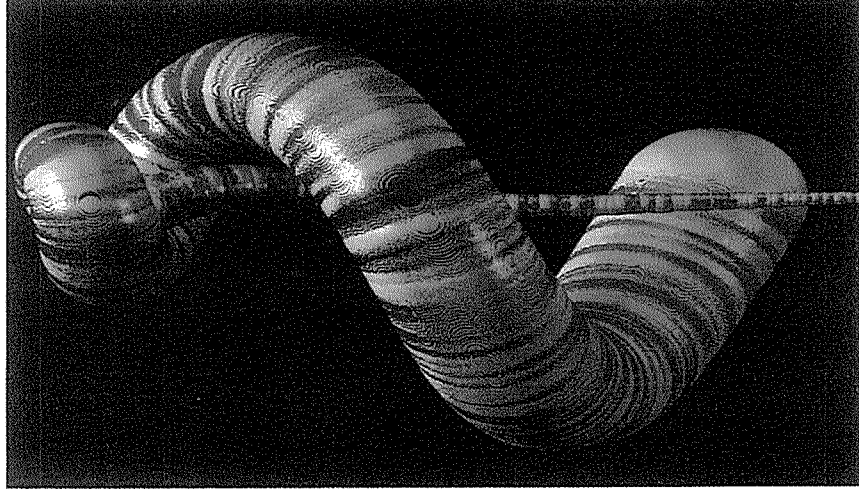
C.P. & C.I.



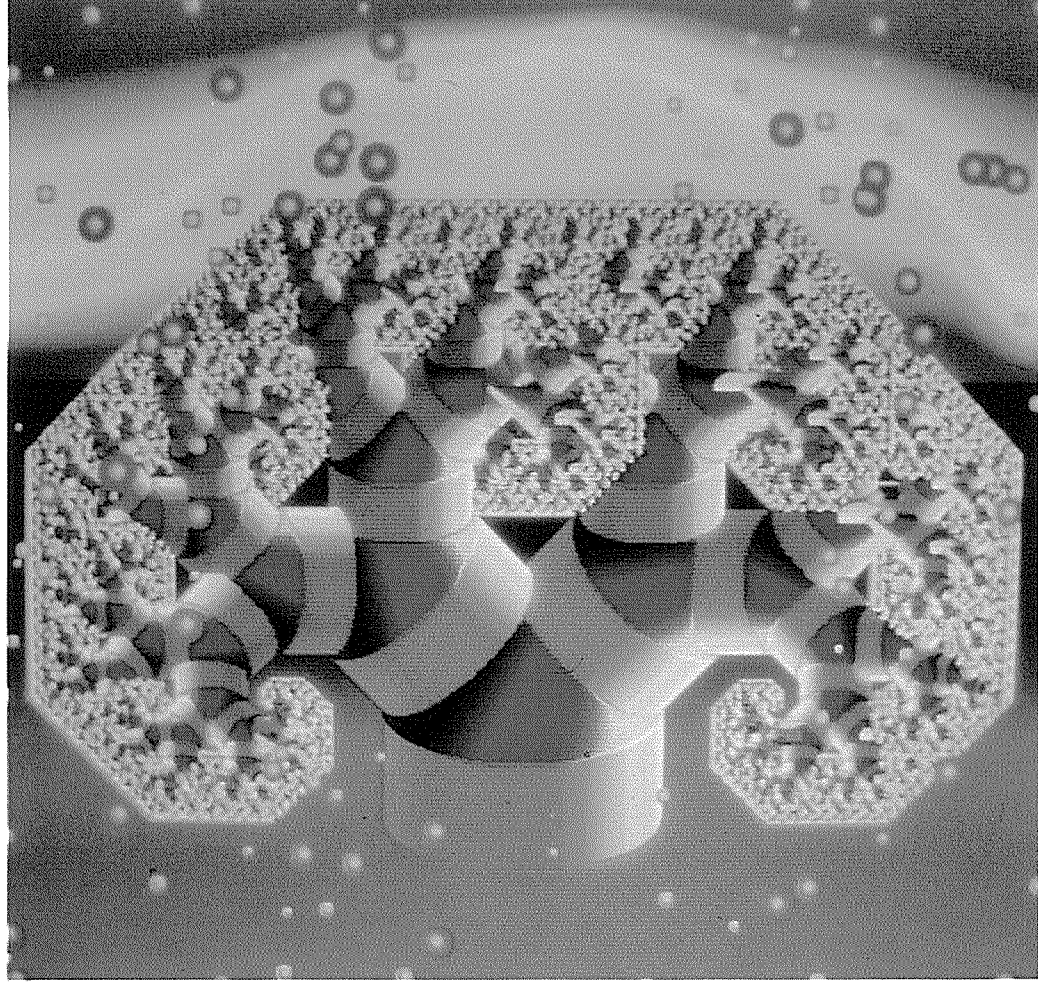
C.P. & C.I.

LEFT: the same adult specimen of *Nipponites mirabilis* as on the opposite page, but with the outermost shell-layer removed ("chipped off"), revealing the underlying silvery "mother-of-pearl" layer.
 ABOVE: another species of *Nipponites*, an open-coiled variety that starts meandering in a serpentine fashion right from the start.

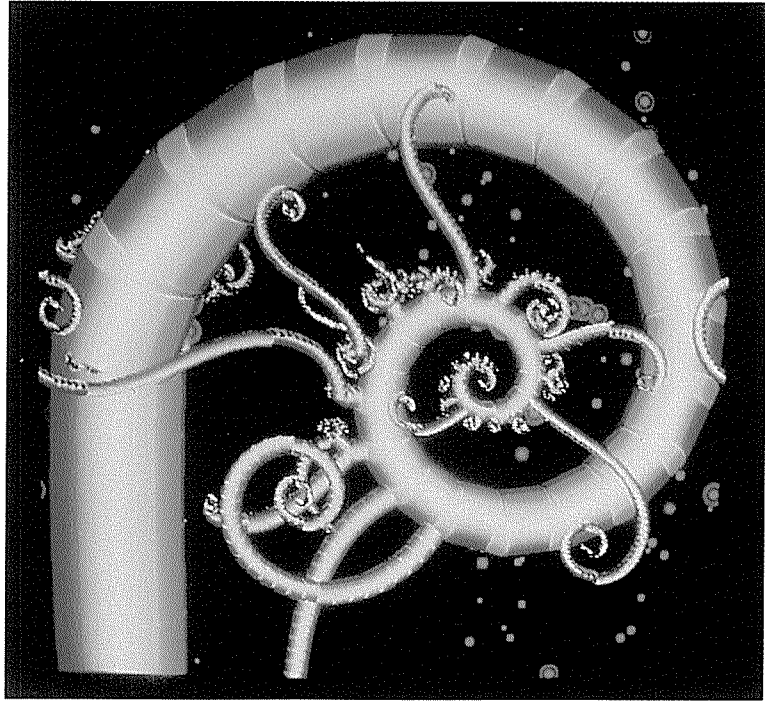
Eubostrychoceras muramotoi



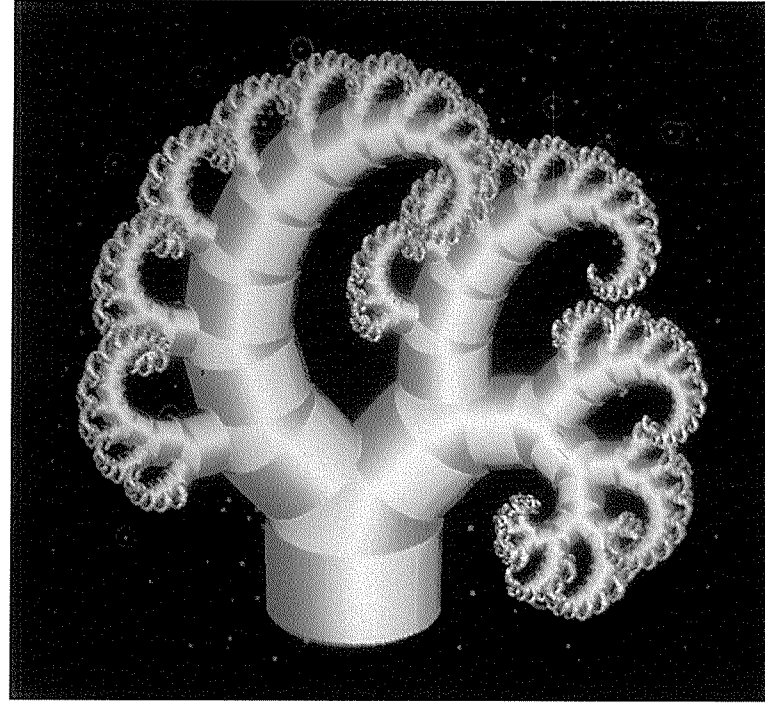
C.P. & C.I.



Y.K.

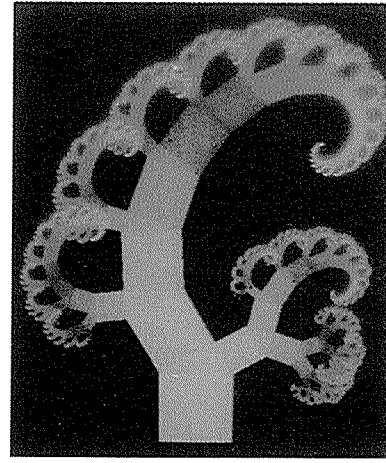


Y.K.

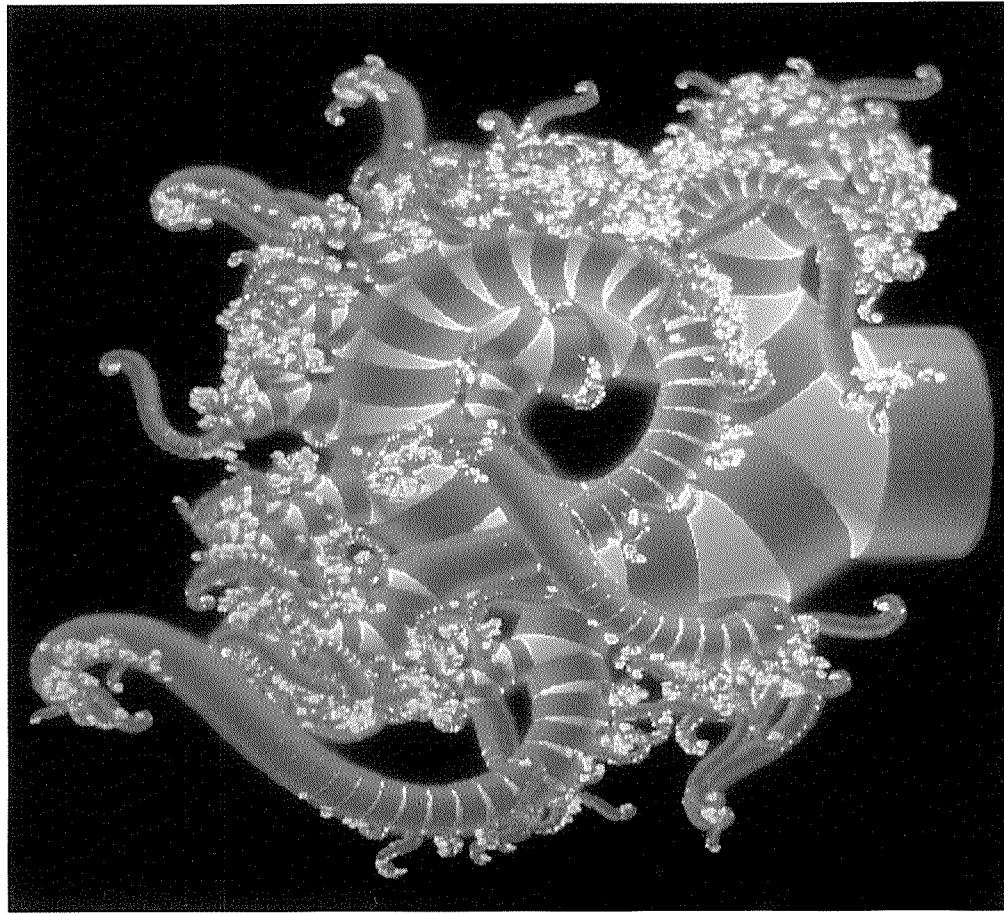


Y.K.

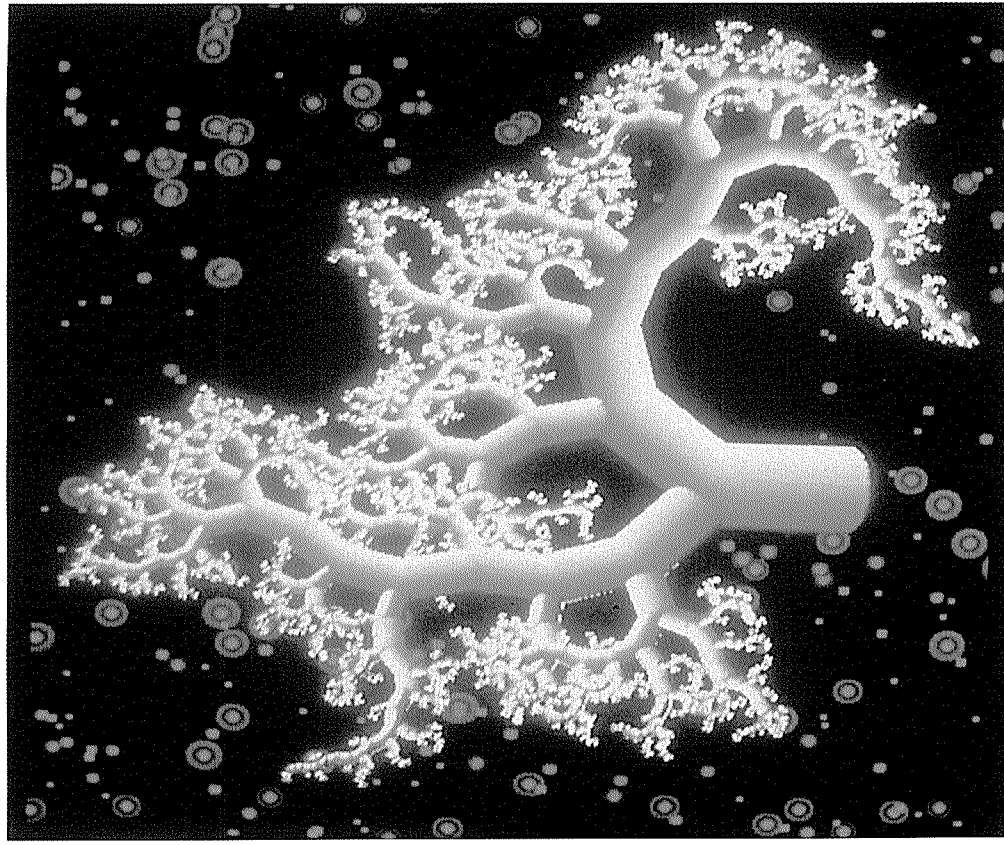
molluscan soft-body anatomy limits the spectrum of branching clockspring geometries that are possible in seashell construction. But bryozoan colonies, certain corals and plants, can and do utilize repeatedly-branching clockspring geometries of the kind shown here and over the page. Our mechanics has only just begun to explore the onset of "chaos" in these kinds of approximately self-similar branching structures. It may also happen that whole classes of elementary particles, each capable of decaying into others, can be topologically represented by some such branching clockspring structure.



Y.K.



Y.K.



Y.K.

ABOUT THE SECOND AUTHOR

Ruggero Maria Santilli was born and educated in Italy where he received his Ph. D. in theoretical physics in 1966 from the University of Torino. In 1967 he moved with his family to the USA where he held academic positions in various institutions including the Center for Theoretical Physics of the University of Miami in Florida, the Department of Physics of Boston University, the Center for Theoretical Physics of the Massachusetts Institute of Technology, the Lyman Laboratory of Physics and the Department of Mathematics of Harvard University. He is currently President and Professor of Theoretical Physics at The Institute for Basic Research, which operated in Cambridge from 1983 to 1991 and then moved to Florida. Santilli has visited numerous academic institutions in various Countries. He is currently a Honorary Professor of Physics at the Academy of Sciences of the Ukraine, Kiev, and a Visiting Scientist at the Joint Institute for Nuclear Research in Dubna, Russia. Besides being a referee for various journals, Santilli is the founder and editor in chief of the *Hadronic Journal* (sixteen years of regular publication), the *Hadronic Journal Supplement* (nine years of regular publication) and *Algebras, Groups and Geometries* (eleven years of regular publication). Santilli has been the organizer of the five *International Workshops on Lie-admissible Formulations* (held at Harvard), the co-organizer of five *International Workshops on Hadronic Mechanics* (held in the USA, Italy and Greece) and of the *First International Conference on Nonpotential Interactions and their Lie-Admissible Treatment* (held at the Université d'Orléans, France). He is the author of over one hundred and fifty articles published in numerous physics and mathematics journals; he has written nine research monographs published by Springer-Verlag (in the prestigious series of "Texts and Monographs in Physics"), the Academy of Sciences of Ukraine and other publishers; he has been the editor of over twenty conference proceedings; he is the originator of new branches in mathematics and physics, some of which are studied in these books; he has received research support from the U. S. Air Force, NASA and the Department of Energy; and he has been the recipient of various honors, including the *Gold Medals for Scientific Merits* from the Molise Province in Italy and the City of Orléans, France and the nomination by the Estonian Academy of Sciences among the most illustrious applied mathematicians of all times. Santilli has been nominated for the Nobel Prize in Physics by various senior scholars since 1985.

ABOUT THE SECOND EDITION

Prof. **C. R. Illert** was the first to discover that sea shells cannot be quantitatively represented via the conventional Euclidean geometry. He achieved comprehensive mathematical representations of sea shells shapes and their growth by using their similarity with non-conservative mechanics which are reproducible via computer visualization, as presented in Part I of this volume.

Prof. **R. M. Santilli** was the first to identify a generalized geometry, his isoeuclidean geometry, which does indeed permit a quantitative representation of sea shells shapes, growth and puzzling time behaviour at bifurcations, also in a form verifiable via computer visualization, as presented in Part II of this volume. The main discovery is that, even though sea shells appear to our senses to belong to our Euclidean geometry, in actuality they belong to a structurally more general geometry with *generalized units* of space and time. The endless, rather complex shapes of sea shells are then all reducible to the perfect sphere in isoeuclidean geometry and they admit as universal-symmetry the conventional rotational symmetry although constructed with generalized units. These novel methods are also applicable to other biological forms, thus initiating a new chapter in theoretical biology.

COMMENTS FROM THE REVIEWERS

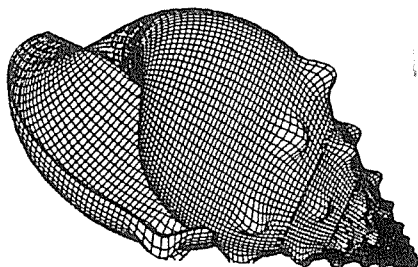
J. V. Kadeisvili (Intern. Center of Physics, Alma-Ata, Kazakhstan): *"This monograph constitutes a true historical development for the entire theoretical biology ..."*

W. Ponder (Curator, Australian Museum, Sydney): *"A truly significant contribution to natural history..."*

T. Rice (Editor, OF SEA AND SHORE): *"Readers will be fascinated by this in depth mathematical study of sea and land shells. Outstanding and highly recommended."*

M. Keats (Chairman, Conchology Section, Royal Zoological Society, N.S.W., Australia): *"The pathway to a new Renaissance in molluscan taxonomy, using computers to model 3D form... highly recommended to theoretical and applied malacologists, biologists and paleontologists"*.

ISBN 0-911767-92-4



HADRONIC PRESS